

https://dspace.org/

Novel synthetic methodology for the assembly of a-carbolines and 7-azaindoles

Henning, Hendrik

2018

https://hdl.handle.net/10539/25742

Henning, Hendrik (2018) Novel synthetic methodology for the assembly of a -carbolines and 7-azaindoles, University of the Witwatersrand, Johannesburg, <http://hdl.handle.net/10539/25742>

Downloaded from a DSpace repository. https://dspace.org/

Novel synthetic methodology for the assembly of α-carbolines and 7-azaindoles

Hendrik Henning

A thesis submitted to the
Faculty of Science,
University of the Witwatersrand,
Johannesburg,
in fulfilment of the requirements for the degree of
Doctor of Philosophy

Johannesburg, February 2018

Declaration of Authorship

I, Hendrik Henning, declare that this thesis titled, 'Novel synthetic methodology for the assembly of α-carbolines and 7-azaindoles' and the work presented in it are my own. I confirm that:

- This work was done wholly or mainly while in candidature for a research degree at this University.
- Where any part of this thesis has previously been submitted for a degree or any other qualification at this University or any other institution, this has been clearly stated.
- Where I have consulted the published work of others, this is always clearly attributed.
- Where I have quoted from the work of others, the source is always given. With the exception of such quotations, this thesis is entirely my own work.
- I have acknowledged all main sources of help.
- Where the thesis is based on work done by myself jointly with others, I have made clear exactly what was done by others and what I have contributed myself.

Signed: _____

Date: _____

"The supreme function of reason is to show man that some things are beyond reason."

Blaise Pascal

Abstract

The α-carbolines and 7-azaindoles are part of a larger family of compounds derived from indoles and other heterocyclic compounds that are prevalent in nature often as biologically active compounds. The synthesis of α-carbolines and 7-azaindoles described in this thesis is built on several key reactions developed in our laboratories, namely the light mediated *t*-BuOK ring closure method used previously to form carbazoles, naphthalenes and anthracenes; as well as an acid mediated ring closure of acetylene containing 2-aminopyridines to form 7-azaindoles; and lastly catalytic palladium chemistry is used in some critical carbon carbon bond forming reactions, namely through the Sonogashira reaction.

The bromine atoms on several 3-bromo-2-aminopyridine compounds is substituted with 1-ethynyl-2-methyl-benzene in a Sonogashira coupling reaction, followed by ring closure forming the respective 2-(2-methylphenyl)-1*H*-pyrrolo[2,3-*b*]pyridines (2-(*o*-tolyl)-1*H*-7-azaindoles). After formylation on the 3 position, forming 2-(2-methylphenyl)-1*H*-pyrrolo [2,3-*b*]pyridine-3-carbaldehydes (3-formyl-2-(*o*-tolyl)-1*H*-7-azaindoles), and *N*-benzylation on the 1 position, furnishing 1-benzyl-5-methyl-2-(2-methylphenyl)-pyrrolo[2,3-*b*]pyridine -3-carbaldehydes (3-formyl-2-(*o*-tolyl)-1-benzyl-7-azaindoles), the compounds were subjected to the light mediated ring closing methodology described, yielding 11-benzyl-benzo -α-carbolines (11-benzyl-11*H*-benzo[*g*]pyrido[2,3-*b*]indoles). The final debenzylation on 11-benzyl-benzo-α-carbolines (11-benzyl-11*H*-benzo[*g*]pyrido[2,3-*b*]indoles) synthesised furnished 11*H*-α-carbolines (11*H*-benzo[*g*]pyrido[2,3-*b*]indole). The novel synthesis of α-carbolines and 7-azaindoles through these methods proved successful, even though in low overall yields. The methodology was further extended to allow further substitution on α-carbolines. This was achieved by bromination on the initial 2-aminopyridine starting material in the 5 position, followed by iodination on the 3 position. The iodide of the 2-aminopyridine could then be selectively substituted using Sonogashira coupling as discussed, followed by Suzuki coupling on the bromide, in this case with 3,4-dimethoxy-phenyl boronic acid. The synthesis of 11*H*-3-(3,4-dimethoxyphenyl)-benzo-α-carboline was then completed using Suzuki coupling methodology to add the 3,4-dimethoxyphenyl functionality from (3,4-dimethoxyphenyl)boronic acid.

The heterocycles synthesised in this thesis were tested against African sleeping sickness parasite *Trypanosoma brucei*. The compound 5-(3,4-dimethoxyphenyl)-2-(2-methylphenyl) -1*H*-pyrrolo[2,3-b]pyridine-3-carbaldehyde was found to have an IC_{50} value of 10 μM, with several others showing activity in the range of 12-27 μM. The antimalarial studies in contrast showed only one significant hit, 11-benzyl-3-(3,4dimethoxyphenyl)-benzo-α-carboline had an IC_{50} value of 26 μM.

Overall, the study resulted in the successful synthesis of α-carbolines and 7-azaindoles, as well as the discovery of biologically active heterocycles effective against malaria and African sleeping sickness. These heterocycles could be used as lead compounds for further research.

Acknowledgements

My dear Saviour, the sustainer of my all
You have given me all these sweet thoughts
The world you made keeps me enthralled
You keep me doing what I ought

Chemistry, although void of prose seems to be what I chose
It is a poor friend, yet one who's regards I must send
It left me somewhat tattered and battered
Yet, I will not leave and grieve it

Charles, you never seem to amaze
You regularly fill my days
With plenty of chemistry, plans and tales
Of your' and other people's sails

Benita, yes, my dearest soul
You fill me with such love and delight
You seem to be my precious all
My days start off truly bright with you by my side

Jean, I even left you a space
You have been my friend through this mad race
You motivated and reasoned with my dreamy schemes
Kept me company through the reality of my schemy dreams

Further 321 and the *fish-tank*, my later lab
My last day was truly sad
We had such fun days and discussions
There were many occasions with many repercussions

There is my family, my father, mother and brothers
You seem to have influenced me a great deal
They say what you sow impacts on what you gather
You in turn have placed your eternal seal

Further there is Cedric, Adam and Bradley
The people that have looked after me at UJ
Your input has moulded me greatly
It was good that I didn't with you stay

The bread, the water and the shelter from the rain
All of this money from the NRF came
I did not do this project as a homeless man
Nor on my own would I have been able to stand

Then there is whizzbang and its crazy friends
I had some fun and amazingly great days
You gave me bangs and scares and daze
Most of my scars will hopefully mend

There are some others that I forgot
Trust me, in my mind you did not rot
I am grateful, you may have been there
Many memories forgotten we now share

This is getting ridiculous, how many verses do you need
Poetry is beautiful, but your thesis with it you cannot read

Hendrik Henning

There is absolutely no reason to have this footnote.

Contents

Declaration of Authorship i

Abstract iii

Ackowledgements v

Contents vii

Abbreviations x

1 Introduction 1
- 1.1 The importance and mechanism of biological activity of molecules 1
  - 1.1.1 DNA binding and activity 4
- 1.2 Cancer, mechanism and treatment 5
  - 1.2.1 Cancer and apoptosis 7
  - 1.2.2 Platinum containing drugs 8
  - 1.2.3 Organic based cancer treatments 9
- 1.3 Protozoan parasitic diseases and their treatments (Malaria and African sleeping sickness) 11
  - 1.3.1 Malaria 11
  - 1.3.2 African sleeping sickness 14
- 1.4 Indoles and Carbazoles 18
  - 1.4.1 Indole 18
  - 1.4.2 Carbazole 23
- 1.5 Azaindoles 26
- 1.6 Azacarbazoles and α-Carbolines 28
- 1.7 Project aims 31

2 Synthesis of α-carbolines 33
- 2.1 Introduction 33
  - 2.1.1 Important reactions 33
  - 2.1.2 Initial synthesis plan 38
- 2.2 Synthesis of the organic framework 39
  - 2.2.1 Sonogashira reaction of substituted 2-aminopyridines with ethynyltrimethylsilane 41
  - 2.2.2 Desilylation of ethynyltrimethylsilane substituted compounds 46
  - 2.2.3 The Sonogashira reaction of acetylene substituted 2-aminopyridines and 2-iodotoluene 48

2.2.4 Cyclization of 2-aminopyridines to form 7-azaindoles 57
2.2.5 Formylation at C-3 and protection of the azaindole at N-1 60
2.2.6 *t*-BuOK and light mediated ring closure 63
2.2.7 The final benzyl deprotection of 11-benzyl-α-carbolines 70
2.3 Further functionalization of α-carbolines 76
2.3.1 The synthesis of 3,4-dimethoxy substituted α-carboline 78
2.4 Conclusion 82

3 Modification and biological activity evaluation of 7-azaindoles 83
3.1 Introduction 83
3.1.1 Hybrid compounds in medicine 83
3.1.2 From biologically active 2,2^i-bisindole natural occurring compounds to 7-azaindole containing ligands 87
3.2 Synthesis of coordinating ligand 94
3.3 Coordination of azaindole ligands with metals 105
3.3.1 Future work 108
3.4 Biological testing 109
3.4.1 African sleeping sickness and Malaria assays 109
3.5 Conclusion 116

4 Experimental 117
4.1 Standard experimental techniques 117
4.1.1 Chromatography 117
4.1.2 Anhydrous solvents and reagents 118
4.1.3 Spectroscopic methods 118
4.1.4 Mass spectroscopy (m/z) 118
4.1.5 Infrared spectroscopy (IR) 118
4.1.6 Crystallography 119
4.2 Chemical methods 119
4.2.1 A typical bromination procedure 119
4.2.2 Esterification reactions 121
4.2.3 An adapted Corey-Fuchs method in the formation of 2 bromo benzofuran 122
4.2.4 A typical iodination of 2-amino-pyridine analogues 123
4.2.5 A typical iodination by lithiation procedure 123
4.2.6 A typical aryl diazotization followed by iodination procedure . . . 124
4.2.7 A typical Sonogashira coupling procedure 125
4.2.8 A typical Boc protection procedure 130
4.2.9 A typical Suzuki coupling procedure 131
4.2.10 A typical Boc deprotection procedure 133
4.2.11 A typical trimethylsilyl deprotection procedure 134
4.2.12 A typical ring closure of 2-amino-pyridines to form corresponding 7-azaindole 136
4.2.13 A typical formylation procedure with 1,1-dichlorodimethyl ether . 139
4.2.14 A typical formylation procedure with $POCl_3$ 141
4.2.15 A typical benzylation procedure 141
4.2.16 A typical light mediated ring closure procedure 143

4.2.17 A typical oxidative debenzylation procedure 146
4.2.18 A typical copper catalyzed alkyne dimerisation procedure 147

References **149**

Appendix: NMR spectra **164**

Appendix: Crystallography data **195**

Abbreviations

A

Å angstrom

Ac acetyl

Ar aryl

Arom. aromatic

B

Bn benzyl

Boc *tert*-butoxycarbonyl

BP boiling point

BuLi butyl lithium

C

°C degrees Celsius

CAN ceric ammonium nitrate

CIMS chemical ionisation mass spectroscopy

COSY correlation spectroscopy

CSD Cambridge structure database[1]

D

DCM dichloromethane

DDQ 2,3-dichloro-5,6-dicyano-1,4-benzoquinone

DIA diisopropylamine

DMAP 4-(*N*,*N*-dimethylamino)pyridine

DMSO dimethyl sulfoxide

E

EIMS electron ionisation mass spectroscopy

ESIMS electrospray ionisation mass spectroscopy

Et ethyl

EtOAc ethyl acetate

eq equivalents

H

h hour

HMBC heteronuclear multiple bond correlation

HSQC heteronuclear single-quantum correlation

I

***i*-Pr** *iso*-propyl

IR infrared

M

Me methyl

min minute

MP melting point

N

NBS *N*-bromosuccinimide

***n*-Bu** *n*-butyl

NMP *N*-methylpyrrolidone

NMR nuclear magnetic resonance

***n*-Pr** *n*-propyl

P

Ph phenyl

PMB *para*-methoxybenzyl

R

rt room temperature

T

T.b. *Trypanosoma brucei*

TBAF tetrabutylammonium fluoride

TBDMS *tert*-butyldimethylsilyl

***t*-Bu** *tert*-butyl

TEA triethylamine

Tetrakis $Pd(PPh_3)_3$)

THF tetrahydrofuran

TLC thin layer chromatography

TMS tetramethylsilane/trimethylsilyl

Tosyl toluenesulfonyl

TOF Turn over frequency

TON Turn over number

Q

quant quantitative

Chapter 1

Introduction

The discussion in this chapter starts with a selected discussion on the role of heterocycles in diseases such as cancer, sleeping sickness and malaria. This is followed by a literature survey on the synthesis of indoles, carbazoles, azaindoles and α-carbolines. Finally, the aims of this PhD project on the novel synthesis of 7-azaindoles and α-carbolines are outlined.

1.1 The importance and mechanism of biological activity of molecules

Biological activity of any compound is determined by the effect exerted on tissue.[2] This biological activity is characterised by the binding of compounds to their respective target molecules, such as enzymes and DNA, stopping their function.[3–6] Compounds can also affect the red-ox state of a cell through excessive oxidative stress, such as seen in the use of cis-platin.[7,8] The mechanisms employed by these biologically active compounds that affect biological systems are the same that are utilised through various naturally occurring invaders of tissue namely virus binding to receptors on cells in order to gain access to the cytoplasm,[9,10] and the excretion of toxic substances by fungi that kill bacteria.[11,12]

Biologically active compounds are important in medicine today, as they enable the body to fight against many ailments and diseases. Research is required to identify and develop biologically active compounds and this research includes the isolation of naturally

occurring compounds, biological testing of these compounds and then the synthesis of these compounds and analogues. The structure activity relationship that exists between biologically active compounds and their respective targets can be used by the synthetic organic chemists to design drugs that are selective and effective.[13–15] This is achieved through the synthesis of compounds that structurally exhibit similarities to naturally occurring compounds that show biological activity, or through computational studies that calculate the specific binding of compounds to the desired active site of enzymes targeted. The selectivity and effectiveness of an active compound is achieved through preferential binding to the active site, and the non-preferential binding to the active site of other enzymes. Non-selectivity binding will result in various side effects, and increased toxicity as multiple enzymes will be effected, and their functions strained. Therefore, the interaction of enzymes with small molecules is one of the critical design concepts of living systems. Enzymes have many functions, ranging from the transformation of small molecules (e.g. hydrogen peroxide into water), to the transcription and translation of DNA which contains all the information required for organisms to function. Enzymes react with a very limited number of substrates, and have very specific roles in the complex biological system. This specific reactivity is due to the complex 3-D structure of the enzyme, which only allow molecules that fit into the active site to bind. There are also a number of binding interactions which occur in the active site which keep the desired compounds in the active site. Since these enzymes are important for all the active biological processes, their inhibition will halt a certain biological process. Enzymatic inhibition is in essence the primary target for drug developers. The design of small molecules that only targets a very specific enzyme and binds strongly is the ultimate goal in this research field. Therefore, the study of enzyme kinetics and binding will help us understand binding and regulatory activity.[3]

The normal function of enzymes is one in which an enzyme binds to a substrate and a chemical reaction occurs. This process allows for the synthesis of compounds in biological systems, as well as control functions required for these biological systems to endure. A cartoon of this function is shown in Figure 1.1.

The binding of the substrate to the enzyme can be blocked by another compound or substrate that takes the appearance of the substrate and has some key binding interactions that keep it in the active site.[3] This kind of binding is called competitive binding and is shown in Figure 1.2.

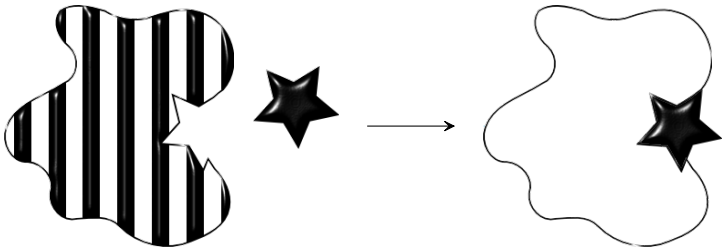


FIGURE 1.1: Normal binding of an enzyme to a substrate allowing the required reaction to occur

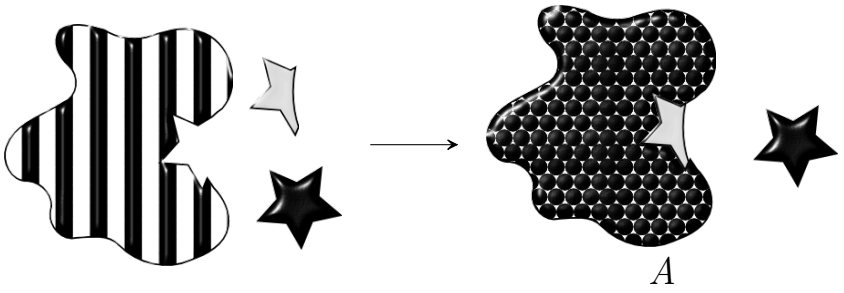


FIGURE 1.2: Competitive binding of a molecule with an enzyme to give the inactivated enzyme A.

The kinetics of this interaction is determined by whether the binding is reversible or irreversible. If the binding is reversible, the substrate and compound blocking the enzymatic function compete for the active site, the compound will move in and out of the active site with a certain residence time. When the molecule is out of the active site, the substrate has a chance to bind and allow normal enzymatic activity. The longer the molecule stays inside the active site, the longer the enzyme will be inactive. Therefore, the more strongly the compound binds to the active site, the more the enzymatic process will be retarded.[3]

The next type of inhibition is that of non-competitive inhibition in which the molecule binds to another section of the enzyme, known as the allosteric site, which is not part of the enzyme active site. The enzyme then changes shape and the substrate is unable to enter the active site, or is unable to bind to the active site effectively, causing no enzymatic reaction to take place as shown in Figure 1.3.

This kind of inhibition in enzymatic processes is common. Enzymes are phosphorylated in order to activate or inhibit them, enzymes respond to messenger molecules in this manner. The concentration of molecules often determine their synthesis by stopping their overproduction when the concentration is too high, or enabling their production

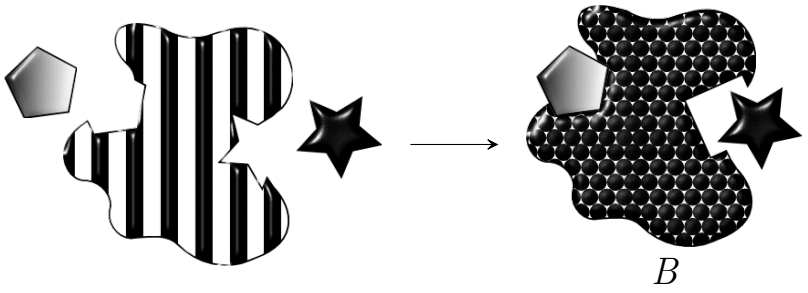


FIGURE 1.3: Non-Competitive binding of a molecule with an enzyme to give the inactivated enzyme *b*.

when the concentration is too low.[3] The kinetics of non-competitive inhibition is independent of the substrate concentration and can be distinguished from competitive inhibition through kinetic studies. The binding of the molecule to the allosteric site is only determined by its strength of interaction to the site, when the molecule detaches it is free to attach again without competing for the allosteric site, which the natural substrate does not bind. Competitive inhibition can be overcome by substrate binding with high substrate concentrations, whereas non-competitive inhibition cannot be overcome in the same manner.[16] This makes the non-competitive binding compound a stronger inhibitor than that of the competitive binding compound.

The next class of inhibitors are irreversible binding inhibitors that chemically form a bond to the enzyme active or allosteric site.[16] These molecules effectively decrease the enzyme concentration and stops the enzyme function until more of the enzyme is produced by the cell.[3,17] This form of inhibitor is very powerful, however, due the irreversible nature of binding can bind to enzymes that are not targeted and disrupting processes unintentionally. This binding to non intended enzymes occur, even when binding is not favoured, because the binding is irreversible yet the draw back is the very non-reversible binding that makes them very effective. This gives this class of inhibitors general toxicity, and is therefore, less favoured in drug design as compared to reversible inhibitor compounds.[3,17]

1.1.1 DNA binding and activity

Molecules that bind to DNA can have varied interactions from interconnection of base pairs, alkylation (mechlorethamine),[18] intercalation (anthracycline antibiotics)[19] and cleavage of the phosphate back bone (vanadium complexes)[20] leading to loss of cell

viability.[21] Loss in cell viability is to due to limited or loss of function of DNA replication, transcription or translation causing cellular panic leading to alteration in gene expression, cell life cycle inhibition and stimulation of DNA repair.[21] In multicellular organisms this can potentially lead to apoptosis.[21–23]

Small molecules that intercalate with DNA are generally flat aromatic or heteroaromatic compounds, often with a carbohydrate moiety attached. The flat aromatic section inserts between the base pairs in the DNA helix and the carbohydrate moiety is generally located in the minor groove. These favourable interactions disallow enzymes of important functions such as transcription, translation and replication of those sections of DNA.[19,24,25] This PhD project will focus on the synthesis of flat heteroaromatic that are potential DNA intercalators.

1.2 Cancer, mechanism and treatment

Cancer can be seen as a genetic disorder in which the cells in an organism mutate. A single damaged parent cell is all that is required to form a tumour and as such is identified as monoclonal.[26,27] There are two types of cancer, it is either benign or malignant with the latter being the very aggressive and dangerous form. This genetic damage can be brought about in various ways, together with environmental effects and DNA transforming agents such as retro-viruses.[26,28] All humans have some cancerous cells in their body as mutations naturally occur over time, yet malignancy is only present after very specific genes are altered and then only after several of these mutations have occurred in the same cell. This damage can be attributed to several events that need to take place within the cell that acts as the origin of the disease. Benign tumours stay in boundaries and adapt to signals from the environment that control their growth. Malignant tumours do not respond to signals and invade and infect many parts of the organism.[26,27] The changed genes usually suppress or stimulate different stages of cell growth and proliferation in the cell cycle.[29] Therefore we need to look at cancer as a series of events in which different parts of the genetic code become damaged.

The changes which occur to genes can be as small as a single nucleotide replacement or something as large as chromosomal rearrangement, the addition or deletion of a

chromosome and even the addition of viral genomes to the host cell.[29] The important genes that can be affected are discussed in the next few sections.

Proto-oncogenes

These are genes which normally promote cell growth and division, but are sufficiently regulated. Changes to these genes or severe up-regulation form oncogenes, which put the cell in a permanent growth and division state according to the severity of the mutations developed or irregular regulation.[26,27,29] Such oncogenes include growth factors (external signalling receptor genes), g-proteins (enzymes of the *ras* family that bind to GTP and are important in signalling inside the cell), cytoplasmic kinases (important in signalling transduction) and nuclear oncogenes (transcription factors). There are some oncogenes that effect the triggering of apoptosis in the cell. In healthy cells apoptosis is triggered when DNA damage is detected, stopping cells from becoming cancerous.[30] When apoptosis is inactivated through oncogenes cells with mutations are not terminated, and can undergo further mutations, which could lead to malignancy.

Tumour suppressor genes

Tumour suppressor genes control cell growth and division.[26,29] These are genes which are not always clearly understood, yet have been identified in different tumour types. For instance it has been shown that breast cancer, colon cancer and kidney cancer have very specific tumour suppressor genes which undergo mutation. Some of these genes include 11p13 (WT1 protein), 11p15 (c-Ha-*ras* protein), 18q21 (DDC protein), 5q21 (RFLP) and 17q21.2.[29] In almost half of cancers studied the tumour suppressor gene p53 has undergone mutation, which shows its important regulatory function in the cell and its critical function in apoptosis to bring about cell death.[29,30]

DNA repair and checking mechanisms

DNA repair in cells is a very important function for cells to stay in a healthy state, as many things like UV light, radicals and other reactive species damage DNA in cells.[31] The failure of DNA repair allows for permanent mutations in the DNA of a cell. It has

been suggested that all cancerous cells have had their DNA repair mechanisms affected in one way or another.[31]

Activation of telomerases

Telomeres are the repetitive end sections on chromosomes that act as a buffer when DNA replication occurs. After every copy of the chromosome is made the telomere gets a little shorter as the replication process skips a few base pairs at the end of the replication process due to the nature in which the enzymes bind and in the direction in which they replicate.[32] If a cell reaches the point where telomeres are depleted and some of the genetic material is destroyed, no further replication can take place and the cell either dies or undergoes apoptosis. Telomerases are enzymes which counter this shortening, lengthening the amount of times a cell can divide to produce daughter cells. In somatic cells, however, the level of telomeres is very low or non existent, making any type of somatic cell mortal - meaning that at some point the division of cells will stop and the cells will die. The only cells in which high levels of telomerases are present are stem cells and cancerous cells.[32] Over 90% of human cancers have some telomerase up-regulation or gene mutation. These cells are immortal in the sense that they can keep on dividing as long as they are provided with nutrients and other such physical constraints.

1.2.1 Cancer and apoptosis

Apoptosis is a process in which a single cell is killed for the greater good of the organism.[31] Apoptosis is triggered mainly through two separate pathways.[30] The two pathways are initiated either through external cellular signalling or by signalling on the mitochondrial surface.[30] Many factors affect these signalling membrane bound enzymes, all are affected by different kinds of external and internal stresses placed upon the cell. Apoptosis can be initiated through many pathways, including activating caspases, a collection of cysteine proteases that bring about the termination.[30] These caspases are activated by proteolytic cleavage, and are always expressed in the cell in the inactive form. Initiator caspases are the caspases that activate other caspases that bring about cell death (cleavage of all the macromolecules found in the cell), these affected caspases are called effector caspases. Suppression of apoptosis creates the perfect environment for gene instability and allows mutated cells to flourish and grow, becoming independent

from external signals and resisting immune based destruction.[30] Interestingly cancers do not have a large number of caspase gene mutations and as such can still undergo apoptosis, the critical point is the activation of these caspases.[30] Apoptosis can be brought about through extensive damage to DNA, heat shock and other cellular stresses such as oxidative stress. Therefore apoptosis is the target for drugs and other therapies and its induction is one that needs careful attention when designing these treatments.[30]

1.2.2 Platinum containing drugs

The widely used anti-cancer drug cisplatin, showing in Figure 1.4 is cytotoxic to cancerous cells and has been used for decades in the fight against cancer. Cisplatin was first described in 1845 by Michele Peyrone and was known as Peyrone's salt.[33] The structure of the complex was not known until 1893. In 1965 it was noted that a soluble platinum complex generated from a platinum electrode in an electrophoresis reaction caused bacteria to grow unusually large, the ability to divide was inhibited by the platinum complex.[34] The medical importance of platinum complexes was thus first noted and research initiated into the biological impact of platinum. In 1969 a report was published by Rosenberg *et al.* detailing the effect of some platinum compounds on cancer cell growth in rats.[35]

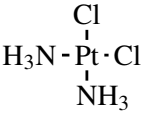


FIGURE 1.4: Cisplatin

Cisplatin was then later approved by the FDA (U.S. Food and Drug Administration) and has been used extensively in the treatment of cancer.[36] Cisplatin does, however, show many side effects and is not very specific in targeting cancerous cells only, but does affect the normal and healthy cells in the human body that are rapidly dividing. The mode of action is targeted cell death or apoptosis. In this process the cell is unable to function due to irregularities in the regulation of proteins, integrity of DNA and metabolites. Platinum containing compounds induce apoptosis by activating signal transduction pathways in the cell.

Platinum containing complexes damage the DNA by preferentially binding to nitrogen atoms found in DNA. This leads to further reactions resulting in DNA damaged. Platinum complexes also produce reactive oxygen species which place the host cell under oxidative stress and leads to further chances of the induction of apoptosis. Necrosis also occurs in cells in patients undergoing treatment, causing cell contents to be dumped into general tissue and causing most of the side effects associated with chemotherapy, such as nausea and vomiting. Drug resistance in tumour cells leads to rampant growth of tumours and spreading throughout the body as other local cells weakened by the platinum poisoning in the treatment are unable to suppress the advancement of the disease. The mechanism of this resistance can be found in the increased production of cellular thiols which bind strongly to the platinum, as well as increased DNA repair rates due to increased production of DNA repair enzymes. Both effects show increased transcription due to activation of certain areas of DNA.[37]

There are a number of other platinum complexes that have been approved for cancer treatment and are shown in Figure 1.5. However, they do not show the same activity as cisplatin and are often used in a combination treatment with cisplatin.[37]

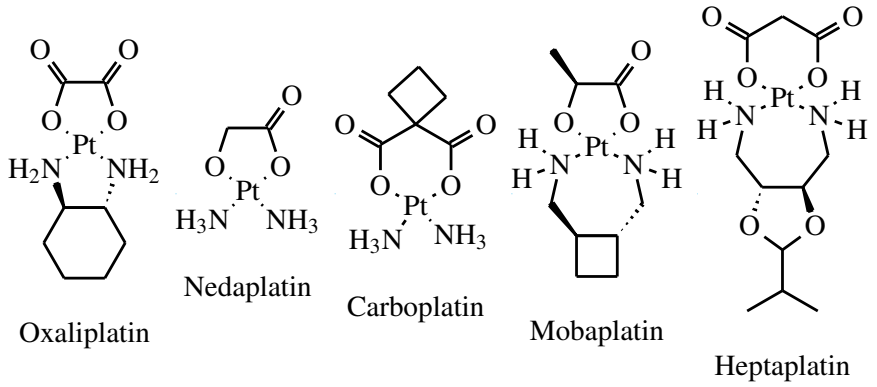


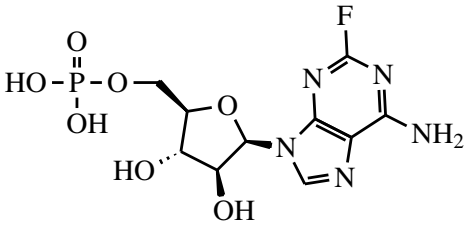
FIGURE 1.5: Platinum based chemotherapeutic drugs

1.2.3 Organic based cancer treatments

Platinum compounds have been used in over 50% of cancer treatments since 1978 when cisplatin was approved by the FDA. Other forms of treatment for cancer include complex organic compounds, such as quinones that contain no metal atoms. One of the most potent classes of organic compounds are the anthracyclines.[38] This class of compounds was first isolated from *Streptomyces peucetius* in the 1960s and posses a quinone unit as

well as carbohydrate moieties.[38] This family of compounds however induces cardiomyopathy and may lead to heart failure in the patient being treated.[38] The mode of action of this family of compounds has not yet been confirmed, however, there is evidence that the organic compounds result in free radical formation which leads to DNA damage and lipid per-oxidation.[38]

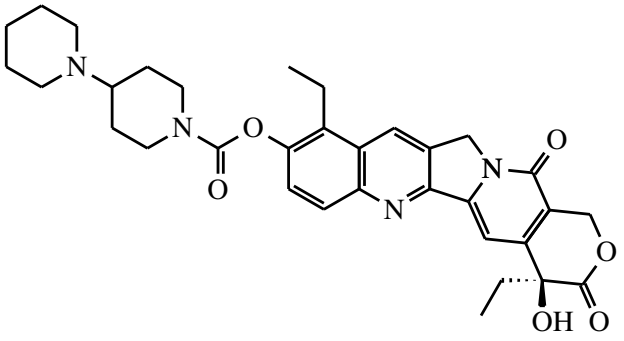
There are some general classes of organic anti-cancer compounds based on their activity. These include the antimetabolite fludarabine (**1** in Figure 1.6), alkaloid and terpenoid compounds, topoisomerase inhibitors such as irinotecan (**2** in Figure 1.7), tyrosine kinase inhibitors and lastly alkylating agents such as mechlororethamine (**3**) and and altretamine (**4**) in Figure 1.8. The method of action for altretamine is through N-demethylation by the release of formamide after oxidation of methyl groups by cytochrome P450.[39]



1

Fludarabine

FIGURE 1.6: Fludarabine, an example of an antimetabolite inhibitor



2

Irinotecan

FIGURE 1.7: Irinotecan, an example of a topoisomerase inhibitor

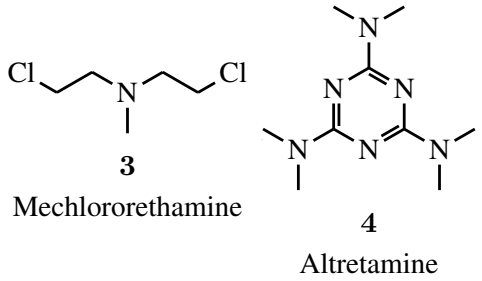


FIGURE 1.8: Examples of methylating agents

1.3 Protozoan parasitic diseases and their treatments (Malaria and African sleeping sickness)

Protozoa is the term used to describe single cellular eukaryote species.[40] The sicknesses known as malaria (caused by *Plasmodium* from the apicomplexan phylum family)[41] and African sleeping sickness (caused by *Trypanosoma brucei*)[42,43] are caused by these protozoa type species. Malaria in particular has been described as "the most deadly parasitic disease" with over 500 million people affected every year. There are over a million deaths annually and most of these are in the third world.[41,44,45] African sleeping sickness causes the deaths of thousands of livestock every year, particularly in places where they are kept in a subsistence capacity in Africa, Asia and South America.[43] Both of these diseases are brought about by blood sucking insects that act as carriers and it is during feeding that the transmission of these parasites occurs. These are now discussed in more detail in the following sub-sections.

1.3.1 Malaria

The infection of *Plasmodium* parasites

The life and infection cycle of malaria causing *Plasmodium* parasites is complex. The parasite starts its journey in the gut of the mosquito where it is in the sporozoite transmission stage. These oocysts release sporozoites which then enter the saliva of the mosquito and then when the mosquito feeds, enter the bloodstream of the host. The parasite has the ability to cross into and out of human cells through proteins on its surface together with special secretary organelles. Here the sporozoites travel to the liver and enter hepatocyte cells in which they then multiply until hundreds of thousands of merozoites are released into the blood circulatory system. These merozoites now

infect red blood cells, causing the erythrocytic replication cycle in which the symptoms of malaria are seen. Some of these merozoites form mature gametocytes which are then taken up by a mosquito. These gametocytes then mature to form gametes, and now take part in the sexual reproduction stage in which zygotes are formed. These mature into oocysts and the whole life cycle is then repeated.[41,46,47]

Therefore, in combating malaria there are many options for possible treatment. It is possible to control mosquitoes and prevent mosquito bites, or it is possible to treat the parasite within the host through the use of medicine.[44] The medical approach will now be further investigated.

Treatment of Malaria

The treatment of malaria has been something of a frustrated journey, as the parasite adapts quickly, especially in highly affected areas, and quickly becomes resistant to drugs used for treatment. This can be seen as a product of the sexual reproduction stage of the parasite in which genetic recombination occurs which gives the parasite great adaptability.[48]

The first known treatment for malaria was the bitter bark of the a high altitude tree (*cinchona*) found in South America, and has been used as a cure for fever since the late 1600s.[49] The isolation of quinine (shown in Figure 1.9) was performed in 1820 and has since received some attention, not for its medicinal properties, but for the mixing of gin and tonic, brought about by British soldiers in India who did not like the bitter taste of their medicine and subsequently mixed it with gin. It must be noted that Woodward and Doering completed the first total synthesis of quinine in 1944.[50]

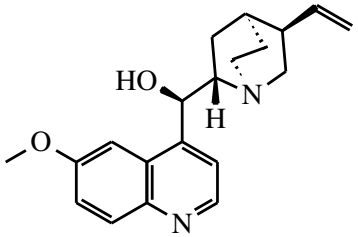


FIGURE 1.9: Quinine

The first synthesised commercially available drug for malaria was chloroquine, from Bayer and the structure is shown in Figure 1.10.

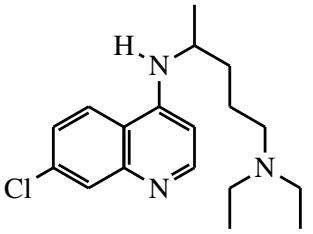


FIGURE 1.10: Chloroquine

After the introduction of chloroquine, resistance grew to the point where the drug is now considered ineffective in most malarial regions.[49,51] The mechanism of action of chloroquine is lysosome dilation through build up of chloroquine in lysosomes, affecting the pH and causing dysfunction.[52] Unfortunately chloroquine has a number of side affects and can be overdosed easily, giving the miracle cure from the early 20th century a great draw back. Interestingly, chloroquine triggers apoptosis with p53 acting as the signalling factor in human cells and has even been examined as an anti-tumour agent.[53]

The next fifty years saw the rise of the mixture sulfadoxine and pyrimethamine as well as mefloquine and artemisinin as anti-malarials (shown in Figure 1.11).[49]

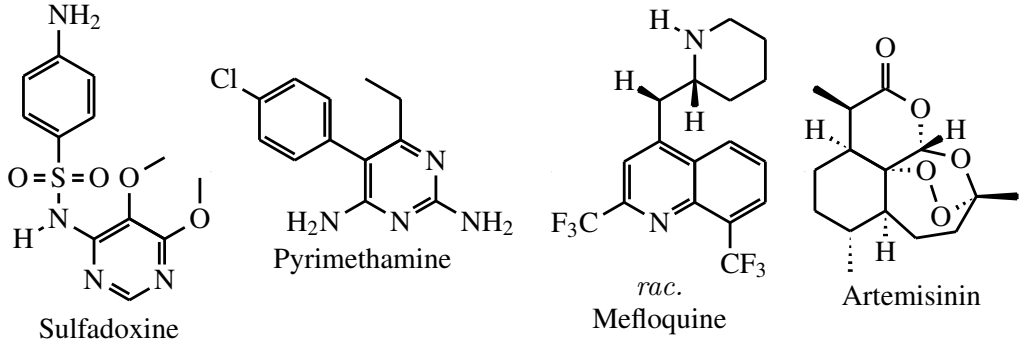


FIGURE 1.11: Sulfadoxine, Pyrimethamine, Mefloquine and Artemisinin

Sulfadoxine and pyrimethamine came into use during the early fifties, but resistance grew rapidly to the mixture as the parasites adapted and changed their enzyme active sites. Severe side effects also followed subsequent doses and the combination is no longer used in medical practice.

Mefloquine came in to use in the 1980s and is used in a preventative manner (malaria chemoprophylaxis), where the drug is taken for a number of days before entering a malaria area. The drug has found great use due to safety in pregnant women and small children, allowing for safe travel to malaria zones.[54]

Artemisinin is isolated from the plant *Artemisia annua*,[55] and currently shows the most rapid action against *Plasmodium falciparum*, which is the most lethal type of malaria.[56] Youyou Tu who discovered Artemisinin in her research towards finding anti-malarial agents received the Nobel prize in medicine in 2015, jointly with William C. Campbell.

Vaccination against malaria

Investigational stage vaccination against malaria has been found to be effective.[46] The vaccine includes modified late liver parasites. Genes are removed from these parasites and thus effectively stop any form of infection, but allows the human immune system to recognise the parasite and prevent future infections.

1.3.2 African sleeping sickness

The infection of *Trypanosoma brucei* parasites

Trypanosoma brucei and its two strains of parasite *Trypanosoma brucei rhodesiense* and *Trypanosoma brucei gambiense* cause the disease known as African sleeping sickness. It initially causes fever, joint pains and headaches; with progression leading to confusion, numbness and disruption of normal sleep and wake cycles due to the infection of spinal fluid. The infection initially starts in tissue surrounding the insect bite, and stays localised. The *Trypanosoma brucei* enters a stage of reproduction for a period of time and when numbers reach a substantial level they invade the blood stream where it spreads through the body. This is the first stage of infection, and the stage in which most drugs are effective and where the minor symptoms are presented. The second stage sees the *Trypanosoma brucei* crossing the blood brain barrier, and brain affecting symptoms are revealed.[57] The parasite releases several cytokines and other signalling factors that affect the surrounding somatic cells generating inflammation.[57]

The parasite is transmitted through the tsetse fly between human and animal hosts through blood feeding.[42,58] *Trypanosoma brucei* is characterised by short periods of outbreaks and long periods of inactivity. The time between feedings must be as short as possible for successful transmission of the parasite - the viability in the saliva of the fly is limited and time dependant. There are several life cycles that the parasite goes through,

however, this is mostly a transition between replication and transmission stages.[43] The changes include differences in the organelles of the cell, most notably through differences to the mitochondria.

Treatment of African sleeping sickness

The treatment of African sleeping sickness is difficult as it is one of the most neglected diseases; cases are few, diagnosis difficult, and treatment is not trivial and often is not administered effectively. The long life cycle of the parasite requires constant and continuous preventative action, which are often neglected during political instability, causing resurgence. The medicines used are old, and somewhat ineffective, and a search for new active drugs is urgently required.[58]

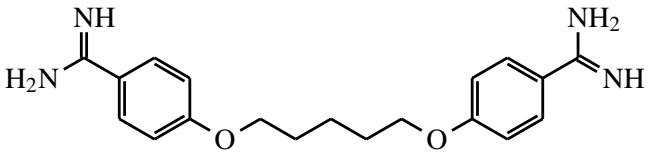


FIGURE 1.12: Pentamidine

Pentamidine as seen in Figure 1.12 is the standard drug for treatment of African sleeping sickness while the disease is still in its first phase. The drug has to be inhaled or injected, causing varying side effects which are very uncomfortable, including hypo-tension, headaches, hypoglycaemia, vomiting and myalgias through the release of histamine.[59–61] Diamidines were first studied in the late 1930s for their ability to act as synthetic insulin analogues and were then found to be active against a range of protozoa, but were found to be most effective against *Trypanosoma brucei gambiense* and have been been used ever since without the rise of major resistance. Diamidines such as pentamidine are selective because the drug accumulates in the protozoa, and not in somatic cells. This is due to the transport of various enzymes across the cell membrane, as an example the enzyme P2 aminopurine actively draws pentamidine into the cell and stops it from binding to its natural substrate adenosine. This leads to a higher concentration level in the infectious protozoa leading to death, even at an intracellular concentration of 1 mM.[61]

Another treatment, suramin as seen in Figure 1.13 is a naphthylamine containing compound with several amide linkages in a long poly-phenyl chain with several sulfonic acid

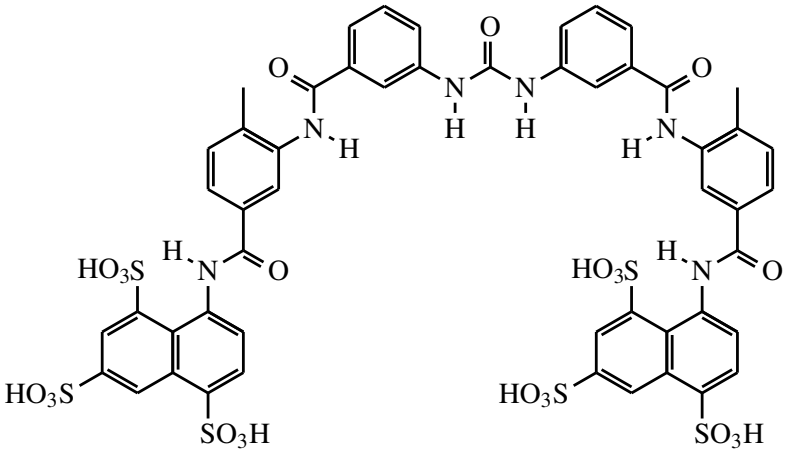


FIGURE 1.13: Suramin

functional groups first used in 1922. The family of compounds including trypan blue and trypan red, are not taken up by somatic cells, but are selectively taken up by the parasite *Trypanosoma brucei* - giving the drug its effectiveness and selectivity. Suramin binds to many proteins, because at physiological pH it has a six negative charge, causing very strong polar interactions. This stops the functionality of a range of proteins, giving it general toxicity once in the cell, leading to cell death. The drug, however, binds strongly to serum proteins, causing very slow release from the blood and can be detected after 3 months of administration. Due to very low membrane permeability the effectiveness of the drug is limited to the first stage of African sleeping sickness due to the inability of accessing neural tissue. Renal toxicity is a major drawback, leading to limited medical use.[62,63]

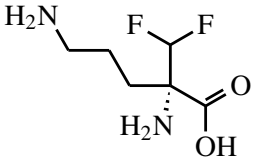


FIGURE 1.14: Eflornithine

Eflornithine as seen in Figure 1.14 was the first African sleeping disease drug registered in over 50 years when it came to the market in the late 1980s. The drug binds to ornithine decarboxylase, however, due to high turn over rates in the parasite the dosages need to be rather high and constant. A typical treatment would be 100 mg/kg (150 mg/kg for children) every six hours for a period of 14 days, making treatment very expensive. The drug is also removed from the blood very quickly, making this treatment difficult to administer. Even with all of these difficulties, the drug is useful enough to be used

in all the stages of the infection of *Trypanosoma brucei*, especially in the brain stage of the disease where many other drugs are ineffective and so has been used as a backup when other drugs fail or are ineffective. The drug has many cytotoxic side effects similar to that of anti-cancer chemotherapy, leaving it as a last resort. The drug allows the immune system of the host to effectively deal with the parasite and as such it has been shown that HIV positive patients have no benefit from the drug. The drug stops the production of poly-amines in the parasite which influences the signalling pathways of protein and DNA synthesis, therefore retarding cell growth and division cycles. This state causes vulnerability to the immune system, however it has been shown that the drug is ineffective in HIV patients for this reason.[63,64]

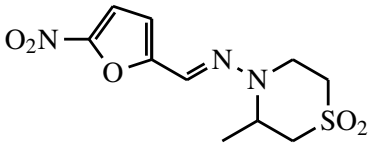


FIGURE 1.15: Nifurtimox

Nifurtimox as seen in Figure 1.15 is a prodrug that has been used for 40 years to combat Chagas disease and has recently been included in the fight against *Trypanosoma brucei* in the form of multi-drug combinations. The drug generates reactive oxygen and nitrogen species, killing parasites, but also causing general cytotoxicity and adverse side effects. The drug is mostly used in combination with eflornithine which has a much slower mode of action and is used in very late stages of the diseases when no other therapy proves effective. The prodrug undergoes reduction via nitrogen reductase generated nitroso compounds, that with further reduction go to the corresponding hydroxylamine derivative, or nitro radicals via a one electron reduction resulting in super-oxide anions and regeneration of the parent compound. Other possible reactive species are generated from the intermediates formed, these allow DNA damage and oxidative stress in cells causing terminal effects.[65]

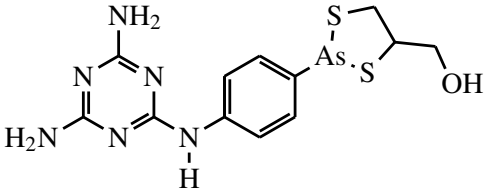


FIGURE 1.16: Melarsoprol

Melarsoprol as seem in Figure 1.16, an arsenic containing drug, is the first line of defence against the second brain stage of African sleeping sickness. The drug dissolves poorly in most solvents and as such is dissolved in propylene glycol and given intravenously (with pain experienced). The drug causes encephalopathy in some of the cases with a mortality rate of 50% in those effected. Other side effects include diarrhoea, vomiting, chest pains and maculopapular rash. A typical treatment lasts for at least 10 days with hospital stays that are up to 36 days, causing immense pressure on hospitals that are typically underfunded. The activity of the drug is due to non-selective binding to enzymes, causing disruption in cell function.[63,66]

1.4 Indoles and Carbazoles

1.4.1 Indole

Indole, a well known and extensively researched compound, is a common embedded motif found in many biologically active compounds.[67–75] Indole was first synthesised in 1866 through the reduction of oxindole by Baeyer and Knop and the structure elucidated by Baeyer and Emmerling in 1869.[67] Indole is important in the dye, flavour and fragrance industry as the core for many compounds. One of the important applications that came from the early 1900s is synthetic indigo, a valuable commodity in an era where blue dyes were rare and expensive. As an example, indigo gives jeans their typical blue colour. The structures of indole and indigo is shown in Figure 1.17.

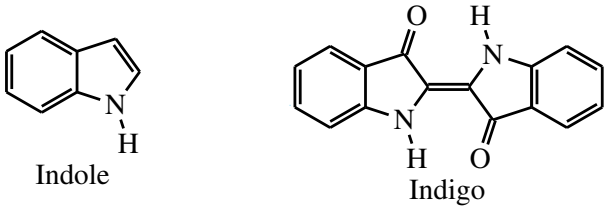


FIGURE 1.17: Indole and indigo

Indole is a central motif in the amino acid tryptophan, and so occurs naturally. Tryptophan is an important precursor in the biosynthesis of serotonin, a neurotransmitter important in the regulation of mood, sleep and appetite.[76] The structures of tryptophan and serotonin is shown in Figure 1.18.

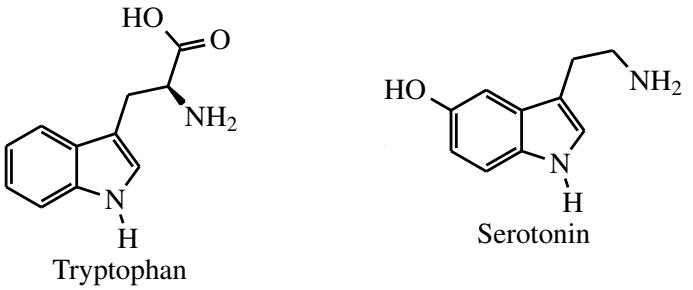


FIGURE 1.18: Tryptophan and serotonin

The biological activity of some indole containing natural products is varied as shown in Figure 1.19. Eudistomin-E was isolated from *Eudistoma vannamei* and showed cytotoxic activity.[77] The alkaloid Gelliusine-E is a marine natural product and shows antiviral activity as well as serotonin receptor binding.[78] The sea sponge *Chelonaplysilla sp.* isolated from a lake in Palau contained the indole Chelonin-A, which shows general anti-microbial activity.[79] Konbamidin, isolated from the sea sponge *Ircinia sp.* from Okinawa was synthesised by Shinonaga *et al.* from D-tryptophan, from which its biological synthesis is also derived.[80]

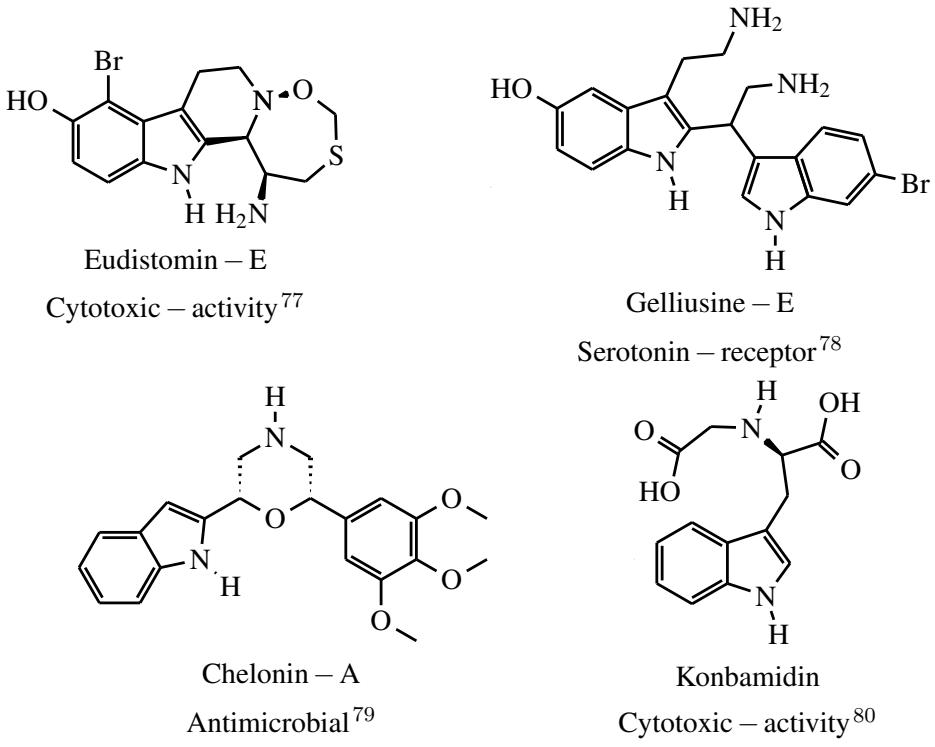
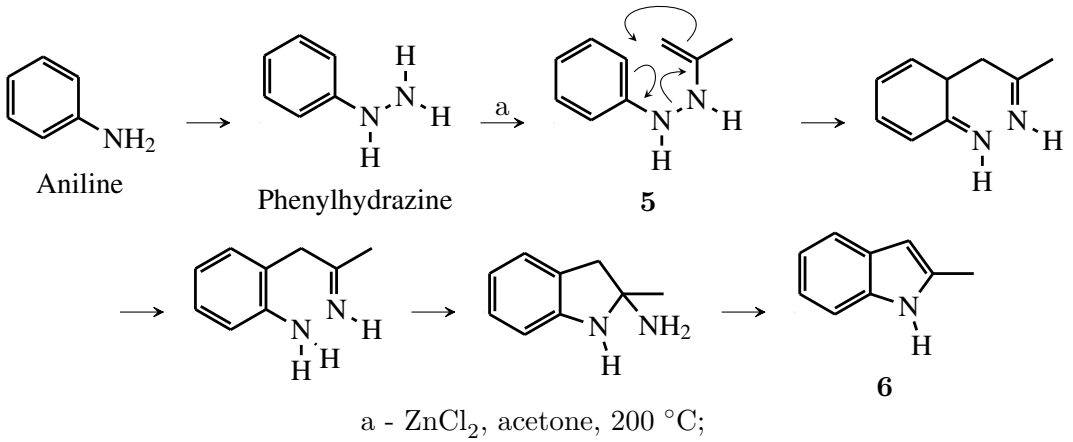


FIGURE 1.19: Indole containing natural products

The synthesis of indole has since received much attention. For instance the classical Fischer indole synthesis utilising aniline. The aniline is first converted to the hydrazine and coupled to the desired ketone, in this case acetone, which allows for the formation

of **5** as shown in Scheme 1.1.[67] This can then undergo a [3,3] sigmatropic rearrangement as the key step with a further elimination of ammonia to form **6** as substrate.



SCHEME 1.1: The synthesis of indole derivatives using Fischer methodology.[67]

Other methods used to synthesise indole has been developed and a brief summary is shown in Figure 1.20 showing the various names of the synthetic routes and bond disconnections, some of which will be discussed in the next section.[81,82]

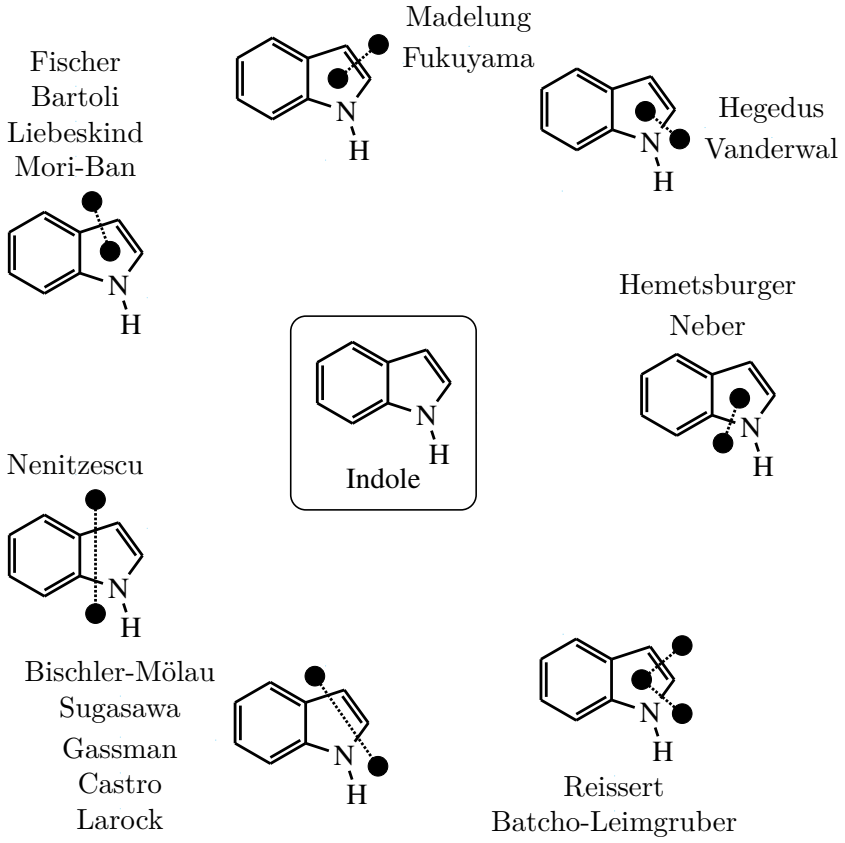
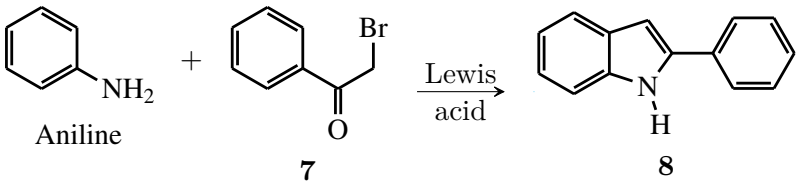


FIGURE 1.20: The synthetic routes towards indoles with the bond disconnections shown.[81]

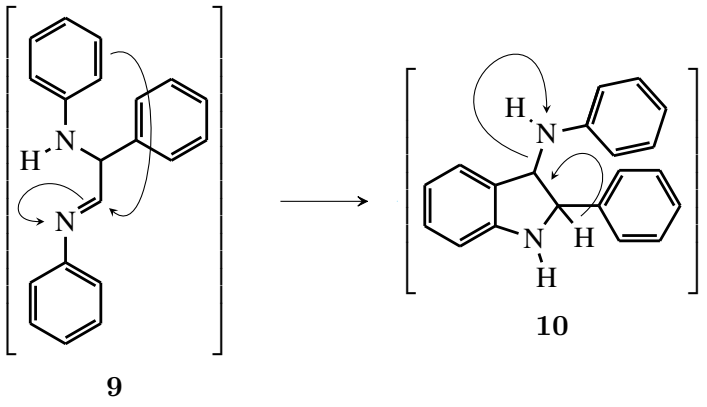
The synthesis of indoles has progressed further since the development of Fischer's method over a hundred years ago. A few critical syntheses will be noted in detail in the next few pages.

The synthesis of indoles by the Bischler-Möhlau indole synthesis route has been known since 1892 and is shown in Scheme 1.2.[83] A recent paper uses a microwave solvent free method, showing continuing development in this methodology.[84]



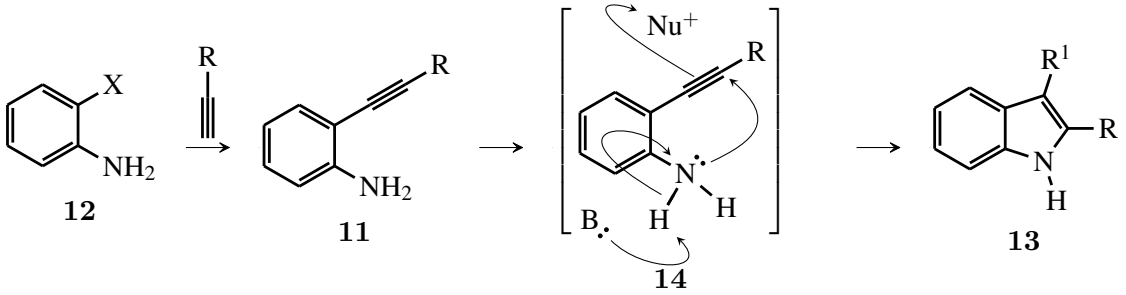
SCHEME 1.2: The synthesis of indole derivatives using Bischler-Möhlau indole synthesis.

The course of this reaction includes the addition of two anilines to **7** forming **9**. This is followed by a ring closing reaction of **9** which sees nucleophilic attack of the phenyl ring onto the imine (requires Lewis acid catalysis) followed by elimination of aniline from **10** to form the desired indole as shown in Scheme 1.3.



SCHEME 1.3: The mechanism of the Bischler-Möhlau indole synthesis starting after the addition of two molecules of aniline to **7**.

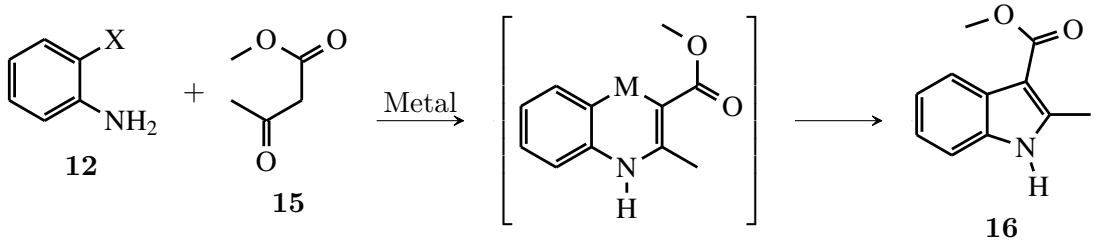
Several methods incorporating Sonogashira coupling reactions followed by a ring closure step of **11** from the halo-aniline **12** to form indoles **13** has been developed with the general synthesis shown in Scheme 1.4.[68–70,75] This Sonogashira type approach has generated a very large library of both alkyl and aryl 2,3 substituted indoles and is relevant in this thesis.



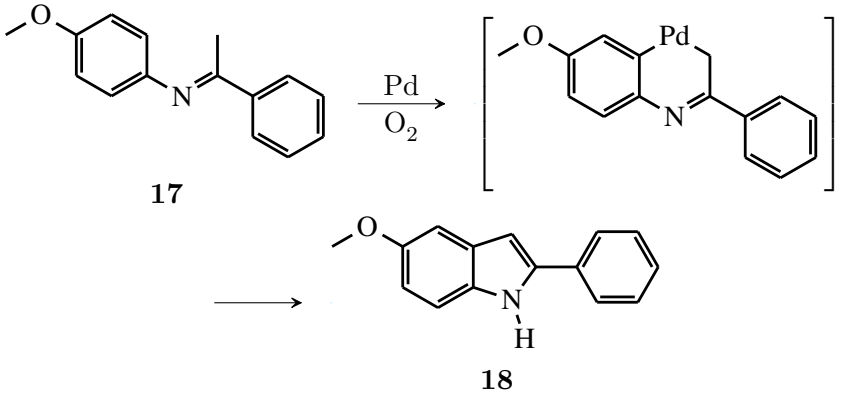
Nu = Nucleophile, B = Base or hydrogen acceptor, X = Br, I; R = Aryl, Alkyl; R^1 = H,[68] I,[69] Aryl (NH-TFA required)[75];

SCHEME 1.4: The synthesis of indole derivatives Sonogashira coupling methodology followed by several ring closure reaction methodologies.

The use of other palladium or other metal mediated processes is also common. These include the use of halo-anilines (**12**) coupled with carbanion stabilised carbonyl compounds such as **15** to form **16** as shown in Scheme 1.5.[70,73,85] Another example uses an oxidative process in which palladium oxidatively adds to **17**, followed by a C-H activation process and forms a metal carbon bond with **15**. The required indole **18** is then formed via a reductive elimination process as shown in Scheme 1.6.[72]



SCHEME 1.5: The synthesis of indoles using oxidative addition of anilines together with stabilised carbo anions containing carbonyl functional groups.[70,73,85]



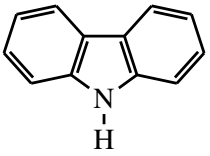
SCHEME 1.6: The synthesis of indoles using palladium catalysed oxidative ring closure methods.[72]

Some other methods for synthesising indoles include the rearrangement of fluorine substituted aniline based imines,[86] and the condensation of substituted propargyl alcohols

and substituted anilines with zinc triflate as catalyst.[71]

1.4.2 Carbazole

The carbazole class of compounds is based on indole, and contains an extra fused benzene ring. The synthesis and biological activity of carbazoles have been studied in great detail with many different synthetic approaches being utilised.[86–95]

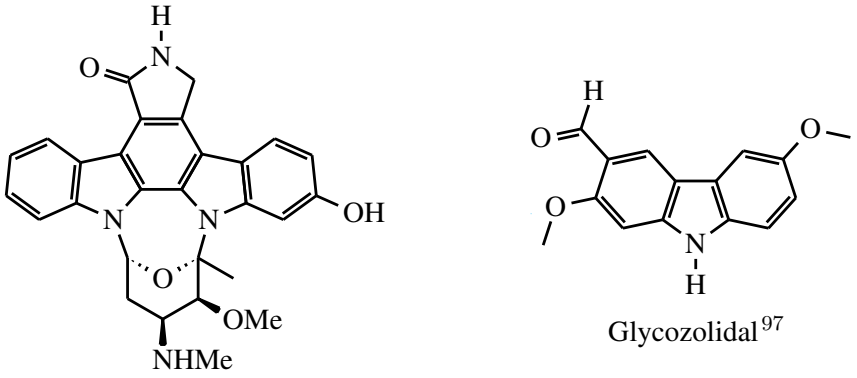


Carbazole

Carbazoles form a part of a rich group of natural products that have been isolated and show interesting biological activity as shown in Figure 1.21. Staurosporine, isolated from *Streptomyces staurosporeus*, has generated a large amount of interest from synthetic chemists due to its general biological activity and has been synthesised utilising various methods.[96] The alkaloid Glycozolidal was isolated from the root of *Glycosmis pentaphylla*, which is known for its rich library of carbazole compounds.[97] The carbazole family of ellipticines are topoisomerase inhibitors, which is important in tumour cells, with Celiptium as an example.[94] Mahanimbilol is a carbazole with anti-HIV activity with an IC_{50} of 23.0 μg/ml.[98]

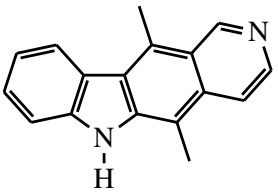
At the forefront of carbazole synthesis is Knölker, who has developed several novel methodologies for the synthesis of carbazole natural products.[87,99–101] Amongst the strategies developed is a novel method using an iron mediated process as shown in Scheme 1.7 for a typical case.[101] This process takes an aniline to the carbazole through a reactive η^4-hexadiene iron complex (**19**) which reacts with **20** to form **21**, followed by spontaneous dehydrogenation allowing the final ring closure of the five membered ring and the final aromatisation by de-metalation forming the carbazole.

Another popular method is the Buchwald–Hartwig coupling of an aniline (as an example **22** with **23** to form **24**) followed by oxidative cyclization with palladium and air, forming **25** in this example as shown in Scheme 1.8.[87,95]

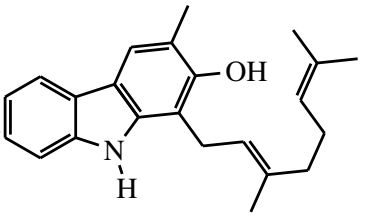


Staurosporine[96]

Glycozolidal[97]

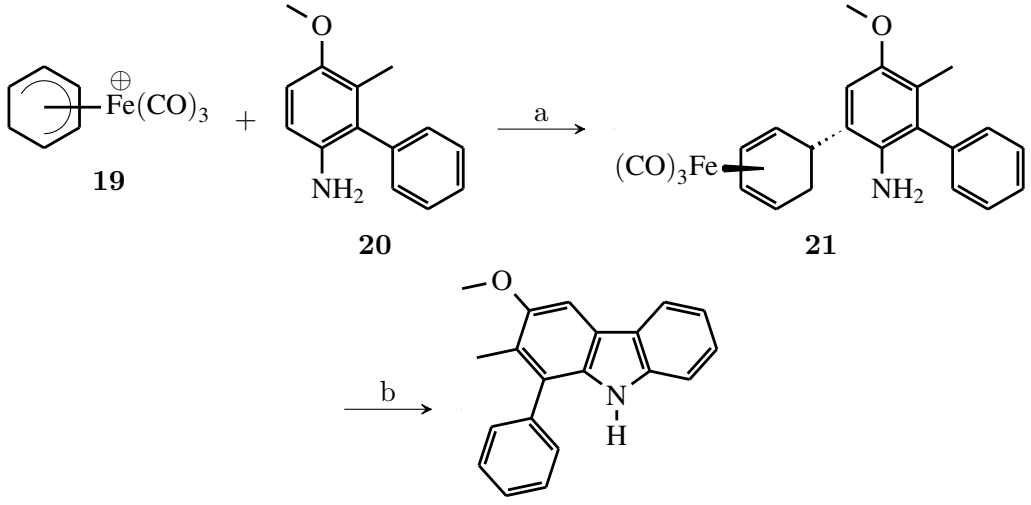


Celiptium[94]



Mahanimbilol[98]

FIGURE 1.21: Carbazole natural products



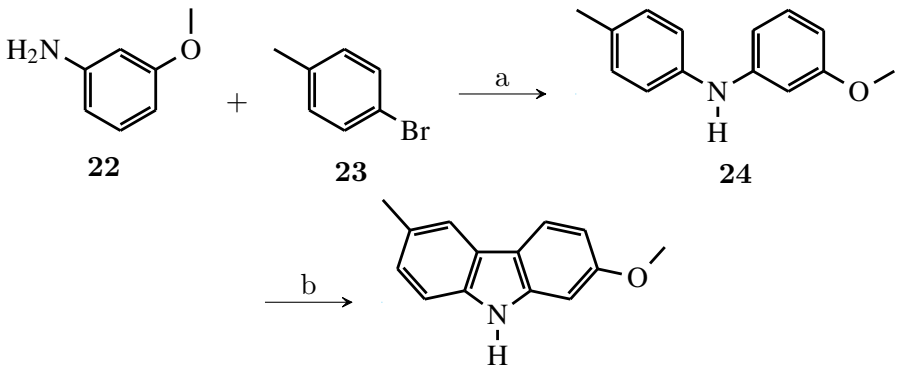
Hyellazole

a - MeCN, 82°C; b - (i) Cp_2FePF_6, DCM, Na_2CO_3 (ii) Me_3NO, Me_2CO (iii) MeI, K_2CO_3, Me_2CO

SCHEME 1.7: The synthesis of carbazole alkaloid hyellazole using Fe mediated coupling and ring closure strategy.[99]

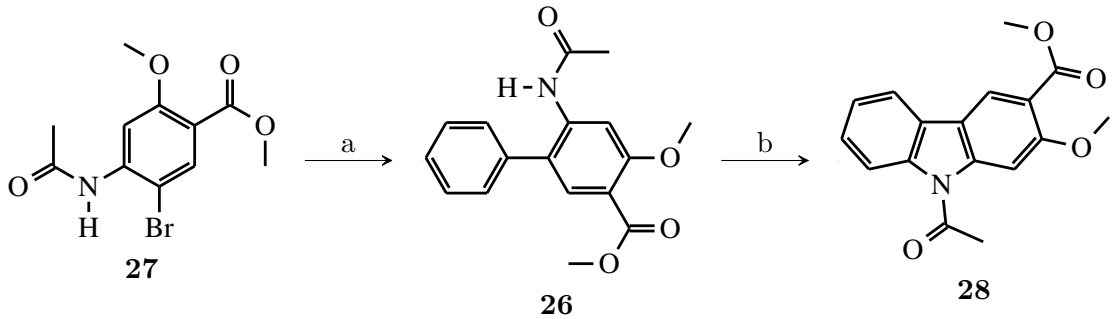
Another approach is to first form the biaryl bond through Suzuki coupling (**26** from **27**) and then through oxidative palladium coupling the aryl-hetero bond in compound **28** is formed as shown in Scheme 1.9.[87]

Other approaches to forming the carbazole will receive a brief mention. The double



a - $Pd(OAc)_2$, BINAP, Cs_2CO_3, toluene; b - $Pd(OAc)_2$, $Mn(OAc)_3 \cdot 2H_2O$, pivalic acid, air

SCHEME 1.8: The synthesis of carbazoles using palladium chemistry through Buchwald–Hartwig coupling of an aniline followed by oxidative cyclization with palladium, copper as co-oxidant and air.[87]

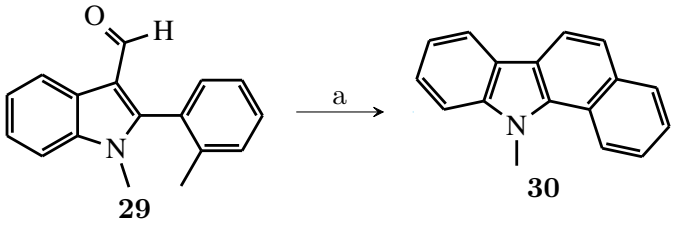


a - $Pd(PPh_3)_4$, $PhB(OH)_2$; b - $Pd(OAc)_2$, CuI, O_2

SCHEME 1.9: Carbazole synthesis through Suzuki coupling followed by oxidative cyclization.[87]

Buchwald–Hartwig coupling reaction approach has been developed that reacts a 2,2'-dihalo-biaryl compound with a primary amine to yield the carbazole.[87,102] The Heck approach is also used in which the palladium oxidatively adds to an 2-(2-halo-phenyl)-phenyl amine and adds across the double bond of the aromatic system on the second ring, in some cases the two rings are joined by Buchwald–Hartwig coupling.[87,103] A *t*-BuOK and light mediated ring closure method has been developed in which an indole (**29**) is transformed into the corresponding benzo[*a*]carbazole (**30**) as shown in Scheme 1.10.[88,89,91] This reaction will be discussed in greater detail in Chapter 2.

It can thus be seen that many strategies have been found to be effective in the synthesis of carbazoles.



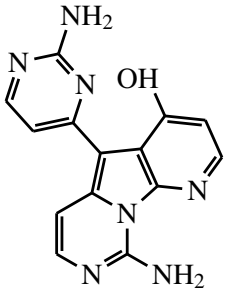
a - DMF, hν, *t*-BuOK

SCHEME 1.10: The synthesis of benzo[*a*]carbazole through a light mediated ring closure reaction

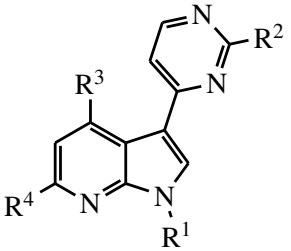
1.5 Azaindoles

Azaindoles are similar in structure to indoles. They are characterized by their inclusion of a nitrogen atom in the six membered ring. This pyridine nitrogen atom is a hydrogen bond acceptor giving it the ability to form hydrogen bonds with biologically active molecules such as enzymes. Investigating the biological activity of 7-azaindoles will therefore generate new insight and will perhaps give some potentially active and selective agents which can lead to further development of biologically active molecules.

The natural occurrence of azaindoles in nature has been documented. The variolins are examples of such natural products as illustrated in Figure 1.22, with the meriolins being a group of compounds which stem from variolins.[104,105] These compounds show powerful kinase binding activity and are strong candidates for any diseases (including that of cancer) that can be combated with this kind of approach.



Variolin – B

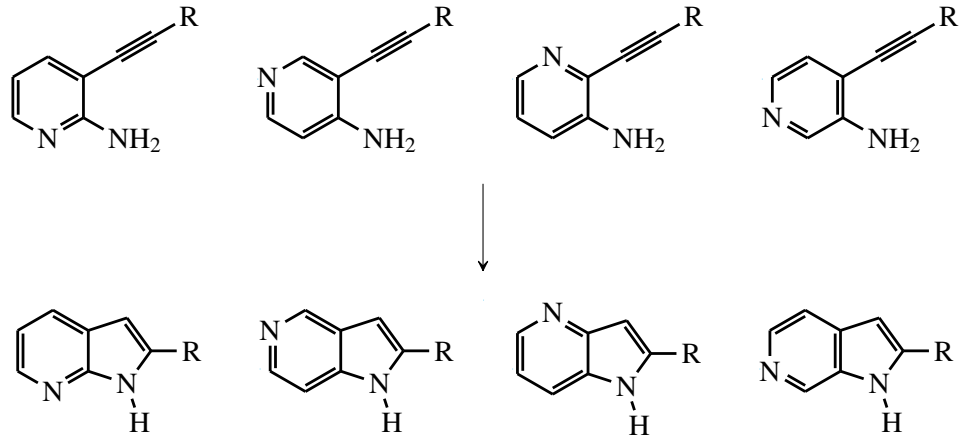


Meriolins

FIGURE 1.22

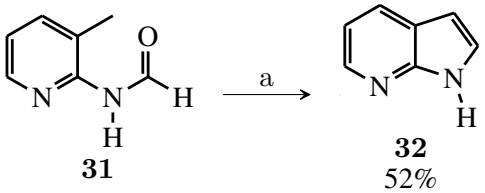
The synthesis of azaindoles is well developed.[106–113] The presence of an electron deficient pyridine ring as compared to indole changes the synthetic routes towards azaindoles significantly. The synthesis of azaindoles generally start from aminopyridines. A common method of ring closure is the nucleophilic attack of the nitrogen atom of the amine

on aminopyridines on an adjacent triple bond system introduced by Sonogashira coupling.[109–111] Often a base is required for the reaction to occur *t*-BuOK is often employed. A general scheme showing the formation of a range of azaindoles from the corresponding acetylene and amine containing pyridines is shown in Scheme 1.11.



SCHEME 1.11: Base catalysed ring closure to form azaindole cores from the acetylene substituted pyridine through the use of heat in the presence of a strong base such as *t*-BuOK

Several other methods utilise a strong base where the acidic methyl group on position 3 of the pyridine is utilised. For example, Robinson and Robison used the base sodium ethoxide together with **31** to form **32** as shown in Scheme 1.12.[113] The addition of the nucleophile to the carbonyl of the amide of **31** is followed by the spontaneous elimination of water to afford 7-azaindole **32**. An alternative method is that of Davis *et al.* who used excess LDA in the presence of **33** and **34**.[112] The condensation to form **35** follows as result as shown in Scheme 1.13. The mechanism includes a double lithiation by subsequent nucleophilic attack on the nitrile on **34** to form **36**.

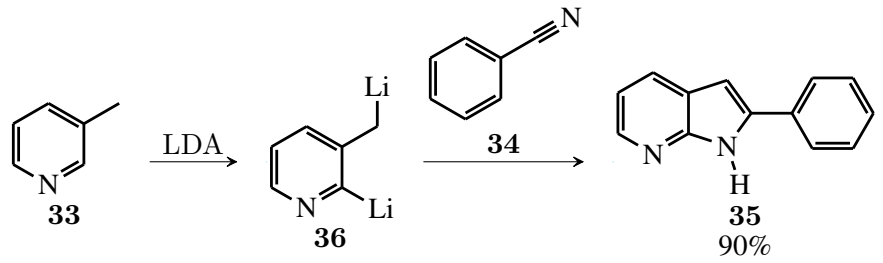


31 **32** 52%

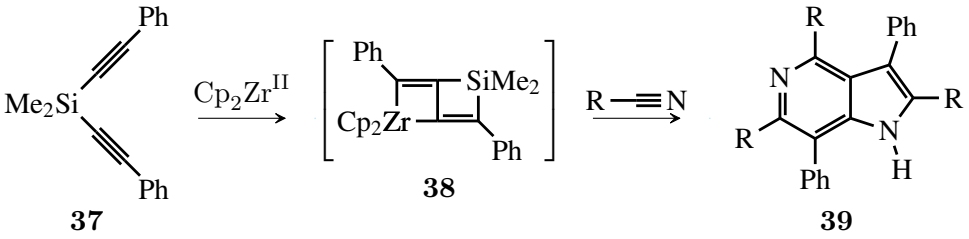
a - Sodium ethoxide

SCHEME 1.12

A zirconocene mediated ring closure reaction used by Sun *et al.* was shown to be effective in the synthesis of substituted 6-azaindoles from the bis-acetylene **37**. On reaction with $CpZr^{II}$ forms a zirconacyclobutene-silacyclobutene fused ring intermediate **38** which reacts further with nitriles to give the 5-azaindole **39** as shown in Scheme 1.14.[107]



Scheme 1.13



Scheme 1.14

1.6 Azacarbazoles and α-Carbolines

Azacarbazoles and carbolines are compounds in which a nitrogen atom is contained in the carbazole nucleus, in addition to that of the indole nitrogen atom. The position of the nitrogen atom can be determined from the name - α, β and γ, as shown in Figure 1.23 The compounds are widely found in nature and have a range of biological activities, making their synthesis an important area of research.

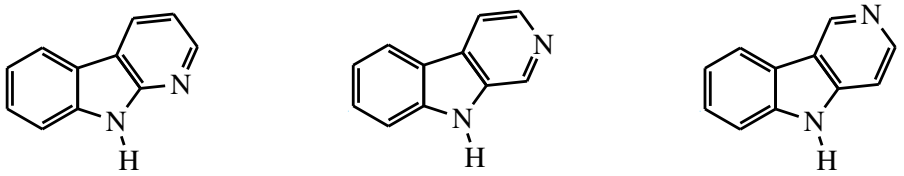


Figure 1.23

The biological activity of azacarbazoles in relation to many diseases including cancer, malaria and alcoholism has been studied.[106,114–117] Some of the active compounds studied are natural products and serve as cores for the development of other biologically active drugs. Some of the natural products discovered are shown below in Figure 1.24

The syntheses of these benzo-fused azaindoles are more developed and varied than those of the azaindoles.[106,108,114–122] Some of the earlier strategies for the synthesis of azacarbazoles involve using the Graebe-Ullmann synthesis.[119,120] The synthesis includes the formation of the triazole **40**, which upon heating, resulted in the release of nitrogen gas

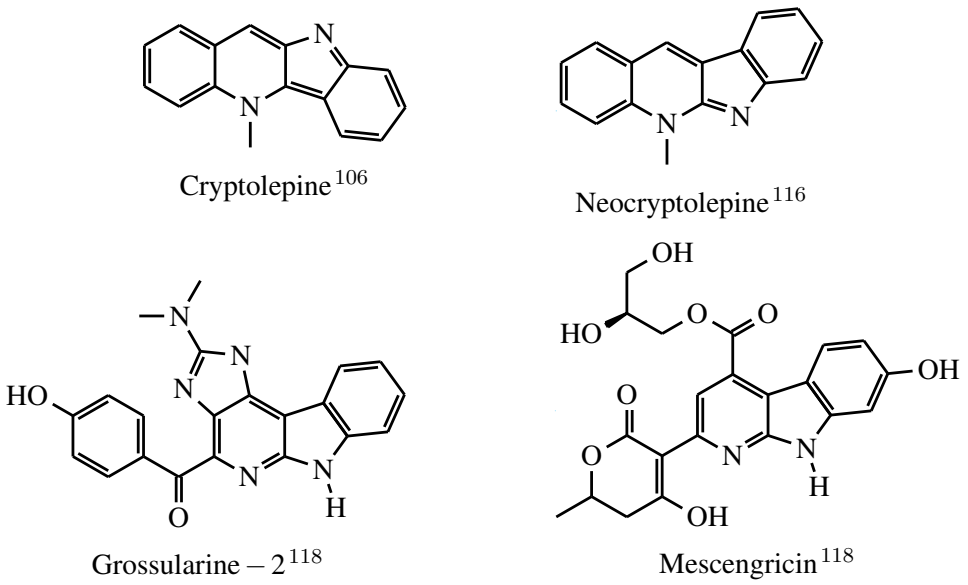
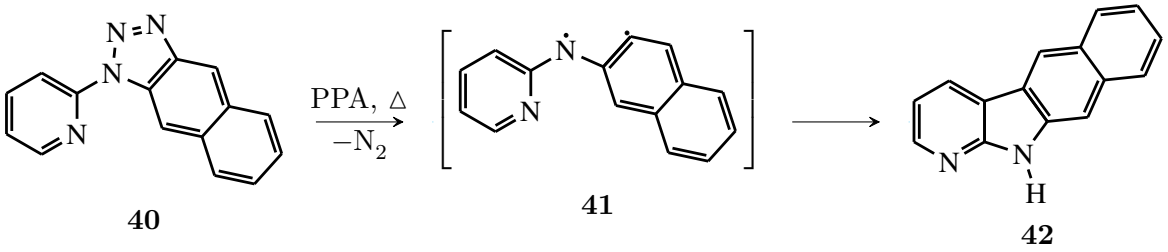


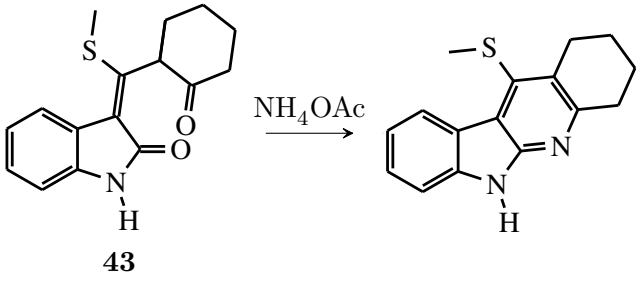
FIGURE 1.24

to form the intermediate biradical **41** which spontaneously undergoes a final cyclisation to form azacarbazole **42** as shown in Scheme 1.15. The range of compounds prepared using this methodology by Aukasz Kaczmarek showed significant anti-cancer activity.



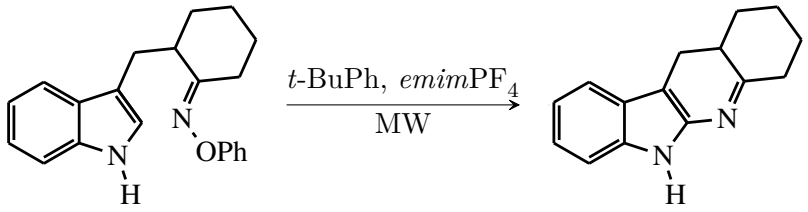
SCHEME 1.15

Bracca *et al.* used several methods in the synthesis of azacarbazoles. Other than the Graebe-Ullmann method Bracca *et al.* used a heterocyclization method in which oxindole **43** is condensed with ammonia as shown in Scheme 1.16.[119]



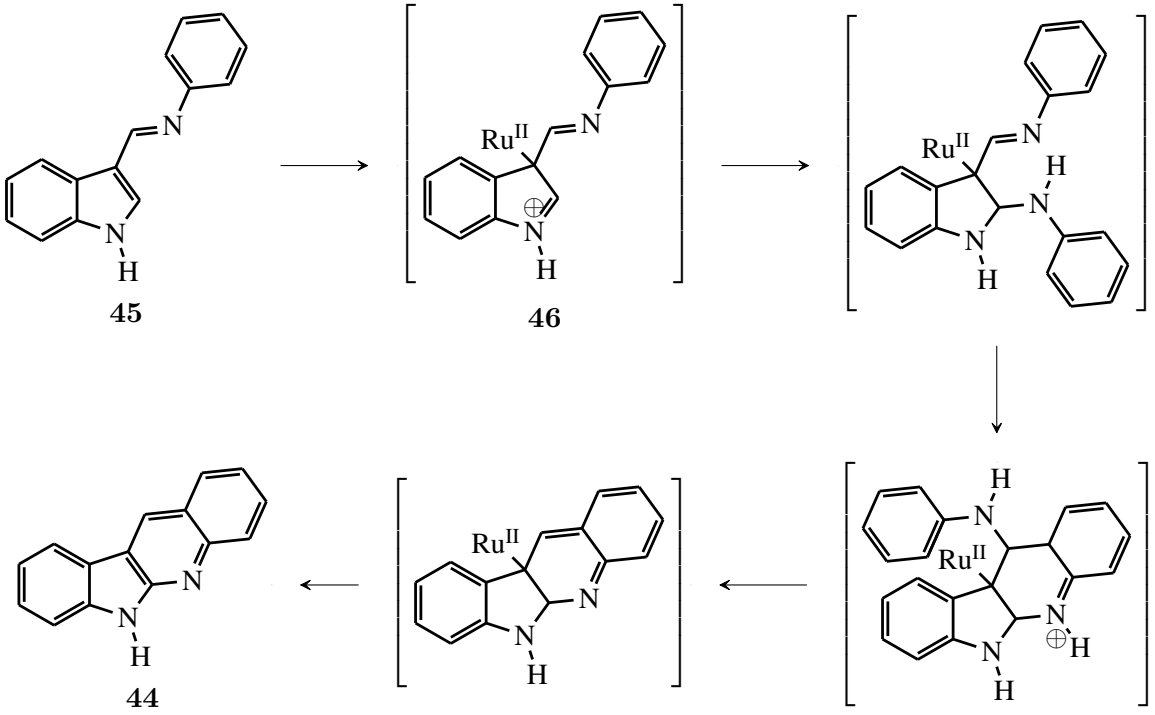
SCHEME 1.16

Bracca *et al.* employed a radical ring closing process as shown in Scheme 1.17.[119]



Scheme 1.17

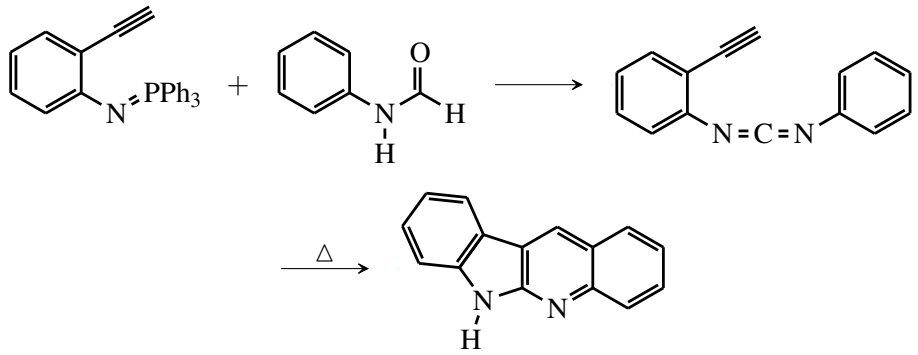
Another interesting method is the reaction of 3-formyl-indole with aniline to afford **44** in the presence of catalytic ruthenium as shown in Scheme 1.18. Mechanistically the imine **45** undergoes a reaction in which ruthenium adds to the indole double bond to afford **46**. This is then followed by the addition of aniline to the 2-position of the indole nucleus which is followed by cyclisation and hydrogen elimination reaction to ultimately lead to **44**.[119]



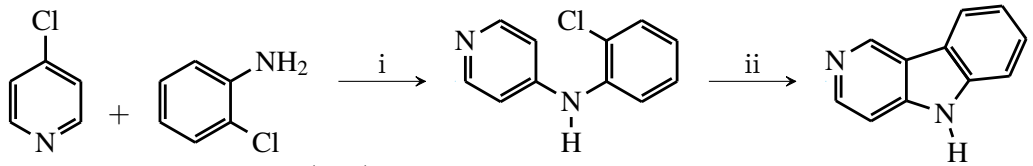
Scheme 1.18: The formation of **44** in a catalytic ruthenium reaction employing **45** and aniline

The azacarbazole nucleus can also be synthesised by using a novel aza-Wittig type reaction followed by ring closure with heating as shown in Scheme 1.19.[108,121]

Catalytic palladium based chemistry has found use in the formation of the azacarbazole nucleus.[106,116–118] As shown in Scheme 1.20, the Buchwald-Hartwig amination reaction, can be prepared using exotic phosphine ligands.



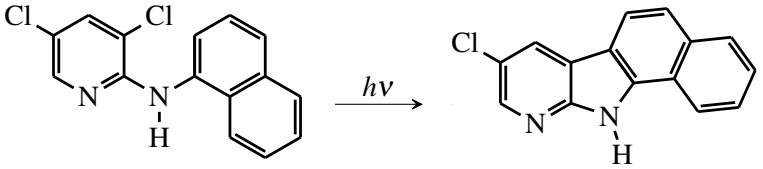
Scheme 1.19



i = $Pd_2(dba)_3$, Xantphos, $CeCO_3$, Dioxane, MW
ii = $Pd_2(dba)_3$, $t-Bu_3P$, DBU, Dioxane, MW

Scheme 1.20

Lastly, an interesting light mediated ring closure reaction was discovered by Frolov and Baklanov in which for example, the substituted pyridine **47** undergoes cyclisation in the presence of light to form azacarbazole **48** as shown in Scheme 1.21.[122] There are, however, only a few examples to illustrate the scope of the reaction.



47 **48**

Scheme 1.21

1.7 Project aims

The purpose of this PhD project is to develop novel methods for the synthesis of nitrogen containing heterocycles belonging to the azaindole and azacarbazole classes. However, it was also thought to be prudent to test a number of our synthesised heterocycles against the parasite of African sleeping disease and malaria as well as against cancer.

Malaria and African sleeping sickness are some of the most neglected diseases in our world today due to their prevalence in the third world in poorer areas where there is no

financial base to cover the costs of development and manufacturing of these drugs. A breakthrough in this field will help with the adaptability of malaria, its ability to gain quick resistance over medical treatments and *Trypanosoma brucei* where the treatments are difficult and tedious with long and painful treatment programs. We live in Africa, therefore we should make a difference on our own continent.

Cancer is another large research field where the focus is on more specific treatments that effectively remove all types of tumour cells. Current chemotherapy has many side effects, and some can even further DNA damage. A breakthrough in this field would transform the way we look at and diagnose cancer.

The 7-azaindole and α-carbolines nucleus was chosen as synthetic targets in this project because of the potential for biological activity due to the corresponding activity seen by their indole counterparts. The methodology required for their synthesis will follow the logic which carbazoles and 7-azaindoles have been synthesised and hopefully adapted to the synthesis of α-carbolines (Figure 1.25).[89,91,123] The novel approach undertaken in this study will give a range of available 7-azaindole and α-carbolines that will compliment those found in literature, as well show the versatility of key reaction steps. For example one key reaction would be the light mediated ring closure reaction to form the final α-carboline core which was discovered and developed at the University of the Witawatersrand. The study will include the synthesis of not only α-carbolines, but 2,2'-bis-7-azaindoles as shown in Figure 1.25 as coordinating ligands for metals. The coordination of metals to these nitrogen rich organic molecules will be attempted in order to improve their activity according to what has been seen when other hybrid molecules have been developed for their biological activity and selectivity.[124–130]

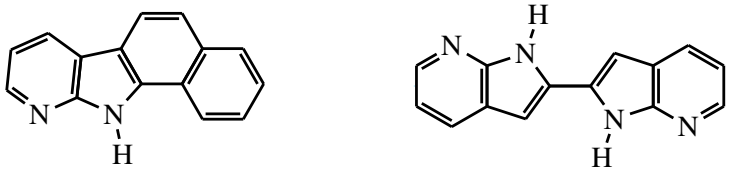


FIGURE 1.25: The target compounds of this study: α-carbolines and 2,2'-bis-7-azaindoles

Chapter 2

Synthesis of α-carbolines

2.1 Introduction

The literature survey of the synthesis and biological activity of indoles, carbazoles and azaindoles is covered in great detail in the introductory chapter of this thesis. It is clear that the synthesis of this class of biological compounds is of great interest and generating novel methods for their synthesis is critical.

α-Carbolines are the focus of this chapter, and their synthesis is described. α-Carbolines are similar in structure to carbazoles, with an added nitrogen atom as shown in Figure 2.1

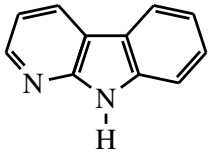


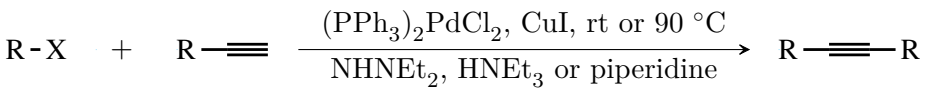
FIGURE 2.1: α-Carboline

2.1.1 Important reactions

The synthesis of α-carbolines in this project requires some important reactions. These reactions will be discussed in greater detail in this section.

The Sonogashira reaction - linking the many parts together

The use of palladium in C−C bond forming reactions has a rich history, spanning several decades and several Nobel prizes as reward for those who drove the development of this field.[131–133] The C−C bond forming reaction that will be focused on in this project is the Sonogashira coupling reaction as this reaction couples organo halides with terminal acetylenes. This reaction was first independently noted by several groups in 1975, however only Sonogashira *et al.* made use of copper as a co-catalyst.[133–135] The first example of this is shown in Scheme 2.1



R = Aryl, Alkenyl; X = I, Br, Cl, OTf;

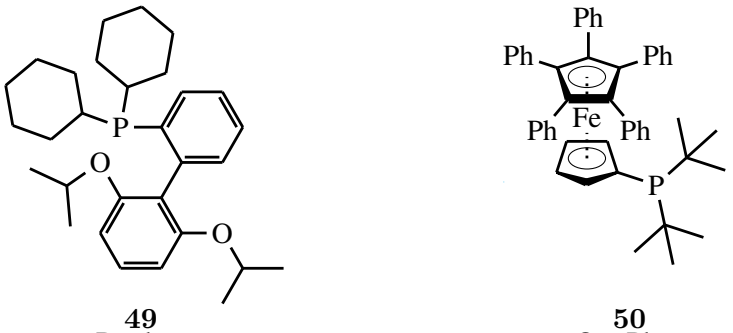
SCHEME 2.1: The first example of the copper catalysed Sonogashira reaction.[133]

For the next 30 years there was very little development of this reaction. Three problems plagued its use namely: the formation of homo-coupled products through oxidative dimerisation, the lack of catalytic systems that are active enough to use organo chlorides as substrates and finally the increase of TON (turn over number), which is a measure of catalyst stability.[131,133]

These challenges are discussed in detail in this chapter where these very issues plagued our synthesis of the desired Sonogashira coupling products.

Over the past two decades researchers have overcome many of these challenges by shifting to Heck catalytic type systems as this reaction does not require the copper co-catalyst.[133] However, this is not strictly the same reaction any more, as the mechanism of these reactions differ greatly. The Heck reaction relies on the migratory insertion of the alkyne, whereas the Sonogashira reaction relies on the transmetalation of the alkyne from the copper co-catalyst which readily reacts with terminal acetylenes.

Catalysts that are active enough for such catalytic systems employ the use of bulky ligands such as **49** and **50** phosphine ligands which are shown in Figure 2.2.[131,132,136]



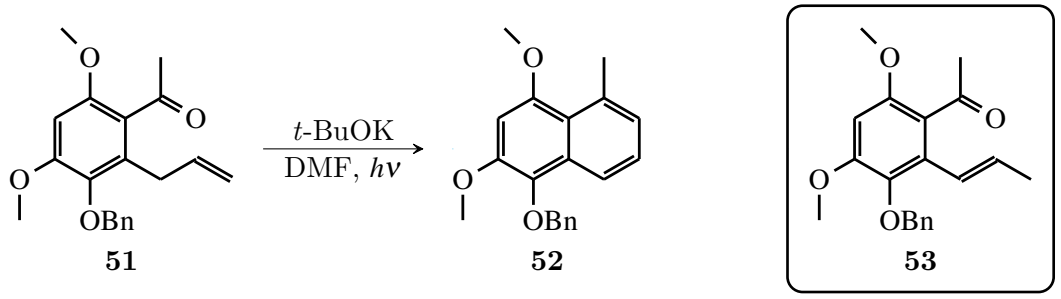
49
Ruphos

50
Q – Phos

FIGURE 2.2: HIgh performing ligands used in Sonagashira reactions

t-BuOK and light mediated ring closure - forming the final aromatic ring

At the University of the Witwatersrand the serendipitous reaction of 2-allyl substituted benzaldehyde **51** to form naphthalene **52** in 48% yield instead of forming the expected styrene **53** as shown in Scheme 2.2 was discovered when the reaction was left over night.[137] Failure in this case led to a new research area, and has been used to synthesise several fused aromatic systems. Interestingly it was found that using light influenced the reaction, increasing the yield to *56%* in this example.

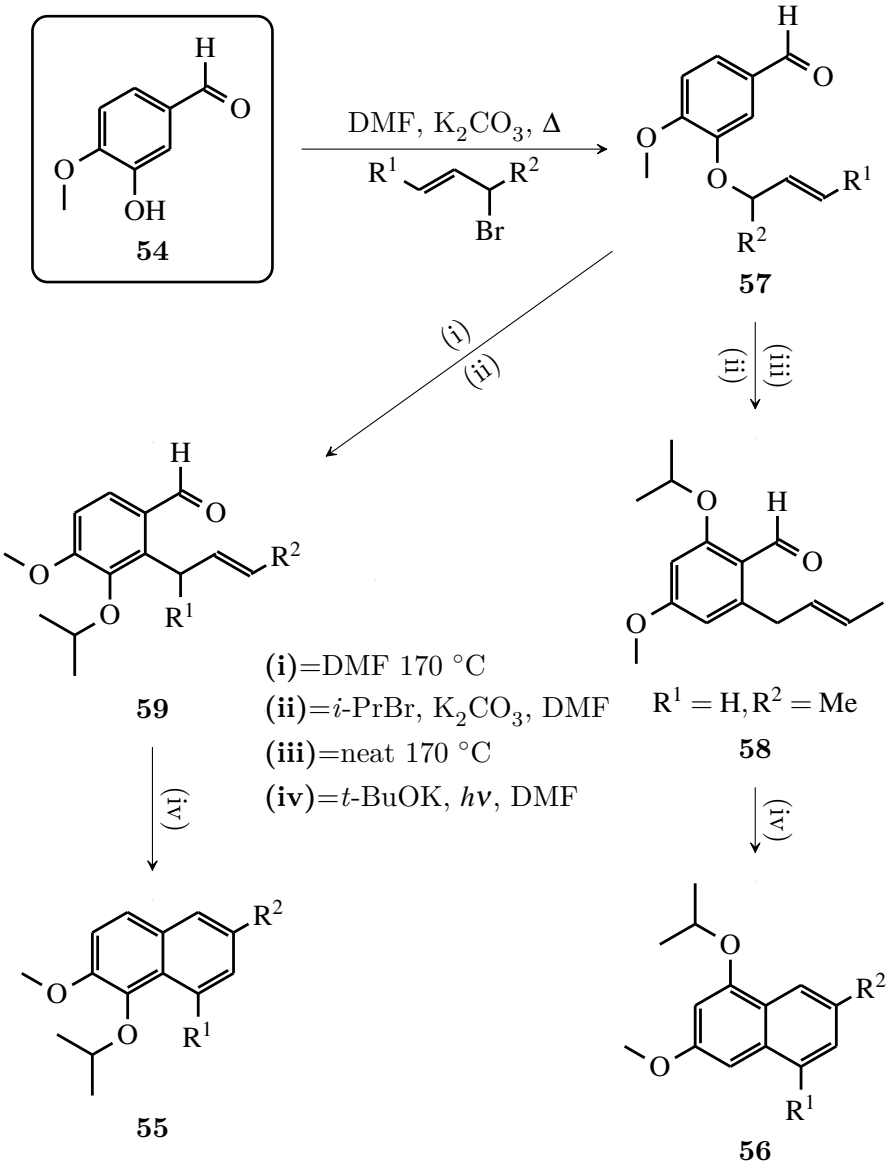


51 **52** **53**

SCHEME 2.2: The serendipitous discovery of *t*-BuOK and light mediated ring closure of substituted benzaldehydes to form naphthalenes.[137]

This novel process was then carried out on a larger library of compounds and a general method for synthesising naphthalenes from isovanillin was proven successful as shown in Scheme 2.3 where **54** is transformed into **55** and **56**.[137]

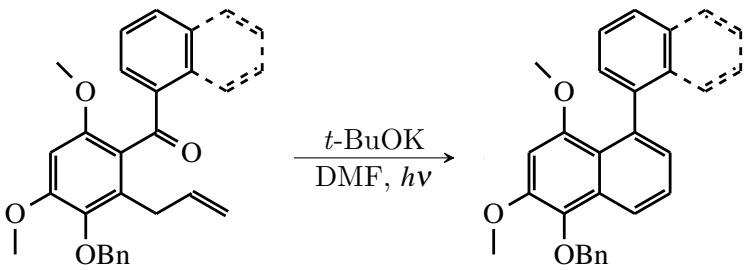
This is achieved by first functionalising the phenol of **54** with a substituted allyl group to form **57** which then further undergoes a Claisen rearrangement to form **58** and **59**. The Claisen rearrangement products differ due to different substituents on the allyl group. This was then followed by protecting the resulting phenol with an *i*-Pr group and performing the novel *t*-BuOK and light mediated ring closing reaction to yield the corresponding naphthalene products **55** and **56**.



SCHEME 2.3: A general method of the synthesis of naphthalenes from 3-hydroxy-benzaldehydes.[137]

It was also noted that ketones (**60**, **61**) could also be used as substrates as shown in Scheme 2.4 to form biaryl naphthalene products **62** and **63**.[137] The formation of a new biaryl axis through the formation of the new benzene ring shows the versatility of this reaction.

A subsequent paper showed an increased scope on this novel reaction, the allyl group was replaced with a tolyl group, which was shown to undergo the same ring closure in order to yield polyaromatic compounds such as phenanthrenes.[88] The reasoning was that a similar double bond system intermediate arises as in the allyl functionality series of compounds, which would then react further with an aldehyde or ketone as shown



60, 61 **62, 63**

SCHEME 2.4: The further scope of a typical *t*-BuOK light mediated ring closure including bulky ketone substrates.[137]

in Figure 2.3. The result was a novel method for synthesising phenanthrene products.

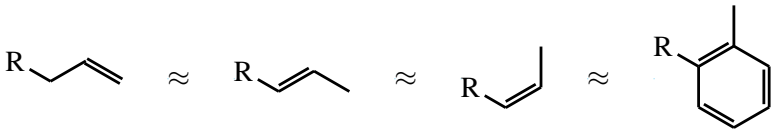
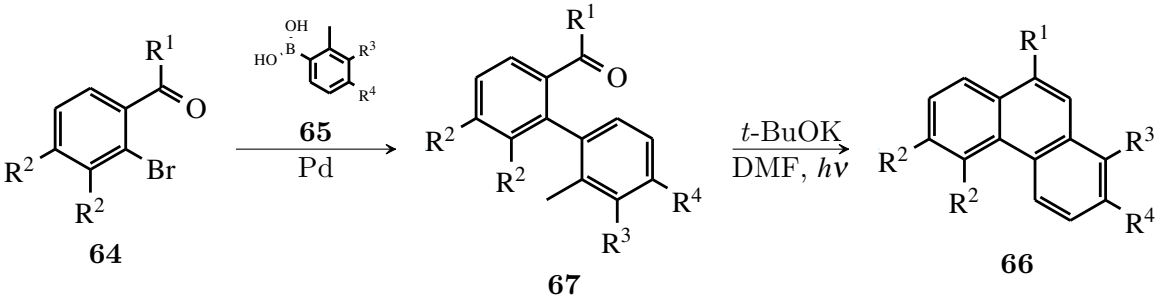


FIGURE 2.3: The similarity in using allyl and tolyl substrates in the *t*-BuOK and light mediated ring closure reaction.[88]

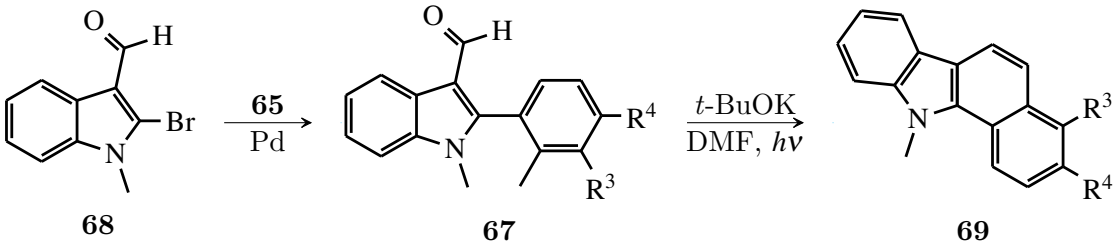
The general method for synthesising these o-tolyl-benzaldehydes start with the acetophenone bromide (**64**), which is then coupled to a boronic acid (**65**) through a Suzuki coupling reaction and lastly subjected to *t*-BuOK, light and DMF to form (**66**) as shown in Scheme 2.5.[88]



SCHEME 2.5: A general method for the synthesis of phenanthrenes.[88]

The scope of this reaction was then further expanded to the synthesis of benzo[*a*]carbazoles from indole as shown in Scheme 2.6.[88,89]

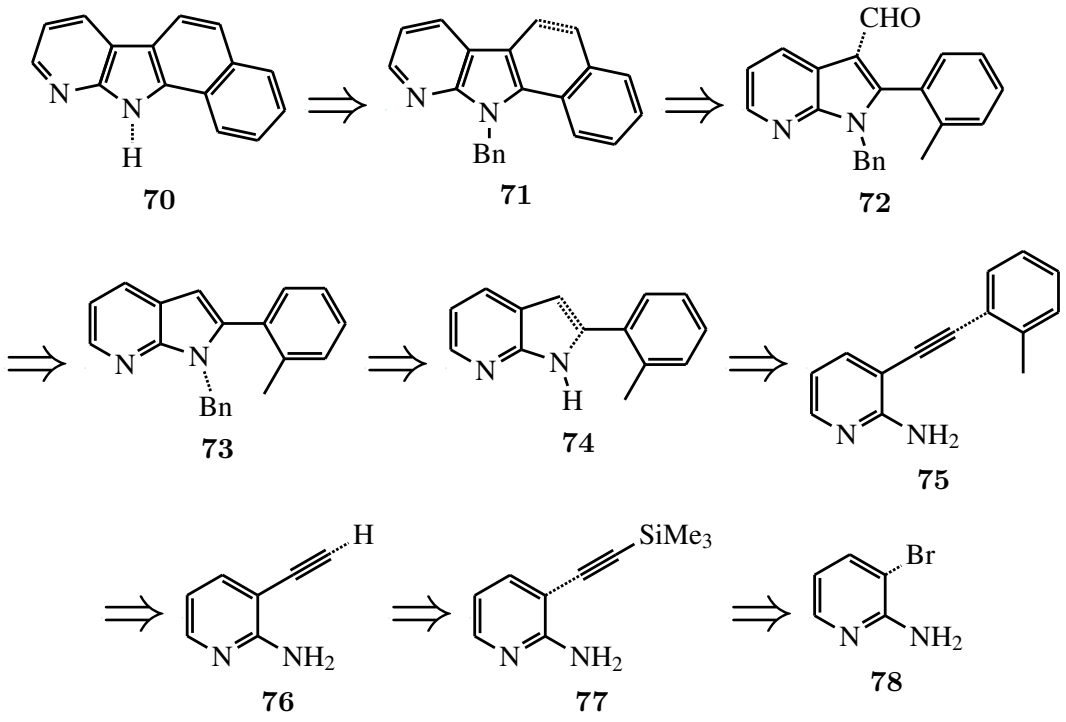
The expansion of this work to α-carbolines, the focus of this chapter, was therefore a novel concept and an important aspect to address in this PhD.



SCHEME 2.6: A general method for the synthesis of benzo[a]carbazoles.[88,89]

2.1.2 Initial synthesis plan

The initial synthesis plan of this project is built on previous work done on 7-azaindoles and benzo-fused carbazoles in our laboratories. The retrosynthesis is shown in Scheme 2.7.



SCHEME 2.7: The retro synthetic analysis of benzo- fused α-carbolines with bond dissociations shown with dashed lines

The retrosynthetic steps are based on methods we have used for the synthesis of benzo-fused carbazoles and 7-azaindoles.[89,91,123] The α-carboline core can be separated into two smaller fused units, namely a fused 7-azaindole and naphthalene core as shown in Figure 2.4. The breaking up of these two sub units with the reactions described allow us to synthesise the smaller precursors from 2-aminopyridine and methylbenzene.

α-Carboline **70** can be synthesised from α-carboline **71** by utilising a debenzylation procedure. The procedure chosen in this synthesis was that utilised in our laboratories

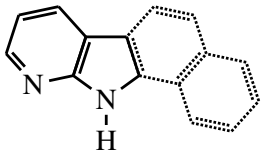


FIGURE 2.4: The two units of the desired α-carboline core, namely that of 7-azaindole and naphthalene

previously in the synthesis of carbazoles, namely through the use of $AlCl_3$.[89] We hoped the formation of the α-carboline core **71** could be achieved through a *t*-BuOK and light mediated ring closure reaction on azaindole **72**, as previously utilised in the synthesis of carbazoles from similar indolic compounds.[89] The formylation of azaindole **73** can be accomplished through the Vilsmeier–Haack reaction, again, as utilised by de Koning *et al.* in the synthesis of carbazoles from indoles.[89] The indolic nitrogen in position 1 requires a protecting group in order for azaindole **72** to undergo the light mediated ring closure reaction, and can be achieved through benzylation. Benzyl protected azaindole **73** can be formed from azaindole **74** by utilising a base and BnBr. The synthesis of the 7-azaindole core can be achieved through the use of an acid mediated ring closure method devised by Leboho *et al.* in our laboratories from the 2-aminopyridine core.[123] This ring closure reaction will attempt to transform 2-aminopyridine **75** into azaindole **74**. The methylbenzene functionality can be included through the use of a Sonogashira coupling reaction of 2-aminopyridine **76** and 1-iodo-2-methylbenzene. The triple bond bridge required to join the 2-aminopyridine and methylbenzene cores can be introduced by first coupling 2-aminopyridine **78** with ethynyltrimethylsilane to form 2-aminopyridine **77** through a Sonogashira cross-coupling reaction, followed by the removal of the silicon protection group through the use of TBAF to form 2-aminopyridine **76**.

2.2 Synthesis of the organic framework

Bromination and iodination of substituted 2-aminopyridines

The introduction of the acetylene functionality for the formation of **75** on the 2-aminopyridine starting material requires a halide from which the palladium can oxidatively add to and then introduce the acetylene. The halide used in this case is the bromine atom. Bromination on the 3 position of the 2-aminopyridines is needed for the acetylene to be in the correct position. Fortunately the amine on the pyridine is an *ortho* and *para*

director, which allows selective substitution on the 3 and 5 positions. It was decided to choose several starting materials that were substituted in the 5 position as to allow only substitution on the 3 position. The 2-aminopyridines substituted with a chloride and a methyl group on the 5 position were chosen. The reasoning behind this decision was to synthesise α-carbolines that were relatively electron poor with the chloride substitution, and relatively electron rich with the methyl substitution. Commercially available 3-bromo-2-aminopyridine was bought and used as a starting material to generate the most simple form of the α-carboline scaffold and to be used as a comparison in the different synthetic steps in relation to the chloride and methyl substituted intermediates.

It was also decided to functionalise the 2-aminopyridine with a bromide in the 5 position. This can only be done when an iodide is used as the oxidative coupling partner in the Sonogashira reaction later in the synthetic route as the iodide is magnitudes more reactive than the bromide in palladium catalysed reactions, allowing for no coupling to occur on the 5 position and and for the bromide to remain in place.

Bromination of 5-methyl-2-aminopyridine 2-aminopyridine and 5-chloro-2-aminopyridine by the use of Br_2 and NBS worked well with yields greater than 70% as shown in Figure 2.5 below. The more electron rich 5-methyl-2-aminopyridine showed higher yields as compared to 5-chloro-aminopyridine, as the increased electron density on the ring allows increased reactivity with bromine. The bromination of 2-aminopyridine, however, was a little more challenging as di-bromination could take place in both the 3 and 5 position. Dibromination was avoided by selectively reacting on the 5 position. The reaction was cooled down to 0 °C and 1 equivalent NBS (N-bromo-succinimide) was added slowly. The bromine atom in the 5 position of 2-aminopyridine **79** ensures that the subsequent iodination would be directed to the 3-position.

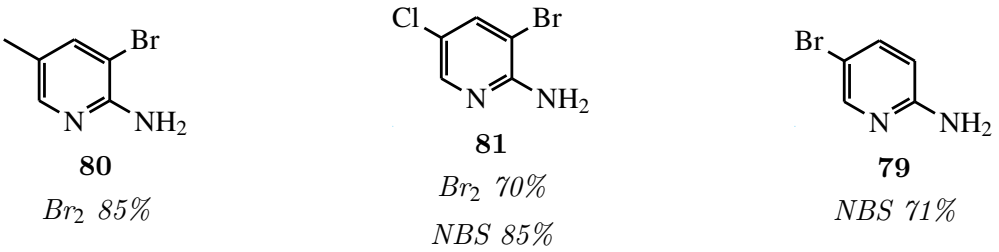


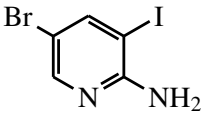
FIGURE 2.5: Bromination of 2-aminopyridines

Inspection of the ^{1}H NMR spectra of **80** and **81** showed the disappearance of an aromatic peak, with only two doublet peaks that have coupling of less than 2 Hz, which is in the

range of *meta* coupling. The ^{13}C NMR spectra showed 3 quaternary carbon sites, marked by much smaller peaks, showing that substitution occurred. The NMR spectra of **79** similarly showed the disappearance of an aromatic signal in the ^{1}H NMR spectrum, but in contrast to **80** and **81** showed three signals, two doublets (positions 6 and 3) and one doublet of doublets (position 4) and the appearance of another *ipso* carbon in the ^{13}C NMR spectrum.

The NBS showed better reactivity than molecular bromine, as is seen in the synthesis of **81** which had a deactivating chloride in the 5 position. It was found unnecessary to use NBS in the synthesis of **80** as the reaction with Br_2 proceeded satisfactorily.

Due to the poor electrophilic nature of iodine, it needs to be activated in order for direct iodination of aromatic compounds to occur. This is usually achieved through oxidation of the iodine and additives such as silver salts can be employed.[138] In our laboratories this proved ineffective in the electrophilic substitution of 2-aminopyridines.[111] It was found by Leboho that the mixture of iodic acid, KI and I_2 in strong acidic conditions at elevated temperatures was required for the direct iodination of 2-aminopyridines.[111] The iodination of **79** proved successful in this project, and **82** formed with a yield of 80% as shown in Figure 2.6.



82

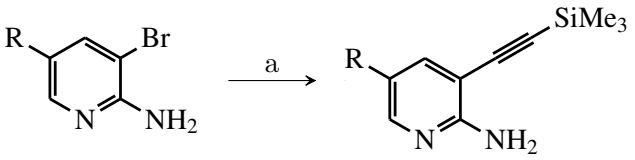
80%

FIGURE 2.6: Iodination of **79** to form **82**

The simplification of the ^{1}H NMR spectrum by the disappearance of an aromatic peak so as to be similar to the NMR spectra of **80** and **81** showed that the substitution was successful.

2.2.1 Sonogashira reaction of substituted 2-aminopyridines with ethynyltrimethylsilane

The coupling of 2-aminopyridines with ethynyltrimethylsilane was the next step in the synthesis towards α-carbolines and was required to form the core 7-azaindole scaffold. A general scheme is shown in Scheme 2.8



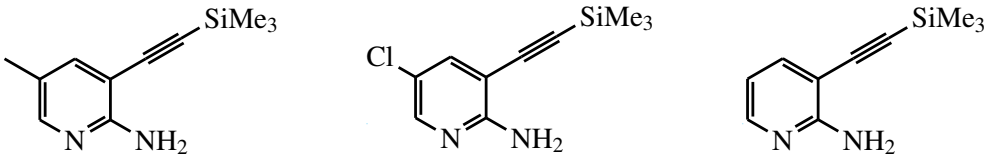
R = H (**78**→**77**), Me (**80**→**83**), Cl (**81**→**84**)
a - THF, TEA, $Pd(PPh_3)_4$, CuI, ethynyltrimethylsilane

SCHEME 2.8: The Sonogashira reaction in the synthesis of substituted 2-aminopyridines

The Sonogashira coupling reactions with 2-aminopyridine bromides 3-bromo-2-aminopyridine, **80** and **81** with ethynyltrimethylsilane failed initially. Palladium black would often form on heating, showing removal of active palladium species from the reaction mixture, leading to no observed coupling. The reaction methodology used was developed in our laboratories previously and utilised $Pd(PPh_3)_4$ as catalyst with THF as solvent and triethyl amine as base. The catalyst loadings were in the range of 5-10 mol %. In the presence of a little oxygen the reaction would fail, and it was found to be difficult to consistently set-up the reaction so that oxygen was excluded. All solid components of the reaction were placed in a two neck round bottom flask and fitted with a dropping funnel. The oxygen was then removed be repeatedly evacuating the round bottom flask and filling it again with N_2. The THF, triethyl amine and ethynyltrimethylsilane was then degassed in the dropping funnel by bubbling N_2 through for a period of of over 10 minutes. It was difficult to see how oxygen could get into the reaction mixture.

The focus was then shifted towards stabilising the catalyst and was achieved through several optimisations. Firstly, it was found that the solvent system used caused the catalyst to have an unnecessarily low concentration. The v/v ratio of THF to triethyl amine was adjusted to 1:1 and the equivalents of triethyl amine kept to 6 in relation to the 2-aminopyridine as was described in the previous method. This reduction in reaction mixture volume from the typical 100 ml to 40 ml would allow the palladium species generated to be in an environment in which the phosphine concentration is high enough so as to stabilise it and to stop the the aggregation of palladium species which forms palladium black. Further, the equivalents of PPh_3 in relation to the palladium was increased to 5 from the 4 initially received in $Pd(PPh_3)_4$, so as to increase the phosphine concentration further. This was achieved by adding PPh_3 in addition to $Pd(PPh_3)_4$ to the reaction mixture. The change of catalyst from $Pd(PPh_3)_4$ to the precatalyst $Pd(OAc)_2$ was also employed, which reduced the need of freshly preparing oxygen and light sensitive $Pd(PPh_3)_4$ on a regular basis, because, $Pd(OAc)_2$ is stable

to air and bought commercially. The Pd^{2+} species would then be activated to the 0 oxidation state in the reaction mixture through dimerisation of the acetylene present. Further it was found that addition of the CuI after everything has been added to the round bottom flask and the reaction mixture stirred for several minutes so as to allow the formation of a stable catalyst system was critical. It was observed that the presence of CuI in the initial stages of catalyst formation would induce palladium black formation. The changes to the method proved robust and so stable that even when the solvent and triethyl amine was not sufficiently degassed or when the N_2 source proved to fail and air was allowed in to the system no palladium black formed and high yields were obtained consistently. The equivalents of catalyst loading was then reduced to 1 mol % in relation to the 2-aminopyridine without any loss of catalytic activity. The yields of **83**, **84** and **77** are shown in Figure 2.7.



83 *82%* **84** *74%* **77** *96%*

Conditions - Substituted 2-aminopyridine (1 eq.), $Pd(OAc)_2$ (0.01 eq.), PPh_3 (0.05 eq.), CuI (0.01 eq.), (TEA 6 eq.), THF (equal volume in regards to TEA), ehthynyltrimethylsilane (1.2 eq.)

FIGURE 2.7: Yields of the initial Sonogashira reaction of bromide substituted 2-aminopyridines

The purification of these compounds were previously done by silica chromatography in our laboratories. This was found to be unnecessary as the basic properties of 2-aminopyridines allowed for the separation through acidic extraction of the reaction mixture. This extraction using aqueous HCl allowed for the separation of 2-aminopyridine compounds from the phosphine used in the reaction, as well as any other non-basic organic material that might have resulted from some decomposition side reactions. In low pHs 2-aminopyridines become readily soluble in water. The isolated water layer from the work up can then be made basic to a pH in which the 2-aminopyridine and triethyl amine from the reaction forms another liquid layer. this can then be isolated from the water using another work up and by running the crude through a short plug column to ensure the removal of any metal contaminants and removal of solvent and triethyl amine

by vacuum. It was found that the 2-aminopyridine product was in sufficient purity to not need further purification.

Crystal structures of **83**, **84** and **77** were solved from data collected after growing crystals in a saturated solution in hexane and are shown in Figure 2.8, Figure 2.9 and Figure 2.10 respectively.

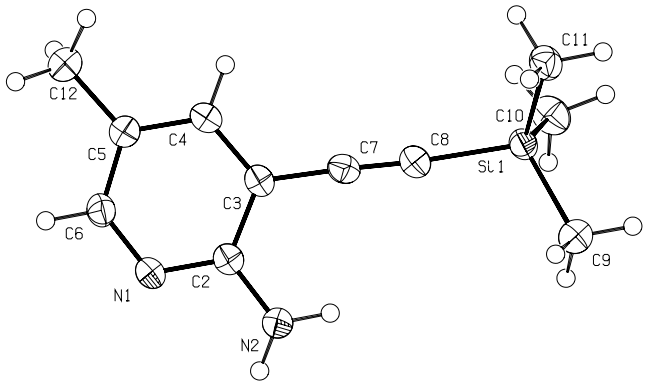


FIGURE 2.8: Crystal structure of **83** drawn with 50% probability ellipsoids

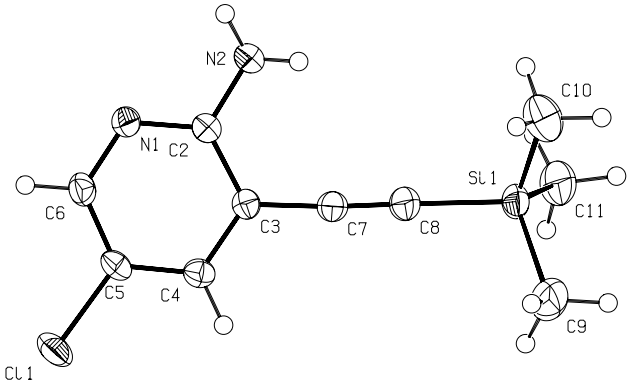


FIGURE 2.9: Crystal structure of **84** drawn with 50% probability ellipsoids

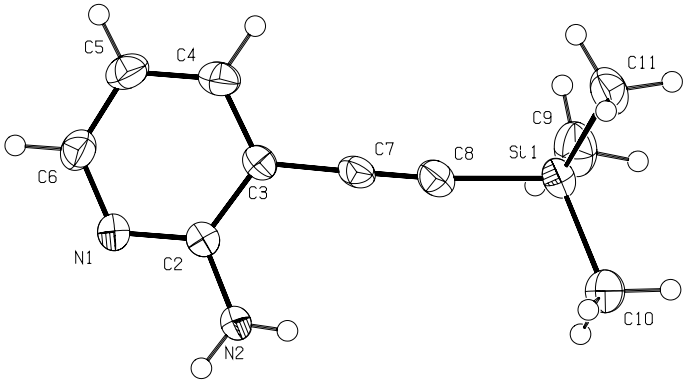
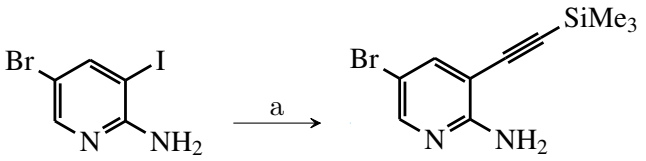


FIGURE 2.10: Crystal structure of **77** drawn with 50% probability ellipsoids

The selective Sonogashira reaction shown in Scheme 2.9 of the iodo-substituted 2-aminopyridine **82** at room temperature with ethynyltrimethylsilane to form **85** proved successful.



82 **85**

78%

a - **82** (1 eq.), $Pd(OAc)_2$ (0.01 eq.), PPh_3 (0.05 eq.), CuI (0.01 eq.), (TEA 6 eq.), THF (equal volume in regards to TEA), ehthynyltrimethylsilane (1.2 eq.), r.t

SCHEME 2.9: The Sonogashira coupling reaction utilised to form aminopyridine **85**

The reaction procedure was the same as that of optimised procedure used with the bromide containing compounds, only that the reaction mixture was not heated and only 4 equivalents of PPh_3 was added. This proved effective as the bromide in the 5 position of **82** was untouched and the iodide in the 3 position was substituted. This is most likely due to the lower bond dissociation energy of C-I (270 $kJ.mol^{-1}$) as compared to C-Br (330 $kJ.mol^{-1}$), as the oxidative addition step is the limiting step in the palladium catalysed Sonogashira cycle.[131] The crystal structure of **85** is shown in Figure 2.11.

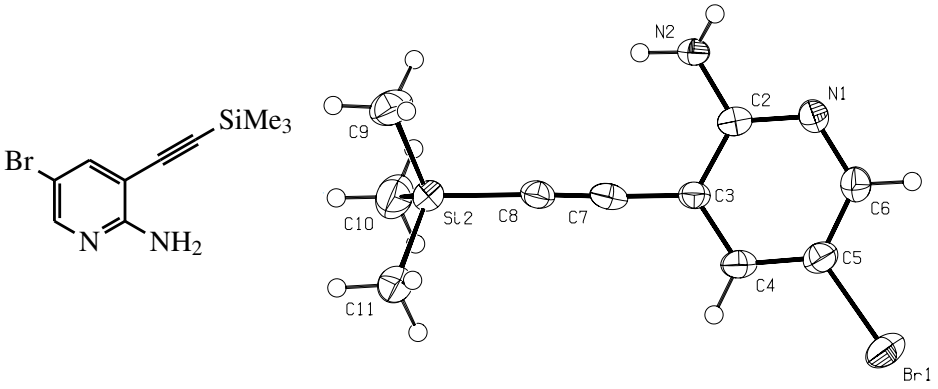


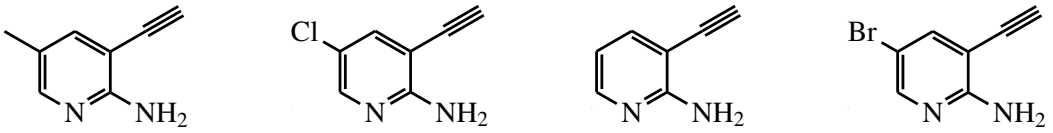
FIGURE 2.11: Crystal structure of **85** drawn with 50% probability ellipsoids

In addition to the crystal structures, the NMR spectra of the substituted 2-aminopyridines showed the presence of the acetylene functionality. In the ^1H NMR spectra a new singlet close to 0 ppm was observed that had an integration of 9H. This peak shows the three methyl groups from the silane functional group. In the ^{13}C NMR spectra the addition of two new peaks close to 100 ppm showed the acetylene functionality was present.

The modifications to the Sonogashira coupling reaction conditions proved critical in the substitution of halides in the 3 position in 2-aminopyridines to improve the catalyst stability and transform the reaction into a robust and repeatable reaction with sufficiently high yields.

2.2.2 Desilylation of ethynyltrimethylsilane substituted compounds

The deprotection of **83**, **84** and **77** would furnish the reactive acetylene C−H required in the second Sonogashira coupling reaction for our synthetic route. The silyl group is removed in the presence of fluoride ions, and is replaced by a hydrogen atom. As fluoride salts are usually very insoluble in organic solvents TBAF (tetrabutyl ammonium fluoride) is used as the fluoride source, as it is both very soluble in most organic solvents and is a fluoride salt. In most cases TBAF is added in a 1:1 molar ratio to the silane group that is to be removed, however, after optimising the reaction it was found that only 10 mol % was required. The usual solvent system used in these reactions is THF, either wet or dried depending on the nature of the reaction. The modified solvent system uses water:THF in a 1:4 ration. If this reaction mixture is left overnight in the presence of either **83**, **84**, **77** or **85** at room temperature the reaction furnishes the acetylene substituted 2-aminopyridine. The reaction could also be heated at reflux for an hour, but would, however, not give such a clean reaction as compared to when done at room temperature. The yields for this reaction are shown in Figure 2.12.



86 *96%* **87** *96%* **76** *96%* **88** *96%*

FIGURE 2.12: The silyl deprotection of substituted of 2-aminopyridines

The use of only 10 mol % TBAF shows that the active desilylating agent is regenerated in the reaction. The two active species that could remove the silyl group is either the fluoride ions present, or the hydroxyl ions generated upon the neutralisation of the acetylene anion formed after the silyl group leaves.

$$F^- + RSiMe_3 \rightarrow R^- + Me_3SiF$$
$$R^- + H_2O \rightarrow RH + OH^-$$
$$OH^- + RSiMe_3 \rightarrow R^- + Me_3SiOH$$

It was noted, however, that when these reaction conditions were tested on more hydrophobic compounds that only a small portion of the starting material would desilylate. This could potentially show that hydrogen bonding with water is required in this system in order for the active species to interact with the starting material effectively.

Crystal structures of **86**, **87**, **76** and **88** are shown below in Figure 2.13, Figure 2.14, Figure 2.15 and Figure 2.16. The crystals were grown from saturated solutions of the subsequent 2-aminopyridine in hexane.

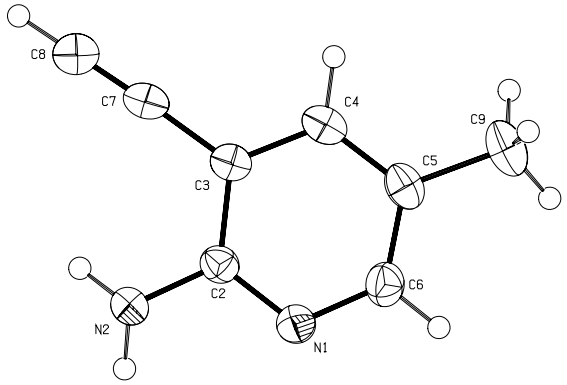


FIGURE 2.13: Crystal structure of **86** drawn with 50% probability ellipsoids

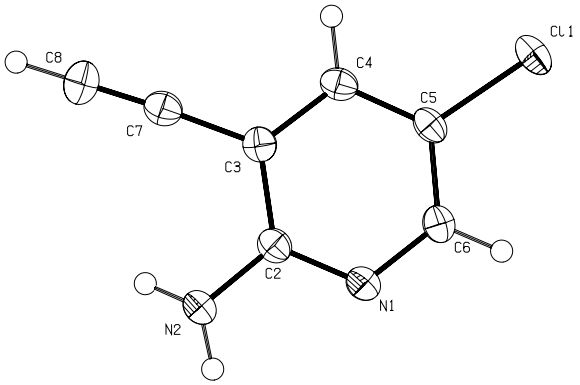


FIGURE 2.14: Crystal structure of **87** drawn with 50% probability ellipsoids

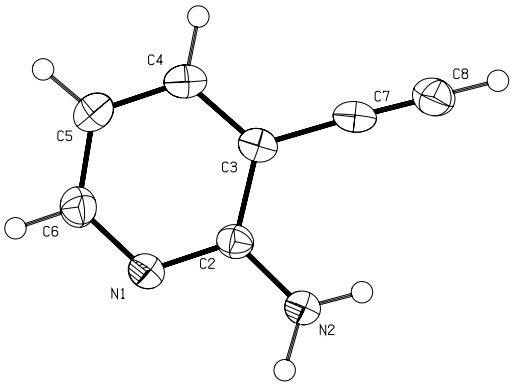


FIGURE 2.15: Crystal structure of **76** drawn with 50% probability ellipsoids

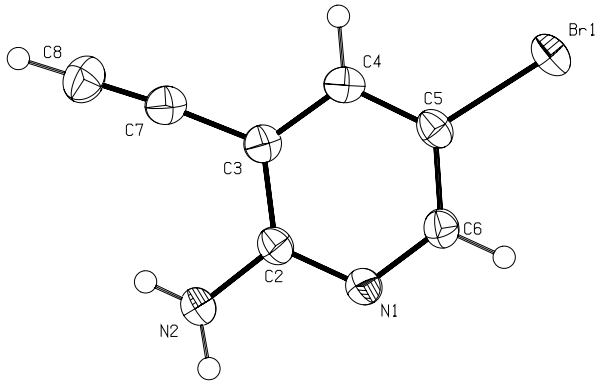


FIGURE 2.16: Crystal structure of **88** drawn with 50% probability ellipsoids

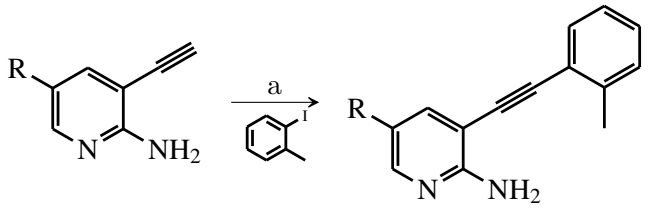
The removal of the silyl group can be seen very clearly in the NMR spectra of the products. The ^{1}H NMR spectra show the removal of the singlet at close to 0 ppm that integrated for 9H, and is replaced by a singlet at roughly 3.4 ppm that integrates for only 1H. This singlet is from the terminal acetylene proton. The ^{13}C NMR spectra shows both acetylene peaks move from close to 100 ppm in the starting material to close to 80 ppm.

The reactions proved very efficient and with the modifications to the reaction procedure the amount of TBAF required for the reaction is reduced significantly.

2.2.3 The Sonogashira reaction of acetylene substituted 2-aminopyridines and 2-iodotoluene

The coupling of the terminal acetylene compounds **86**, **87** and **76** with 2-iodotoluene to give **89**, **90** and **75** respectively is the next step in our synthesis. Note that brominated compound **88** was not subjected to the following reaction conditions, but was instead subjected to the improved condition later discussed in this chapter as its synthesis was performed at a later stage in the project. This coupling gives us our second aromatic ring for the assembly of azacarbazole, and gives the methyl group that will later be used in the *t*-BuOK and light mediated ring closure reaction to form our final aromatic ring and yield our desired α-carboline. the general reaction scheme is shown in Scheme 2.10.

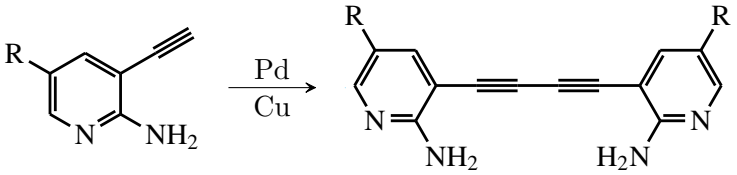
The second Sonogashira was initially expected to proceed as the first with high yields, especially since an aromatic iodide will be used in conjunction with the acetylene substituted 2-aminopyridine. This was, however, not the case. The reactions performed on



R = H (**76**→**75**), Cl (**87**→**90**), Me (**86**→**89**)
a - $Pd(OAc)_2$, CuI, TEA, THF, PPh_3

SCHEME 2.10: The second Sonogashira coupling of acetylene substituted 2-aminopyridines with 2-iodotoluene

86, **87** and **76** produced mostly dimer homo-coupled products **91**, **92** and **93** as shown in Scheme 2.11.



R = H (**76**→**93**), Cl (**87**→**92**), Me (**86**→**91**)

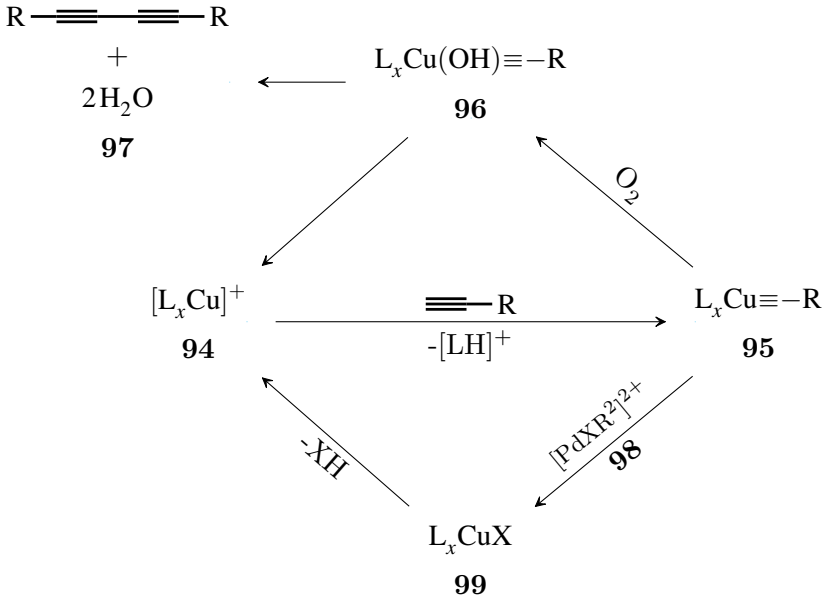
SCHEME 2.11: The formation of homo-coupled product from the Sonogashira coupling reaction as a side reaction product

The homo-coupled product appears as a yellow precipitate and upon inspection of NMR spectroscopy showed the disappearance of the acetylene proton at 3.4 ppm on the ^{1}H NMR spectrum. Compound **86** gave a mixture of products. The yellow precipitate could be filtered off using a Celite plug. The reaction mixture could then be further worked up and compound **89**, which was the intended o-tolyl substituted 2-aminopyridine product, was isolated in a 15% yield. The expected o-tolyl substituted products of **87** and **76** were in even lower yields, with the chloride compound **90** isolated in trace amounts. This shows some loose correlation with electron density on the pyridine ring, with the more electron rich compounds giving higher yields.

The formation of homo-coupled products was further tested by using known copper catalysed dimerisation reaction procedures from literature.[139] The reaction procedure uses copper(I) acetate and piperidine in acetonitrile in the presence of air.[139] The same yellow precipitate was recovered and gave the exact NMR spectra observed as the yellow precipitate from the Sonogashira coupling reaction. The presence of the copper in the reaction can thus be seen as the reagent that brings about the homo-coupling side reaction.

The mechanism of the copper catalysed homo-coupling was then further investigated, and it was found to be well documented in literature.[140] The overall reaction pathways of copper in the Sonogashira coupling reaction can be seen in Scheme 2.12. A copper complex formed by coordination of amine molecules present in the reaction (**94**) first reacts with the acetylene by coordinating to the triple bond. The base present in the reaction mixture deprotonates the acetylenic proton, which is now much more acidic due to coordination of the triple bond to the copper. The copper then migrates to the new carbanion at the end of the acetylene forming **95**. Once this neutral complex forms it is readily oxidised by oxygen, generating a +1 species (**96**) with a hydroxyl group attached. This +1 species then interacts with another molecule that is in the same state, i.e. bound to the acetylene and oxidised. This forms a copper dimer type complex which then decomposes to form the acetylene dimer (**97**) and regenerate the copper species.[140]

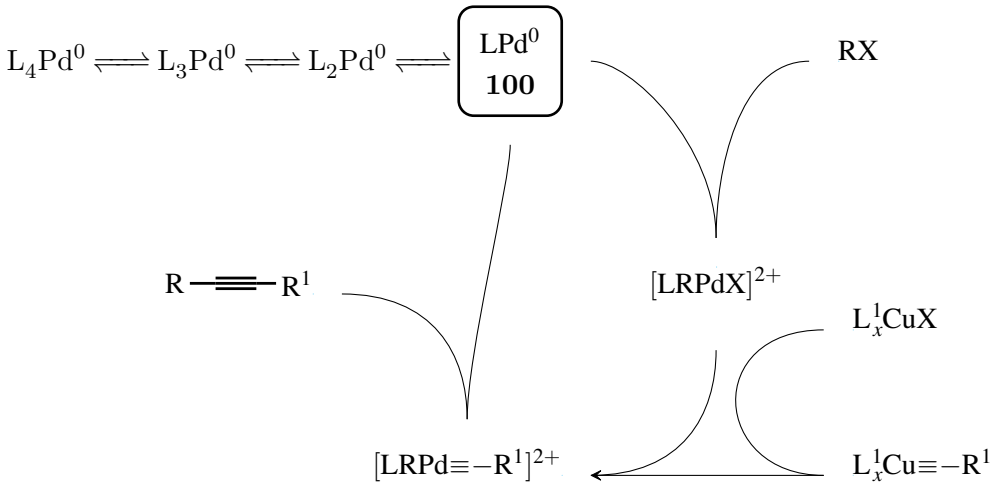
In a Sonogashira coupling reaction the stated copper pathway is a side reaction, and reduces the yield of the desired product significantly, as seen in the results of this section so far. In the Sonogashira reaction the coupling of the copper to the acetylene is desired, but then must transmetalate with **98** in order to form **99** which can be reactivated by the removal of the halide which was received from the palladium in the transmetalation reaction.



R: any aliphatic or aromatic functionality; R^2: any aromatic functionality; X: Cl, Br, I; L: amine

SCHEME 2.12: The oxidation cycle of copper in the Sonogashira reaction[131,140,141]

In the Sonogashira coupling reaction we can see two opposing reaction pathways for the copper acetylide **95**. The two pathways compete with one another, and in the Sonogashira coupling reaction the homo-coupling pathway needs to be slowed and out competed by the transmetalation pathway. As seen from the results of Sonogashira coupling reactions in this chapter the nature of the acetylene influences which pathway is preferred. The electron rich ethynyltrimethylsilane couples well with the 2-aminopyridine substrates used previously in the Sonogashira coupling reactions. In this synthetic step it is also seen that the more electron rich substrate **86** has a higher yield than the more electron poor substrate **87**. The acidity of the acetylene is increased, causing higher concentrations of **95**, as the coordination and deprotonation reactions are accelerated. If the palladium species **98** is present in low concentrations and sufficient oxygen is present more **96** would be formed than **99** as a result. In order to accelerate the formation of **99** over that of **96** several adjustments must be made to the catalytic system in the reaction mixture. Firstly, oxygen must be excluded as vigorously as possible. Small amounts of oxygen still seemed to be present in the reaction mixture, even under the best attempts of excluding it and so needed to be worked around. Secondly, the concentration of **98** needs to be increased. This oxidative step is the rate limiting step in the catalytic process.[131] The $Pd(PPh_3)_4$ catalyst system used until this point has decent activity and is easily accessible and affordable. These properties make $Pd(PPh_3)_4$ widely used, and as a first option in many coupling reactions. There have been, however, many advances in ligand design with ligands that show orders of magnitudes greater activity in palladium systems.[131] The increase in activity can be achieved by increasing the electron donating potential of the phosphine, as increased electron density on the palladium will increase its oxidation potential and increase the affinity for oxidative addition. The active palladium species in the reaction is not the fully coordinated palladium species. This fully coordinated palladium species is inert and stable and will not react with any aryl halide present in the reaction mixture. The palladium needs to undergo the loss of a ligand in order to become active. According to Colacot the active palladium species is one with only one phosphine attached (**100**) and a short reaction pathway is shown in Scheme 2.13. This palladium species is very unstable and so very reactive. Pushing the equilibrium towards the generation of this very reactive species can be done by increasing the bulkiness of the ligand. When the ligand design is very bulky unfavourable interactions occur between these bulky ligands coordinated to the palladium and they become more labile.[131,142]



SCHEME 2.13: The catalytic cycle of the Sonogashira reaction[131]

In the first reaction of this synthetic project the concentration of this species was lowered through addition of excess ligand, as catalyst stability was desired and the ethynyltrimethylsilane was reactive enough to furnish coupling products in high yields. The next logical step of solving this homo-coupling problem was then to increase the activity of the palladium species through modifying the ligand used in the reaction. It was decided that catalyst stability should not be compromised, as robust and repeatable reaction procedures are important in synthetic projects. In palladium ligand systems catalyst stability and increased activity can be achieved through the use of bis-phosphine ligands. This class of phosphine ligands have two phosphines on one molecule and form bidentate complexes. Bidentate ligands are not removed from the metal so easily, as even when a phosphine dissociates from the metal it is always kept in close proximity through the physical link to the other phosphine on the molecule that is still coordinated. The close proximity of this detached phosphine allows it to re-engage quickly and so keep the palladium in this case stable. Due to the strong binding affinity of these bidentate ligands they can be added in equimolar quantities as compared to that of the palladium and still furnish a stable catalyst as in comparison to the catalytic system devised in the first part of this synthesis where 5 equivalents of phosphine was added in order to furnish a stable catalyst. Several ligands were proposed, namely dppf (1,1'-bis(diphenylphosphino)ferrocene), BINAP (2,2'-bis(diphenylphosphino)-1,1'-binaphthyl) and ethylbis-diphenylphosphine. It was also decided to increase the catalyst loading to 5 mol % as compared to that of 1 mol % used in the first step of this synthesis.

Attention was also given to the amine used in the reaction. Most Sonogashira coupling reactions use triethyl amine, and use it in large concentrations as compared to that of the palladium and copper. The use of the amine in this reaction has a dual purpose. Firstly it neutralises the halide acid formed in the reaction, and the salt formed is often seen precipitating out of the reaction mixture. Secondly, the amine coordinates to the copper present in the reaction mixture. This coordination to the copper is critical. Homo-coupling is reduced when the copper species present is highly coordinated. The increase in complex stability will reduce the copper's affinity to dimerize with another active copper species present. In the reaction conditions used the concentration of the amine is in excess 150 times that of the copper. This pushes the equilibrium in the reaction as shown in Scheme 2.14 to that of $[L_3Cu]^+$ and $[L_4Cu]^+$.

$$Cu^+ \rightleftharpoons [L_1Cu]^+ \rightleftharpoons [L_2Cu]^+ \rightleftharpoons [L_3Cu]^+ \rightleftharpoons [L_4Cu]^+$$

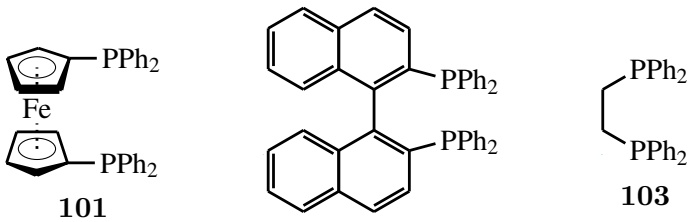
SCHEME 2.14: The complexation of copper when excess ligand is present

The amine in the reaction, however, does more than just coordinate to the copper. The amine also coordinates to the palladium present, even if weakly. This coordination to the palladium will lower the reactivity of the palladium in the reaction, as the concentration of **100** will be lowered. This coordination occurs, because triethyl amine is relatively small and flexible allowing the amine to easily bind to the palladium. In order to combat this coordination an amine that is a poor nucleophile must be used. In our case diisopropyl amine was chosen. the amine is still able to act as a base in the reaction, and due to copper's high affinity for amines still coordinate to it, but, will not be able to coordinate to the palladium species present in the reaction mixture and will as result furnish a much more active palladium species.

With the new reaction conditions tests were done on the ligands described. The 2-aminopyridine chosen was **76**. It was found that the dppf **101** gave the highest yields as shown in Figure 2.17 with **75** at 65%, which is more than a four fold increase.

This result can be linked to both the electron donating potential of ferrocene into the phosphine atoms and thus into the palladium atom, and the large bite angle of the dppf on the palladium.[131,143–145] The bite angle of the phosphines are as follows: **101**-dppf-99°; **102**-BINAP-93°; and **103**-ethylbis-diphenylphosphine-86°.

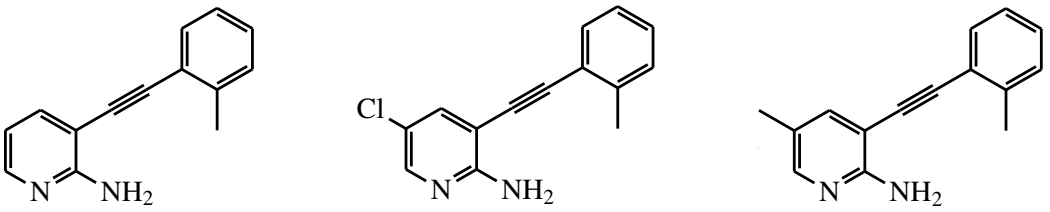
It was decided to use dppf as the ligand of choice and the other 2-aminopyridines were also reacted to yield **90** and **89**. The chloride **87** gave a lower yield of 45% (**90**) and



101 *65%* **102** *40%* **103** *0%*

FIGURE 2.17: The effect of bidentate ligands in the reaction shown in Scheme 2.10

reacting the methyl substituted **86** gave a yield of 75% (**89**) as shown in Figure 2.18. This corresponds to what is stated above that the more electron deficient the alkyne, the more homo-coupling will predominate.



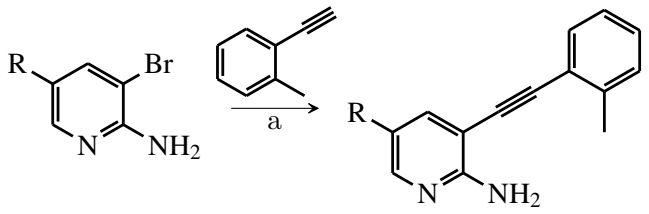
75 *65%* **90** *45%* **89** *75%*

FIGURE 2.18: The effect functional groups on the pyridine in the modified Sonogashira reaction

The NMR spectra of **75**, **90** and **89** showed the introduction of a new aromatic methyl signal in both ^{1}H and ^{13}C NMR spectroscopy experiments, as well as the disappearance of the acetylene hydrogen peak at 3.4 ppm. The methyl peak is from the coupled o-tolyl moiety and shows the coupling was successful.

The optimisations were successful, but, the yields were still not sufficiently high enough for the continuation of the synthesis. It was decided to change the synthetic route so as to avoid using acetylenes that were as electron poor as those of the substituted 2-aminopyridine **86**, **87** and **76**. The brominated 2-aminopyridines would be coupled directly with 1-ethynyl-2-methyl-benzene to furnish **75**, **90** and **89** as shown in Scheme 2.15.

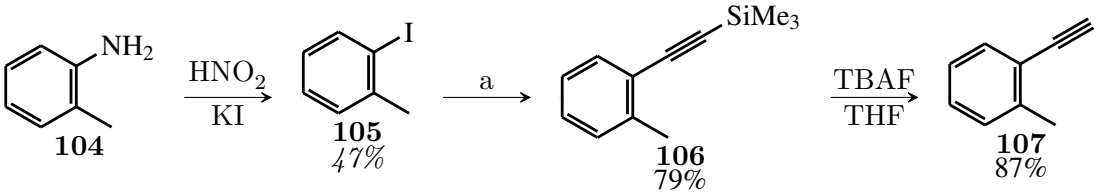
The methyl substituted benzene ring 1-ethynyl-2-methyl-benzene would be more electron rich than that of 2-aminopyridine promoting less homo-coupling and better overall yields. It was decided to synthesise the 1-ethynyl-2-methyl-benzene and use it freshly prepared



R = Cl (**81**→**90**), H (**78**→**75**), Me (**80**→**89**)
a - THF, $Pd(OAc)_2$, CuI, dppf, DIA

SCHEME 2.15: The synthesis of **75**, **90** and **89**

as the electron rich alkyne can readily undergo polymerisation in air. The synthesis of 1-ethynyl-2-methyl-benzene is shown in Scheme 2.16.



a - THF, TEA, $Pd(OAc)_2PPh_3$CuIethynyltrimethylsilane

SCHEME 2.16: The synthesis of 2-methyl-phenyl-acetylene **107** with an overall yield of *32%*

The synthesis of **105** from **104** gave low yields with a maximum of 47%. The reaction conditions were varied so as to test the effect of different acids, different temperature and different substrate concentrations. The reaction proceeds by first diazotizing the amine to $[R{-}N{\equiv}N]^+$ by using HNO_2, followed by the addition of KI which facilitates the decomposition of the diazo intermediate and the addition of the iodine atom to the ring. An acid is added to $NaNO_2$ in order to generate HNO_2. An initial yield of 23% was achieved using HCl at 5°C with one equivalent of KI in the second portion of the reaction. A method by Ullmann was then adapted in which H_2SO_4 was used at 5°C and 2 equivalents of KI were used.[146] A significant difference in the procedure was that KI solution was cooled to 5°C and then the reaction mixture was added to this solution. The second method gave the reported 47% yield. The reaction is so low yielding because the intermediate is very reactive and readily decomposes to the corresponding phenol in the presence of water. The phenol is removed in the work up by washing the hexane used to wash the reaction mixture with concentrated NaOH. The phenol forms a salt which is then solubilised in the NaOH solution. The ^{1}H NMR spectrum of **105** shows the disappearance of the amine peak, showing the displacement of the amine in **104** with an iodide in **105**.

The Sonogashira coupling reaction of **105** with ethynyltrimethylsilane to form **106** worked without any problem. The reaction condition used was triethyl amine as base, together with $Pd(OAc)_2$ as palladium source and PPh_3 as ligand as described in Scheme 2.16. Only **106** was isolated. The work up was done using hexane, so as to exclude the phosphine used, as well as a short plug column on flash silica using hexane as eluent. The ^{1}H NMR spectrum of **106** showed the presence of a singlet at 0.256 ppm that integrated for 9H, and the ^{13}C NMR spectrum showed the presence of the acetylene with shifts at 104 and 98 ppm, showing that the coupling was successful.

The use of TBAF for the deprotection was not accomplished as previously stated with the 2-aminopyridine substituted compounds. The 10 mol % catalytic loading of TBAF in a mixture of water, THF and **106** only yielded 20% of **107** at room temperature and 50% under reflux overnight. Therefore, it was suspected that the hydrophobicity of **107** was the cause of this poor reactivity. The reaction was accomplished with good yields by adding 1 molar equivalent of TBAF and stirring the reaction at room temperature for 1 hour after which water was added and the work up done. The ^{1}H NMR spectrum of **107** showed the presence of an acetylene peak at 3.26 ppm. The shift of the acetylene peak in comparison to that of the acetylene substituted 2-aminopyridines give an indication of the electron density in these compounds. The shift of 3.26 ppm of **107** shows more shielding as compared to the 3.4 ppm of the 2-aminopyridine compounds.

The overall yield for this synthesis was 32%, but, was low due to the low yield of the diazotization reaction.

The reaction of the acetylene **107** with the substituted pyridines **80**, **81** and **78** as seen in Scheme 2.15 in the presence of palladium gave **75**, **90** and **89** in moderate to high yields as seen in Figure 2.19.

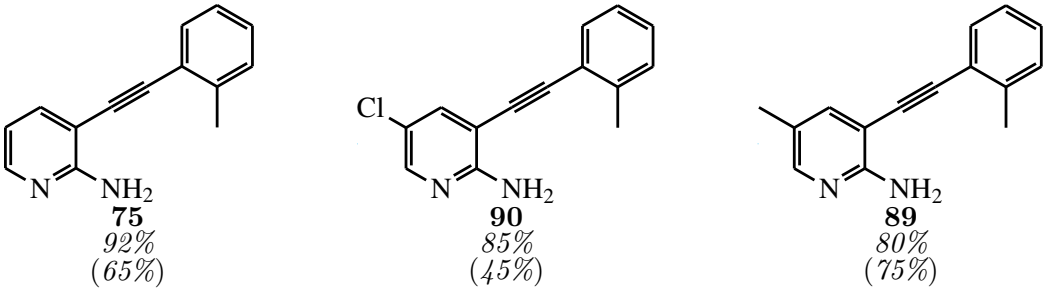


FIGURE 2.19: The yields of **75**, **90** and **89** in the convergent synthesis using acetylene **107** in comparison with using 3-alkynyl-2-aminopyridines **86**, **87** and **76** (yields in brackets for comparison)

It was therefore found that using the convergent synthesis was of great success. The dimerisation of 3-alkynyl-2-aminopyridines were avoided, making the work-up easier and giving higher yields of **75**, **90** and **89**.

From the results observed the stronger the electron withdrawing potential on the substituted alkyne lowers the yield of the Sonagashira reaction as shown in Figure 2.20.

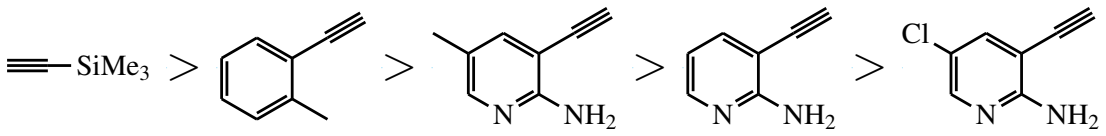
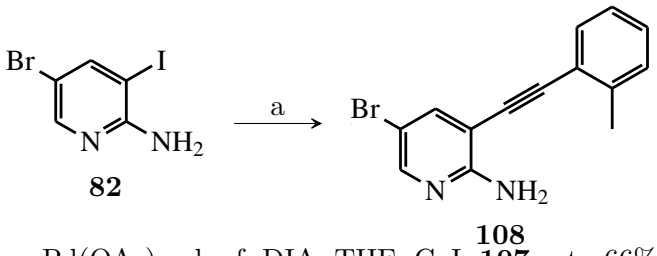


FIGURE 2.20: The comparison of reactivity of substituted alkynes in the Sonogashira reaction

The formation of **75**, **90** and **89** gave some challenges, but changes to the Sonogashira coupling reaction conditions and a small change in the synthesis plan aided in giving **75**, **90** and **89** in sufficient yields.

The methodology was then further applied to 2-aminopyridine **82** to generate **108** with a yield of 66%. The substitution of the iodide in the 3 position was effectively achieved at r.t., leaving the bromide intact at the 5-position. This is shown in Scheme 2.17.



82 **108**

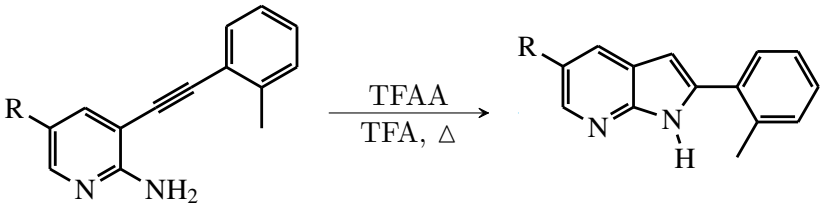
a - $Pd(OAc)_2$, dppf, DIA, THF, CuI, **107**, r.t., 66%

SCHEME 2.17: The synthesis of **108** utilising selective Sonogashira coupling of an iodide

2.2.4 Cyclization of 2-aminopyridines to form 7-azaindoles

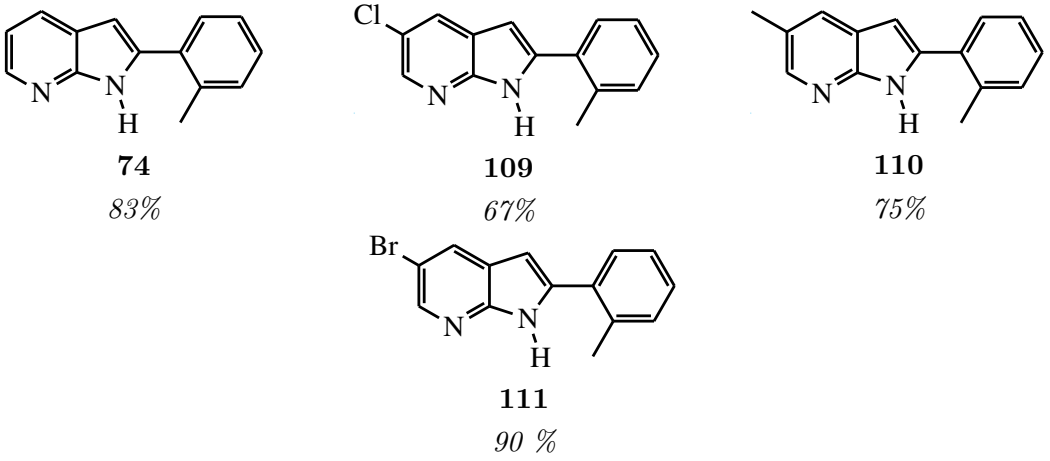
The general cyclisation reaction of 2-amino-pyridines to form 7-azaindoles is shown in Scheme 2.18

The method developed in our laboratories by Leboho *et al.* is the first reported acid mediated ring closure of 2-amino-pyridine systems to yield 7-azaindoles.[123] The reaction gave good to moderate yields of the desired products in the work done in this project as shown Figure 2.21. It was however important to note that leaving the reaction for only eight hours is critical as yields drop drastically due to decomposition after this time.



R = Cl (**90**→**109**), H (**75**→**74**), Me (**89**→**110**), Br (**108**→**111**)

SCHEME 2.18: The general TFAA and TFA mediated ring closure of 2-amino-pyridines to form the desired 7-azaindoles



74 *83%*

109 *67%*

110 *75%*

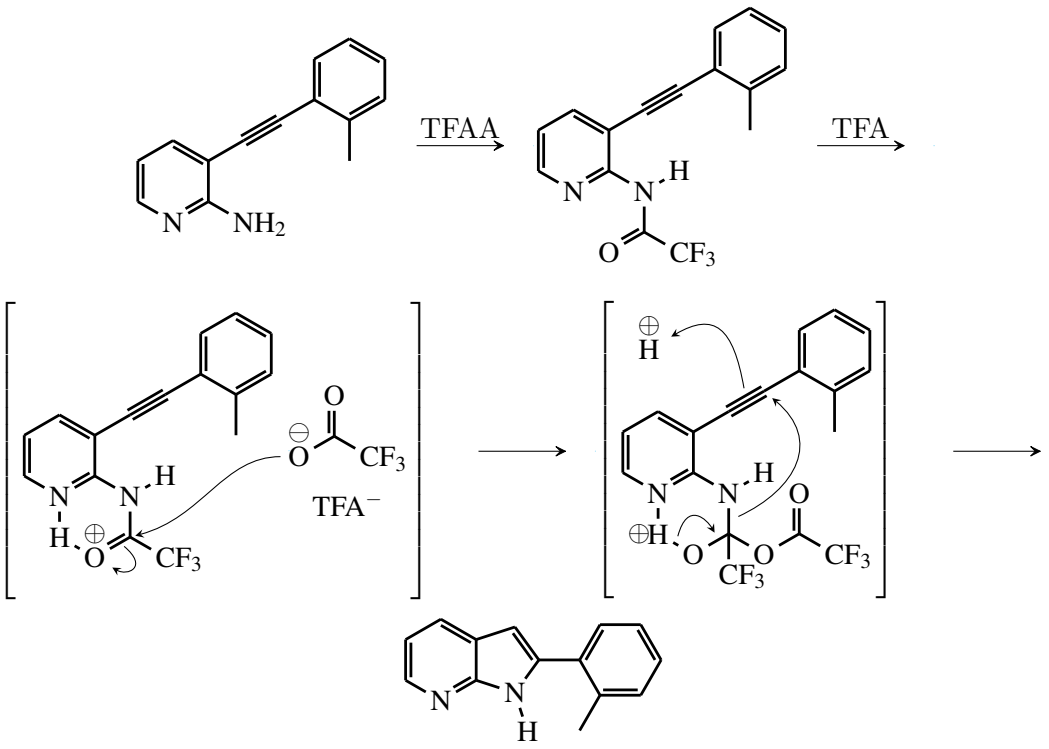
111 *90 %*

FIGURE 2.21: The yields of 7-azaindoles from the the ring closure of 2-aminopyridines

The ^{1}H NMR spectra of compounds **74**, **109**, **111** and **110** show the disappearance of the amine peak at roughly 5-6 ppm and the appearance of an N-H peak at roughly 8-13 ppm. The ^{13}C NMR spectra shows the shifting of the acetylene peaks to the aromatic region as the azaindole ring is formed.

The amino group in the ring is acidic and can be deprotonated using a strong base such as *t*-BuOK followed by heating, in which nucleophilic attack on the triple bond occurs, yielding the desired azaindole system as is seen in most literature procedures.[123] In our reaction an acidic reaction mixture is used. As nucleophilic attack on an electron rich acetylene functional group is unlikely, the use of an acid to activate the triple bond system is required. However, this in turn limits the nucleophilicity of the amine by protonation on an already poor electron donor. This was solved by generating the trifluoroacetamide, which collapses, generating an anion that can react further. The proposed mechanism is shown in Scheme 2.19.

The high shift of the N-H peak in the ^{1}H NMR spectra can be understood by strong hydrogen bonding dimers forming in solution as seen in the crystal structures of these



SCHEME 2.19: The general TFAA and TFA mediated ring closure of 2-amino-pyridines to form the desired 7-azaindole.

types of compounds as shown in Figure 2.23. This makes the 7-azaindoles readily crystalline, with higher melting points than the acetylene 2-aminopyridines (below 100 °C as compared to above 150 °C for 7-azaindoles) 7-Azaindoles can be recrystallised from ethyl acetate and isopropanol, whereas the 3-alkynyl-2-aminopyridine cannot since they are too soluble. This shows that new flat π system and strong hydrogen bonding decreases solubility of the 7-azaindole as compared to other heterocycles previously made in this synthesis.

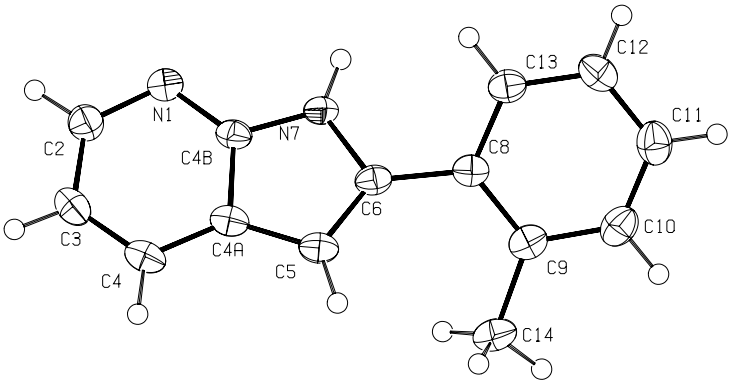


FIGURE 2.22: Crystal structure of **74** drawn with 50% probability ellipsoids

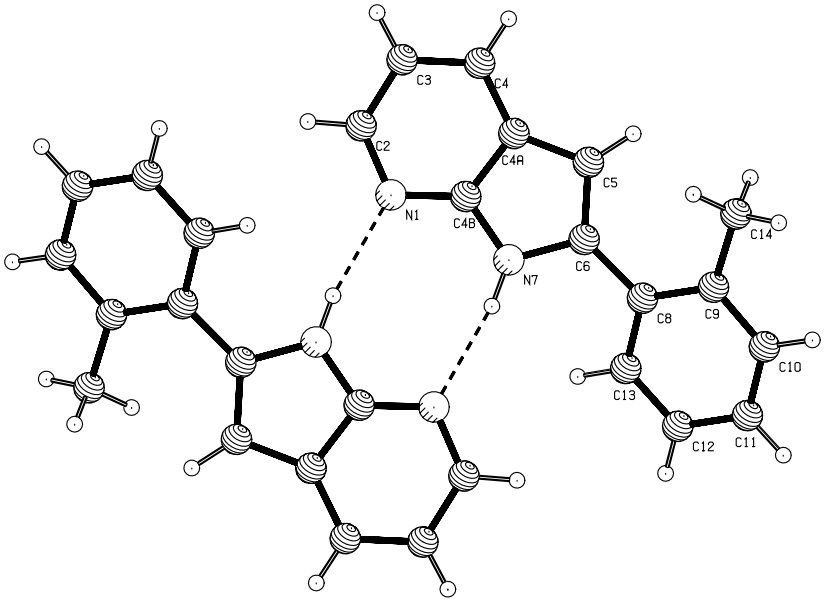
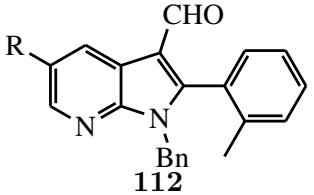


FIGURE 2.23: Crystal structure of **74** showing H bonding dimer formation

2.2.5 Formylation at C-3 and protection of the azaindole at N-1

The formylation and benzyl protection of 7-azaindoles was necessary for the formation of the final α-carboline structure of the final product. The *t*-BuOK and light mediated ring closure reaction does not proceed without a protecting group at the N-1 position. This was also seen in the indole counterparts.[88,89]

Therefore, the aim of this section of the synthesis is to generate the class of compounds as shown in Figure 2.24 *i.e.* **112** that can undergo the final ring closure reaction step to form the desired α-carbolines.

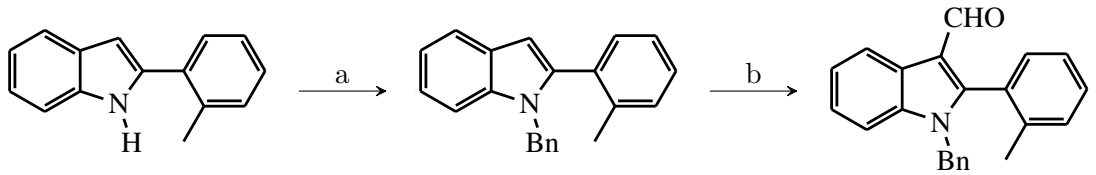


112

R = Cl (**113**), Me (**114**), H (**115**)

FIGURE 2.24: The synthetic goal for this section in the synthetic route

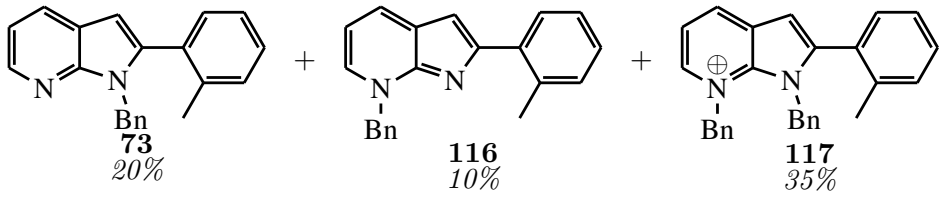
In the previous synthesis of carbazoles, the indole containing compounds were first benzylated and then formylated using $POCl_3$ and DMF as shown in Scheme 2.20.[88,89]



a - BnBr, KOH, NMP; b - 1) DCM, DMF, $POCl_3$ 2) water, NaOH;

SCHEME 2.20: The synthesis of benzo-fused carbazole precursors from indole by formylation and benzyl protection

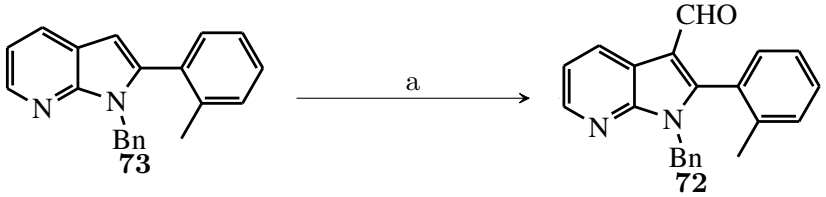
The methodology described, however, worked poorly with the 7-azaindoles as the benzyl protection step generated multiple products as shown in Scheme 2.21. The pyridine nitrogen atom is nucleophilic with a lone pair that is not conjugated with the aromatic system. This allows the formation of several side products from this reaction. The aromatic system in 7-azaindoles can facilitate N-benzylation on the 7 position as seen with **116**. The benzylated 7-azaindole **73** and **116** can be further benzylated to form **117** as a salt. Silica chromatography is required to separate these three different products generated.



SCHEME 2.21: Products generated from the benzyl protection of **74**. Note that starting material was also recovered

Unfortunately, the attempted optimisation of this reaction yielded no better results. Using stronger bases, lowering the reaction temperature and changing solvents still did not stop the formation of **116** and **117**.

Azaindole **73** was then taken and formylated by using $POCl_3$ and DMF, and **72** was isolated with a 70% yield as shown in Scheme 2.22.

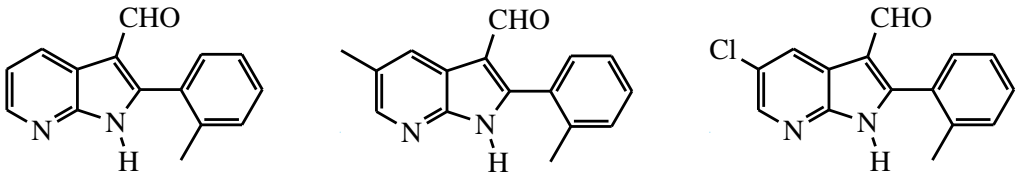


a - 1) DCM, DMF, $POCl_3$ 2) water, NaOH;

SCHEME 2.22: The synthesis of **72** from **73** using $POCl_3$ and DMF

It was then decided after some consideration to reverse the reactions so as to formylate **74** first and benzyl protect after. The reasoning behind this was that the introduction of a formyl group to the 7-azaindole system would decrease the electron density of the 7-azaindole and will as a result decrease the electron density on the nitrogen atom in the 7 position. If this nitrogen atom is made less reactive the selective benzylation on the 1 position could be favoured. However, the formylation of **74** using $POCl_3$ and DMF was not successful and starting material was recovered. This reaction typically works with indole, and so the failure of this reaction can be attributed to the lowered electron density in the 7-azaindole system. The active electrophile generated in the $POCl_3$ reaction is not sufficiently electrophilic enough for the reaction to proceed, whereas in the case of the benzylated 7-azaindole **73** this was not the case. The benzyl group donates electron density into the 7-azaindole system, giving it the ability to react with the active intermediate generated in this reaction.

In order to formylate the 7-azaindole an alternative formylating agent was required. Another formylation method was found in which $AlCl_3$ and dichloromethyl-methyl-ether in DCM is reacted with aromatic systems, which is in our case 7-azaindole.[147] The yields of this formylation procedure on the 7-azaindoles synthesised were modest ranging from *35%* to *65%* depending on the electronic properties of the system with the chloride substituted 7-azaindole **113** giving the lowest yield. It was also found that coordination to the aluminium occurred, causing a precipitate which was difficult to work with, which reduced the yields of this reaction in all cases. Another Lewis acid was then tested, namely $TiCl_4$ as recovery of any coordinated product could be recovered by using a concentrated solution of NaOH which transforms the titanium complexes to titanium oxide. The precipitate formed with $TiCl_4$ remained as a suspension, allowing for normal handling of the reaction mixture. The optimised formylation yields for **115**, **114** and **113** are shown in Figure 2.25



115 *57%* **114** 96% **113** *35%*

FIGURE 2.25: The formylation results from the optimised reaction conditions

The formylation products **113**, **114** and **115** showed the typical sharp aldehyde signal upfield of 10 ppm in the ^{1}H NMR spectrum and a peak close to 180 ppm in the ^{13}C NMR spectrum showing that the reaction was successful.

The benzylation of the formylated 7-azaindoles **113**, **114** and **115** were more successful than the reactions on the 7-azaindoles. The electron withdrawing nature of the formyl group was sufficient to encourage mono-benzylation in the correct position of the 7-azaindole. The benzyl CH_2 peak in the ^{1}H NMR spectrum would show the reaction was successful, as well the typical pyridine proton pattern in which H-6 had a ppm shift of between 8.5 and 8.9 ppm, and H-4 with a ppm shift just a little lower by roughly 0.2 ppm on the NMR spectrum. If the benzyl group attaches to the nitrogen atom in the 7 position these peaks shift into the range of 7 - 7.6 ppm. The final yields for the benzylation reaction resulting in **72**, **118** and **119** is shown in Figure 2.26. 7-Azaindoles **72** and **118** were not isolated and treated as intermediates.

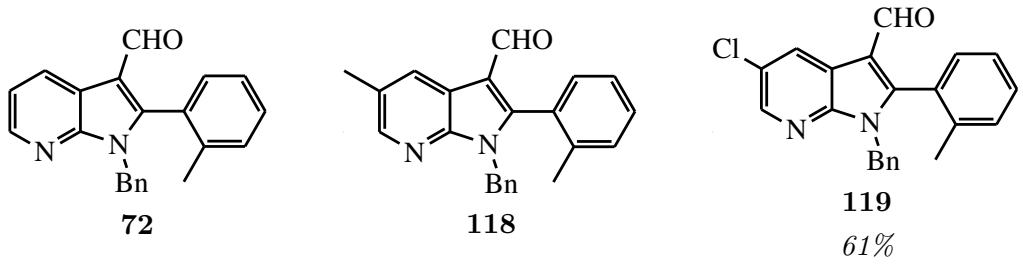
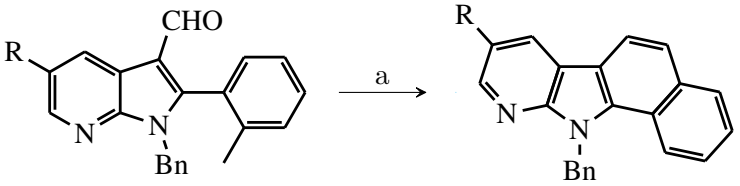


FIGURE 2.26: The N-1 benzylation yields of 3-formyl-7-azaindoles

2.2.6 *t*-BuOK and light mediated ring closure

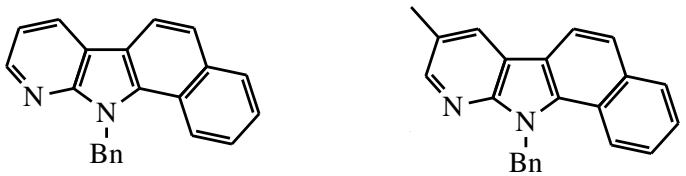
The *t*-BuOK and light mediated ring closure to form the desired α-carbolines worked from the initial reactions performed on the 3-formyl substituted 7-azaindoles from the previous section of the synthesis. The general outline for the reaction is shown in Scheme 2.23.



R = H (**72**→**71**), Cl (**119**→**120**), Me (**118**→**121**)
a - *t*-BuOK, hν, DMF

SCHEME 2.23: The synthesis of α-carbolines from previously synthesised formyl 7-azaindole compounds

The general method included dissolving the formyl compound in DMF, heating it to 70 °C, adding *t*-BuOK and then stirring the reaction while exposed to UV light. The UV light source used was a high pressure mercury vapour lamp, which gives general emission in the UV spectrum from 253 nm to above 350 nm. Isolation of products from the reaction mixture required the pouring of the reaction mixture into water, from which the product precipitated as a solid. The reaction mixture must be exposed to the UV light source for only 15 minutes, as decomposition of product was noted with exposure times of greater than 15 minutes. α-Carboline **71** as shown in Figure 2.27 was isolated with a yield of 82% using this method. α-Carboline **121** as shown in Figure 2.27 was isolated with a yield of 35% from over two steps, namely the benzylation protection reaction and the ring closure reaction.



71 *82%*

121 *35%*

Note that the yield calculated for **121** was for over two steps

FIGURE 2.27: Yield of α-carboline **71** and **121** from the stated ring closure reaction

The products were identified through their characteristic ^{1}H NMR spectra which showed the disappearance of the methyl peak from the tolyl group of the starting material in this step, as well as the disappearance of the aldehyde peak and the further introduction of two protons in the aromatic region. The crystal structures of **71** and **121** were determined and shown in Figure 2.28 and Figure 2.29, and act as further confirmation of the success of the ring closure reaction performed in this section.

During the course of this project the high pressure mercury vapour lamp used was broken, and was unable to be replaced before the completion of this project. A low pressure mercury vapour lamp was employed instead for the synthesis of the chloride substituted α-carboline **120**. The change in lamps effected the yield greatly and **120** was isolated in a low yield of 4% as shown in Figure 2.30.

The low pressure mercury vapour lamp has an emission spectrum with a sharp peak at 253 nm, which is in contrast to the broader spectrum of light emitted from the high pressure mercury vapour lamp. It was also noted that no other organic compounds

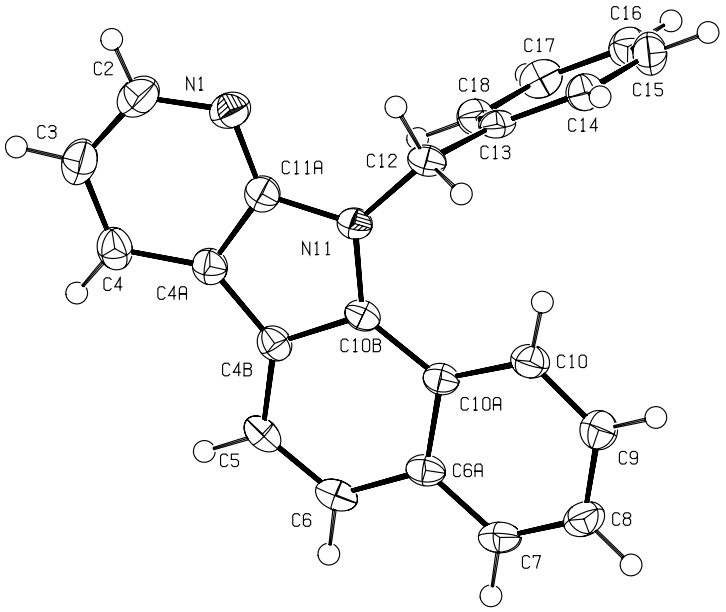


FIGURE 2.28: Crystal structure of **71** drawn with 50% probability ellipsoids

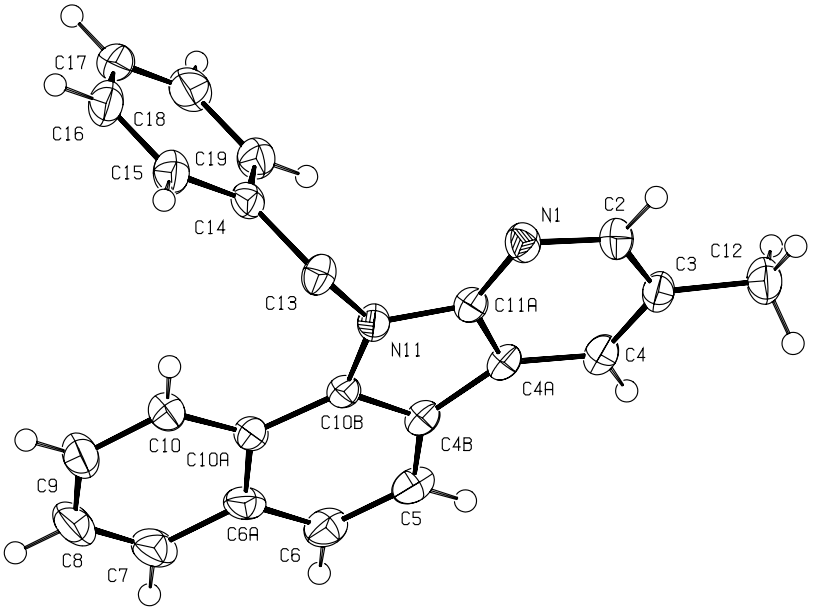
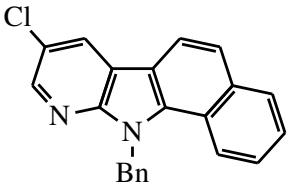


FIGURE 2.29: Crystal structure of **121** drawn with 50% probability ellipsoids



120

4%

FIGURE 2.30: Yield of α-carboline **120** from the stated ring closure reaction using a low pressure mercury vapour lamp

were isolated in the synthesis of **120**. However, large amounts of a dark material was observed that was uncharacterised. This material was attributed to decomposition of the material present in the reaction. This change from the previous reaction conditions in which the high pressure mercury lamp was used suggests that the wavelength of 253 nm allowed for only low yields in this reaction, even if the wavelength is sufficient in bringing about the desired ring closure reaction as seen with the isolation of **120**. As a reference the emission spectra of high and low pressure mercury vapour lamps are shown in Figure 2.31

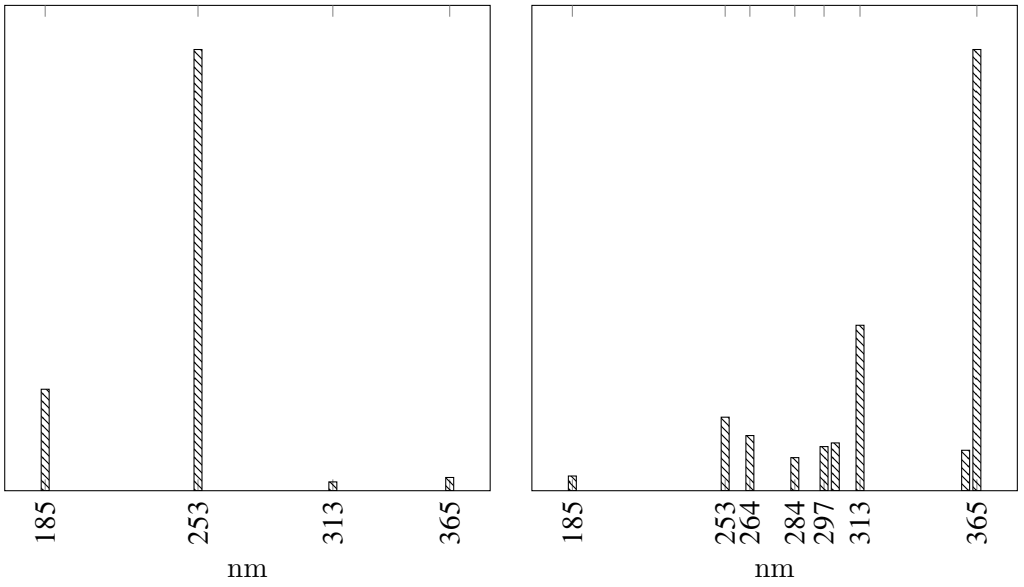
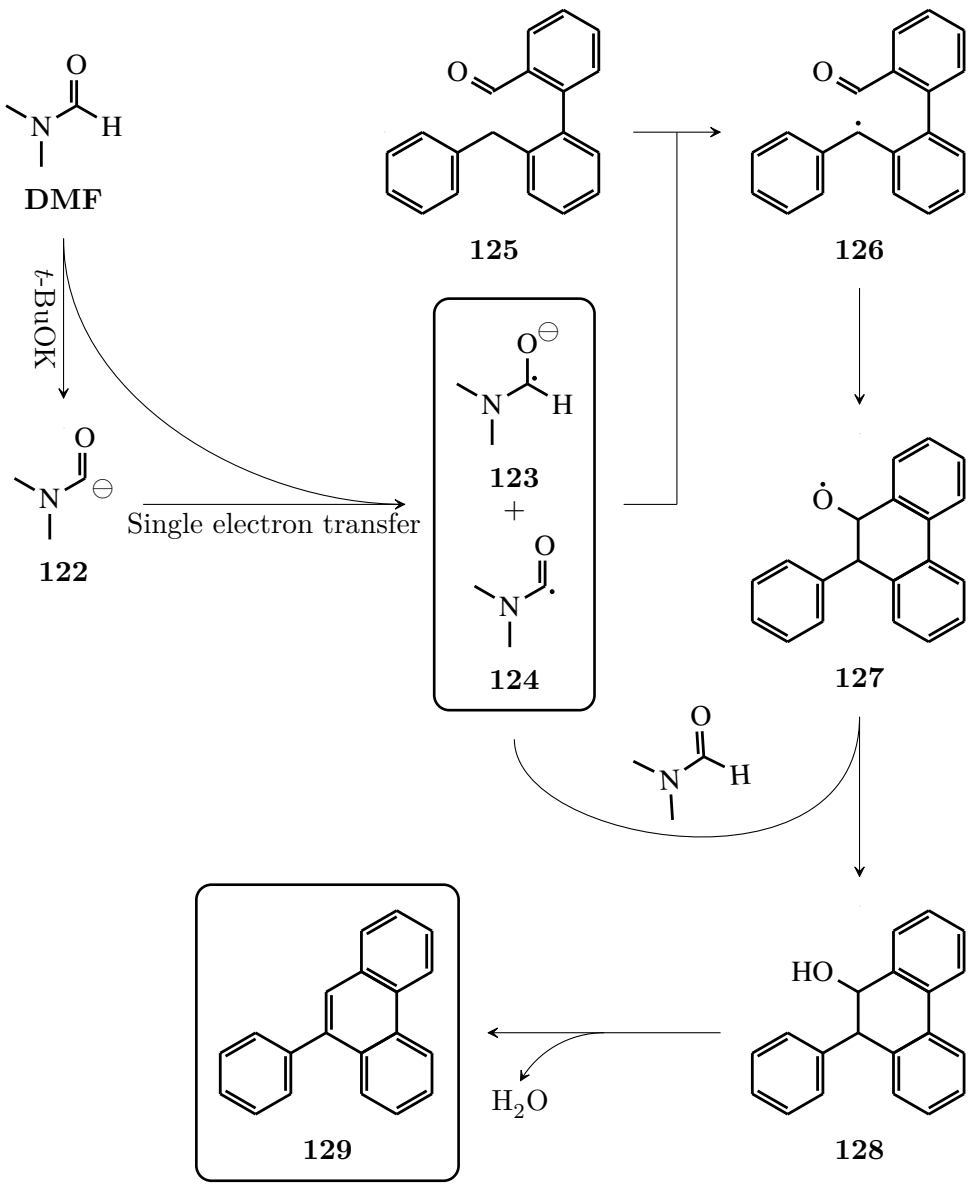


FIGURE 2.31: The emission spectra of a low (left) and a high (right) pressure mercury vapour lamp. Note that the quartz lamps used filters out the peak at 185 nm

A proposed mechanism by Chen *et al.* based on a similar reaction in which light is not utilised is shown below in Scheme 2.24.

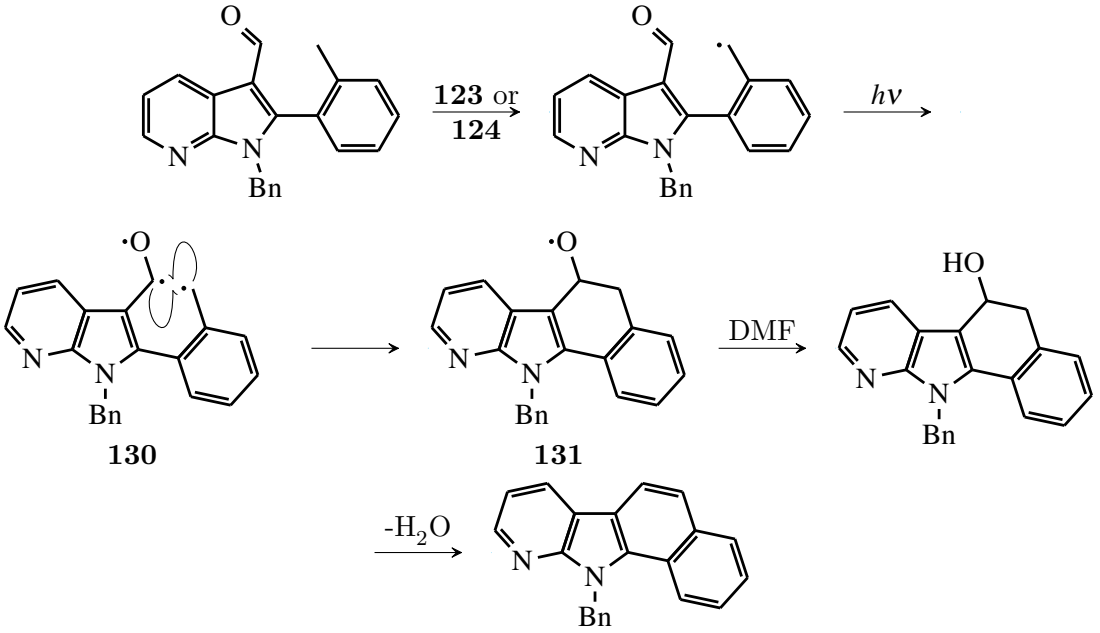
The reaction depends on the deprotonation of DMF to **122**, which in the presence of DMF will form **123** and **124**. It was proposed in this mechanistic study that the radical **124** reacts further with **125** to form the benzyl radical **126**. This radical is stabilised through resonance on the adjacent aromatic rings. This radical can then react with the aldehyde on the molecule, forming a new C-C bond. The very reactive C−O· radical on **127** can then abstract a proton from the DMF solvent forming **128** and **124**. Dehydration of **128** to form the aromatic ring is the final step of the synthesis forming the anthracene product **129**. The details of this mechanism were elucidated by radical scavengers confirming a radical reaction. Light is then not required in the ring closure reaction studied, yet shows a catalytic effect when used, as well as an increase in



SCHEME 2.24: Proposed mechanism of the *t*-BuOK without light mediated ring closure reaction by Chen *et al.*.[148]

yield. The light can aid the reaction through the activation of the aldehyde. Aromatic aldehydes have absorbance values in the range of 270 - 340 nm, as well as a secondary absorbance value around 250 nm.[149] The excitation of the aldehyde through light can lead to a singlet or a triplet state, and a single electron on both the carbon and the oxygen. The synthesis of oxetanes for instance require the formation of the triplet state for a successful reaction.[150] Radicals are generally in higher energy states than that of other ground state electrons. Bonding forms through the interactions of orbitals with these corresponding energy states, with orbitals of similar energy states showing the greatest energy gaining effects and therefore greater bonding interaction.[150] With the

example shown in Scheme 2.24 radical **126** is highly stabilised as noted, which gives an energy lowering effect to this radical state. This energy lowering effect would as result be sufficient to allow strong bonding interactions between the radical and the aldehyde on the molecule as the orbitals involved would be close in energy levels. In the work done in this study and in the synthesis of naphthalenes, anthracenes and carbazoles which utilise at most only one adjacent aromatic ring as in contrast to the two in **125**. This gives a lesser degree of stabilisation in the radical formed, leading to lower yields in these reactions because of less favourable orbital interactions. The light used in these studies therefore show that the activation of the aldehyde to either the singlet or triplet state aids in the C-C bond forming through bringing the required energy states of orbitals in the reaction closer in energy level. In the ring closure reaction of this study intermediate **130** would thus be formed and allow for the formation of **131** as shown in Scheme 2.25.



SCHEME 2.25: Proposed mechanism of the *t*-BuOK and light mediated ring closure reaction.

This interaction will now be explained in greater detail and it will be assumed that a triplet state is formed upon activation through light on the aldehyde. In Figure 2.32 we see the interacting orbitals of the participating oxygen and carbon atoms. The one pair combine to generate the σ and σ^* orbitals. This is the formal single bond. The next pair of orbitals combine to generate the π and π^* orbitals. Notice that the π system generated is the now the HOMO and the LUMO of the new system. Also notice that π is closer to the previous O_p orbital used, and that the π^* system is closer to the C_p

system. This in turn reveals that the HOMO is in principle more similar to the O_p orbital than the C_p and the π^* is thus the opposite.

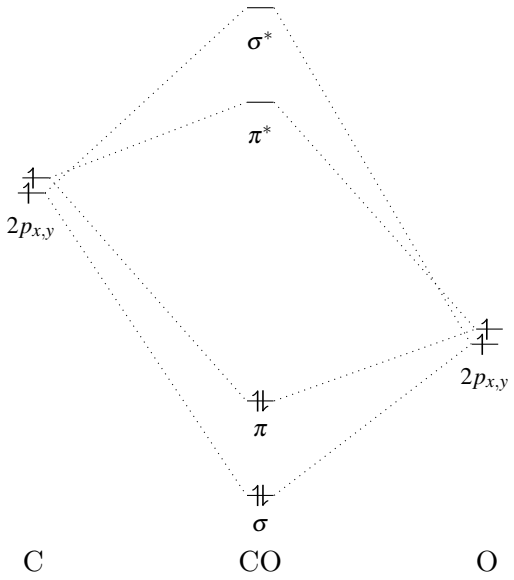


FIGURE 2.32: The combination of the p orbitals on C and O to generate the new σ and π system.

In Figure 2.33 we see the combination of the radical and the π system. On the left side of the figure we see the ground state reaction, on the right the excited state. The idea is that the SOMO interacts with the π system to generate a C−C σ bond, which is low in energy, and a O$\cdot$ which is higher in energy than the C$\cdot$. The bond is formed between the carbon atoms because the radical is closer in energy level to the LUMO than the HOMO and the HOMO sits mostly on the carbon atom.[150] In the excited state the C=O is in the triplet state as seen in the synthesis of oxetanes from carbonyl and double bond systems.[151,152] In this state the double bond is effectively broken, this system closely resembles the intermediate **131** which has the high energy radical on the oxygen atom. This new system allows for the π^* and the SOMO to overlap generating a new σ bond. The oxygen radical energy level is then raised. If we look at the net energies of both systems the excited state system has a much greater lowering of energy than the ground state system. This would explain why the reaction would proceed without light, but is accelerated by the addition of light.

The final ring closure in the synthesis of α-carbolines were shown to be successful with moderate to high yields achieved when the reaction was done with a high pressure mercury vapour lamp. It must be noted the the wavelength of 253 nm emitted by a low

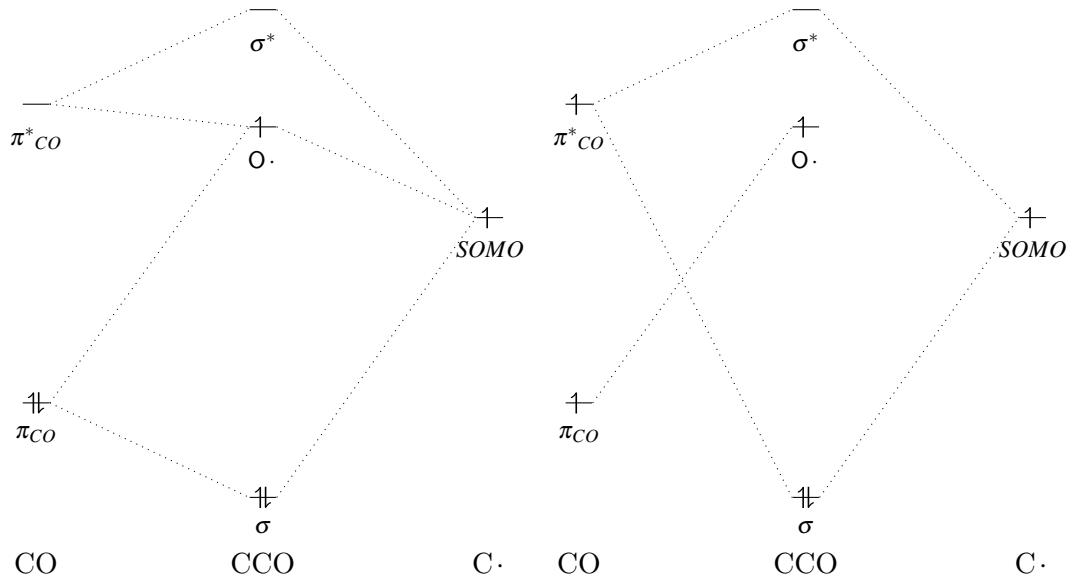
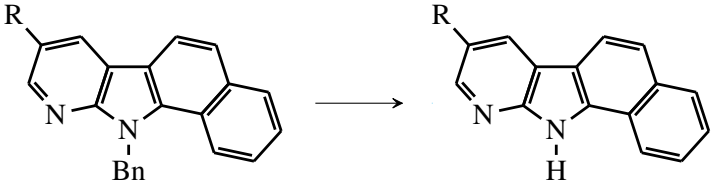


FIGURE 2.33: The interaction of C· and C=O to generate the new C−C bond. The ground state reaction is shown on the left and the $h\nu$ reaction shown on the right.

vapour mercury lamp does not allow for successful transformation to the α-carboline product.

2.2.7 The final benzyl deprotection of 11-benzyl-α-carbolines

The final step in the synthesis of benzo- fused α-carbolines was that of the deprotection of the benzyl group in order to generate the unprotected α-carboline as shown in Scheme 2.26.



R = Cl (**120**→**132**), Me (**121**→**133**), H (**71**→**70**)

SCHEME 2.26: The final debenzylation step toward the synthesis of 11-benzyl-α-carbolines

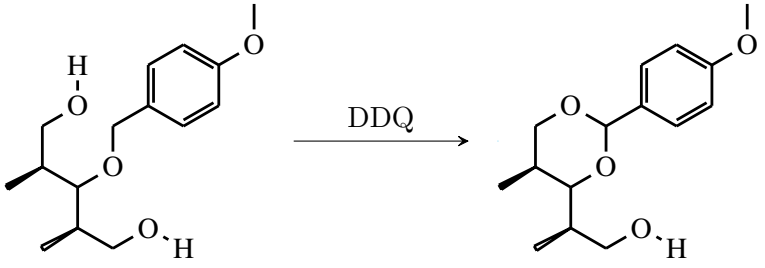
The final debenzylation proved troublesome. de Koning *et al.* removed the benzyl group from protected carbazoles by using $AlCl_3$ in benzene.[89] This method, however, was not successful when used in conjunction with 11-benzyl-α-carbolines. Reacting **71** at room temperature overnight with $AlCl_3$ did not yield α-carboline **70**. This was thought to be

the pyridine nitrogen atom interfering by coordinating with the aluminium present, deactivating the Lewis acid. The reaction mixture was then heated in order to promote the bond breaking required. The reaction proved unsuccessful as decomposition occurred.

Benzyl groups can be removed through reductive processes using palladium on carbon in the presence of hydrogen, and became the focus in the pursuit of producing α-carbolines from the corresponding 11-benzyl-α-carbolines. Basic reductive methods as stated proved unsuccessful. Upon work up only starting material was isolated, and that not all of it was recovered. This suggested that coordination to the palladium was likely, deactivating the palladium and causing no reaction to proceed. The reaction was then tried again with higher catalyst loadings and increased H_2 pressure, all to no avail.

Literature revealed that nitrogen bonded benzyl groups were much harder to de-benzylate than their ether counterparts.[153–155] In this class of nitrogen compounds, aromatic and imadazolic nitrogens are the most resistant to reduction.[153]

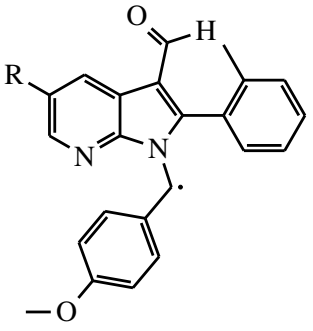
It was then decided to use another protecting group, one which would be easier to remove. The first protecting group attempted was *para*-methoxy-benzyl. The group can be removed through both oxidative and Lewis acid conditions.[156] The protection worked similarly to that of the benzyl protection, however, the *t*-BuOK and light mediated ring closure reaction proved unsuccessful. This is possibly due to the radical nature of the ring closure reaction as the PMB benzylic position is prone to radical oxidation as shown in acetal synthesis using DDQ from the ethers shown in Scheme 2.27.[156,157]



Scheme 2.27: DDQ mediated synthesis of acetals from the PMB ether in diols.[156]

Therefore, in the *t*-BuOK ring closure reaction a radical intermediate (**134**) is expected to be formed as shown in Figure 2.34. This intermediate would not allow for the formation of the desired α-carboline.

Another protecting group that was tested was the Boc group, which can easily be removed with an acid.[156] The *t*-BuOK and light mediated reaction proved unsuccessful



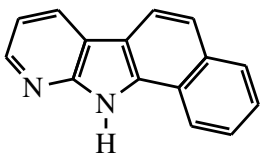
134

FIGURE 2.34: The suspected reactive intermediate **134** formed in the *t*-BuOK ring closure reaction

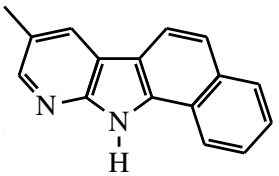
and no α-carboline was formed. Competition between the aldehyde and the Boc group must have resulted in no reaction, as the Boc group is electrophilic even if very sterically hindered. No starting material was recovered.

The next approach was to attempt removal of the benzyl group through oxidative means. In contrast to benzyl ethers, which are easily removed through reductive methods, nitrogen benzylic compounds are more reactive through oxidative means as found by Haddach *et al.*.[153] It was found in the work done in this paper that nitrogen benzylated compounds can be selectively deprotected in the presence of benzyl ethers. The reaction utilises DMSO in the presence of oxygen and *t*-BuOK. The mechanism proposed by Haddach *et al.* is shown in Scheme 2.28. Deprotonation on the benzylic position is first achieved by *t*-BuOK to furnish **135** from **136**. Compound then reacts with O_2 to form **137** which is then reduced by DMSO to form hemi-acetal anion **138**. Hemi-acetals are not stable compounds and react in a reversible manner to form **139** and benzaldehyde.

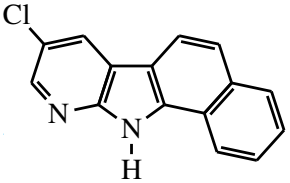
The debenzylation proved successful with only the recovery of the α-carbolines **70**, **133** and **132** with yields shown in Figure 2.35. Low yields were experienced in the reactions due to the small reaction scale worked on and the large degree of insolubility of α-carbolines, making the work up of the reactions difficult.



70
24%

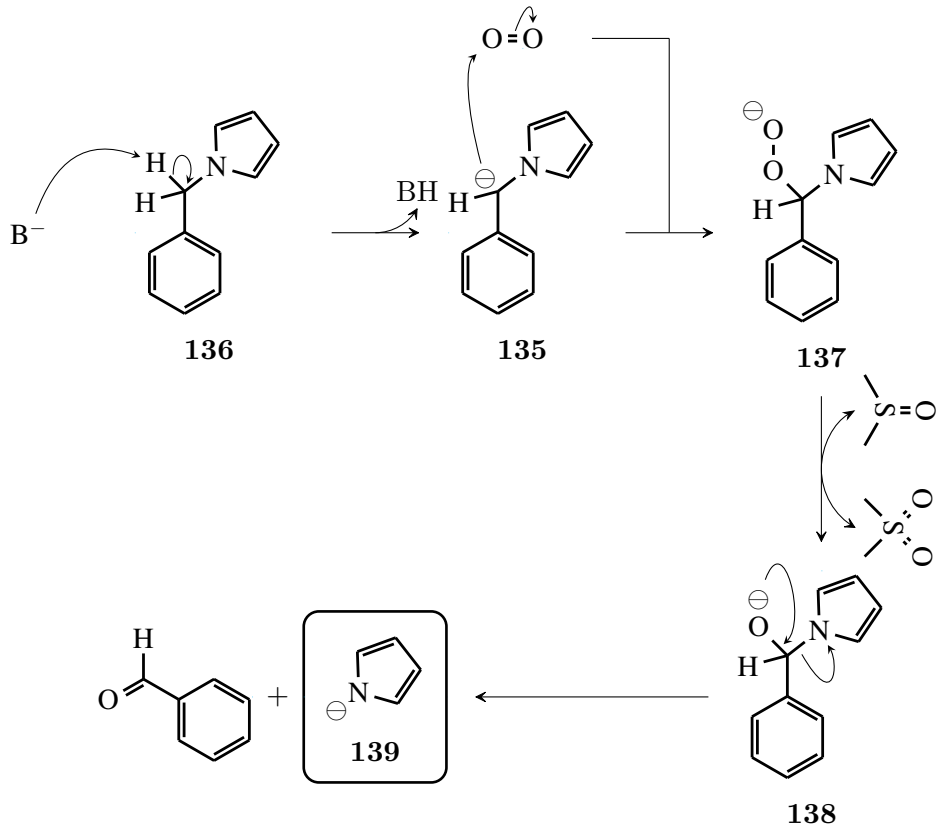


133
18%



132
25%

FIGURE 2.35: Yields of α-carbolines synthesised



SCHEME 2.28: Proposed mechanism of the deprotection of the benzyl group by oxidation with O_2 in the presence of *t*-BuOK and DMSO.[153]

The ^{1}H NMR spectra of α-carbolines showed the disappearance of the benzyl CH_2 peak and the total integration of aromatic protons of 9 or 8 depending on whether the compounds had substitution on the 3 position. The presence of the N-H peak at above 12 ppm was also a confirmation that the reaction had been successful. Figure 2.36 shows the single crystal X-ray structure of **70**. It must be noted that there was a larger degree of difficulty in growing crystals of α-carbolines in comparison to 11-benzyl-α-carbolines as powders would often form. The slow evaporation of solvent over several months was required for the acquisition of a single crystal of sufficient quality to run a XRD experiment.

The total synthesis of substituted α-carbolines was as result of the final debenzylation reaction proved successful. Some modification of the synthetic approach was required, and several reactions were optimised in order to achieve the final desired α-carbolines with the synthetic route shown in Scheme 2.29.

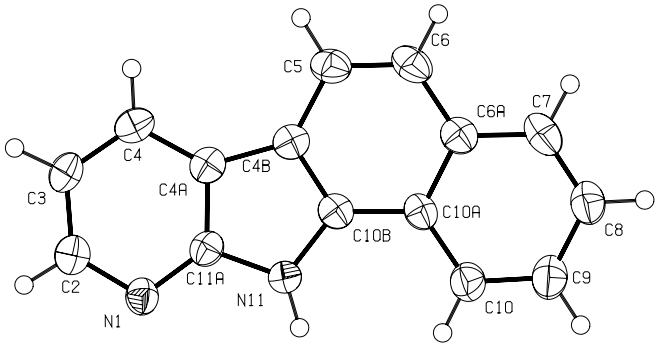
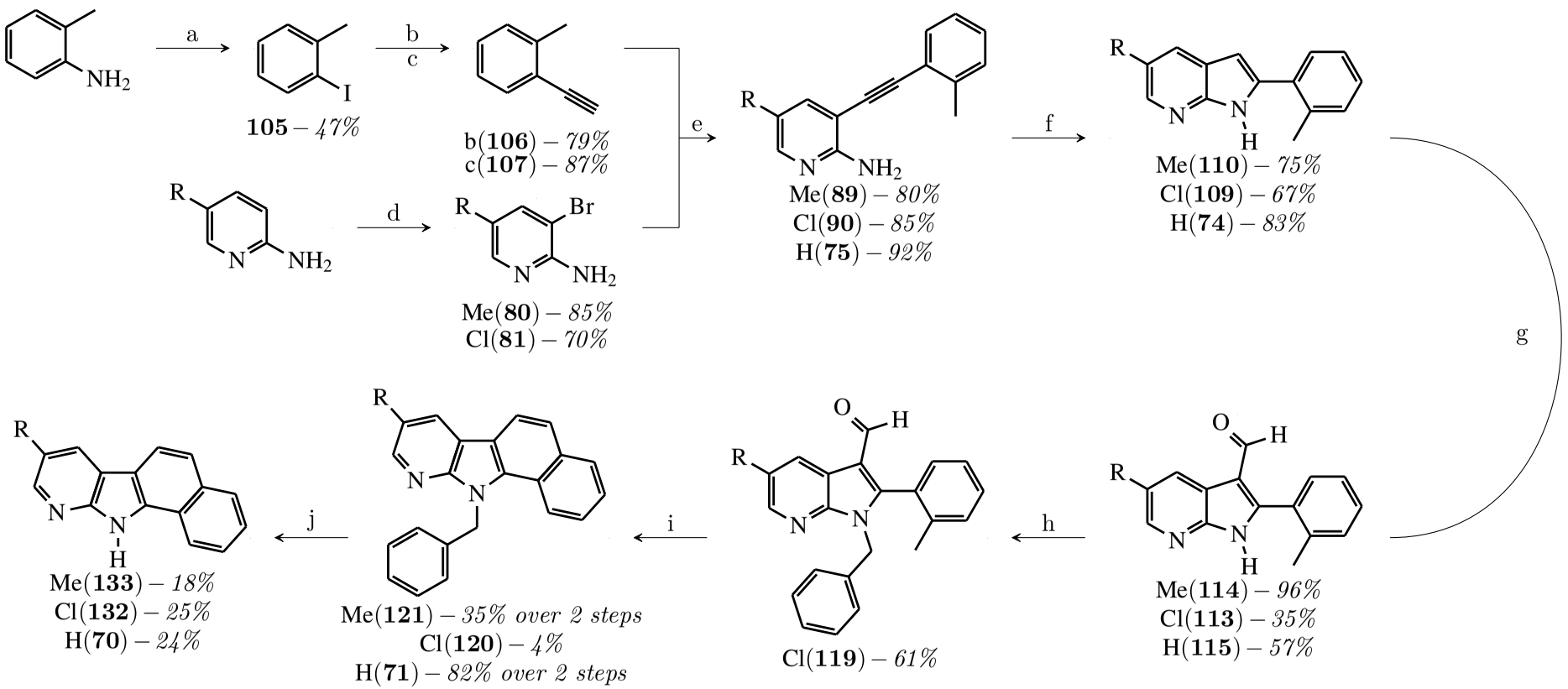


FIGURE 2.36: Crystal structure of **70** drawn with 50% probability ellipsoids - the final product of this synthetic project

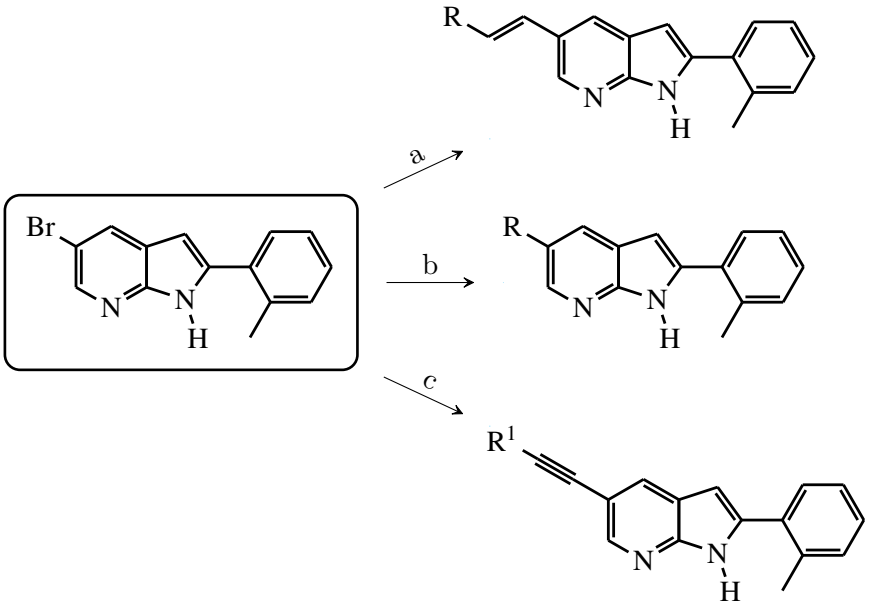


a - 1) H_2SO_4, $NaNO_2$, 5°C 2) KI; b - $Pd(OAc)_2$, CuI, NEt_3, PPh_3, ethynyltrimethylsilane, THF; c - TBAF, THF; d - CCl_3H, Br_2; e - $Pd(OAc)_2$, CuI, DIA, dppf, THF; g - 1) $TiCl_4$, dichloro-methyl methyl ether, DCM 2) water; h - BnBr, KOH, NMP; i - DMF, *t*-BuOK, hν; j - O_2, DMSO, THF;

Scheme 2.29: The final synthetic route for the synthesis of α-carbolines

2.3 Further functionalization of α-carbolines

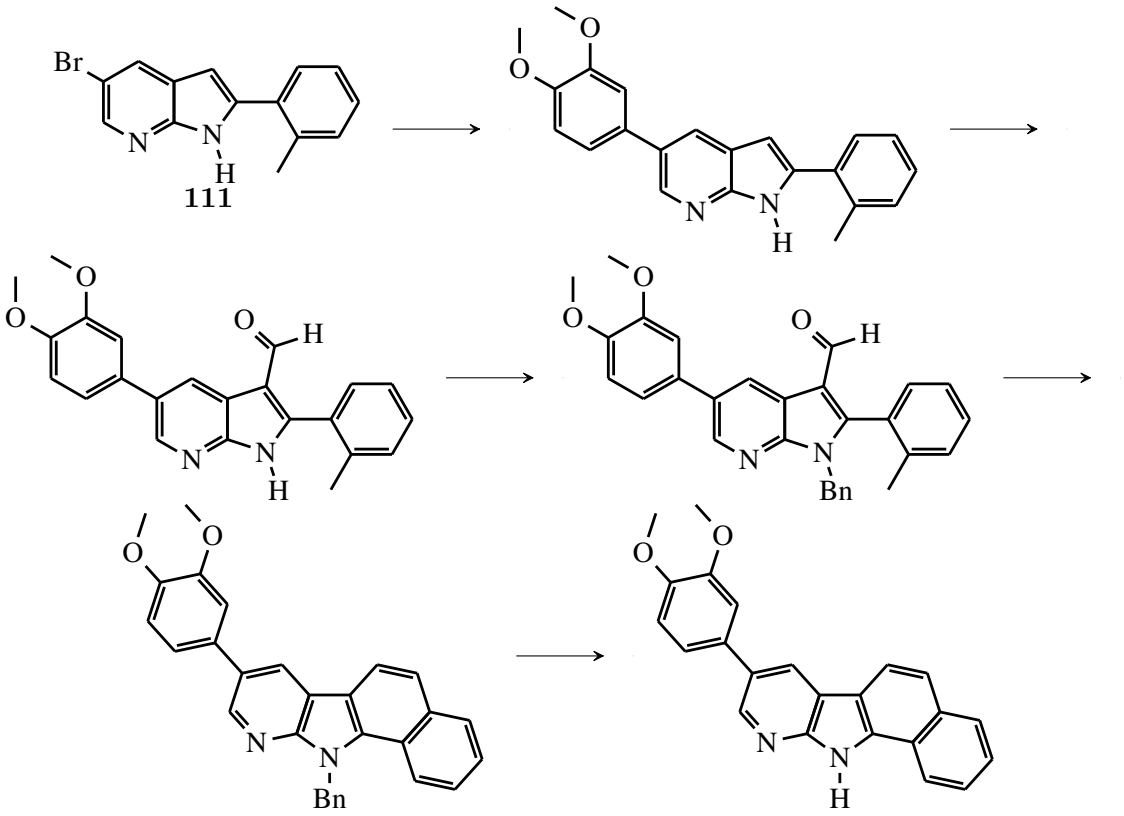
After the initial synthesis was completed and most of the problems successfully solved it was decided to expand on the functionality included on the α-carbolines prepared thus far. The α-carbolines have all been substituted at the 3 position with either a halide, hydrogen or a methyl group. It was then decided to expand the library of α-carbolines through a later functionalization reaction in the synthetic route. A handle was then required on the 2-aminopyridine molecule which could then be transformed into various different functional groups. The handle decided on was a bromine atom. The compound 3-bromo-5-iodopyridin-2-amine (**82**) was already synthesised in the early part of this project, however, taking the synthetic route further as the time was desired. From the radical nature of the light and *t*-BuOK ring closure mechanism it was decided to avoid bromine atom containing molecules in this step. This is because the bromine atom reacts readily with radicals, forming stable radical Br· species which can combine to form Br_2. In the new proposed synthetic scheme the bromine atom would be reacted in a palladium catalysed coupling reaction before the ring closure reaction is performed, therefore preventing any undesired products to form. Coupling reactions that use bromides as substrates include palladium based Sonogashira, Suzuki or Heck coupling reactions as shown in Scheme 2.30.



R - aryl; R^1 - aryl or alkyl
a - Heck coupling; b - Suzuki coupling; c - Sonogashira coupling

SCHEME 2.30: The further functionalization of brominated 7-azaindoles to lead to several analogues through simple palladium based coupling reactions

A single α-carboline target was chosen as proof of concept for this study. It was decided to use an electron rich phenyl ring in the form of 3,4-dimethoxy phenylboronic acid and to utilise the Suzuki coupling reaction. The addition of hetero atoms results in some expected difficulties in the synthesis. If successful, the reaction shows some robustness in the methods used and discussed in this chapter. Electron rich phenyl rings are also prone to oxidation and other effects which could limit their scope, adding further credibility to the synthesis if successful. It has also been shown that having the chloride in the 3 position helps with the benzylation protection reaction, however, the formylation reaction proceeds best when electron donating substituents are present. Therefore, it was decided to attempt the Suzuki coupling reaction before the formylation, as the electron rich phenyl system might improve the formylation reaction as compared to the bromide. A short sequence for the synthesis is shown in Scheme 2.31 with the starting 7-azaindole **111** synthesised with methodology described in this chapter.

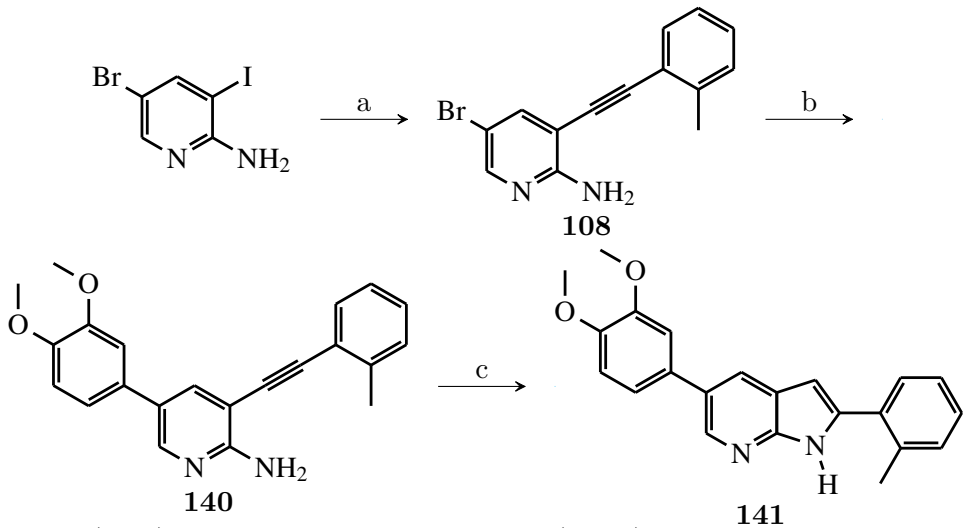


SCHEME 2.31: The synthesis plan for further substitution using the Suzuki coupling reaction

2.3.1 The synthesis of 3,4-dimethoxy substituted α-carboline

The initial synthesis of the substituted 5-bromo-7-azaindole **111** has been covered in previous sections of this chapter and will not be repeated in this section. Unfortunately, the Suzuki coupling reaction of 5-bromo-7-azaindole **111** with 3,4-dimethoxyphenylboronic acid was not successful despite the use of several different strategies. The Suzuki coupling methods utilised include a microwave method, and a conventional heating method.[88,89,158] In both methods there was no product formation and starting material was recovered. Formylation of **111** was then attempted, followed by the Suzuki coupling reaction, which was unsuccessful as before. From the failed Suzuki coupling reactions it was decided to attempt the Suzuki coupling before the ring closure of the 2-aminopyridine to the corresponding 7-azaindole. Substituting two different moieties with two separate reactions has been shown to be successful by Leboho *et al.* in which two Sonogashira coupling reactions were performed. One can substitute the iodide in 3-iodo-5-bromo-2-aminopyridine **82** first, as shown previously in this chapter, by controlling the temperature and using PPh_3 as ligand for the palladium catalyst. The bromide can then be substituted upon heating at reflux in a second reaction with which a second group, different from the first introduced, can be substituted in the 5 position. The first reaction in the synthesis would then be the substitution of the iodide with 1-ethynyl-2-methyl-benzene (**107**) through the Sonogashira coupling reaction as described to give **108**. The bromide will then be displaced in a Suzuki coupling reaction with 3,4-dimethoxyphenylboronic acid forming **140**, followed by a TFAA/TFA ring closure yielding the desired 7-azaindole **141** as shown in Scheme 2.32.

This worked rather well with a yield of 61% for the Sonogashira reaction in forming **108**, and 56% for the Suzuki coupling reaction resulting in **140**. The acid mediated ring closure reaction gave a yield of 80% and was satisfactory. It must be noted that the attempted purification by column chromatography at this stage proved disastrous. The 7-azaindole product showed limited solubility in EtOAc, with generous amounts of solvent required for dissolution. Taking advantage of this the 7-azaindole compounds synthesised throughout this last section were purified by recrystallisation from isopropanol, which had little solubility of compounds at room temperature and sufficient solubility when heated. Silica chromatography was generally avoided as large losses of material precipitating on the silica was noted, even when DCM/Methanol was used as solvent

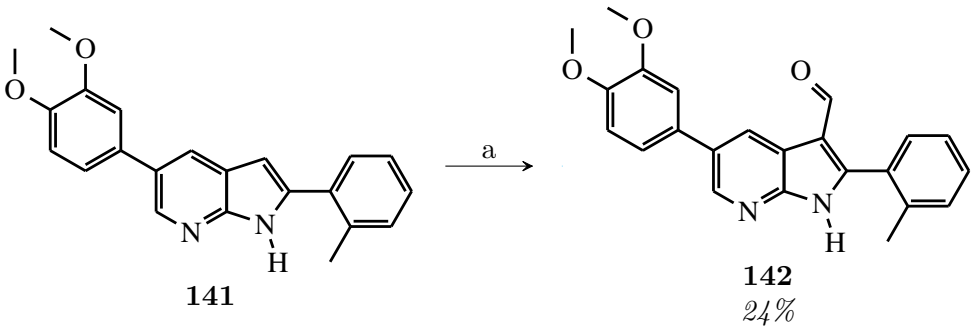


a - $Pd(OAc)_2$, CuI, DIA, THF, r.t.; b - $Pd(PPh_3)_4$, Na_2CO_3, DME, water, 3,4-dimethoxyphenylboronic acid; c - TFA, TFAA, MeCN;

SCHEME 2.32: The synthesis strategy for the assembly of 6-substituted 7-azaindoles

systems. The typical singlet of C-3 was seen in the down-field aromatic region of 5-6 ppm, and a broad singlet at 13 ppm (N-H, 1H) showing the formation of the indole ring, as well as the presence of two singlets, each integrating for 3H in the methoxy region.

The formylation of **141** with dichloromethyl methylether and $TiCl_4$ was the next reaction in this synthetic route with **142** isolated in a yield of 24% as shown in Scheme 2.33

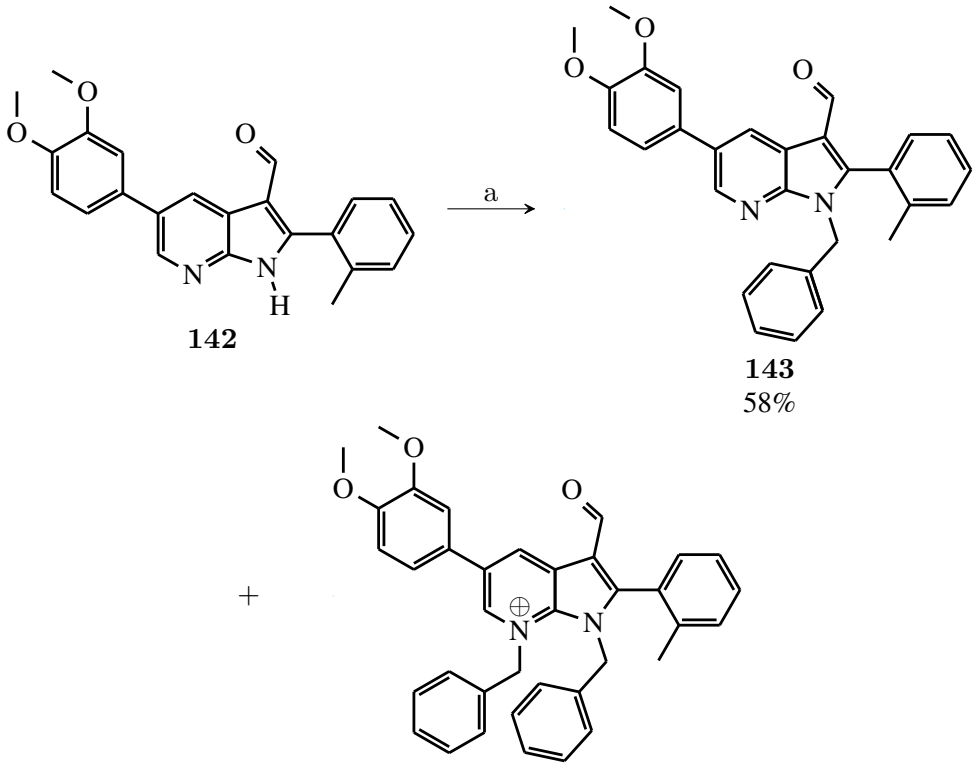


a - 1) Dichloromethyl methylether, $TiCl_4$, DCM 2) water

SCHEME 2.33: The formylation of azaindole **141**

The modest yield from the formylation reaction was unfortunate, with no improvement of yield seen when the reaction was repeated. The NMR spectrum showed the expected aldehyde peak close to 10 ppm, proving the synthesis of **142** successful.

The benzyl protection of **142** gave a 58% yield of **143** with some isolation of some dibenzylated product as shown in Scheme 2.34.



142 **143** 58%

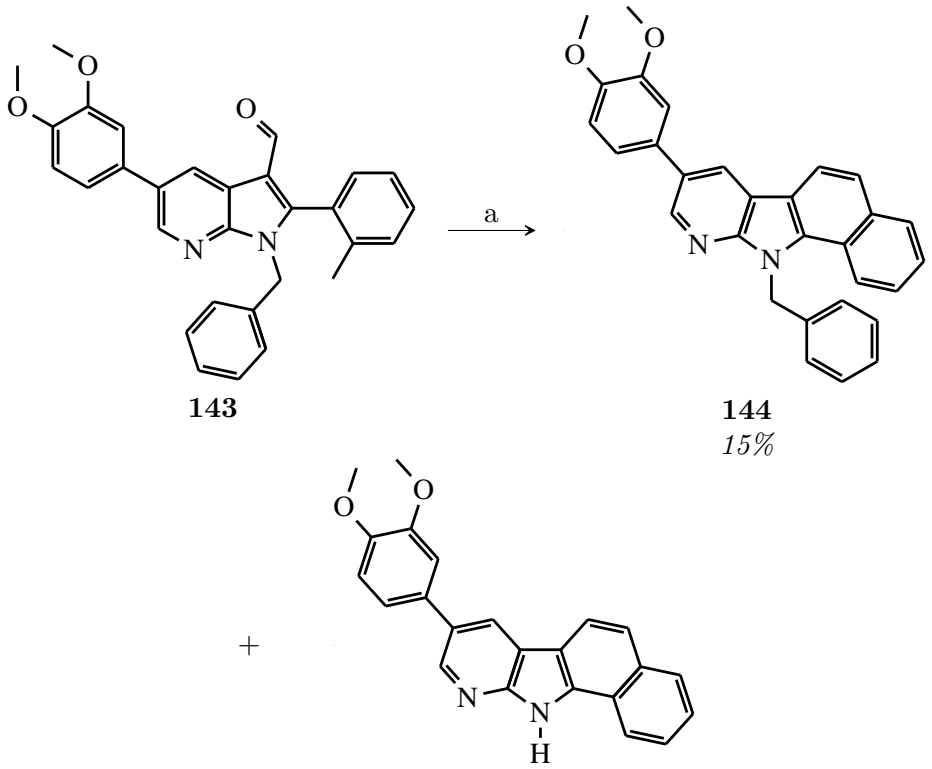
a - NMP, KOH, BnBr

SCHEME 2.34: Benzylation of **142**

The ^{1}H NMR spectra show the typical CH_2 peak at 6.01 ppm, a singlet integrated for 2H and the removal of the N-H proton that is at 11.20 ppm in **142**.

The final ring closure reaction of **143** was attempted with the low pressure mercury lamp available. The reaction proceeded differently as seen to the other α-carbolines synthesised as both the desired ring closed product **144**, as well as the unexpected debenzylated ring closed product **143** was isolated as shown in Scheme 2.35. This was a rather interesting result.

As discussed the 253 nm of the low pressure mercury lamp encourages decomposition and is not in the optimal range for aldehyde bonding electron excitation, as shown in the low yields observed. The debenzylation of **145** into **144** shows that oxygen had not been completely excluded from the reaction performed, effectively producing oxidative conditions as seen in the oxidative debenzylation reaction performed and discussed. A crude work up was done, and the material washed with isopropanol and dried. A crude ^{1}H NMR spectrum was then acquired showing no starting material (easily observed by the aldehyde and methyl peak from **143**) and the a mixture of both **144** and **145**, in which the latter was readily recognised by the N-H peak at 12.81 ppm.



SCHEME 2.35: The formation of α-carbolines **145** and **144** by the ring closure reaction under UV and *t*-BuOK conditions from **143**

The mixture was separated by silica chromatography with DCM and methanol, after which the silica was washed with a DMF/DCM solvent mixture removing any **144** that had crystallised off the column (50% of **145** isolated). The clean ^{1}H NMR spectrum of **144** and **145** confirmed the earlier assumption of two products from the reaction, as the characteristic N-H signal was present in **145** and the benzylic CH_2 at 6.34 ppm in **144**.

A small portion of the crude mixture obtained from the ring closure reaction discussed was then dissolved in THF and DMSO and *t*-BuOK added and stirred under bubbling of O_2. It was noted that the solubility of this crude mixture was poor. A ^{1}H NMR spectrum of the crude mixture showed no change in the ratio of compounds **144** and **145**. The reaction was then attempted with pure **144** whereupon no de-benzylated product **145** was formed. It was concluded that solubility had been the main reason for the poor reaction results. However, since synthesis route goal compound **145** had formed in the light mediated ring closure reaction the synthesis was still seen as successful, even if the last reaction failed.

2.4 Conclusion

The light mediated reaction in which carbazoles and α-carbolines are formed has proven to work on this range of compounds, further showing the potential of this reaction in other areas of organic synthesis. The Sonogashira reactions utilised proved incredibly powerful and key in the synthesis of α-carbolines and other 7-azaindole related molecules. The debenzylation step proved problematic when using traditional methods (reductive debenzylation as well as lewis acid methods). The use of oxidative methods mostly solved this issue, even though the debenzylation reaction in the formation of **145** had failed.

The further substitution of α-carbolines proved successful, palladium catalysis can be utilised in the C-C bond forming step and other palladium based reactions could be used to great success. The substitution, however, is limited to the 2-aminopyridine molecule, and should therefore be done before the 7-azaindole ring closure formation step. Almost all the reactions for this synthetic route proceeded, with the exception of the oxidative debenzylation reaction due to solubility problems, showing that there is some robustness in the synthesis used, giving the method a potentially large scope.

The synthesis of α-carbolines using novel methodology was successful, allowing the synthesis of several molecules that can be tested for biological activity.

Chapter 3

Modification and biological activity evaluation of 7-azaindoles

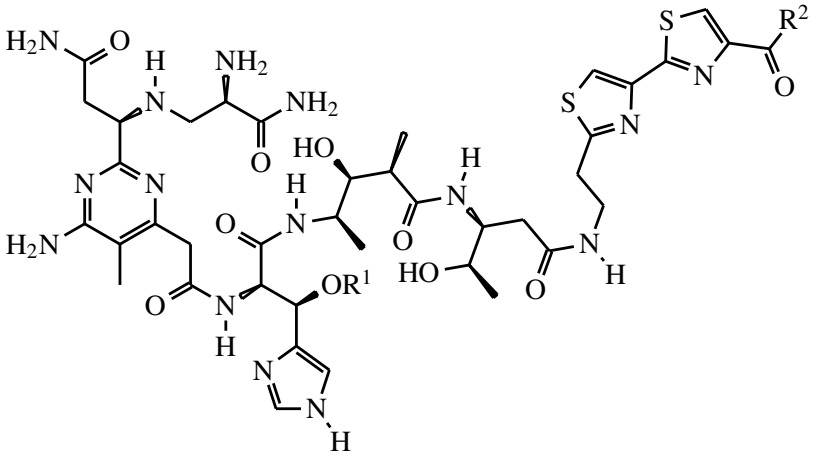
3.1 Introduction

3.1.1 Hybrid compounds in medicine

Hybrid compounds are compounds that contain more than one active pharmacological core. These hybrid compounds show significant improvement in activity over compounds that only contain one active pharmacological core. The fight against malaria, African sleeping sickness and cancer is riddled with drugs that are ineffective, old, toxic and consequently growing resistance. Very active compounds can have side effects due to toxicity to healthy cells or other such draw backs, whereas those compounds which seem to have little side effects do not have much activity at all. Selectivity and ease of treatment is not a reality today. This can be observed in the activity of platinum complexes in the treatment of cancer. When the metal is coordinated to small organic ligands instead of ammonia as is on cisplatin, the activity drops significantly. In African sleeping sickness, the drug melarsoprol contains arsenic and displays adverse side reactions. Malaria, the adaptable epidemic renders drugs ineffective in short periods of time. It seems, that the dream is tantalisingly out of reach, therefore, novel approaches are essential.

One approach utilised is the use of "hybrid compounds". These drugs are multi-faceted and have more than one biologically active domain. Each region acts as a separate pharmacophore, and so acts independently of the other.[124] Most hybrid drugs are generally two small organic molecules bound by a linker. Some examples include are bleomycin (**146**) and DU1302 (**147**).

Bleomycin as shown in Figure 3.1 is an effective anti-cancer agent that was first isolated from *Streptomyces verticillus* and shows the power of having multiple biologically active units on a single molecule.[124] The method of biological action is believed to be the induction of DNA strand breaks, and oxidative RNA degradation.[160]



146

Bleomycin

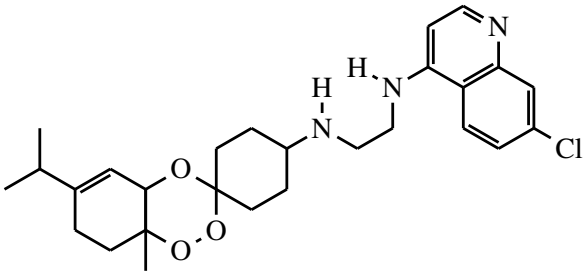
$R^1 = L-gulose-D-mannose$

$R^2 = -NH-(CH_2)_4-NH-C(=NH)-NH_2$

FIGURE 3.1: Bleomycin with its metal binding domain (pyrimidine core); cell penetration domain (R^1); and DNA binding domain (bis-thiazole unit);

DU1302 (**147**) as shown in Figure 3.2 is an anti-malarial drug that has two separate domains. The quinoline domain with which malaria species has developed resistance against and a trioxane domain which operates by a different mechanism. The drug showed effectiveness against a resistant strain of malaria parasite.[124]

The expansion of this idea to metal containing coordinating compounds is a logical next step. Metals are a crucial component to many enzymes and show powerful redox activity. Their activity in general is not very selective, and many metals have been found to be poisonous, causing a great deal of harm when ingested or injected. Some metals such as copper and iron are required for normal biological function, however the regulation in uptake and cell concentration is critical for cell viability. When metals are introduced



147
DU1302

FIGURE 3.2: The anti-malarial drug DU1302 with the quinoline and trioxane units.

into the body for the treatment of diseases their selective uptake of the non-somatic cells and parasites in the body is important. Many cancer related chemotherapies using platinum containing complexes are good examples. Using metals in hybrid molecules can have advantages, especially if both the metal and organic ligand act through separate pathways. The metal with its broad range of activity can be released from the labile/semi labile ligand in the areas where the action is required, giving them lower general toxicity. The organic ligands acting as the carrier, once released can act at a specific target site, bringing about the required effect. The benefit of using this approach is that a linker molecule is not required as with the organic hybrid molecules and due to separation of the metal core and the ligand the activity of each subunit can be well established independently from one another. In the case where the ligands are not very labile, the coordinated metal might show some interesting activity, perhaps enhancing its function in disruption in the cell, for example stopping chelating agents that can remove it from the cell in order to regulate its concentration. It must be noted that through this approach drug resistant diseases have been treated with a hybrid molecule containing the original core for which resistance was shown. Resistance against these types of hybrid drugs is less likely as resistance against both pharmacophores is required to stop the action of the metal-organic ligand complex, showing potential in fields such malaria where resistance is a chronic problem.[125]

An example of such a metal containing drug was published by Cafeo *et al.* who linked platinum to a calixpyrrole sub-unit as shown in Figure 3.3. Calixpyrroles have been shown to bind to anions and so attracted some attention as a possible delivery system for bringing the active platinum to the DNA which is rich in phosphates and other bases. In the study, apoptosis was shown to be induced in cancerous cells and was shown to be more active than cisplatin which was used as the benchmark.[161]

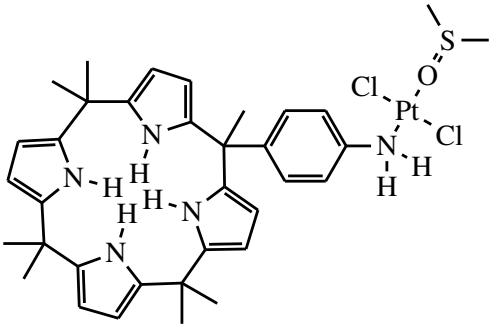
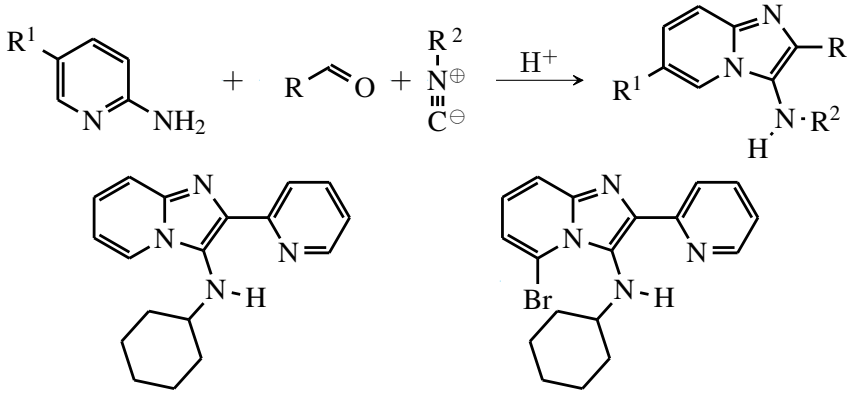


FIGURE 3.3: Calixpyrrole linked to platinum as a metal containing hybrid molecule

A more recent study into this domain was done in our laboratories in which imidazo[1,2-*a*]pyridines were synthesised and coordinated to several metals.[162] The library of imidazo[1,2-*a*]pyridines synthesised utilised the Groebke–Blackburn–Bienaymé reaction that allows for the reaction of an aldehyde, isocyanide and 2-aminopyridine as shown in Scheme 3.1. This method is powerful and allows the generation of highly functionalised compounds in a one pot reaction as shown in Scheme 3.1.



SCHEME 3.1: General method used in the synthesis of imidazo[1,2-*a*]pyridines by Dam *et al.*

The copper complexes synthesised utilised the library of imidazo[1,2-*a*]pyridines made from the Groebke–Blackburn–Bienaymé reaction, and showed good anti-tumour activity against HT-29 and Caco cell lines. The imidazo[1,2-*a*]pyridines were also reported to be coordinated to zinc and copper, with the copper complexes showing increased activity and general lower cytotoxicity. The activity of the complex was greater than that of the copper salt used in the complex formation and the organic molecule coordinated and showed a synergistic effect. The most active complex is shown in Figure 3.4

The 7-azaindole core, with its many nitrogen atoms has the potential to act as a ligand in coordination, fit as a prime candidate in this kind of hybrid molecule study in which

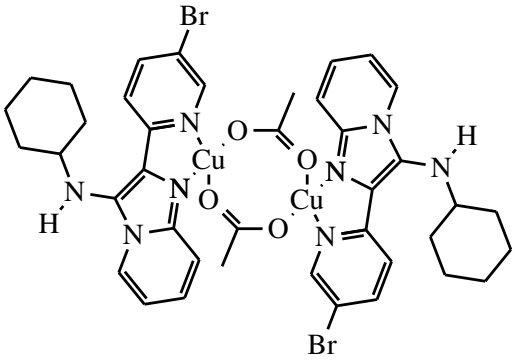
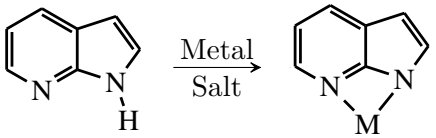


FIGURE 3.4: The hybrid copper and imidazo[1,2α]pyridine complex synthesised by Dam *et al.* which shows synergistic effects against several cancer cell lines

metals can be incorporated. The nitrogen atoms in the 7-azaindole core are in close proximity, allowing for chelation with a metal atom as shown in Scheme 3.2 It was in our interest to study the biological activity of this class of compounds.



M - Metal

SCHEME 3.2: The proposed coordination of 7-azaindoles with metal ions

3.1.2 From biologically active 2,2^i-bisindole natural occurring compounds to 7-azaindole containing ligands

Introduction

The bisindole moiety is prevalent in nature under a class of carbazoles. The most famous of this class of compounds is staurosporine as shown in Figure 3.5.

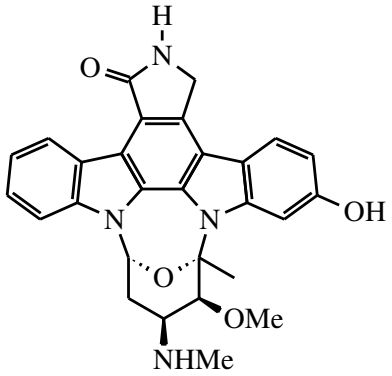


FIGURE 3.5: Staurosporine

Staurosporine itself shows interesting biological activity through having protein kinase C (PKC) activity.[163–165]. Staurosporine induces cascade processes in cells that lead to apoptosis.[166–168] This PKC activity is due to the similarity in structure to metabolites that fit into the ATP binding site of the enzyme.[163] The activity of staurosporine is so general that other kinases have shown to also undergo regulatory activity, including the Ca^{2+}/phospholipid dependent protein kinase.[164] This general activity makes staurosporine a poorly selective molecule showing general cytotoxicity.[169]

The search for more selective and more potent biologically active compounds that are staurosporine derivatives started in 1977, the year of its first isolation in Japan (known as AM-2282) from the bacterium *Streptomyces* found in a soil sample.[170] The complete structure elucidation of staurosporine was achieved in 1994 when the stereochemistry was determined by X-ray crystallography.[171] The first total synthesis was first published in 1995.[172] This synthesis incorporated two indole molecules reacted with dibromomaleimide **148** through Grignard type chemistry to form **149**. The sugar moiety **150** was then added and the final ring closure to form the carbazole **151** was done by utilising oxidative chemistry through hν and iodine as catalyst as shown in Scheme 3.3.

In the last decade a more selective staurosporine analogue midostaurin (PKC412) was synthesised and proceeded far through clinical trials.[173] Midostaurin has a modified sugar moiety which includes a benzamide as shown in Figure 3.6

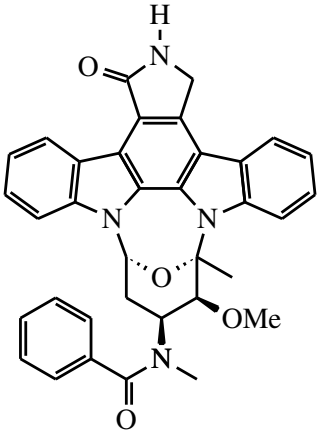
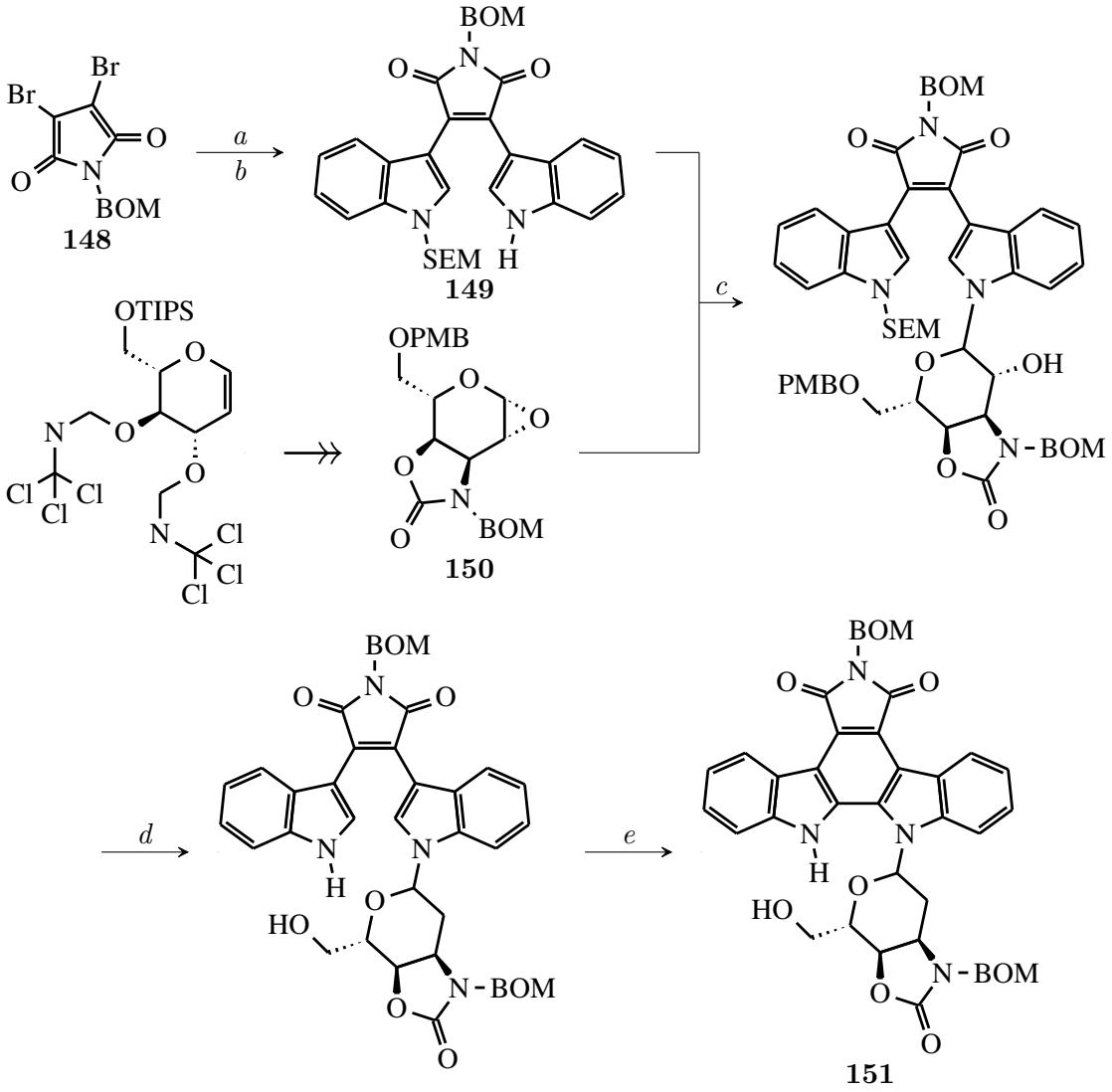


FIGURE 3.6: Midostaurin

Further, the molecule rebeccamycin shown in Figure 3.7 which has a similar core to staurosporine has also shown some significant biological activity.[174,175]



a - Indole Grignard; *b* - 2-SEM-Indole Grignard; *c* - NaH; *d* - (i) Thiophosgene, DMAP, C_6F_5OH (ii) Bu_3SnH, AIBN (iii) DDQ; *e* - I_2, air, *hv*

SCHEME 3.3: First reported synthesis of Staurosporine (1995) with some of the key steps involved, namely the introduction of the indole groups (*a, b*) and the oxidative ring closure (*e*)

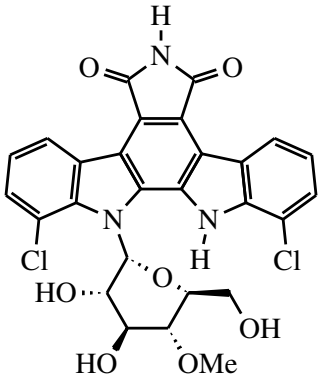
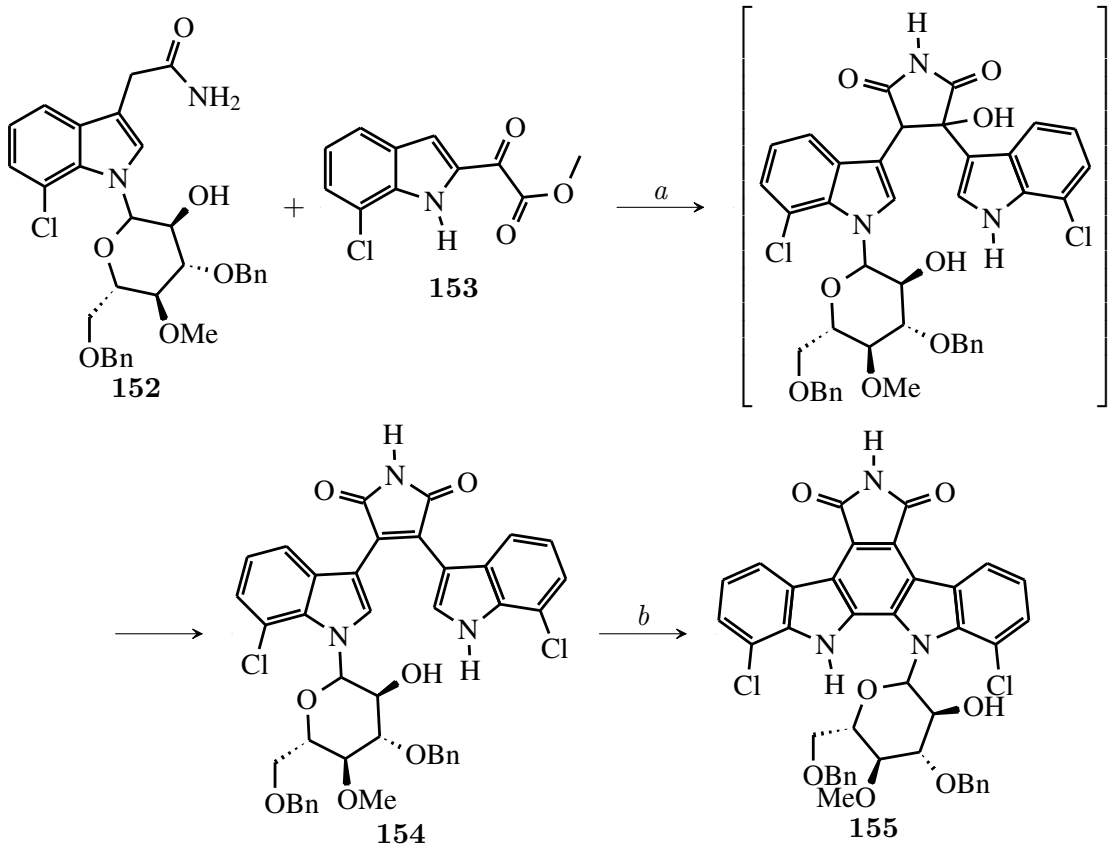


FIGURE 3.7: Rebeccamycin

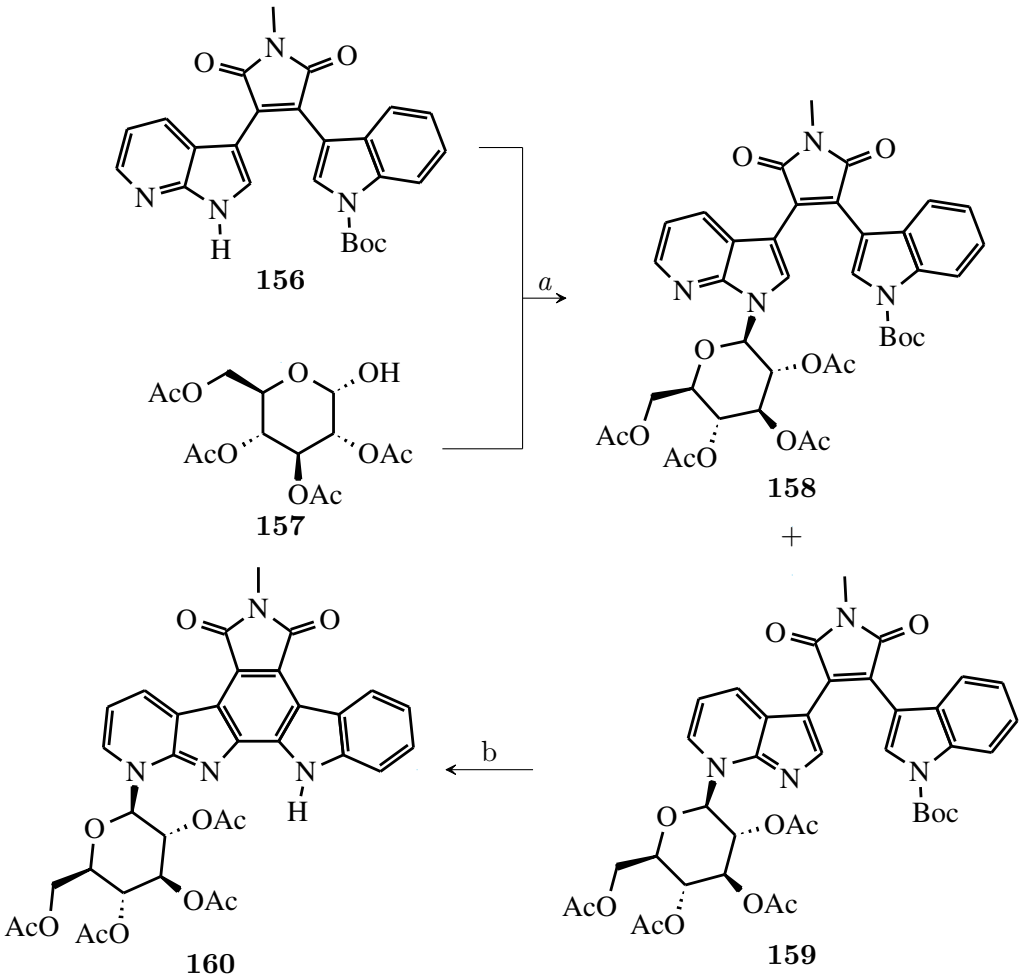
The synthesis approach is much similar to that shown in Scheme 3.3 with some minor difference such as using palladium to perform the oxidative cyclisation reaction to form the aromatic core. One paper describes the condensation of **152** and **153** to afford **154** followed by oxidative cyclisation to give **155** as shown in Scheme 3.4



Scheme 3.4: Synthesis of Rebeccamycin showing key steps

7-Azarebeccamycin as also been synthesised using similar approaches to that of the rebeccamycin and staurosporine syntheses described and is shown in Scheme 3.5.[176]

The synthesis of 7-azarebeccamycin starts with the condensation of azaindole **156** and carbohydrate **157** to afford **158** and **159** as a mixture. This is followed by deprotection of **159** and light mediated ring closure in the presence of I_2 to give ring closed carbazole **160**. 7-Azarebeccamycin shows cancer activity through both Chk1 inhibition and DNA binding.



a - DIAD, THF, PPh_3; b - (i) HCO_2H, (ii) hν, I_2

SCHEME 3.5: The synthesis of 7-azarebeccamycin

Aglycones of staurosporine

Even though most natural products isolated in the staurosporine class of compounds have a carbohydrate moiety included in the structure, this is by no means necessary, as compounds such as aglycone arcyriaflavin B (**161**) have been isolated and is shown in Figure 3.8.[96,177] It was isolated from the fruiting bodies of the slime moulds of *Arcyria denudata*, arcyriaflavin B and has a red colour and pigments the fruiting bodies. The structure is analogous to that of staurosporine and rebeccamycin, where the crucial difference is the absence of the carbohydrate. The biological activity of arcyriaflavin B was established through activity against *Bacillus brevis* and *B. subtilis*. Therefore it is seen that even in the absence of the carbohydrate the biological activity is still present.

Another important carbazole is K-252c better known as staurosporinone is the aglycone of staurosporine. This is thought of as a synthesis precursor of staurosporine and has

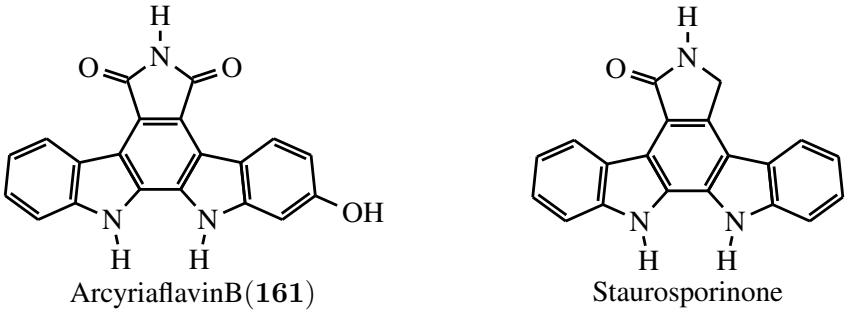
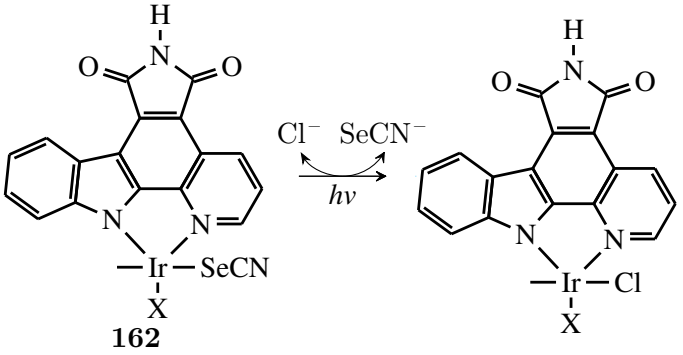


FIGURE 3.8: Arcyriaflavin B and staurosporinone

received some interest with several syntheses over the years.[178–182]

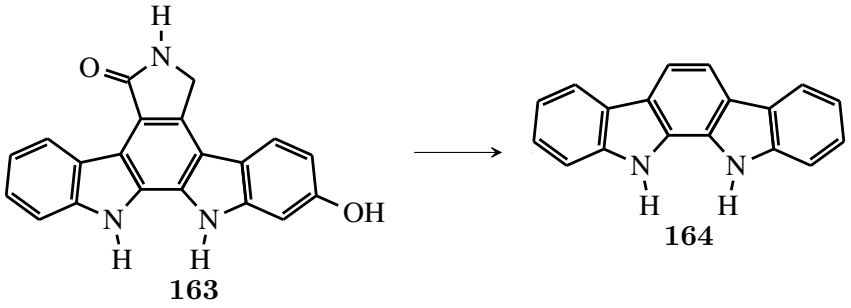
There has been development engaging in the further development of the carbazole core with the coordination of metals, such as iridium by Kastl *et al.* in which an indole is substituted by pyridine to aid in chelation.[183] Iridium complex **162** showed some activity against cancer cell lines (IC50 of 8 μM), however, when the cell culture in the presence of **162** is irradiated with light, a great improvement of activity with an IC50 of 0.8 μM is seen. The mechanism of action for **162** is believed to be the release of $SeCN^-$ through the substitution with a chloride ion as shown in Scheme 3.6. The $SeCN^-$ released causes distress in the biological system present, increasing the activity of the complex in addition to the activity of the biologically active organic ligand.



SCHEME 3.6: The mechanism of action for iridium complex **162**

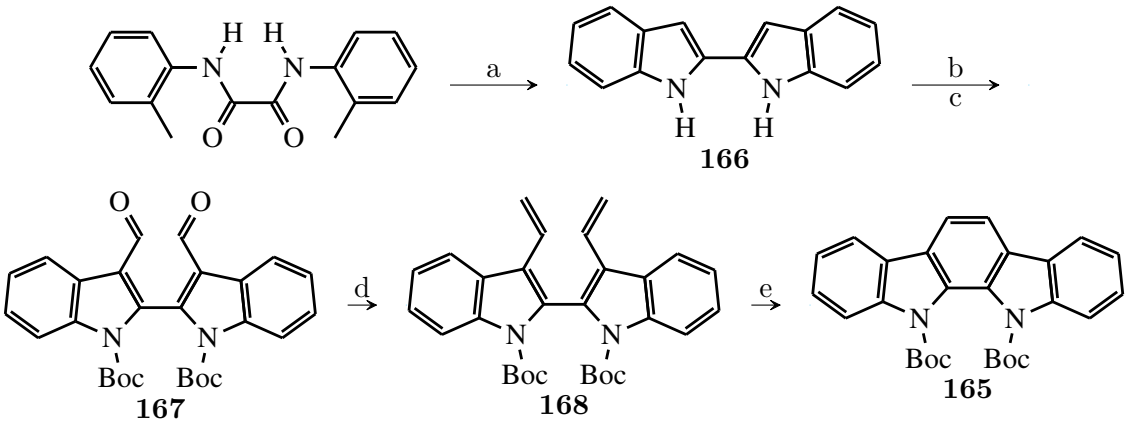
Further simplification of the staurosporine structure to a carbazole

Further simplification of the staurosporine core leaves the carbazole core. Research on this subunit ties into the theme of this thesis which is the synthesis of azaindole containing compounds. Research done by Pelly *et al.* at this university in this field allowed for the synthesis of the carbazole **165** by utilising metathesis.[184] Their synthetic method



SCHEME 3.7: The simplification of the Staurosporine molecule to give the aromatic core

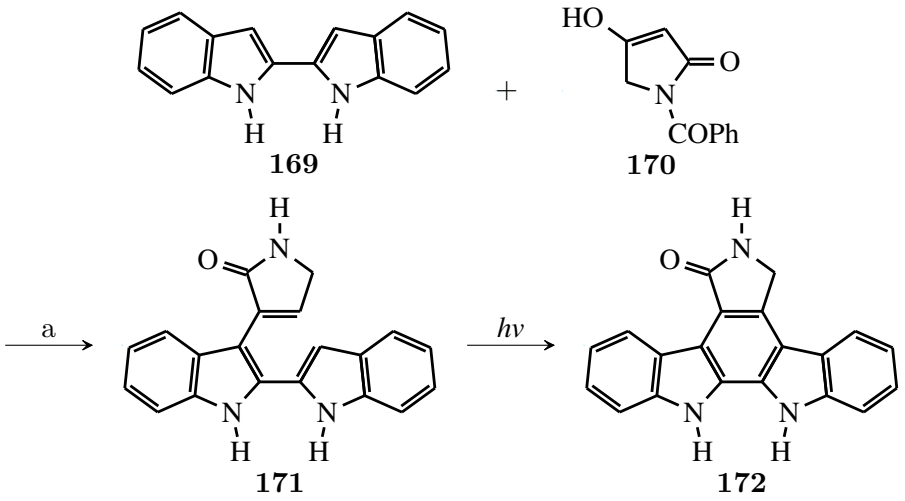
incorporated the formation of the bis-indole core **166**, followed by formylation to give indole **167**. Which then underwent a Wittig transformation to afford the diene compound **168**. Metathesis on diene **168** formed the carbazole **165** as shown in Scheme 3.8.



a - Microwave, base; b - 1) DCM, $POCl_3$, DMF, 2) water, NaOH; c - Boc_2O, THF, DMAP; d - base, $MePPh_3^+$ Br^-; e - Grubbs I catalyst;

SCHEME 3.8: The synthesis of the carbazole core by Pelly *et al.* using metathesis methodology.

The synthesis of staurosporinone aglucone through the use of a bis-indole containing compound has also been recorded.[178] This synthesis includes the coupling of the bis-indole **169** with tetramic acid **170** to afford bis-indole **171**. Ring closure of **171** with light yields carbazole **172**. This type of coupling adds the two rings to the bis-indole core in two steps as shown in Scheme 3.9



a - $BF_3 \cdot OEt_2$, DCM, molecular sieves

SCHEME 3.9: The synthesis of staurosporinone through the use of bis-indole as the starting core.

The transformation to the bis azaindole system

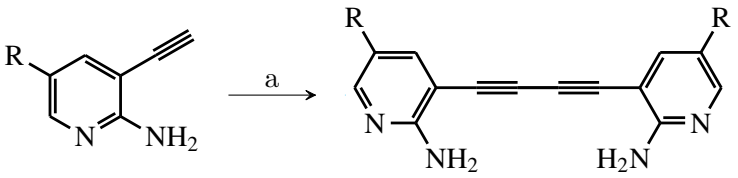
As shown in Scheme 3.8 the formation of bis-indole systems are beneficial to the synthesis of the greater structure of natural products such as staurosporine, rebeccamycin and other biological compounds that fall in between in complexity. The central idea of this study is to transform this concept to that of the azaindole system. The ground work for more complicated systems will be done together with biological studies of these basic core molecules to try and investigate activity and selectivity.

3.2 Synthesis of coordinating ligand

Bis 2,2^1-7-azaindole system

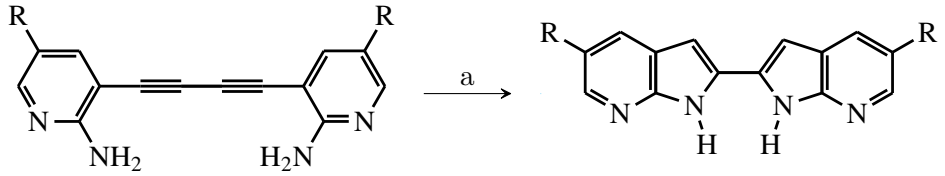
The synthesis of bisazaindoles was initially built on the work covered in the previous chapter through the incorporation of a copper mediated oxidative homo-coupling acetylene reaction.[139] This would take the functionalised 3-acetylene 2-aminopyridines **173** and generate a library of bis-acetylenes **174** as shown in Scheme 3.10

A further ring closure reaction using TFA/TFAA on **174** would then generate the respective bis azaindole **176**.[123] This is shown in Scheme 3.11



R = H (**76**→**93**), Cl (**87**→**92**), Me (**86**→**175**)
a - $Cu(OAc)_2$, piperidine, acetonitrile, air.

SCHEME 3.10: Dimerisation of 2-aminopyridines as a bis azaindole precursor



R = H (**93**→**177**), Cl (**92**→**176**), Me (**178**→**175**)
a - Acetonitrile, TFA, TFAA.

SCHEME 3.11: Ring closure on bis acetylene compounds in the formation of bis azaindoles

The dimerisation of **76** and **87** proceeded smoothly. A yellow precipitate formed in both cases which could be washed with DCM to remove any impurities. The absence of the acetylene peak in ^{1}H NMR spectra and the indication of dissimilar aromatic proton environments due to limited rotation indicated the compounds successfully synthesised. It must be noted that a drop in solubility was seen. DMSO was now required to dissolve the sample for NMR spectra analysis and weakly acidic media was found sufficient to fully dissolve the material.

The ring closure reaction to form the bis azaindole compound **176** was found to be successful. The bis acetylene compounds dissolved well in acetonitrile after the addition of TFA and TFAA. The acid-base reaction, forming the aminopyridine trifluoroacetate salt, aids in solubility as the salt formed would have less intermolecular hydrogen bonds, and would now contain a charge causing repulsion between the azaindole molecules. Heating with reflux produced a pale precipitate which could be filtered and washed with a slightly acidic aqueous solution of HCl to remove any excess starting material. This proved ominous, as solubility of the product was poor. The precipitate had formed a powder similar to brick dust and the only analysis used successfully on the synthesised material was that of solid state NMR spectroscopy as shown in Figure 3.9. It was found that the ^{13}C NMR spectrum showed similar shifts to that of other 7-azaindoles synthesised. The drop in solubility and the NMR spectral evidence was convincing

enough to conclude that the desired bis-azaindoles were synthesised.

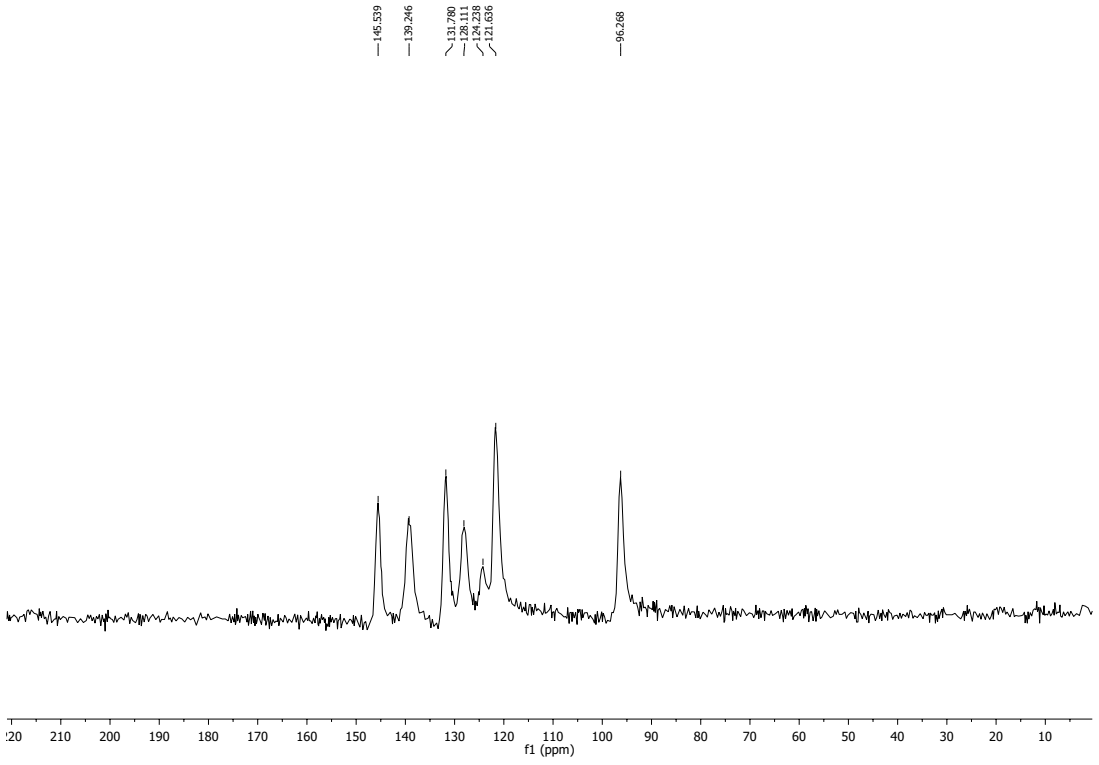


FIGURE 3.9: Solid state ^{13}C NMR spectrum of bis-2,2^{i}-(5-chloro-7-azaindole)

The bis(7-azaindoles) **176** were further subjected to highly acidic aqueous solutions of HCl and H_2SO_4 and solvents at high temperatures with little to no evidence of solubility. Aqueous solubility of compounds are necessary to exert some biological function. It was clear that these molecules would show no biological activity due to their lack of solubility.

Due to the solubility problems encountered some other solutions were required in order to progress with this research. Some possible solutions included the protection of the indole nitrogen atom N-1 in order to break the hydrogen bonding and in so doing help with solubility issues encountered. Boc protection of the indole nitrogen atom N-1 did not proceed and starting material was recovered. Hence, more radical solutions were required in order to progress.

Furan containing 7-azaindole systems

It was clear from the research thus far that solubility issues would not allow use of these bis azaindoles for the formation of metal complexes. The problem with 7-azaindoles

and α-carbolines is the strong hydrogen bonding as seen through crystal structures of both the 2-aminopyridines, 7-azaindoles and α-carbolines as noted in Figure 3.10. The acidic proton of H-1 in 7-azaindoles is strongly deshielded in the ^{1}H NMR spectra of these compounds, with a shift above 12 ppm. A more acidic proton would infer a stronger hydrogen–hydrogen accepter bond leading to greater stability.

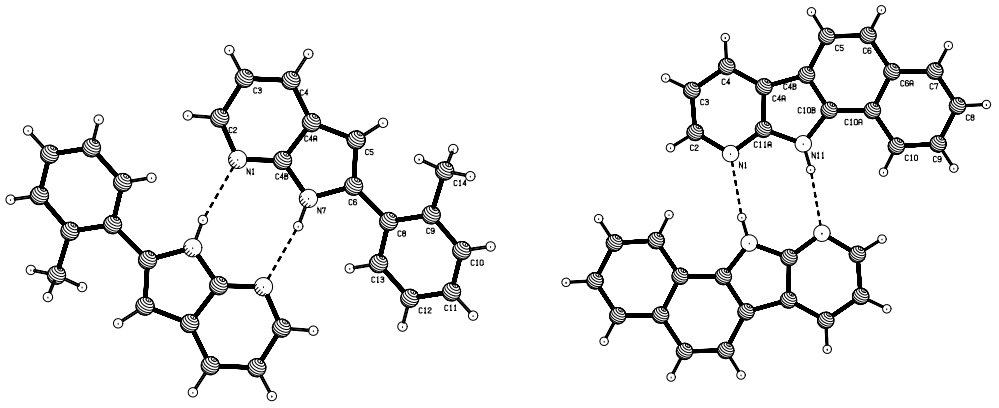


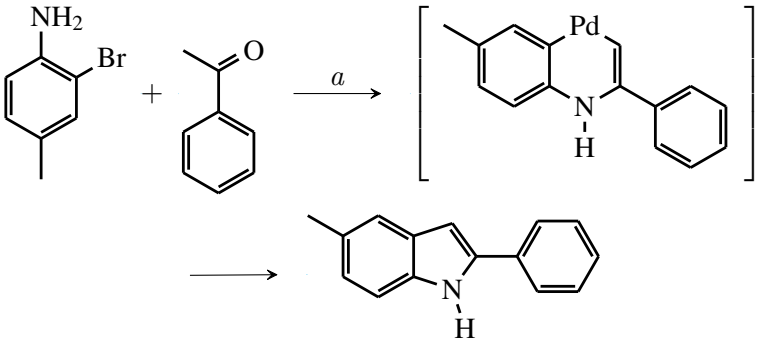
FIGURE 3.10: Crystal structure diagrams of **74** and **70** showing strong hydrogen bonding

Symmetry in molecules affects the melting point and solubility. This is due to the fewer possible arrangements that can be generated when the molecule is rotated and flipped. This would then allow the heterocycle to stay in the crystal structure or localised molecular patterns in solution for longer causing an increase in the melting point and a higher possibility of aggregation in solution lowering the solubility.[185,186]

Several solutions to this problem were obvious, namely the breaking of symmetry and reducing the possible number of hydrogen bonds. The breaking of symmetry would be done by replacing one indole with a furan or benzofuran moiety. We wished to attempt the synthesis on a simple indole containing compounds and then further expanded this to the 7-azaindoles.

There are several synthetic methods that can form the desired indoles in a single step. The first method utilised palladium to condense a 2-bromo-aniline with a ketone as shown in Scheme 3.12.[187]

In our hands several different ligands and palladium precursors were used in conjunction with several different experimental conditions including heating with several different solvents, as well as heating with a microwave, in all cases only palladium black was

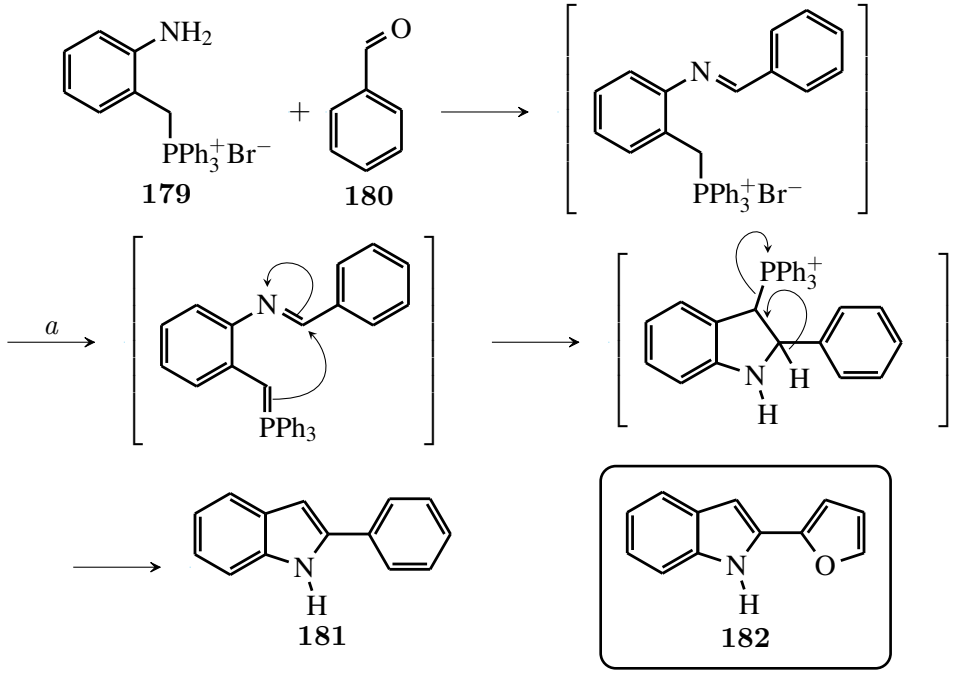


a - Pd^0, Ligand, Base

SCHEME 3.12: The one pot synthesis of indoles utilising the condensation of bromoaniline and a ketone with palladium as catalyst

formed.[187] Non of the procedures tested produced any indole product, even with the testing reaction seen in Scheme 3.12.

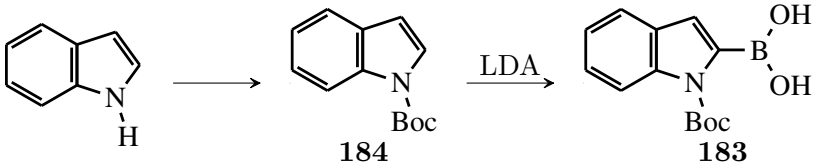
Kraus and Guo have devised a method utilising 2-amino benzyl phosphonium salts.[74] The phosphorus ylide formed under basic conditions from phosphine **179** undergoes a Wittig type reaction with the imine initially formed from aldehyde **180** and after subsequent dehydration forms indole **181** as shown in Scheme 3.13. The paper showed many examples, and in our hands none of them was found to be reproducible. The desired 2-substituted indoles **181** and **182** could not be formed.



a - *t*-BuOK

SCHEME 3.13: The one pot synthesis using 2-amino benzyl phosphonium salts using benzaldehyde as an example and **182** as a second attempted molecule

With the poor results from the one pot synthesis reactions, it was decided to follow a multi-step route where the reactions were easier to track and which utilised reactions performed previously in our laboratory. Initially this would require the synthesis of the boronic acid (**183**) of the Boc protected indole **184** and furan containing a halogen in the 2-position that could undergo coupling with a palladium catalyst. Indole can be converted to the corresponding 2-boronic acid indole through directed ortho metalation (DOM) using lithium diisopropylamide as the metalation agent and Boc behaving as the director as shown in Scheme 3.14.[88] This would then first require the Boc protection of indole to afford **184**.



184 **183**

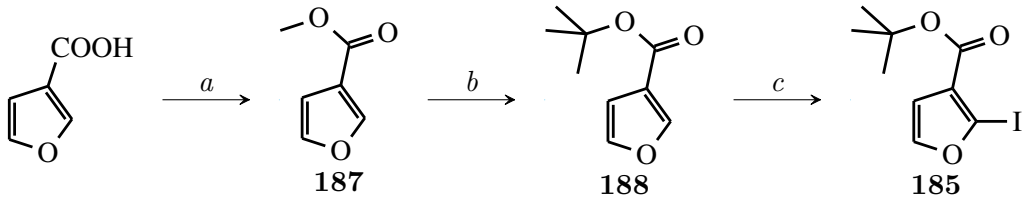
a - Boc_2O; *b* - (i) LDA, (ii) $B(i\text{-}PrO)_3$

SCHEME 3.14: Formation of the boronic acid at the 2 position of indole

The Boc protection reaction of indole was performed as described in the literature and was high yielding with a quantitative yield observed.[89] The lithiation and transformation to the indole boronic acid gave varying yields of between 90% and 40% depending on the quality and concentration of the butyl lithium and the scale the reaction was performed on. It must be noted that great care must be taken in drying the diisopropyl amine for the reaction, as the moisture content increases easily when exposed to air.

The synthesis of the furan **185** and benzofuran **186** took two separate routes. The furan moiety chosen was the 3-carboxylic substituted furan as this was available at the time in sufficient quantities. The iodide was introduced through a DOM reaction using butyl lithium at -100 °C. However, this required the transformation of the carboxylic acid functionality to a *t*-Bu-ester group that can withstand butyl lithium due to the groups bulkiness. The lithiated furan can then react with iodine to yield **185**. The reactions used are shown in Scheme 3.15 with the synthesis of **185** through first forming the methyl ester **187** by an esterification reaction using H_2SO_4 as catalyst (52%), followed by *t*-BuOK to transform the ester to the *t*-Bu functionality to yield furan **188** (40%). If acid catalysis together with *t*-BuOH was utilised this would generate large amounts of $t\text{-}Bu_2O$ due to the ease at which the carbocation is formed due to the stabilisation introduced by the methyl groups on the tertiary carbon. By first forming the methyl

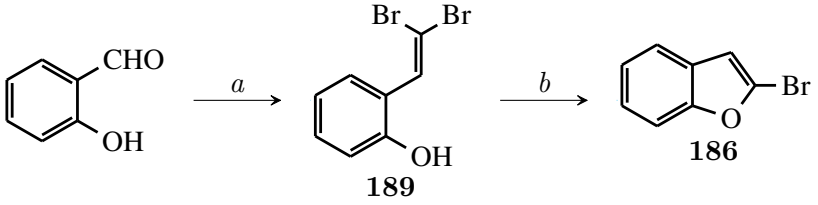
ester all this is avoided and allows for the basic conversion to the *t*-Bu group. The iodide was introduced through lithiation of the 2 position with BuLi, followed by addition of iodine to yield **185** (quantitative).



a - MeOH, H_2SO_4, 52%; *b* - *t*-BuOH, △, 40%; *c* - (i) BuLi (ii) I_2, Quant.

Scheme 3.15: Formation of 2-iodo *t*-Bu 3-furoate (**185**)

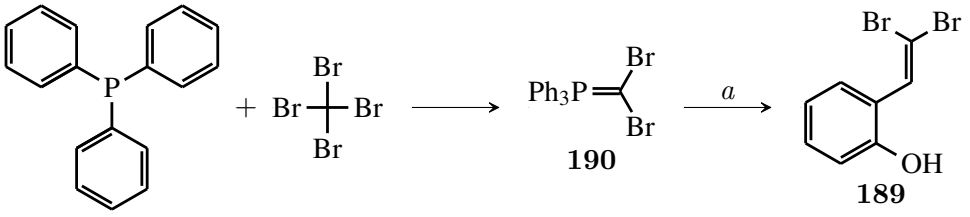
The second required substrate was the derivatization of 2-salicylaldehyde to 2-bromo benzofuran. This transformation is done by using the Corey-Fuchs reaction, introducing an extra carbon and two bromine atoms (**189**), followed by ring closure under TBAF to yield benzofuran **186** as shown in Scheme 3.16. The overall yield was 77% over 2 steps with **189** treated as an intermediate.



a - CBr_4, PPh_3; *b* - TBAF; 77% yield over 2 steps

Scheme 3.16: Formation of 2-bromobenzofuran (**186**) from salicylaldehyde

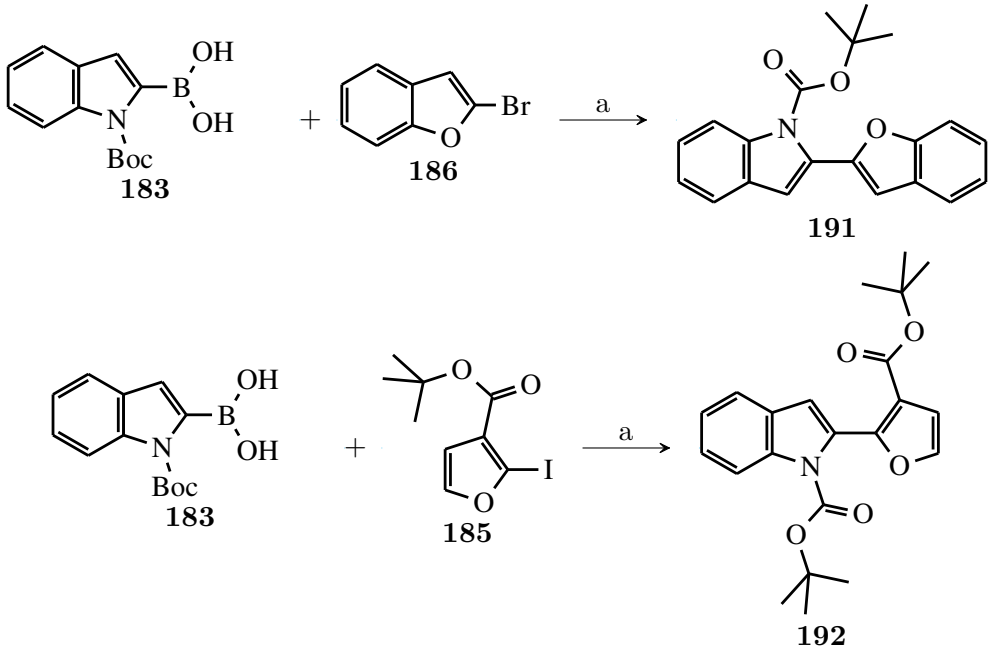
The Corey-Fuchs reaction proceeds by the reaction of PPh_3 and CBr_4 to form ylide **190** as shown in Scheme 3.17. This then undergoes a Wittig type addition to an aldehyde or ketone, in our case generating **189**. The TBAF reaction proceeds via the deprotonation of phenol **189**, and with some possible stabilisation of the *tetra*-butyl amine allows the ring closure onto the double bond formed in the first reaction to give the ring desired 2-bromo-benzofuran **186**.



a - Salicylaldehyde, DCM

Scheme 3.17: The mechanism of the Corey-Fuchs reaction

The Suzuki reactions of **185** and **186** with **183** proved successful, yielding benzofuran **191** and furan **192** quantitatively. The ^{1}H NMR spectra of **191** and **192** showed the presence of the Boc group with a methyl at 1.35 and 1.40 ppm, both integrating for 9H, as well as increased proton integration in the aromatic region of 10H for **191** and 7H for **186** showing an increase of 5H from starting furans **185** and **186**. The reactions are shown in Scheme 3.18. The method utilized was as explained previously with $Pd(PPh_3)_4$ and $NaHCO_3$ as base and DME as solvent.

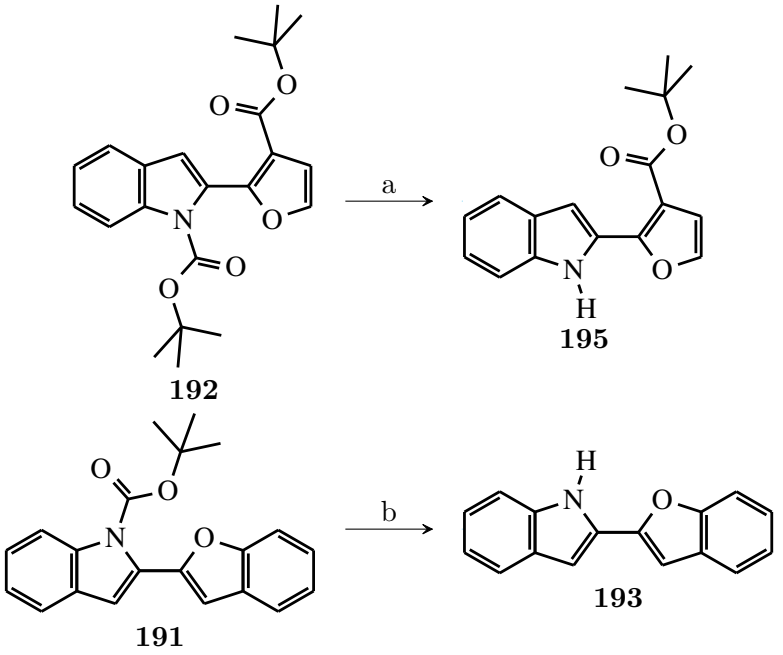


a - $Pd(PPh_3)_4$, DME, Na_2CO_3 (aq.)

SCHEME 3.18: The formation of 2-substituted indole through Suzuki coupling to furans **185** and **186**, both in quantitative yields

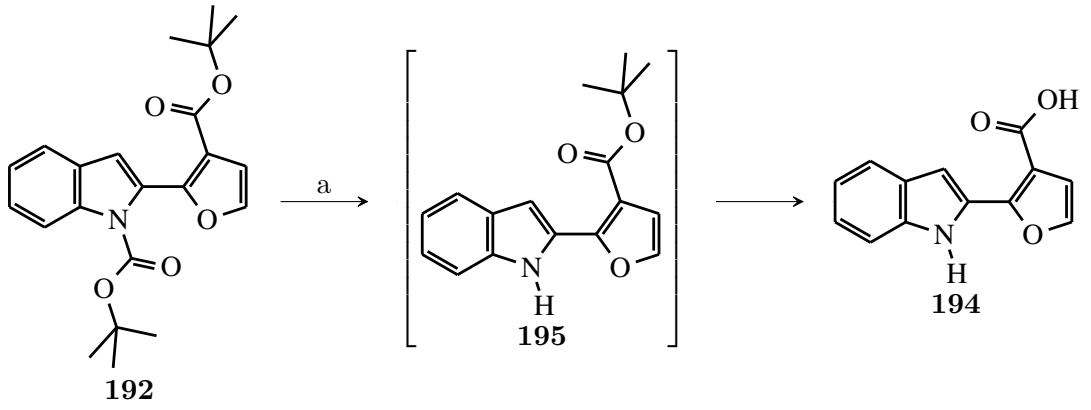
To deprotect the indole nitrogen atom of **191** and **192** the removal of the Boc was necessary as shown in Scheme 3.19. The benzofuran analogue **191** gave a clean product **193** (54%) with the presence of an NH in the ^{1}H NMR spectrum at 8.65 ppm and the disappearance of the Boc methyl groups at 1.35 ppm. No other products were isolated. It was, however, expected that **192** would give some trouble as the *t*-Bu ester is sensitive to the acidic conditions of 30% TFA in DCM and would perhaps transform into the acid **194** as shown in Scheme 3.20, or form a reactive *t*-Bu cation that could react further on the molecule. Care was taken to make sure the reaction was dry and the DCM dried and distilled, as to prevent addition to the ester group. The product **195** (51%) was retrieved without the need for any purification and without the loss of the *t*-Bu ester as seen in the ^{1}H NMR spectrum with only the disappearance of one 9H singlet at 1.40

ppm and the presence of a singlet at 1.63 ppm integrating for 9H. The appearance of an NH signal at 11.63 ppm gave further confirmation that the reaction had been successful. The crystal structures of **195** and **193** are shown in Figure 3.11.



a (51%) and b (54%) - DCM/TFA 30%

SCHEME 3.19: Formation of the final indole compounds **193** and **195**



a - DCM/TFA 30%

SCHEME 3.20: The possible formation of the carboxylic acid from the indole **192**

The synthesis of the azaindole counterparts was then attempted. 7-Azaindole was first Boc protected using the same methodology as described with indole, with a quantitative yield of **196** as shown in Scheme 3.21, followed by the formation of boronic acid **197**, which was used directly in the following Suzuki coupling reaction.

However, the coupling of boronic acid **197** to benzofuran **186** and furan **185** proved unsuccessful. As noted in the previous chapter when 5-bromo-azaindole was subjected

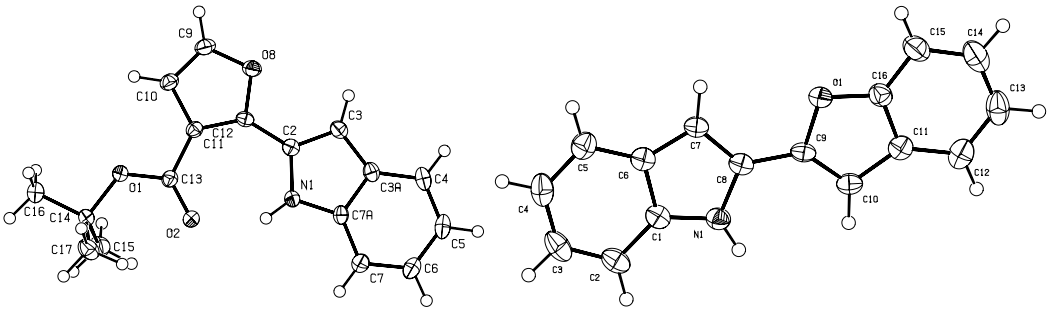
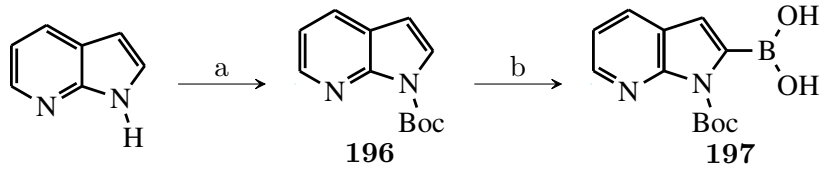


FIGURE 3.11: Crystal structures of **195** and **193** drawn with 50 % probability ellipsoids



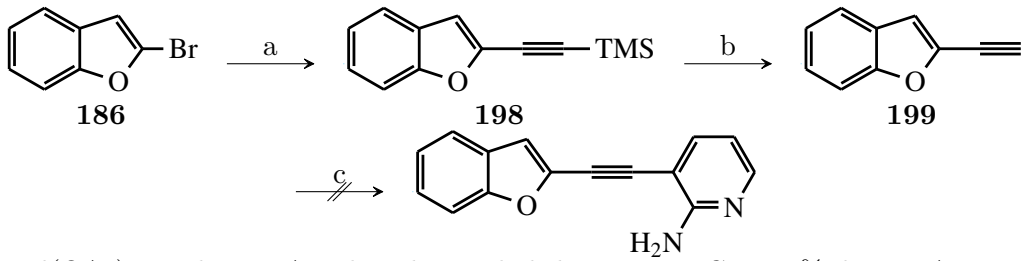
196 **197**

a - Boc_2O, DCM, 96%; b - (i) LDA (ii) $B(i\text{-}PrO)_3$ (iii) HCl, used directly in next reaction

SCHEME 3.21: Boc protection of 7-azaindole

to Suzuki conditions, no coupling product was obtained. The coupling reaction of 7-azaindole boronic acid **196** showed similar results and as such it can be concluded that 7-azaindoles do not perform well in coupling reactions such as the Suzuki coupling reaction. The possible coordination of the palladium between the two nitrogen atoms on the azaindole moiety is likely, therefore, not allowing for the recycling of the palladium catalyst. A rule of thumb, it seems emerging from all the failures of certain reactions - namely that 7-azaindoles and their respective family of molecules do not participate well in metal catalysed reactions. It became clear that performing cross-coupling reactions on 7-azaindoles with palladium was not a feasible route. As before, the Sonogashira coupling reaction of 2-aminopyridines would prove vital in the coupling of the different moieties involved, and would build on the work done previously. This would entail adding an acetylene on to the substituted furan and then reacting it with the brominated 2-aminopyridine and then subjecting it to the TFA/TFAA ring closure reaction as shown in Scheme 3.22. The electron rich nature of the furan should limit homocoupling and promote hetero coupling in the reaction as seen similarly with electron rich acetylenes. The formation of the alkynes **198** and **199** were successful, but the following Sonogashira coupling reactions were not. This surprising result could not be explained and repetition produced similar results.

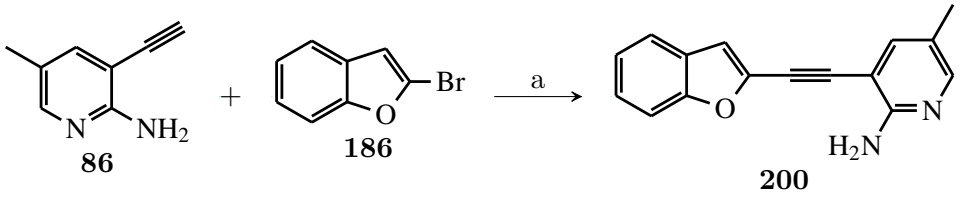
It was then decided to change the reaction order and instead form 2-aminopyridine **86** followed by Sonogashira coupling to **186** in order to form as **200** shown in Scheme 3.23.



a - $Pd(OAc)_2$, PPh_3, TEA, ethynyltrimethylsilane, THF, CuI, 28%; b - TBAF, THF, 73%; c - $Pd(PPh_3)_4$, DME, Na_2CO_3, 3-bromo-2-aminopyridine

SCHEME 3.22: The synthesis of substituted 2-aminopyridines towards the synthesis of azaindole-furan analogues

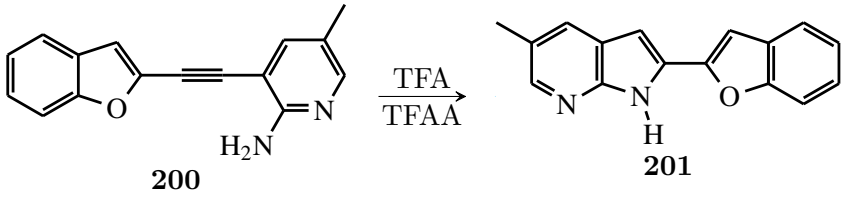
The potential shortcomings were clear, homo coupling could dominate and that the reactions would not be successful. The reactions however, ran smoothly under diisopropyl amine and with the aid of dppf as ligand affording **200** in 94% yield with creating little dimer homo-coupled product. The substrate chosen for the reaction was crucial, the 5-methyl 2-aminopyridine derivative had the least amount of homo coupling from the work done in the previous chapter, the rational being the electron donating nature of the methyl group aiding in the trans-metalation step as discussed before.



a - $Pd(OAc)_2$, dppf, CuI, diisopropylamine

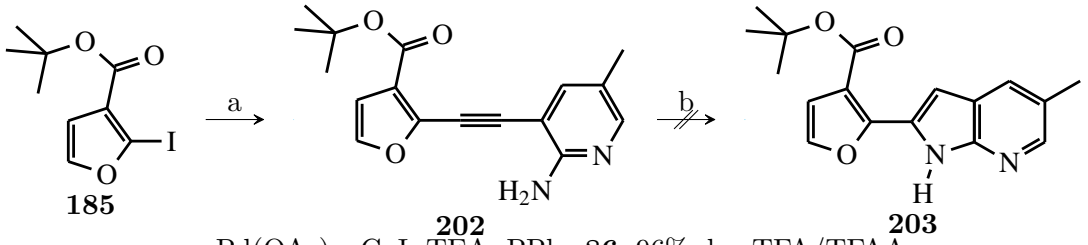
SCHEME 3.23: The synthesis of **200** in 94% yield

The next required step was the ring closure of the 7-azaindole **200**, giving the furan-azaindole as shown in Scheme 3.24. The ring closure of **200** using TFA/TFAA yielded **201** as a powder in 21% yield, with some poor solubility in most solvents. The ^{1}H NMR spectrum showed the disappearance of the NH_2 singlet at 4.95 ppm and the appearance of a doublet at 6.04 ppm integrating for 1H, which is the proton on the 3-position of the azaindole ring.



SCHEME 3.24: The synthesis of the azaindole-benzofuran **201** in 21% yield

The synthesis of furan **202** was then attempted using Sonogashira methodology from the furan **185** as shown in Scheme 3.25. The reaction gave a quantitative yield of furan **202**. The ring closure of **202** to form azaindole **203** was not successful. It is believed the acid sensitive ester functionality on the furan may have allowed decomposition, as no starting material was recovered from the reaction mixture. The ring closure was then attempted using iodine and again only decomposition occurred, with no isolated starting material and the synthesis route was abandoned.



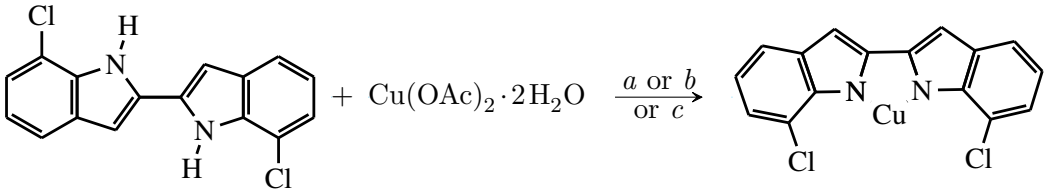
a - $Pd(OAc)_2$, CuI, TEA, PPh_3 **86**, 96%; b - TFA/TFAA;

SCHEME 3.25: The unsuccessful synthesis of the azaindole-furan compound

3.3 Coordination of azaindole ligands with metals

Bis-indole coordination reactions

The first metal coordination studies were performed utilising bis-indoles left from a previous student.[184] The metal coordination revolved around the idea of deprotonation of the indole nitrogen, followed by introduction of the desired metal as shown in Scheme 3.26.



a - Diisopropyl amine; *b* - Triethyl amine; *c* - Acetic acid;

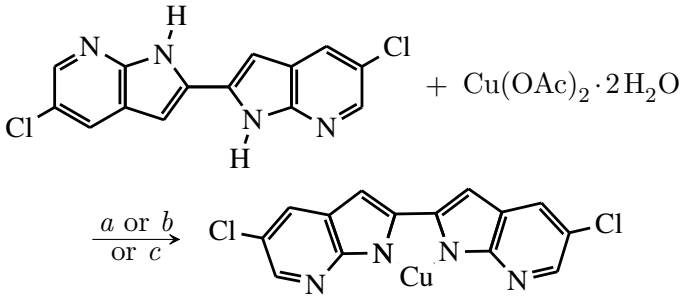
SCHEME 3.26: The coordination of copper with 2,2^i-bis indoles

As the bis-indoles used were rather insoluble in most solvents this methodology proved problematic. Firstly, diisopropyl amine was used as base and solvent. The diisopropyl amine would act as a non nucleophilic base, and coordinates weakly to the metals in solution, allowing for solubility, but not affecting the metal coordination, however, this was unsuccessful. A green powder formed that was insoluble in organic solvents. Simultaneously in a separate reaction was set-up in which the salt and ligand was heated at

reflux in acetic acid. The principle of this reaction was the favouring of the chelation of the two nitrogen atoms over that of the acetates in solution. The neutral bis-indole formed would then precipitate out once cooled or once water was added. In the end this resulted again in insoluble powder that had a green colour. The green colour showing coordination of the copper, yet no crystal was successfully grown. As copper was used in the experiment this was taken as a sign that coordination had occurred, but it was likely that a charge-less molecule formed making solubility difficult.

Bis-azaindole coordination reactions

The next step was to attempt the same reaction with the synthesised bis-azaindoles, even when these compounds exhibited poor solubility. Several reaction were attempted, as shown in Scheme 3.27 namely heating with acetic acid, diisopropyl amine and triethyl amine as separate reaction, with no success.



a - Diisopropyl amine; *b* - Triethyl amine; *c* - Acetic acid;

SCHEME 3.27: The coordination of copper with 2,2^{i}-bis 7-azaindoles

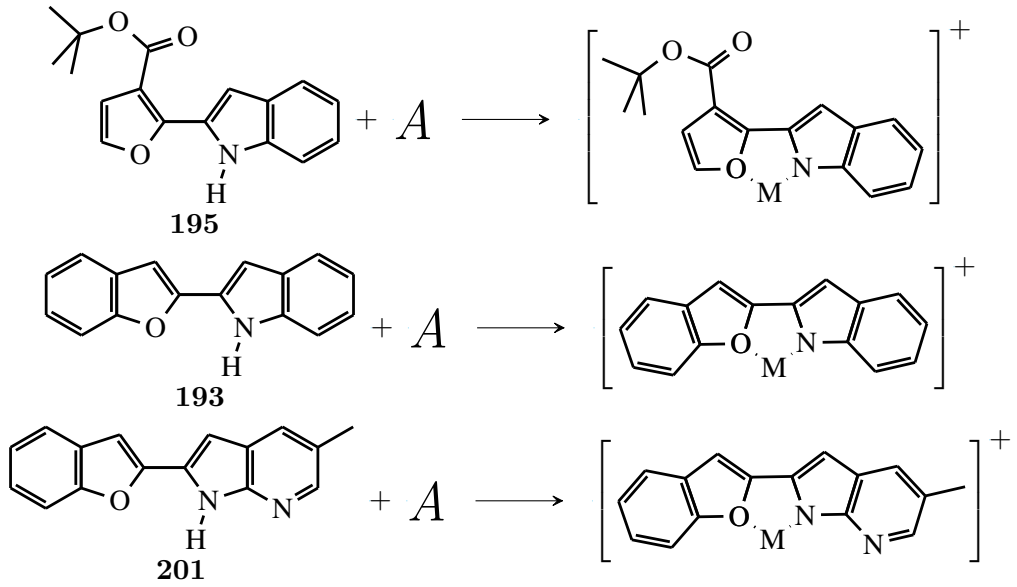
In addition, the bis-azaindole was placed in methanol and stirred with the metal salt. The reaction was stirred over a period of 48 hours with copper acetate and produced a light green precipitate. The precipitate appeared to be a mixture of a possible copper complex and starting material, which had a white colour, and both were very insoluble. The reaction could not be driven to completion and it was clear that an equilibrium existed between the coordinated compound and the product, ensuring the mixture remained.

The failure in the formation of complexes with the bis-indoles and 7-azaindoles raised some points. Firstly, the salts used were all in the 2+ oxidation state and would be neutralised by the 2- charged bisindole, causing poor interaction with solvent molecules and counter ligands. Once the neutral metal complex is formed, it was of poor solubility

most likely to extensive π-stacking type interaction due to the flat nature of the azaindole and exclusion from the solvent due to little bonding interactions. Changing the metal complex to a state in which the ligand will only have one proton that can be removed with a base and result in only a +1 charge could potentially assist with solubility.

The asymmetrical indoles

As the furan-indoles synthesised (**193**, **195** and **201**) were used as ligands in this sections. The furan ligand **195** was soluble in THF in contrast to the bis-indoles and bis-azaindoles. The coordination reaction was modelled after work done by Liu *et al.* in which butyl lithium was used as the base, followed by the addition of the metal salt.[188] In this paper the method proved effective in the synthesis of 7-azaindole containing complexes. The reaction tried in our case was with the asymmetrical indoles and azaindoles synthesised previously as shown in Scheme 3.28



Scheme 3.28: Attempted formation of 7-azaindole/indole metal complexes

The reaction with the benzofuran substituted indole **193** and zinc acetate yielded a crystalline solid which was isolated and the single crystal diffraction pattern observed and solved. The crystal structure did not include any metal atom, and only had furan **193** as shown in Figure 3.12. The crystals isolated were all uniform, and it was clear that no metal coordination had taken place.

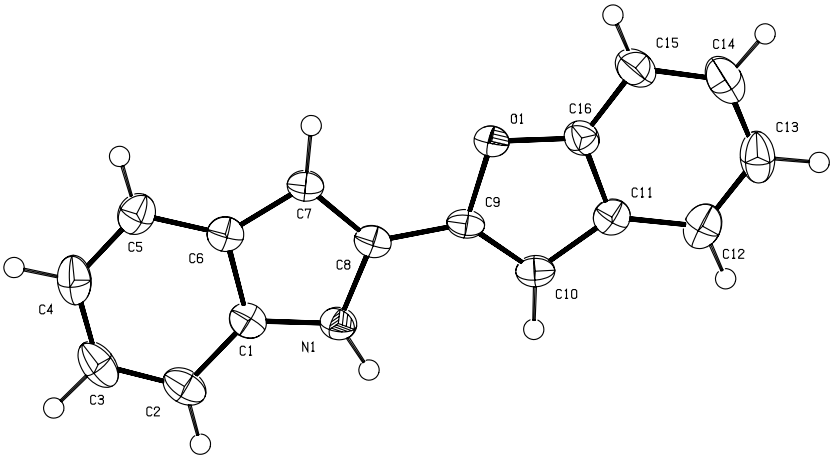
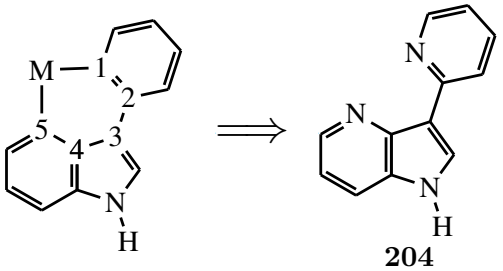


FIGURE 3.12: Crystal structure of **193**

It was decided that another method in which sodium hydride is used as a base. This proved futile as the same crystals were once again isolated, showing no metal coordination. The other ligands gave similar results, and no metal coordination had taken place with any of the reactions. From the results obtained it showed that the coordination of indoles and 7-azaindoles in this manner is a very ineffective manner of forming metal containing hybrid biologically active compounds.

3.3.1 Future work

The introduction of a pyridine onto the organic scaffold has found some success in work in our laboratories when coordination of metals was required.[189] Since the metal coordination on the 7-azaindole nucleus was not very successful it will be beneficial to incorporate a pyridine unit. For example in Scheme 3.29 a new metal coordination system with two pyridine groups are part of the 7-azaindole **204**. Molecule **204** would then form the coordinated compound, with a six membered ring forming upon chelation with the metal.



204

SCHEME 3.29: The coordination of **204** through chelation of two pyridine centres

The proposed compound would then mimic adenosine as seen in Figure 3.13 to some degree, and may even fit into the active site of kinases. Further functionalization would be required as **204** might show some general cytotoxicity.

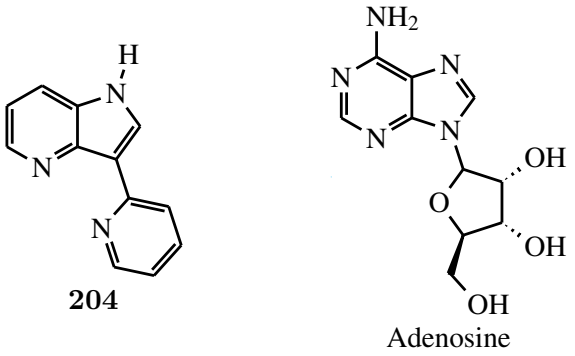
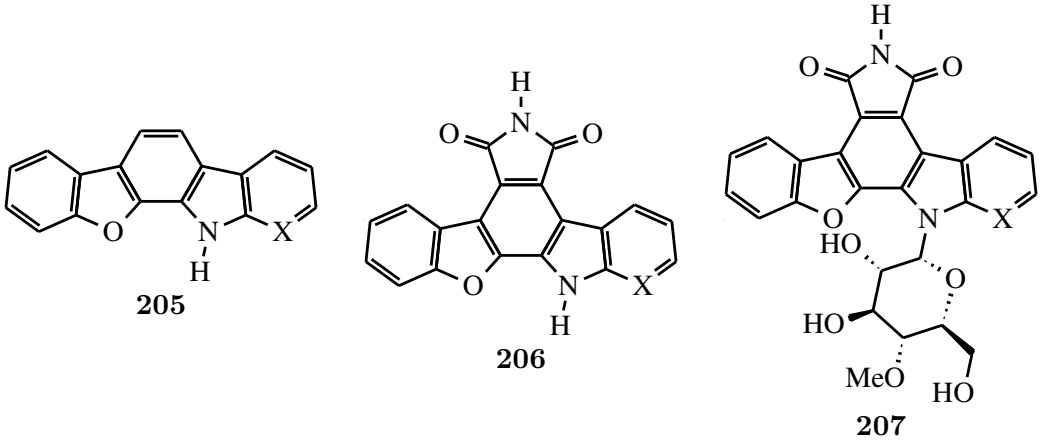


FIGURE 3.13: The similarities in the structures of adenosine and 4-azaindole **204**

The further development of the 7-azaindole and indole linked benzofuran molecules can be further expanded to closer resemble carbazoles such as Rebeccamycin, with the proposed furans **205**, **206** and **207** as shown in Figure 3.14.



X - N *or* C-H

FIGURE 3.14: The proposed further development of benzofuran carbazole derivatives

3.4 Biological testing

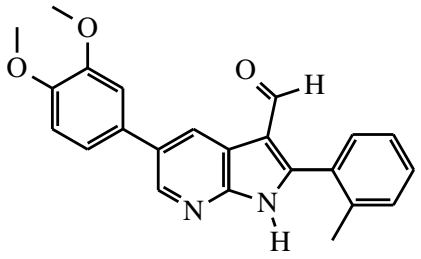
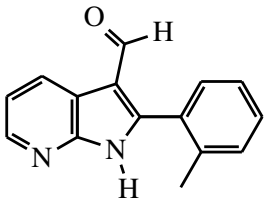
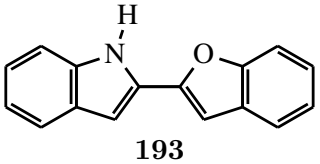
3.4.1 African sleeping sickness and Malaria assays

Results and discussion

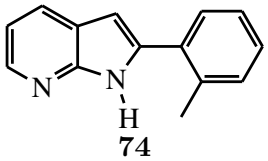
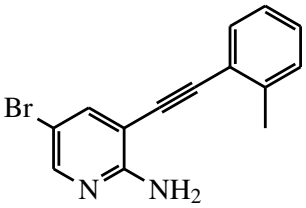
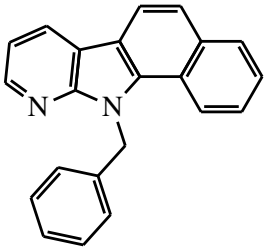
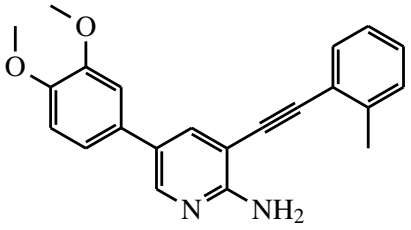
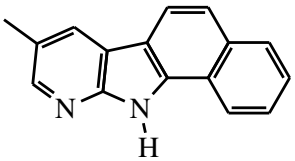
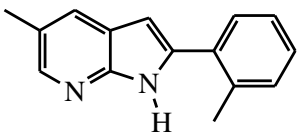
Anti-trypanocidal/malarial activity was measured by testing of live cultures of *Trypanosoma brucei* or *P. falciparum*. To these cultures 20 μM of compound dissolved in

a 1% DMSO in water was added. The cultures were then incubated for 48 hrs. For *Trypanosoma brucei* a resazin based reagent was then added to gauge the amount of surviving *Trypanosoma brucei* and through fluorescence of the resorufin generated by healthy cells and in comparison to an untreated well the percentage viability was calculated. The general toxicity of the synthesised compounds were tested against the HeLA cell line. This was done by exposing a HeLA culture to a solution of the compounds after which the cell viability was calculated. A high viability value indicates lower toxicity. The results are shown in Table 3.1. The biological testing was done at Rhodes University, Grahamstown, South Africa.

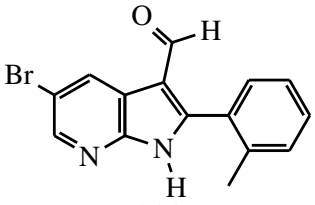
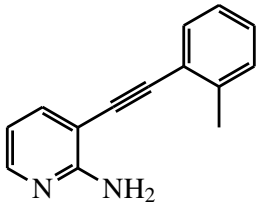
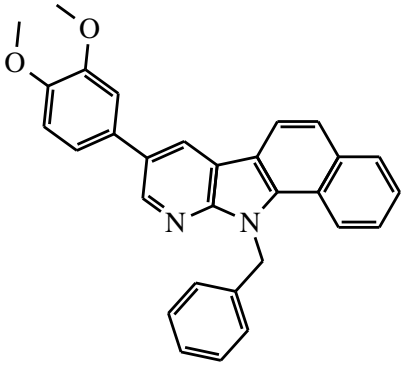
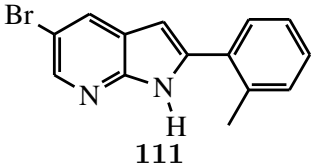
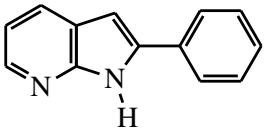
TABLE 3.1: Toxicity of synthesised compounds towards *Trypanosoma brucei* (*T.b.*) and HeLa cells expressed as % viability and IC_{50} values in a *Trypanosoma brucei* (*T.b.*), HeLa and *P. falciparum* (*P. f.*) assay. All experiments were done in duplicate

Compound	**Viability** (%)			IC_{50} (μM)	
	T.b.	HeLa	*P. f.*	*T.b.*	*P. f.*
 **142**	9.1	-	0.1	89	10.23
 **115**	47.3	24.8	88	11.27	-
 **193**	82.4	3.7	77	20.68	-

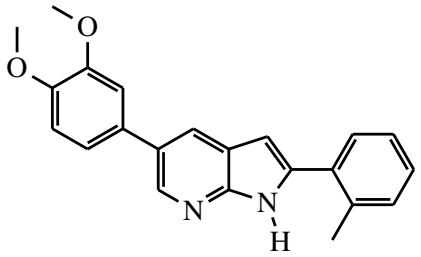
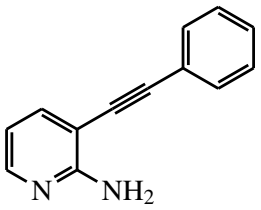
Continued on next page

Compound	**Viability** (%)			IC_{50} (μM)	
	T.b.	HeLa	*P. f.*	*T.b.*	*P. f.*
 **74**	66.6	12.8	98	24.44	-
 **108**	95.1	26.1	103	-	-
 **71**	74.9	87.1	95	-	-
 **140**	97.8	33.4	56	-	-
 **133**	78.0	-	0.2	105	15.13
 **110**	112.1	2.2	111	21.2	-

Continued on next page

Compound	**Viability** (%)			IC_{50} (μM)	
	T.b.	HeLa	*P. f.*	*T.b.*	*P. f.*
 **208**	93.2	81.7	102	-	-
 **75**	74.4	52.9	100	-	-
 **145**	97.6	48.4	23	-	26
 **111**	88.3	66.4	109	-	-
 **209**	83.9	16.4	88	26.88	-

Continued on next page

Compound	**Viability** (%)			IC_{50} (μM)	
	T.b.	HeLa	*P. f.*	*T.b.*	*P. f.*
 **141**	96.4	113.7	89	-	-
 **210**	97.3	60.1	91	-	-
Pentamidine	-	-	-	0.0002588	-
Chloroquine	-	-	-	-	0.06

The anti-malarial testing showed very little activity except for the case of **145**, the only active compound towards *P. falciparum*. This was rather unexpected as the compound shows a high degree of insolubility in most solvents. It is however the compound with the most aromatic rings that form a very flat and rigid structure, perhaps showing some DNA intercalating ability. The means of uptake into the *P. falciparum* cell would be an interesting study and could perhaps shed some light into designing molecules that are selectively taken up by malaria parasites, as **145** does not show general toxicity. It is interesting to note that other dimethoxy molecules did not show any activity, and that it is perhaps necessary to have the dimethoxy group as well as the carbazole moiety in place in order to see anti-malarial activity.

As for the *Trypanosoma brucei* activity, there is a clear correlation with general cytotoxicity and the formyl functional group. The least and most active compound (**142** and **141**) only differ with this functional group. This would suggest that the group of enzymes that interact with this class of molecules, have some interaction with the formyl group in this region, stabilising the interaction and causing inhibition. All the

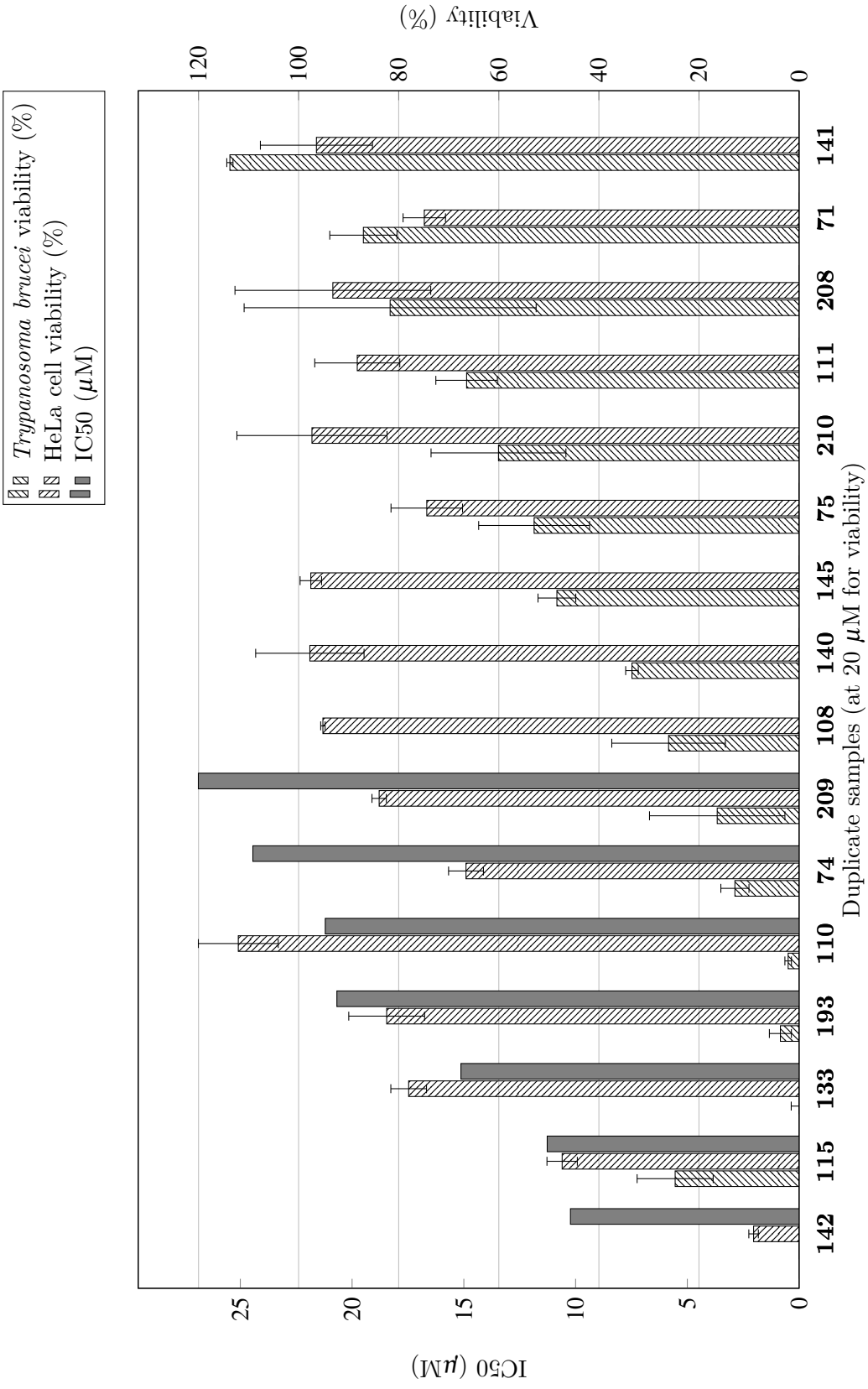


FIGURE 3.15: Figure showing the toxicity of synthesised molecules against HeLa and *T.b.*

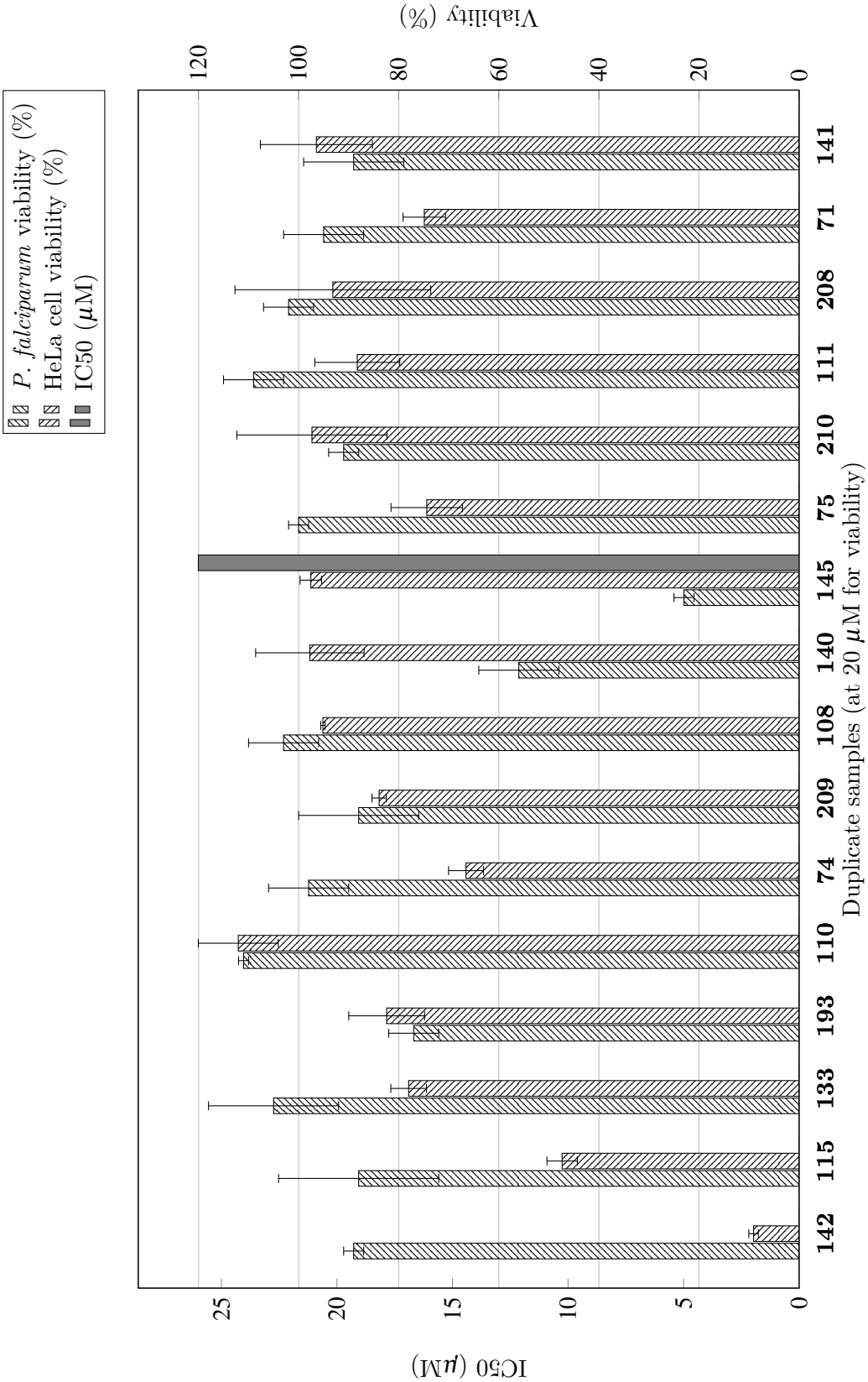


FIGURE 3.16: Figure showing the toxicity of synthesised molecules against HeLa and Malaria

azaindoles with aldehyde functionalities displayed this effect, and it is clear that no selectivity was achieved with this class of compounds. Finding the enzyme azaindoles bind to could show some areas in which functional groups can be added, and possibly make the interaction more selective.

Further, the α-carboline tested (**133**) showed the third highest activity, with low general cytotoxicity, showing a selective interaction with the parasite. With some further work this class of compounds can be optimised to increase the activity.

It must be noted that the 2-aminopyridines showed poor activity, and that all those tested were compounds with a rigid triple bond. This is in contrast with the 7-azaindoles tested, showing that there is possibly some kinase activity as these structure resemble adenosine more closely than the 2-aminopyridines tested. The rigid triple bond could be reduced by hydrogenation and could potentially lead to a much more flexible molecule that could show some interaction.

3.5 Conclusion

The coordination of metals on to the 7-azaindole system was problematic. However, the study afforded some compounds that exhibited biological activity, showing that the further expansion and functionalization of these molecules to be viable. The 7-azaindoles and α-carbolines synthesised showed some varied biological activity and can be expanded and studied further. In conclusion the heteroaromatic compounds synthesised showed general biological activity and shows promise in further development, which is a success in itself.

Chapter 4

Experimental

4.1 Standard experimental techniques

4.1.1 Chromatography

Thin-layer chromatography (TLC) was conducted on Merck GF_{254} pre-coated silica gel aluminium backed plates (0.25 mm layer). Various solvent mixtures were used for the elution of the chromatograms with a mixture of hexane and EtOAc. Compounds were visualised by either UV light (254 nm) or by spraying with either of the following:

- vanillin/H_2SO_4 solution
- $KMnO_4$ solution
- I_2/silica
- DNPH solution

This was followed by a drying period and thereafter by heating if necessary.

Flash column chromatography refers to column chromatography performed under nitrogen pressure (*ca.* 100 kPa). The columns were packed with Merck Kieselgel 60 (230-400 mesh) and eluted with the appropriate solvent mixture. Solid crude mixtures were adsorbed on a portion of silica by dissolving the mixture first in DCM followed by addition of silica and subsequent removal of DCM.

4.1.2 Anhydrous solvents and reagents

THF and toluene were heated under reflux over sodium under N_2 with benzophenone as the indicator. These were distilled prior to use. DCM, acetonitrile and DMF were heated over CaH_2 under N_2 with subsequent distillation. EtOAc and subsequent hexanes were distilled prior to use.

4.1.3 Spectroscopic methods

NMR spectra were recorded using a Bruker Ultrashield 300 or 500 MHz spectrometer in $CDCl_3$ or deuterated DMSO. The ^{1}H NMR data are listed in the order: chemical shift (δ, reported in ppm and referenced to the residual solvent peak of TMS [δ = 0.00 ppm]), the multiplicity (s = singlet, d = doublet, q = quartet, dd = doublet of doublets, dt = doublet of triplets, dq = doublet of quartets, ddd = doublet of doublets of doublets, ddt = doublet of doublets of triplets, p = pentet, sx = sextet, sp = septet), the number of integrated protons, the coupling constant J expressed in Hz, and finally the specific hydrogen allocation. Spin decoupling assisted with the determination of the coupling constants and hydrogen allocation. ^{13}C NMR data are listed in the order: chemical shift (δ, reported in ppm and referenced to the residual solvent peak of TMS [δ = 0.0 ppm]).

4.1.4 Mass spectroscopy (m/z)

Mass spectrometry was performed on Thermo Double Focusing Sector high resolution mass spectrometer. Ionisation techniques include EIMS, CIEMS and ESIMS.

4.1.5 Infrared spectroscopy (IR)

A Tensor 27 spectrophotometer was used to record IR spectra using an ATR fitting. The data are listed with the characteristic peaks indicated in wavenumber (cm^{-1}) followed by a description of the intensity of the signal where l indicates large, m indicates medium and s indicates small.

4.1.6 Crystallography

Intensity data were collected on a Bruker SMART 1K CCD area detector. Data reduction was carried out using the program SAINT+ and absorption corrections were made using the program SADABS.[190,191]

The crystal structures were solved by direct methods using SHELXTL.[192] Non-hydrogen atoms were first refined isotropically followed by anisotropic refinement by full matrix least-squares calculations based on F^2 using SHELXTL. Hydrogen atoms were first located in the difference map then positioned geometrically and allowed to ride on their respective parent atoms. Amino group hydrogen atoms were refined isotropically after being identified in the difference map. Diagrams and publication material were generated using SHELXTL, PLATON[193] and ORTEP-3.[194]

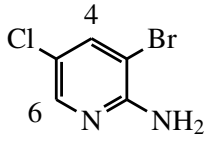
4.2 Chemical methods

4.2.1 A typical bromination procedure

The substituted 2-amino-pyridine (5-methyl-2-aminopyridine or 5-chloro-2-aminopyridine) (15.6 mmol) was dissolved in chloroform (100 ml) to which Br_2 (2.64 g, 17.16 mmol) was added slowly so as to generate a slow reflux. The solution was then stirred for 2 hours. A saturated aqueous potassium carbonate solution was then added slowly until bubbling stopped. A saturated aqueous solution of sodium sulphite was added to react with excess bromine, and the chloroform layer isolated using a separating funnel. The chloroform was then dried over anhydrous Na_2SO_4 and filtered through a short silica plug column (15g). The silica column was then washed with excess chloroform (50 ml). The chloroform was then removed under vacuum. Recrystallisation with toluene can be done if the compound (**81** or **80**) purified is not sufficiently clean.

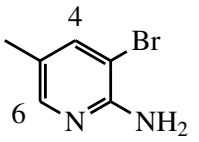
3-Bromo-5-chloropyridin-2-amine (81)

CAS: 26163-03-1[195] **Yield:** 70% **MP:** 81-83 °C **IR (cm^{-1}):** $\bar{\nu}$ 3470 (*s*), 3288 (*s*), 3139 (*s, br*), 1625 (*l*), 1474 (*l*), 1387 (*l*), 1032 (*l*), 887 (*l*), 714 (*l*), 653 (*l*),



540 (*l*) **^{1}H NMR (300 MHz, $CDCl_3$):** δ 7.98 (*d*, J = 2.1 Hz, 1H, H-4), 7.66 (*d*, J = 1.8 Hz, 1H, H-6), 4.99 (*s*, 2H, N**H**$_2$) **^{13}C NMR (125 MHz, $CDCl_3$):** δ 154.1, 145.4, 139.6, 120.4, 104.0

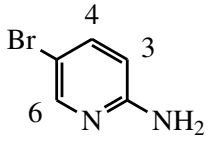
3-Bromo-5-methylpyridin-2-amine (80)



CAS: 17282-00-7[195] **Yield:** 81% **MP:** 73-75 °C **IR (cm^{-1}):** $\bar{\nu}$ 3457 (*m*), 3137 (*m*), 1625 (*l*), 1477 (*l*), 1393 (*l*), 1204 (*l*), 1047 (*l*), 886 (*l*), 743 (*l*), 553 (*l*) **^{1}H NMR (300 MHz, $CDCl_3$):** δ 7.84 (*d*, J = 0.9 Hz, 1H, H-6), 7.49 (*d*, J = 1.5 Hz, 1H, H-4), 4.85 (*s*, 2H, N**H**$_2$), 2.18 (*s*, 3H, C**H**$_3$) **^{13}C NMR (75 MHz, $CDCl_3$):** δ 153.6, 146.7, 141.0, 124.4, 104.3, 17.0 (**C**H$_3$)

5-Bromopyridin-2-amine (79)

2-Amino-pyridine (5 g, 53.2 mmol) was added to chloroform (100 ml) and cooled to 0°C. To the reaction mixture NBS (9.46 g, 53.2 mmol) was added slowly so as to keep the reaction mixture below 5°C and stirred for 2 hours. The reaction mixture was then poured into a saturated potassium carbonate and sodium sulphite solution (50ml) and the organic layer separated. The water layer was washed with chloroform (20 ml) and the combined organic layers washed with brine (20 ml) and dried over anhydrous Na_2SO_4 and the *chloroform* removed. The crude product was then recrystallized from hot toluene to yield light brown crystals (6.5 g).

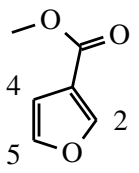


CAS: 1072-97-5[196] **Yield:** 71% **MP:** 131-136 °C **IR (cm^{-1}):** $\bar{\nu}$ 3453 (*s*), 3284 (*s, br*), 3141 (*s, br*), 2360 (*s*), 1622 (*m*), 1586 (*m*), 1475 (*m*), 1327 (*m*), 1261 (*m*), 1141 (*m*), 927 (*m*), 872 (*l*), 642 (*l*) **^{1}H NMR (300 MHz, $CDCl_3$):** δ 8.10 (*d*, J = 2.4 Hz, 1H, H-6), 7.49 (*dd*, J = 2.4 Hz, 8.7 Hz, 1H, H-4), 6.41 (*d*, J = 8.7 Hz, 1H, H-3), 4.55 (*s*, 2H, N**H**$_2$) **^{13}C NMR (75 MHz, $CDCl_3$):** δ 157.1, 148.7, 140.1, 110.0, 108.3

4.2.2 Esterification reactions

The formation of a methyl ester from 3-furoic acid was achieved by dissolving the 3-furoic (4g, 35.7 mmol) in excess MeOH (20 ml) and by the further slow addition of conc. H_2SO_4 (2 ml). The solution was heated under reflux for 2 hrs and extracted using EtOAc (50 ml) and washed with aqueous saturated Na_2CO_3 (30 ml x 3). The organic layer was dried using anhydrous Na_2SO_4 and evaporated under vacuum to yield the respective methyl ester compound **187**.

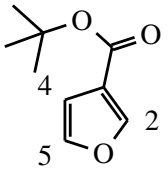
Methyl furan-3-carboxylate (187)



CAS: 13129-23-2[197] **Yield:** 52% **^{1}H NMR (300 MHz, $CDCl_3$):** δ 8.01 (*s*, 1H, H-2), 7.43 (*s*, 1H, H-5), 6.74 (*s*, 1H, H-4), 3.84 (*s*, 3H, C**H**$_3$) **^{13}C NMR (75 MHz, $CDCl_3$):** δ 163.6 (**C**=O), 147.8 (C-2), 143.8 (C-5), 119.3 (C-3), 109.9 (C-4), 51.6 (**C**H_3)

***tert*-Butyl furan-3-carboxylate (188)**

The substitution of the methyl ester for the *t*-Bu ester was achieved by the addition of *t*-BuOK (4eq) in THF (30 ml) to the methyl ester starting material. The reaction mixture was heated under reflux for 2 hrs. The reaction mixture was then poured into a mixture of EtOAc (30 ml) and water (20 ml) and the organic phase was removed and dried over anhydrous Na_2SO_4. The removal of the solvent yielded **188**.

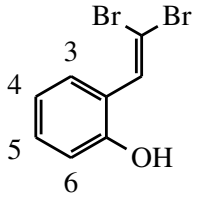


CAS: 125294-46-4[198] **Yield:** 40% **^{1}H NMR (300 MHz, $CDCl_3$):** δ 7.92 (*dd*, J = 1.5 Hz, 1.2 Hz 1H, ,H-2), 7.39 (*t*, J = 1.8 Hz, 1H, H-5), 6.69 (*dd*, J = 1.8 Hz, 1.2 Hz, 1H, H-4), 1.55 (*s*, 9H, C**H**$_3$) **^{13}C NMR (75 MHz, $CDCl_3$):** δ 162.5 (**C**=O), 147.3 (C-2), 143.4 (C-5), 121.1 (C-3), 110.0 (C-4), 80.9 (**C**$(CH_3)_3$), 28.3 (C(**C**$H_3)_3$)

4.2.3 An adapted Corey-Fuchs method in the formation of 2 bromo benzofuran

2-(2,2-Dibromovinyl)phenol (189)

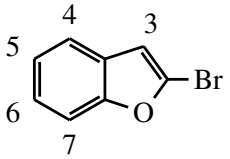
To a solution of triphenyl phosphine (5.24 g, 10 mmol) and DCM (20 ml) at 0° was added tetrabromomethane (3.31 g, 10 mmol) dissolved in DCM (10 ml) and the solution stirred for 30 min after which salicylaldehyde (0.61 g, 5 mmol) was added. The reaction mixture was allowed to warm to rt and stirred for 2 hrs. EtOAc (60 ml) was added and the resulting precipitate filtered off. The organic mixture was then added to *water* and separated using a separating funnel and the organic layer dried with anhydrous $MgSO_4$ and evaporated. The resulting solid was then washed with several portions of hot ether and the ether evaporated to yield (**189**) as white crystals (1.82 g).



CAS: 91703-34-3[199] The product was used as is in the next step as part of a two step reaction. **^{1}H NMR (500 MHz, $CDCl_3$):** δ 7.56 (*s*, 1H, alkene), 7.54 (*dd*, J = 7.6 Hz, 1.2 Hz, 1H, H-3), 7.23 (*td*, J = 7.9 Hz, 1.7 Hz, 1H, H-5), 6.95 (*td*, J = 7.5 Hz, 1.1 Hz, 1H, H-4), 6.82 (*dd*, J = 8.2 Hz, 1.1 Hz, 1H, H-6) **^{13}C NMR (126 MHz, $CDCl_3$):** δ 152.49, 132.38, 130.05, 129.21, 122.86, 120.67, 115.74, 92.04

2-Bromobenzofuran (186)

To (**189**) (4.24 g, 15.3 mmol) was added THF (50 ml) and TBAF$\cdot 3H_2O$ (4.83 g, 15.3 mmol) and heated under reflux for 6 hrs. The reaction mixture goes from a green to a yellow colour. The mixture is then added to water (100 ml) and EtOAc (50 ml) and the organic layer separated and the water layer washed with another portion of EtOAc and the organic layers combined and dried over anhydrous $MgSO_4$ and dried under vacuum. The crude was then purified using silica chromatography with hexane:EtOAc in a ration of 10:1.



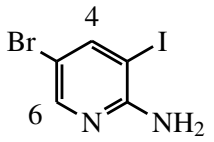
CAS: 54008-77-4[199] **Yield:** 77% (over 2 steps) **^{1}H NMR (500 MHz, $CDCl_3$):** δ 7.49 (*dd*, J = 7.2 Hz, 1.9 Hz, 1H, H-7), 7.44 (*dt*, J = 8.3 Hz, 0.9 Hz,

1H, H-4), 7.23 (*m*, 2H, H-5 & H-6), 6.71 (*d*, J = Hz,
1H, H-3) **^{13}C NMR (126 MHz, $CDCl_3$):** δ 155.79, 128.70, 128.19, 124.21, 123.37, 120.03, 110.90, 108.26

4.2.4 A typical iodination of 2-amino-pyridine analogues

To a solution of H_2SO_4 (920 μl) in water (6.0 ml) was added 5-bromo-2-aminopyridine (10.0 g, 58 mmol), iodic acid (2.4 g, 15 mmol), I_2 (5.4 g, 23 mmol) and acetic acid (36.7 ml). This solution was then heated to 80° overnight and neutralised with conc. NaOH and washed with DCM (3 x 30 ml). The DCM was washed with a dilute sodium thiosulfate solution and dried over anhydrous $MgSO_4$.

5-Bromo-3-iodopyridin-2-amine (82)

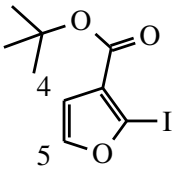


CAS: 381233-96-1[200] **Yield:** 80% **MP:** 111-113 °C
IR (cm^{-1}): $\bar{\nu}$ 3446 (*s*), 3278 (*s*), 3122 (*s*), 2900 (*s*), 2690 (*s*), 2106 (*s*), 1627 (*l*), 1567 (*l*), 1454 (*l*), 1380 (*m*), 1239 (*l*), 1022 (*l*), 891 (*l*), 743 (*l*), 678 (*l*), 642 (*l*) **^{1}H NMR (300 MHz, $CDCl_3$):** δ 7.98 (*m*, 2H, H-4 & H-6), 5.53 (*s*, 2H, N**H**$_2$) **^{13}C NMR (75 MHz, $CDCl_3$):** δ 176.4, 156.6, 148.7, 147.6, 106.8

4.2.5 A typical iodination by lithiation procedure

A solution of THF (15 ml) and furan **188** (2.00 g, 11.89 mmol) was cooled with liquid nitrogen in acetone and further reacted with BuLi (12.49 mmol). This reaction mixture was stirred for 30 min and iodine (3.02 g, 11.89 mmol) in THF (5 ml) added drop wise and stirred for 30 min. The reaction was then quenched with solid ammonium chloride and poured into a mixture of OEt_2 and sat. *sodium sulphite*. The organic phase was isolated and dried over anhydrous $MgSO_4$ and the solvent evaporated. No further purification was required

***tert*-Butyl 2-iodofuran-3-carboxylate (185)**



CAS: Novel **Yield:** Quantitative (liquid) **IR (cm^{-1}):** $\bar{\nu}$ 2983 (*s*), 1706 (*l*), 1489 (*m*), 1305 (*l*), 1145 (*l*), 1002 (*l*), 740 (*l*) **^{1}H NMR (300 MHz, $CDCl_3$):** δ 7.55 (*d*, J = 2.1 Hz, 1H, H-5), 6.69 (*d*, J = 2.1 Hz, 1H, H-4), 1.58 (*s*, 9H, C**H**$_3$) **^{13}C NMR (75 MHz, $CDCl_3$):** δ 161.3 (**C**=O), 147.9 (C-5), 125.3 (C-3), 112.6 (C-4), 97.0 (C-2), 81.7 (**C**$(CH_3)_3$), 28.2 (C(**C**$H_3)_3$) **HRMS:** [M+2H-*t*-Bu]$^+$ Calculated: 238.9200 Found: 238.9338

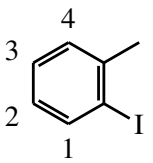
4.2.6 A typical aryl diazotization followed by iodination procedure

The respective amine compounds were synthesised using a modified procedure from Ullmann[146].

o-Toluidine (5.4 ml, 50 mmol) was dissolved in a dilute H_2SO_4 solution (7 ml conc. H_2SO_4 in 70 ml water) and cooled to 0°C. To this solution sodium nitrite (3.5 g, 50.7 mmol) dissolved in water (15 ml) was added slowly so as to keep the reaction mixture below 5°C. The mixture was then stirred for 30 minutes after which it was added to a potassium iodide (15 g, 90.4 mmol) solution in water (60 ml) which was pre-cooled to –5°. The reaction mixture was allowed to warm to room temperature and left overnight or heated at 70° for an hour. The mixture was then extracted with hexane (2 x 50 ml) and the organic layer washed with HCl (1 M, 20 ml, x 2) followed by a sodium hydroxide wash (5 M, 20 ml, x2) and finally by brine (20 ml). The hexane layer was then dried by the addition of anhydrous $MgSO_4$ and filtered through a short silica plug column and washed with excess hexane. The hexane was then removed under vacuum to yield **105**.

1-Iodo-2-methylbenzene (105)

The spectra obtained was in accordance with literature values.[201]



CAS: 615-37-2[202] **Yield:** 52% **BP:** 84°C (6 mmHg) **IR (cm^{-1}):** $\bar{\nu}$ 3054 (*s*), 3007 (*s*), 1563 (*s*), 1452 (*m*), 1378 (*s*), 1274 (*s*), 1012 (*l*), 738 (*l*), 644 (*l*), 537 (*m*) **^{1}H NMR (300 MHz, $CDCl_3$):** δ 7.78 (*d*, J = 7.2 Hz, 1H, H-1), 7.21 (*d*, J = 4.2 Hz, 2H, H-2 & H-3), 6.84 (*m*, 1H, H-4), 2.41 (*s*, 3H, C**H**$_3$)

^{13}C NMR (75 MHz, $CDCl_3$): δ 141.3 (**C**CH_3), 138.9, 129.7, 128.1, 127.4, 101.2 (**C**I), 28.1 (**C**H_3)

4.2.7 A typical Sonogashira coupling procedure

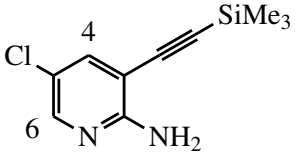
Ethynyltrimethylsilane (4.17 ml, 28.9 mmol) was added to a mixture of dry THF (20 ml) and triethyl amine (20 ml, 144 mmol) and degassed for 15 minutes with bubbling nitrogen. This mixture was then added to the following: palladium acetate (5.4 mg, 0.24 mmol), triphenyl phosphine (316 mg, 1.2 mmol) and the substituted 3-bromo-pyridine (**81**, **80** or 3-bromo-2-aminopyridine) (24.1 mmol) from which oxygen has been excluded by repeatedly placing the solid mixture under vacuum and nitrogen gas. After several minutes of stirring copper iodide (4.6 mg, 0.24 mmol) was added and heated under reflux for 16 hrs. The solution was then cooled and washed with saturated ammonium chloride (20 ml) to remove copper salts. Sodium hydroxide (500 mg) was added to the biphasic system in order to increase the pH, decreasing the solubility of amino pyridine compounds in the water phase. The layers were then extracted with diethyl ether or ethyl acetate (3 x 50 ml). The organic layer was then acidified with 6M HCl (15ml) and the water layer isolated. This was repeated and the water layers were then neutralised using solid Na_2CO_3. The neutralised mixture was then washed with EtOAc (30 ml x 3). The organic layer was then dried with anhydrous Na_2SO_4 and the EtOAc removed under vacuum to give 2-aminopyridine **84**, **83** or **83**.

In the case of 3-iodo-pyridine 3 equivalents of triphenyl phosphine in regards to palladium acetate was added and the reaction kept at 30°C.

Some reactions would generate large amounts of dimer products. In these cases dppf was used as a ligand in equimolar quantities in regards to the palladium acetate instead of triphenyl phosphine. Triethyl amine was also replaced with diisopropyl amine (same molar equivalents) was also necessary.

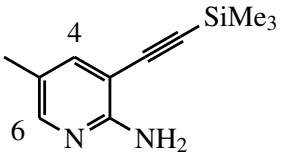
5-Chloro-3-[2-(trimethylsilyl)ethynyl]pyridin-2-amine (84)

CAS: 866318-90-3[123] **Yield:** 74% **MP:** 106-108 °C **IR (cm^{-1}):** $\bar{\nu}$ 3455 (*s*), 3158 (*s*), 2105 (*s*), 1622 (*m*), 1554 (*m*), 1455 (*m*), 1405 (*m*), 1248



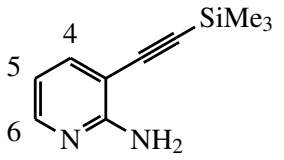
(*m*), 1199 (*m*), 1106 (*m*), 928 (*m*), 904 (*m*), 838 (*l*), 762 (*l*), 648 (*l*), 560 (*m*) **^{1}H NMR (300 MHz, $CDCl_3$):** δ 7.96 (*d*, J = 2.4 Hz, 1H, H-6), 7.50 (*d*, J = 2.4 Hz, 1H, H-4), 5.15 (*s*, 2H, N**H**$_2$), 0.26 (*s*, 9H, Si(C**H**$_3$)$_3$) **^{13}C NMR (75 MHz, $CDCl_3$):** δ 157.7, 146.7, 139.4, 119.9, 104.2, 102.7 (C–**C**≡C), 99.0 (Si–**C**≡C), 0.1 (Si(**C**H$_3$)$_3$)

5-Methyl-3-[2-(trimethylsilyl)ethynyl]pyridin-2-amine (83)



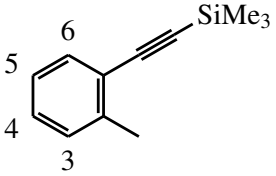
CAS: 500903-95-7[123] **Yield:** 82% **MP:** 105-107 °C **IR (cm^{-1}):** $\bar{\nu}$ 3460 (*s*), 3292 (*s, br*), 3152 (*s, br*), 2142 (*s*), 1627 (*m*), 1561 (*m*), 1472 (*m*), 1403 (*m*), 1249 (*m*), 1218 (*m*), 837 (*l*), 762 (*l*), 654 (*l*) **^{1}H NMR (300 MHz, $CDCl_3$):** δ 7.85 (*d*, J = 1.5 Hz, 1H, H-6), 7.38 (*d*, J = 2.1 Hz, 1H, H-4), 4.87 (*s*, 2H, N**H**$_2$), 0.26 (*s*, 9H, Si(C**H**$_3$)$_3$) **^{13}C NMR (75 MHz, $CDCl_3$):** δ 157.31, 148.07, 140.81, 122.34, 102.68 (C–**C**≡C), 100.86, 100.50 (C–**C**≡C), 17.21 (**C**H$_3$), 0.00 (Si(**C**H$_3$)$_3$)

3-[2-(Trimethylsilyl)ethynyl]pyridin-2-amine (77)



CAS: 936342-23-3[123] **Yield:** 94% **MP:** 80-81 °C **IR (cm^{-1}):** $\bar{\nu}$ 3463 (*s*), 3282 (*s, br*), 3125 (*s, br*), 2134 (*s*), 1629 (*m*), 1568 (*m*), 1247 (*m*), 1201 (*m*), 837 (*l*), 756 (*l*), 642 (*l*) **^{1}H NMR (300 MHz, $CDCl_3$):** δ 8.01 (*dd*, J = 1.8 Hz, 5.1 Hz, 1H, H-6), 7.52 (*dd*, J = 1.8 Hz, 7.5 Hz, 1H, H-4), 6.58 (*dd*, J = 4.9 Hz, 7.5 Hz, 1H, H-5), 5.13 (*s*, 2H, N**H**$_2$), 0.26 (*s*, 9H, Si(C**H**$_3$)$_3$) **^{13}C NMR (75 MHz, $CDCl_3$):** δ 159.3, 148.2, 140.2, 113.3, 103.0, 101.1 (C–**C**≡C), 100.4 (Si–**C**≡C), 0.37 (Si(**C**H$_3$)$_3$)

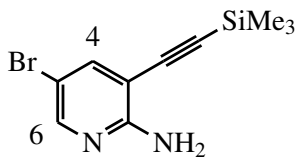
Trimethyl[2-(2-methylphenyl)ethynyl]silane (106)



CAS: 3989-15-9[203] **Yield:** 79% **IR (cm^{-1}):** $\bar{\nu}$ 2959 (*s*), 2154 (*s*), 1482 (*s*), 1248 (*m*), 866 (*l*), 835 (*l*), 714 (*m*), 698 (*m*), 645 (*m*) **^{1}H NMR (300 MHz, $CDCl_3$):** δ 7.41 (*d*, J = 7.5 Hz, 1H, H-6), 7.19 – 7.09

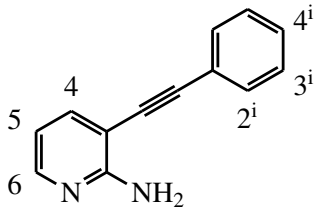
(*m*, 3H, H-3 & H-4 & H-5), 2.43 (*s*, 3H, CC**H**$_3$), 0.256 (*s*, 9H, SiC**H**$_3$) **^{13}C NMR (75 MHz, CDCl$_3$):** δ 140.5, 132.0, 129.3, 128.4, 125.3, 122.9, 104.0 (**C**≡C), 98.1 (**C**≡C), 20.5 (C–**C**H$_3$), 0.00 (Si(**C**H$_3$)$_3$)

5-Bromo-3-[2-(trimethylsilyl)ethynyl]pyridin-2-amine (85)



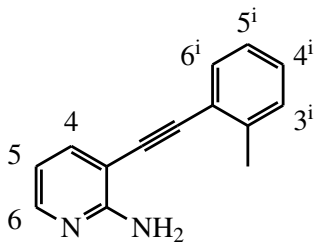
CAS: 905966-34-9[123] **Yield:** 78% **MP:** 131-134 °C **IR (cm^{-1}):** $\bar{\nu}$ 3456 (*s*), 3293 (*s*), 3159 (*s*), 2960 (*s*), 2902 (*s*), 2151 (*s*), 1625 (*m*), 1458 (*m*), 1249 (*m*), 1196 (*m*), 914 (*m*), 837 (*l*), 792 (*l*), 645 (*l*), 607 (*m*) **^{1}H NMR (300 MHz, CDCl$_3$):** δ 8.04 (*d*, J = 2.1 Hz, 1H, H-6), 7.63 (*d*, J = 2.4 Hz, 1H, H-4), 5.09 (*s*, 2H, N**H**$_2$), 0.262 (*s*, 9H, C**H**$_3$) **^{13}C NMR (75 MHz, CDCl$_3$):** δ 157.9, 148.7, 142.1, 107.0, 105.0, 102.9 (**C**≡C), 98.9 (**C**≡C), 0.1 (Si(**C**H$_3$)$_3$)

2-Amino-3-[phenylethynyl]pyridine (211)



Reaxys: 11280435[204] **Yield:** 89% **MP:** 119-123 °C **^{1}H NMR (300 MHz, CDCl$_3$):** δ 8.05 (*dd*, J = 1.5 Hz, 5.1 Hz, 1H, H-6), 7.60 (*dd*, J = 1.8 Hz, 7.5 Hz, 1H, H-4), 7.54 - 7.50 (*m*, 2H, H-3^i), 7.38 - 7.34 (*m*, 3H, H-2^i & H-4^i), 6.65 (*dd*, J = 7.5 Hz, 5.3 Hz, 1H, H-5), 5.07 (*s*, 2H, N**H**$_2$) **^{13}C NMR (75 MHz, CDCl$_3$):** δ 158.8, 148.1, 140.0, 131.5, 128.7, 128.5, 122.7, 113.6, 103.2 (**C**≡C), 95.5 (**C**≡C), 84.5

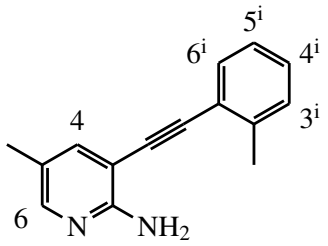
2-Amino-3-[(2-methyl-phenyl)ethynyl]pyridine (75)



CAS: Novel **Yield:** 92% **MP:** 87-89 °C **IR (cm^{-1}):** $\bar{\nu}$ 3469 (*s*), 3284 (*s*), 3124 (*s*), 1629 (*m*), 1562 (*m*), 1450 (*m*), 1242 (*m*), 750 (*l*) **^{1}H NMR (300 MHz, CDCl$_3$):** δ 8.05 (*dd*, J = 5.0 Hz, 1.8 Hz, 1H, H-6), 7.61 (*dd*, J = 7.5 Hz, 1.8 Hz, 1H, H-4), 7.49 (*d*, J = 7.3, 1H, H-6^i), 7.28 - 7.15 (*m*, 3H, H-3^i & H-4^i & H-5^i), 6.66 (*dd*, J = 7.5 Hz, 5.0 Hz, 1H, H-5), 5.09 (*s*, 2H, N**H**$_2$), 2.51 (*s*, 3H, C**H**$_3$) **^{13}C NMR (75 MHz, CDCl$_3$):** δ 158.7,

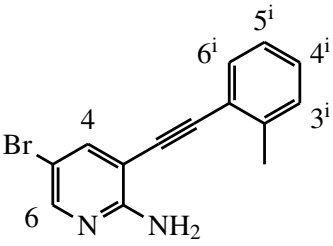
148.0, 139.8, 138.0, 131.9, 129.6, 128.7, 125.8, 122.6, 113.6, 103.5, 94.5 (C–**C**≡C), 88.4 (C–**C**≡C), 20.9 (**C**H_3) **HRMS:** $[M+H]^+$ Calculated: 209.1073 Found: 209.1078

2-Amino-5-methyl-3-[(2-methyl-phenyl)ethynyl]pyridine (89)



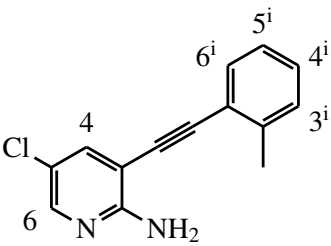
CAS: Novel **Yield:** 80% **MP:** 105-108 °C **IR (cm^{-1}):** $\bar{\nu}$ 3473 (*s*), 3302 (*s*), 3149 (*s, br*), 2927 (*m*), 1627 (*m*), 1568 (*m*), 1244 (*l*), 1244 (*l*), 756 (*l*) **^{1}H NMR (300 MHz, CDCl$_3$):** δ 7.88 (*d*, J = 1.7 Hz, 1H, H-6), 7.48 (*d*, J = Hz, 1H, H-6^i), 7.45 (*d*, J = 2.2 Hz, 1H, H-4), 7.28 - 7.22 (*m*, 2H), 7.19 (*dd*, J = 7.6 Hz, 3.6 Hz, 1H, H-4^i), 4.93 (*s*, 2H, N**H**$_2$), 2.51 (*s*, 3H, C**H**$_3$), 2.12 (*s*, 3H, C**H**$_3$) **^{13}C NMR (75 MHz, CDCl$_3$):** δ 156.8, 147.9, 146.8, 141.0, 140.5, 139.8, 131.8, 129.6, 128.6, 125.7, 122.7, 103.2, 94.3 (C–**C**≡C), 88.6 (C–**C**≡C), 20.9 (**C**H_3), 17.3 (**C**H_3) **HRMS:** $[M+H]^+$ Calculated: 223.1230 Found: 223.1228

5-Bromo-2-amino-3-[(2-methyl-phenyl)ethynyl]pyridine (108)



CAS: Novel **Yield:** 66% **MP:** 124-127 °C **IR (cm^{-1}):** $\bar{\nu}$ 3469 (*s*), 3288 (*s*), 3138 (*s*), 1627 (*l*), 1462 (*l*), 1234 (*l*), 887 (*l*), 758 (*l*) **^{1}H NMR (300 MHz, CDCl$_3$):** δ 8.07 (*d*, J = 2.4 Hz, 1H, H-6), 7.69 (*d*, J = 2.4 Hz, 1H, H-4), 7.47 (*d*, J = 7.3 Hz, 1H), 7.28 - 7.16 (*m*, 3H), 5.16 (*s*, 2H, N**H**$_2$), 2.49 (*s*, 3H, C**H**$_3$) **^{13}C NMR (75 MHz, CDCl$_3$):** δ 157.3, 148.4, 141.4, 139.9, 131.9, 129.7, 129.1, 125.8, 122.0, 107.1, 105.2, 95.6 (C–**C**≡C), 87.1 (C–**C**≡C), 20.5 (**C**H_3) **HRMS:** $[M+H]^+$ Calculated: 287.0178 Found: 287.0188

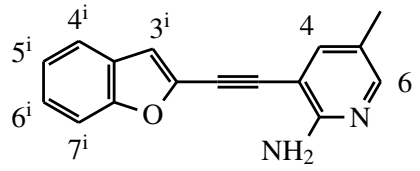
5-Chloro-2-amino-3-[(2-methyl-phenyl)ethynyl]pyridine (90)



CAS: Novel **Yield:** 85% **MP:** 124-126 °C **IR (cm^{-1}):** $\bar{\nu}$ 3467 (*s*), 3290 (*s*), 3126 (*s*), 1627 (*m*), 1556 (*m*), 1462 (*l*), 1230 (*l*), 759 (*l*) **^{1}H NMR (500 MHz, CDCl$_3$):** δ 7.98 (*d*, J = 2.4 Hz, 1H, H-6), 7.57 (*d*, J = 2.5 Hz, 1H, H-4), 7.48 (*d*, J = 7.6 Hz,

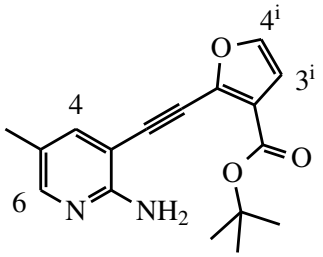
1H, H-6^i), 7.30 - 7.23 (*m*, 2H), 7.19 (*td*, J = 7.2 Hz, 1.4 Hz, 1H, H-5^i), 5.16 (*s*, 2H, N**H**$_2$), 2.50 (*s*, 3H, C**H**$_3$) **^{13}C NMR (125 MHz, CDCl$_3$):** δ 157.1, 146.2, 134.0, 138.9, 131.9, 129.7, 125.8, 122.0, 120.1, 104.6, 95.5 (C–**C**≡C), 87.1 (C–**C**≡C), 20.9 (**C**H$_3$) **HRMS:** [M+H]$^+$ Calculated: 243.0685 Found: 243.0685

3-(Benzofuran-2-ylethynyl)-5-methyl-2-aminopyridine (200)



CAS: Novel **Yield:** 94% **MP:** 82-86 °C **IR (cm^{-1}):** $\bar{\nu}$ 3454 (), 3286 (*s*), 3122 (*s*), 1768 (*m*), 1627 (*m*), 1473 (*m*), 1394 (*l*), 1245 (*m*), 1049 (*m*), 885 (*m*), 746 (*l*) **^{1}H NMR (500 MHz, CDCl$_3$):** δ 7.93 (*s*, 1H, H-6), 7.58 (*d*, J = 7.1 Hz, 1H, H-7^i), 7.48 (*m*, 2H, H-4 & H-5^i), 7.36 (*ddd*, J = 8.4 Hz, 7.1 Hz, 1.3 Hz, 1H, H-6^i), 7.26 (*m*, 1H, H-4^i), 7.01 (*d*, J = 1.0 Hz, 1H, H-3^i), 4.95 (*s*, 2H, N**H**$_2$), 2.21 (*s*, 3H, C**H**$_3$) **^{13}C NMR (126 MHz, CDCl$_3$):** δ 156.99, 154.99, 149.04, 141.04, 140.79, 138.30, 127.62, 125.80, 123.41, 122.68, 121.27, 111.81, 111.25, 90.54, 85.43, 17.25 **HRMS:** [M+H]$^+$ Calculated: 249.1022 Found: 249.1020

***tert*-Butyl 2-[(2-amino-5-methylpyridin-3-yl)ethynyl]furan-3-carboxylate (202)**

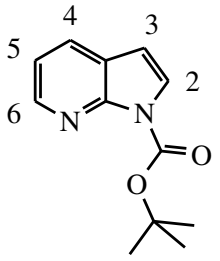


CAS: Novel **Yield:** Quantitative **MP:** 57-58 °C **IR (cm^{-1}):** $\bar{\nu}$ 3388 (*s*), 3145 (*s*), 2987 (*s*), 2196 (*s*), 1701 (*m*), 1652 (*m*), 1575 (*m*), 1487 (*m*), 1055 (*l*), 744 (*l*) **^{1}H NMR (300 MHz, CDCl$_3$):** δ 7.91 (*d*, J = 1.9 Hz, 1H, H-6), 7.43 (*d*, J = 2.0 Hz, 1H, H-4), 7.34 (*d*, J = 2.0 Hz, 1H, H-4^i), 6.69 (*d*, J = 1.9 Hz, 1H, H-3^i), 5.65 (*s*, 2H, N**H**$_2$), 2.18 (*s*, 9H, C(C**H**$_3$))$_3$, 1.57 (*s*, 3H, C**H**$_3$) **^{13}C NMR (75 MHz, CDCl$_3$):** δ 161.9 (**C**=O), 153.5, 140.6, 124.5, 122.8, 121.7, 104.3, 100.64 (C–**C**≡C), 94.7 (C–**C**≡C), 84.8 (**C**(CH$_3$)$_3$), 28.3 (C(**C**H$_3$)$_3$), 17.0 (**C**H$_3$) **HRMS:** [M+H]$^+$ Calculated: 299.1390 Found: 299.1389

4.2.8 A typical Boc protection procedure

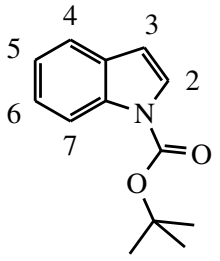
Indole or 7-azaindole (42.6 mmol) was dissolved in THF (50 ml) with DMAP (78.2 mg, 0.64 mmol). To this solution Boc_2O (13.94 g, 63.9 mmol) was added slowly and the reaction stirred until starting material was consumed as seen by TLC. The solution was then extracted using EtOAc and water and the organic layer was isolated and dried using anhydrous Na_2SO_4. Removal of the organic solvent yielded the Boc protected indole **184** or 7-azaindole **196** without the need for further purification.

tert-Butyl 1*H*-pyrrolo[2,3-b]pyridine-1-carboxylate (196)



CAS: 138343-77-8[205] **Yield:** Quantitative **^{1}H NMR (300 MHz, $CDCl_3$):** δ 8.51 (*dd*, J = 4.8 Hz, 1.6 Hz, 1H, H-6), 7.86 (*dd*, J = 7.8 Hz, 1.7 Hz, 1H, H-4), 7.63 (*d*, J = 4.1 Hz, 1H, H-3), 7.17 (*dd*, J = 7.8 Hz, 4.8 Hz, 1H, H-5), 6.49 (*d*, J = 4.1 Hz, 1H, H-2), 1.67 (*s*, 9H, C**H**$_3$) **^{13}C NMR (75 MHz, $CDCl_3$):** δ 147.9 (**C**=O), 145.07, 129.09, 126.53, 123.00, 118.47, 104.48, 85.1 (**C**$(CH_3)_3$), 83.96, 28.10 (**C**H_3)

tert-Butyl 1*H*-indole-1-carboxylate (184)



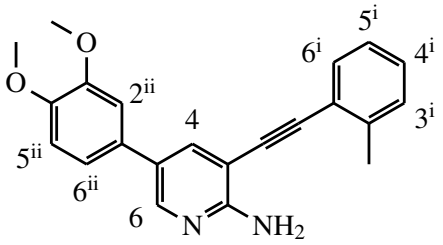
CAS: 75400-67-8[206] **Yield:** Quantitative **^{1}H NMR (300 MHz, $CDCl_3$):** δ 8.14 (*d*, J = 8.2 Hz, 1H, H-7), 7.59 (*d*, J = 3.7 Hz, 1H, H-2), 7.56 (*d*, J = 7.6 Hz, 1H, H-4), 7.31 (*ddd*, J = 1.2 Hz, 7.5 Hz, 8.1 Hz, 1H, H-6), 7.22 (*dt*, J = 1.2 Hz, 7.5 Hz, 1H, H-5), 6.56 (*d*, J = 3.7 Hz, 1H, H-3), 1.67 (*s*, C**H**$_3$, 9H) **^{13}C NMR (75 MHz, $CDCl_3$):** δ 130.6, 125.9, 124.2, 122.6, 120.9, 115.2, 107.3, 83.6 (**C**$(CH_3)_3$), 28.2 (**C**H_3)

4.2.9 A typical Suzuki coupling procedure

$Pd(PPh_3)_4$ (764 mg, 0.662 mmol) was weighed in to a two neck round bottom flask together with the corresponding aromatic boronic acid (9.95 mmol) and the round bottom evacuated to remove O_2 and replace it with N_2. A solution of DME (50 ml) and corresponding halide **108**, **186** or **185** (6.62 mmol) was added to a dropping funnel and degassed by bubbling of N_2 for 15 min. This was then added to the round bottom flask under stirring. A 2M aqueous solution of potassium carbonate (15 ml) was then degassed by the bubbling of N_2 for 15 min after which it was added to the reaction mixture. The reaction mixture was then heated under reflux over night. After cooling the reaction mixture was added to a mixture of EtOAc and water and the organic layer separated and washed with brine. The organic layer was then dried over anhydrous anhydrous Na_2SO_4 and the solvent removed under vacuum. The crude product was then purified using silica chromatography to yield the desired products **140**, **191** or **192**.

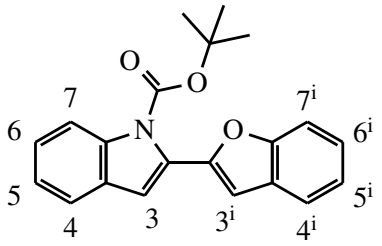
The indole and 7-azaindole boronic acids were synthesised from **196** and **184**. A three neck round bottom was taken and flame dried under vacuum, after which THF (10 ml) and diisopropyl amine (0.72 ml, 5.15 mmol) were added. The reaction was then cooled by using an acetone slurry made by adding liquid nitrogen to acetone. BuLi in hexane (4.80 mmol) was then added slowly and reaction mixture stirred for 30 min while maintaining the acetone slurry. Indole or 7-azaindole **196** or **184** (4.80 mmol) was then dissolved in THF (10 ml) and slowly added to the reaction mixture which was then stirred for an hr while maintaining the acetone slurry. To the reaction was then added triisopropyl borate (7.02 mmol) and the reaction mixture allowed to warm to rt. The reaction mixture was then quenched with a aqueous 1 M HCl until the pH was at 7 after which the reaction mixture was placed in a separating flask and washed with diethyl ether (30ml x 3). The diethyl ether layer was then dried under anhydrous $MgSO_4$ and evaporated under vacuum. Care must be taken to not let the water temperature rise above 30°C, as the boronic acid decomposes readily at elevated temperatures. The boronic acids isolated were used as is in the Suzuki reaction.

5-(3,4-Dimethoxyphenyl)-3-(o-tolylethynyl)pyridin-2-amine (140)



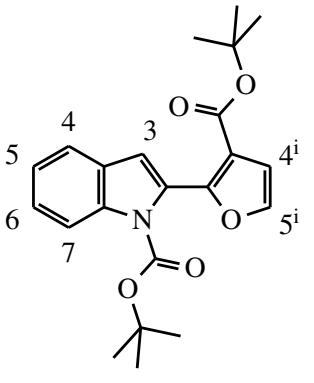
CAS: Novel **Yield:** 12% **MP:** 116-118 °C **IR (cm^{-1}):** $\bar{\nu}$ 3469 (*s*), 3290 (*s*), 3149 (*s*), 2983 (*s*), 1625 (*s*), 1448 (*l*), 1263 (*l*), 1136 (*l*), 914 (*l*), 748 (*l*) **^{1}H NMR (300 MHz, $CDCl_3$):** δ 8.26 (*d*, J = 2.4 Hz, 1H, H-6), 7.80 (*d*, J = 2.4 Hz, 1H, H-4), 7.52 (*d*, J = 7.4 Hz, 1H, H-6^i), 7.30 - 7.15 (*m*, 3H), 7.07 (*dd*, J = 8.2 Hz, 2.1 Hz, 1H, H-6^{ii}) 7.02 (*d*, J = 2.0 Hz, 1H, H-2^{ii}), 6.94 (*d*, J = 8.3 Hz, 1H, H-5^{ii}), 5.13 (*s*, 2H, N$\underline{\mathbf{H}}_2$), 3.95 (O$\underline{\mathbf{C}}$H$_3$), 3.92 (O$\underline{\mathbf{C}}$H$_3$), 2.53 ($\underline{\mathbf{C}}$H$_3$) **^{13}C NMR (125 MHz, DMSO):** δ 158.7, 149.7, 148.5, 146.6, 139.9, 137.8, 132.3, 130.4, 130.0, 129.2, 126.3, 125.1, 122.8, 118.3, 112.8, 110.2, 101.9, 94.0 (C–$\underline{\mathbf{C}}$≡C), 89.7 (C–$\underline{\mathbf{C}}$≡C), 56.11 (O$\underline{\mathbf{C}}$H$_3$), 56.07 (O$\underline{\mathbf{C}}$H$_3$), 21.0 ($\underline{\mathbf{C}}$H$_3$) **HRMS:** [M+H]$^+$ Calculated: 345.1598 Found: 345.1603

tert-Butyl 2-(benzofuran-2-yl)-1*H*-indole-carboxylate (191)



CAS: Novel **Yield:** 96% **MP:** 127-128 °C **IR (cm^{-1}):** $\bar{\nu}$ 3057 (s) 2974 (*s*), 1743 (*l*), 1444 (*l*), 1367 (*l*), 1325 (*l*), 1292 (*l*), 1159 (*l*), 1124 (*l*), 815 (*l*) **^{1}H NMR (300 MHz, $CDCl_3$):** δ 8.24 (*dd*, J = 8.3 Hz, 0.7 Hz, 1H, H-7), 7.60 (*ddd*, J = 6.8 Hz, 3.9 Hz, 0.7 Hz, 2H, H-5), 7.49 (*d*, J = 8.2 Hz, 1H, H-7^i), 7.38 (*ddd*, J = 8.5 Hz, 7.3 Hz, 1.3 Hz, 1H, H-6), 7.31 (*d*, J = 1.4 Hz, 1H), 7.30 - 7.21 (*m*, 2H), 6.93 (*d*, J = 0.8 Hz, 1H, H-3), 6.89 (*s*, 1H, H-3^i), 1.35 (*s*, 9H, C$\underline{\mathbf{H}}_3$) **^{13}C NMR (75 MHz, $CDCl_3$):** δ 154.96 ($\underline{\mathbf{C}}$=O), 149.75, 149.47, 137.67, 129.41, 128.55, 128.49, 125.41, 124.58, 123.11, 122.89, 121.12, 121.03, 115.36, 112.63, 111.04, 105.69, 83.79 ($\underline{\mathbf{C}}$(CH$_3$)$_3$), 27.64 ($\underline{\mathbf{C}}$H$_3$) **HRMS:** [M+H]$^+$ Calculated: 334.1438 Found: 334.1685

tert-Butyl 2-[3-(*tert*-butoxycarbonyl)furan-2-yl]-1*H*-indole-1-carboxylate (192)



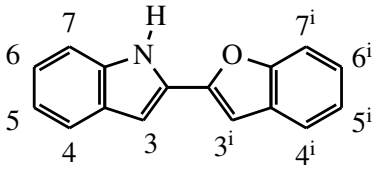
CAS: Novel **Yield:** Quantitative **MP:** 66-70 °C **IR (cm^{-1}):** $\bar{\nu}$ 2983 (*s*), 1712 (*l*), 1452 (*m*), 1332 (*l*), 1159 (*l*), 1066 (*l*), 746 (*l*) **^{1}H NMR (300 MHz, $CDCl_3$):** δ 8.24 (*dd*, J

= 8.4 Hz, 0.8 Hz, 1H, H-7), 7.58 (*dd*, J = 7.8 Hz, 0.7 Hz, 1H, H-4), 7.45 (*d*, J = 1.9 Hz, 1H, H-5^i), 7.40 - 7.35 (*m*, 2H), 7.26 (*dd*, J = 7.4 Hz, 1.3 Hz, 1H, H-5), 6.84 (*d*, J = 1.9 Hz, 1H, H-4^i), 6.81 (*d*, J = 0.7 Hz, 1H, H-3), 1.40 (*s*, 9H, C$\underline{\mathbf{H}}_3$), 1.28 (*s*, 9H, C$\underline{\mathbf{H}}_3$) **^{13}C NMR (75 MHz, CDCl$_3$):** δ 162.19, 150.44, 149.55, 141.70, 137.04, 128.36, 127.69, 125.40, 124.18, 122.90, 121.09, 118.82, 115.43, 113.32, 111.74, 107.26, 83.34, 80.85, 27.98, 27.87 **HRMS:** [M+H]$^+$ Calculated: 384.1805 Found: 384.1736

4.2.10 A typical Boc deprotection procedure

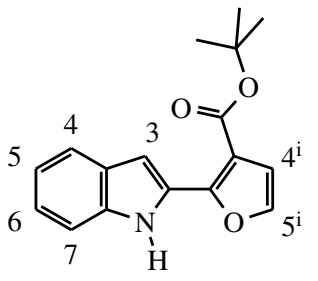
The Boc substituted compound **191** or **192** (5 mmol) was dissolved in a 40% mixture of TFA in DCM (50 ml) and stirred for 1 hr after which the reaction mixture was poured into a sat. $NaHCO_3$ solution. If a solid precipitate formed this was filtered and dried. If not the reaction mixture was extracted several times with EtOAc, dried over anhydrous Na_2SO_4 and evaporated under vacuum to yield **193** or **195**.

2-(Benzofuran-2-yl)-1*H*-indole(193)



CAS: 78842-63-4[207] **Yield:** 54% **MP:** 193-196 °C **^{1}H NMR (500 MHz, CDCl$_3$):** δ 8.65 (*s*, 1H, N$\underline{\mathbf{H}}$), 7.65 (*dd*, J = 8.0 Hz, 1.0 Hz, 1H, H-4^i), 7.59 (*ddd*, J = 7.6 Hz, 1.5 Hz, 0.7 Hz, 1H, H-4), 7.52 (*dd*, J = 8.0 Hz, 0.9 Hz, 1H, H-7^i), 7.43 (*dd*, J = 8.2 Hz, 0.9 Hz, 1H, H-7), 7.27 (*m*, 3H), 7.15 (*ddd*, J = 8.0 Hz, 7.0 Hz, 1.0 Hz, 1H, H-5), 6.99 (*d*, J = 1.0 Hz, 1H, H-3^i), 6.98 (*dd*, J = 2.1 Hz, 1.0 Hz, 1H, H-3)**^{13}C NMR (126 MHz, CDCl$_3$):** δ 154.48, 149.36, 136.46, 129.03, 128.75, 128.54, 124.40, 123.31, 123.16, 120.97, 120.91, 120.60, 111.05, 101.44, 101.22 **HRMS:** [M+H]$^+$ Calculated: 234.0913 Found: 234.0908

tert-Butyl 2-(1*H*-indol-2-yl)furan-3-carboxylate (195)



CAS: Novel **Yield:** 51% **MP:** Decomposed 142 °C **IR (cm^{-1}):** $\bar{\nu}$ 3276 (*s*), 2970 (*s*), 1683 (*s*), 1600 (*s*), 1259 (*m*), 1136 (*l*), 1080 (*l*), 1022 (*l*), 786 (*l*) **^{1}H**

NMR (500 MHz, $CDCl_3$): δ 11.66 (*s*, 1H, N**H**), 7.65 (*d*, J = 7.9 Hz, 1H, H-7), 7.50 (*dd*, J = 8.2 Hz, 0.7 Hz, 1H, H-4), 7.35 (*d*, J = 1.9 Hz, 1H, H-4^i), 7.23 (*t*, J = 7.7 Hz, 1H, H-5), 7.11 (*t*, J = 7.5 Hz, 1H, H-6), 7.07 (*d*, J = 1.0 Hz, 1H, H-3), 6.72 (*d*, J = 1.9 Hz, 1H, H-5^i), 1.63 (*s*, 9H, C**H**$_3$) **^{13}C NMR (126 MHz, $CDCl_3$):** δ 164.58 (**C**=O), 152.16, 140.62, 136.37, 128.27, 127.91, 123.28, 121.04, 120.15, 113.78, 112.65, 111.88, 102.40, 82.02 (**C**$(CH_3)_3$), 28.27 (**C**H_3) **HRMS:** $[M+H]^+$ Calculated: 284.1281 Found: 284.1265

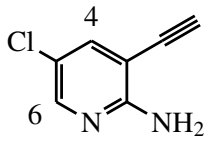
4.2.11 A typical trimethylsilyl deprotection procedure

In the case of 2-aminopyridine substrates the following procedure was followed:

To a solution of THF and water (4:1) (50 ml) was added the substrate **84**, **83**, **85** or **77** (7.44 mmol) and TBAF (0.74 mmol) and the reaction allowed to stir for 12 hrs. Alternatively, the reaction could be heated at reflux for an hour, however, the rt method tends to give a cleaner reaction.

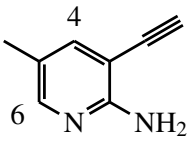
The reaction mixture was then poured into water and extracted with EtOAc, dried with anhydrous Na_2SO_4 and the solvent evaporated under vacuum to yield the product **87**, **107**), **86**, **76** or **88**.

5-Chloro-3-ethynylpyridine-2-amine (87)



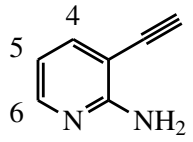
CAS: 866318-88-9[208] **Yield:** 96% **MP:** 98-100 °C **IR (cm^{-1}):** $\bar{\nu}$ 3455 (*s*), 3287 (*s, br*), 3158 (*s, br*), 2959 (*s*), 3149 (*s*), 1622 (*m*), 1554 (*m*), 1455 (*m*), 1405 (*m*), 1248 (*m*), 1199 (*m*), 1106 (*m*), 928 (*m*), 905 (*m*), 837 (*l*), 837 (*l*), 761 (*l*), 647 (*l*) **^{1}H NMR (300 MHz, $CDCl_3$):** δ 7.99 (*d*, J = 2.1 Hz, 1H, H-6), 7.53 (*d*, J = 2.1 Hz, 1H, H-4), 5.2 (*s*, 2H, N**H**$_2$), 3.45 (*s*, 1H, ≡C**H**) **^{13}C NMR (75 MHz, $CDCl_3$):** δ 157.9, 147.0, 139.8, 119.8, 102.8, 84.5 (**C**≡C), 84.5 (**C**≡C)

3-Ethynyl-5-methylpyridin-2-amine (86)



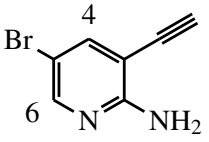
CAS: 863479-77-0[209] **Yield:** 96% **MP:** 55-57 °C **IR (cm^{-1}):** $\bar{\nu}$ 3440 (*m*),3279 (*m*), 3249 (*m*), 3131 (*m, br*), 2096 (*s*), 1629 (*l*), 1568 (*l*), 1468 (*l*), 1400 (*l*), 1222 (*l*), 1085 (*m*), 892 (*l*), 769 (*l*), 709 (*l*), 607 (*l*), 574 (*l*) **^{1}H NMR (300 MHz, $CDCl_3$):** δ 7.90 (*s*, 1H, H-6), 7.41 (*s*, 1H, H-4), 4.88 (*s*, 2H, N**H**$_2$), 3.39 (*s*, 1H, ≡C**H**), 2.17 (*s*, 3H, C**H**$_3$) **^{13}C NMR (75 MHz, $CDCl_3$):** δ 157.6, 148.4, 141.3, 122.4, 101.5, 83.2 (≡**C**H), 79.5 (C–**C**≡C), 17.2 (**C**H$_3$)

3-Ethynylpyridin-2-amine (76)



CAS: 67346-74-1[210] **Yield:** 96% **MP:** 84-86 °C **IR (cm^{-1}):** $\bar{\nu}$ 3461 (*m*), 3286 (*m*), 3239 (*m*), 3154 (*m, br*), 2099 (*s*), 1621 (*l*), 1569 (*l*), 1447 (*l*), 1252 (*l*), 1186 (*l*), 801 (*l*), 768 (*l*), 696 (*l*), 609 (*l*), 592 (*l*) **^{1}H NMR (300 MHz, $CDCl_3$):** δ 8.05 (*d*, J = 3.9 Hz, 1H, H-6), 7.56 (*dd*, J = 1.5 Hz, 7.5 Hz, 1H, H-4), 6.61 (*dd*, J = 4.8 Hz, 7.5 Hz, 1H, H-5), 5.15 (*s*, 2H, N**H**$_2$), 3.41 (*s*, 1H, ≡C**H**) **^{13}C NMR (75 MHz, $CDCl_3$):** δ 159.5, 148.5, 140.7, 113.34, 101.8, 83.4 (≡**C**H), 79.3 (C–**C**≡C)

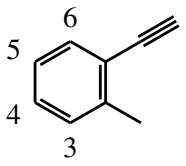
5-Bromo-3-ethynylpyridine-2-amine (88)



CAS: 1210838-82-6[211] **Yield:** 97% **MP:** 120-123 °C **^{1}H NMR (300 MHz, $CDCl_3$):** δ 8.01 (*d*, J = 2.4 Hz, 1H, H-6), 7.65 (*d*, J = 2.1 Hz, 1H, H-4), 5.05 (*s*, 2H, N**H**$_2$), 3.45 (*s*, 1H, ≡C**H**) **^{13}C NMR (75 MHz, $CDCl_3$):** δ 158.0, 149.2, 142.3, 106.8, 103.5, 84.6 (**C**≡C), 78.0 (**C**≡C)

1-Ethynyl-2-methyl-benzene (107)

The procedure for de-protection of acetylene **106** was the same as the procedure stated other than a full equivalent of *TBAF* was added and water was excluded from the reaction by using dry THF. The reaction time was also limited to an hour.

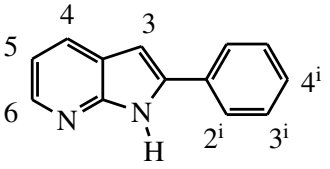


CAS: 766-47-2[212] **Yield:** 87% **IR (cm^{-1}):** $\bar{\nu}$ 3290 (*s*), 3022 (*s*), 2922 (*s*), 2104 (*s*), 1483 (*s*), 1455 (*s*), 1014 (*s*), 755 (*l*), 715 (*m*), 644 (*l*), 610 (*l*) **^{1}H NMR (300 MHz, CDCl$_3$):** δ 7.46 (*d*, J = 7.5 Hz, 1H), 7.24–7.12 (*m*, 3H), 3.26 (*s*, 1H, ≡C**H**), 2.45 (*s*, 3H, C**H**$_3$) **^{13}C NMR (75 MHz, CDCl$_3$):** δ 140.8, 139.0, 132.5, 129.5, 128.7, 125.5, 82.6 (C–**C**≡C), 80.9 (≡**C**H), 20.6 (**C**H$_3$)

4.2.12 A typical ring closure of 2-amino-pyridines to form corresponding 7-azaindole

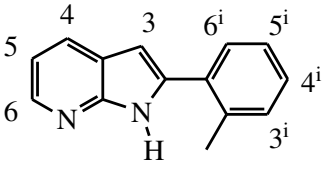
The corresponding alkenyl compounds **211**, **75**, **200**, **89**, **140** or **90** (20.6 mmol) was added to degassed acetonitrile (20 ml) followed by the addition of TFA (2.0 ml, 26.8 mmol) and then TFAA (3.8 ml, 26.8 mmol). The reaction vessel was then evacuated to remove oxygen and kept under N_2. The solution was then heated under reflux for 6 hrs after which it was poured into a 50% saturated aqueous solution of Na_2CO_3 and stirred for 30 min after which the solid was filtered and recrystallised from *i*-PrOH to yield **209**, **74**, **110**, **109**, **141** or **201**.

2-Phenyl-1*H*-pyrrolo[2,3-*b*]pyridine (209)



CAS: 10586-52-4[213] **Yield:** 75% **MP:** 204-205 °C **^{1}H NMR (300 MHz, CDCl$_3$):** δ 12.63 (*s*, 1H, N**H**), 8.31 (*dd*, J = 4.9 Hz, 1.5 Hz, 1H, H-6), 7.96 (*dd*, J = 7.8 Hz, 1.5 Hz, 1H, H-4), 7.90 (*dt*, J = 8.2 Hz, 1.7 Hz, 2H, H-2^i), 7.53 (*t*, J = 7.6 Hz, 2H, H-3^i), 7.40 (*t*, J = 7.4 Hz, 1H, H-4^i), 7.11 (*dd*, J = 7.8 Hz, 4.9 Hz, 1H, H-5), 6.79 (*d*, J = 1.2 Hz, 1H, H-3) **^{13}C NMR (75 MHz, CDCl$_3$):** δ 150.0, 142.2, 139.5, 132.5, 129.0, 128.7, 128.2, 125.9, 122.4, 116.1, 97.4

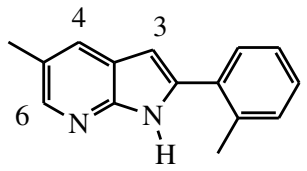
2-(2-Methylphenyl)-1*H*-pyrrolo[2,3-*b*]pyridine (74)



PubChem: 84676211 **Yield:** 83% **MP:** Decomposed at 220 °C **^{1}H NMR (300 MHz, CDCl$_3$):** δ 12.7 (*s*, 1H, N**H**), 8.08 (*d*, J = 3.8 Hz, 1H, H-6), 7.95 (*d*, J = 7.8 Hz, 1H, H-4), 7.73 - 7.67 (*m*, 1H,

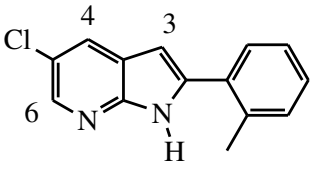
H-6^i), 7.42 - 7.33 (*m*, 3H, H-3^i - H-5^i), 7.05 (*dd*, J = 7.8 Hz, 4.6 Hz, 1H, H-5), 6.58 (s, 1H, H-3), 2.57 (*s*, 3H, C<u>**H**</u>$_3$) **^{13}C NMR (75 MHz, CDCl$_3$):** δ 149.2, 141.7, 139.0, 136.3, 132.6, 131.1, 129.5, 128.6, 128.2, 126.1, 121.9, 117.3, 115.8, 100.4, 21.2 (<u>**C**</u>H$_3$) **HRMS:** [M+H]$^+$ Calculated: 209.1073 Found: 209.1068

5-Methyl-2-(2-methylphenyl)-1*H*-pyrrolo[2,3-*b*]pyridine (110)



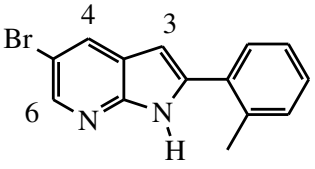
CAS: Novel **Yield:** 75% **MP:** 165-167 °C **IR (cm^{-1}):** $\bar{\nu}$ 3150 (*s, br*), 3010 (*s, br*), 2879 (*s, br*), 1683 (*m*), 1591 (*m*), 1458 (*m*), 1278 (*l*), 1145 (*l*), 750 (*l*) **^{1}H NMR (500 MHz, DMSO):** δ 11.70 (*s*, 1H, N<u>**H**</u>), 8.07 (*d*, J = 2.0 Hz, 1H, H-6), 7.75 (*d*, J = 2.0 Hz, 1H, H-4), 7.57 (*dd*, J = 5.0 Hz, 4.0 Hz, 1H), 7.35 - 7.30 (*m*, 3H), 6.48 (*d*, J = 2.0 Hz, 1H, H-3), 2.46 (*s*, 3H, C<u>**H**</u>$_3$), 2.39 (*s*, 3H, C<u>**H**</u>$_3$) **^{13}C NMR (126 MHz, DMSO):** δ 148.12, 143.79, 138.72, 136.17, 132.61, 131.31, 129.79, 128.39, 127.96, 126.42, 124.57, 120.82, 100.05, 60.23, 21.37, 18.62 **HRMS:** [M+H]$^+$ Calculated: 223.1230 Found: 223.1233

5-Chloro-2-(2-methylphenyl)-1*H*-pyrrolo[2,3-*b*]pyridine (109)



CAS: Novel **Yield:** 67% **MP:** 222-224 °C **IR (cm^{-1}):** $\bar{\nu}$ 3124 (*s*), 2985 (*s*), 1579 (*s*), 1462 (*s*), 1400 (*m*), 1284 (*m*), 941 (*m*), 871 (*m*), 738 (*l*) **^{1}H NMR (500 MHz, DMSO):** δ 12.11 (*s*, 1H, N<u>**H**</u>), 8.21 (*d*, J = 2.3 Hz, 1H, H-6), 8.06 (*d*, J = 2.3 Hz, 1H, H-4), 7.55 (*dd*, J = 6.8 Hz, 2.1 Hz, 1H), 7.34 (*m*, 3H), 6.57 (*d*, J = 1.9 Hz, 1H, H-3), 2.46 (*s*, 3H, C<u>**H**</u>$_3$) **^{13}C NMR (126 MHz, DMSO):** δ 147.72, 140.98, 140.78, 136.38, 132.00, 131.37, 129.95, 128.88, 127.25, 126.50, 122.99, 121.96, 100.37, 21.24 **HRMS:** [M+H]$^+$ Calculated: 243.0684 Found: 243.0685

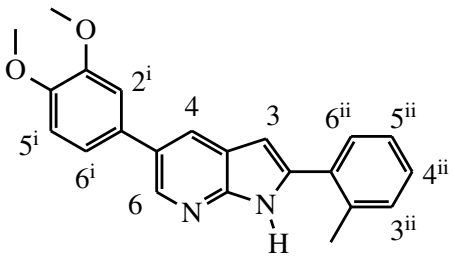
5-Bromo-2-(2-methylphenyl)-1*H*-pyrrolo[2,3-*b*]pyridine (111)



CAS: Novel **Yield:** 90% **MP:** 110-114 °C **IR (cm^{-1}):** $\bar{\nu}$ 3444 (*s*), 3278 (*s*), 3204 (*s*), 1626 (*l*), 1455 (*l*), 1235 (*m*), 1020 (*m*), 871 (*m*), 742 (*m*) **^{1}H NMR**

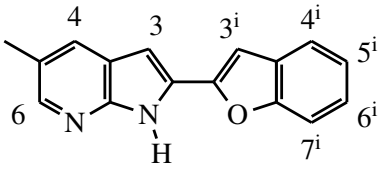
(400 MHz, $CDCl_3$): δ 8.63 (*s*, 1H, N**H**), 8.43 (*d*, *J* = 2.4 Hz, 1H, H-6), 7.93 (*d*, *J* = 2.3 Hz, 1H, H-4), 7.40 – 7.35 (*m*, 1H), 7.25 – 7.21 (*m*, 1H), 7.19 – 7.16 (*m*, 1H), 7.14 – 7.09 (*m*, 1H), 2.40 (*s*, 3H, C**H**$_3$) **^{13}C NMR (101 MHz, $CDCl_3$):** δ 149.36, 143.02, 140.83, 132.74, 130.54, 130.33, 126.50, 121.15, 117.19, 99.90, 84.76, 21.11 **HRMS:** $[M+H]^+$ Calculated: 287.0178 Found: 287.0183

5-(3,4-Dimethoxyphenyl)-2-(2-methylphenyl)-1*H*-pyrrolo[2,3-*b*]pyridine (141)



CAS: Novel **Yield:** 80% **MP:** 186-189 °C **IR (cm^{-1}):** $\bar{\nu}$ 3014 (*s, br*), 2846 (*s*), 1593 (*s*), 1521 (*s*), 1448 (*s*), 1257 (*l*), 1143 (*l*), 844 (*l*), 756 (*l*) **^{1}H NMR (300 MHz, DMSO):** δ 11.90 (*s*, 1H, N**H**), 8.52 (*d*, *J* = 2.1 Hz, 1H, H-6), 8.18 (*d*, *J* = 2.1 Hz, 1H, H-4), 7.58 (*dd*, *J* = 5.1 Hz, 3.8 Hz, 1H, H-3^{ii}), 7.38 - 7.29 (*m*, 5H), 7.24 (*dd*, *J* = 8.3 Hz, 2.0 Hz, 1H, H-6^{ii}), 7.06 (*d*, *J* = 8.4 Hz, 1H, H-6^{i}), 6.51 (*s*, 1H, H-3), 3.88 (*s*, 3H, OC**H**$_3$), 3.80 (*s*, 3H, OC**H**$_3$), 2.48 (*s*, 3H, C**H**$_3$) **^{13}C NMR (75 MHz, $CDCl_3$):** δ 162.3, 149.2, 148.3, 148.1, 141.4, 138.9, 135.8, 130.8, 129.3, 128.5, 126.0, 125.3, 120.5, 118.9, 112.5, 110.8, 106.4, 100.3, 79.1, 55.6 (O**C**H$_3$), 20.8 (**C**H$_3$) **HRMS:** $[M+H]^+$ Calculated: 345.1598 Found: 345.1594

2-(Benzofuran-2-yl)-5-methyl-1*H*-pyrrolo[2,3-*b*]pyridine (201)

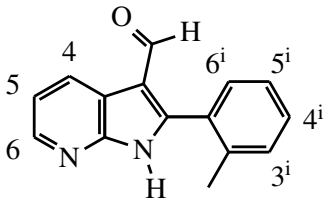


CAS: Novel **Yield:** 21% **MP:** Decomposed 230 °C **IR (cm^{-1}):** $\bar{\nu}$ 3072 (*s*), 2908 (*s*), 1670 (*s*), 1631 (*s*), 1583 (*s*), 1433 (*m*), 1282 (*m*), 1141 (*m*), 738 (*l*) **^{1}H NMR (500 MHz, DMSO):** δ 7.29 (*d*, *J* = 2.1 Hz, 1H, H-6),6.96 (*d*, *J* = 1.9 Hz, 1H, H-4),6.87 (*dd*, *J* = 7.7 Hz, 1.2 Hz, 1H, H-7^{i}),6.79 (*d*, *J* = 8.1 Hz, 1H, H-4^{i}),6.57 (*s*, 1H, H-3),6.50 (*ddd*, *J* = 8.2 Hz, 7.7 Hz, 1.4 Hz, 1H, H-5^{i}),6.44 (*t*, *J* = 7.4 Hz, 1H, H-6^{i}),6.04 (*d*, *J* = 2.0 Hz, 1H, H-3^{i}),1.54 (*s*, 3H, C**H**$_3$)**^{13}C NMR (125 MHz, DMSO):** δ 159.43, 154.41, 153.42, 134.26, 133.70, 133.56, 133.45, 130.08, 128.66, 126.57, 125.41, 116.29, 103.27, 23.30 **HRMS:** $[M+H]^+$ Calculated: 249.1022 Found: 249.1009

4.2.13 A typical formylation procedure with 1,1-dichlorodimethyl ether

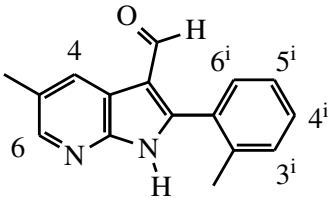
To a solution of 7-azaindole (**74**, **110**, **109** or **141**) (7.02 mmol) in DCM (40 ml) at 0° was added $TiCl_4$ (1.9 ml, 21.1 mmol). 1,1-Dichlorodimethyl ether (2.3 ml, 21.1 mmol) in DCM (10 ml) was added drop wise and the resulting mixture left to stir at rt for 2 hrs after which water (20 ml) was added drop wise and the resulting mixture left to stir for another hour. The resulting mixture was then worked by adding water and DCM and the organic layer separated and dried over anhydrous Na_2SO_4 and evaporated under vacuum. The resulting crude product was then purified using silica chromatography with a 4:1 Hexane:EtOAc mobile phase. Alternatively the product could be recrystallised from *i*-PrOH. TLCs were stained using a DNPH stain under which aldehydes selectively turn orange.

2-(2-Methylphenyl)-1*H*-pyrrolo[2,3-*b*]pyridine-3-carbaldehyde (115)



PubChem: 84699412 **Yield:** 57% **MP:** 215-217 °C **IR (cm^{-1}):** $\bar{\nu}$ 2927 (*s*), 2785 (*s*), 2717 (*s*), 1658 (*l*), 1583 (*m*), 1456 (*l*), 1408 (*m*), 1379 (*m*), 1274 (*l*), 1166 (*m*), 1132 (*m*), 804 (*l*), 727 (*l*), 667 (*l*) **^{1}H NMR (500 MHz, $CDCl_3$):** δ 13.74 (*s*, 1H, N**H**), 9.82 (*s*, 1H, C(=O)**H**), 8.69 (*dd*, J = 7.8 Hz, 1.5 Hz, 1H, H-6), 7.88 (*dd*, J = 4.8 Hz, 1.2 Hz, 1H, H-4), 7.53 (*dd*, J = 12.1 Hz, 4.5 Hz, 2H, H-5^i & 3^i), 7.47 (*d*, J = 7.5 Hz, 1H, H-6^i), 7.41 (*dd*, J = 7.7 Hz, 7.2 Hz, 1H, H-4^i), 7.22 (*dd*, J = 7.8 Hz, 4.9 Hz, 1H, H-5), 2.42 (*s*, 3H, C**H**$_3$) **^{13}C NMR (126 MHz, $CDCl_3$):** δ 186.52 (**C**=O), 150.21, 148.56, 143.00, 137.43, 131.45, 131.37, 130.98, 130.39, 129.38, 126.06, 119.17, 118.75, 113.93, 20.37 (**C**H$_3$) **HRMS:** $[M+H]^+$ Calculated: 237.1022 Found: 237.1024

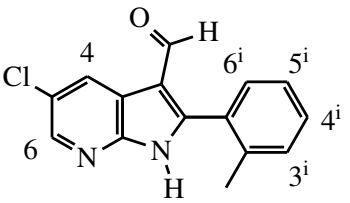
5-Methyl-2-(2-methylphenyl)-1*H*-pyrrolo[2,3-*b*]pyridine-3-carbaldehyde (114)



CAS: Novel **Yield:** Quantitative **MP:** 222-224 °C **IR (cm^{-1}):** $\bar{\nu}$ 2682 (*s, br*), 1658 (*l*), 1460 (*l*), 1240 (*l*), 1217 (*l*), 1066 (*l*), 1045 (*l*), 769 (*l*), 727 (*l*), 659 (*l*) **^{1}H NMR (500 MHz, $CDCl_3$):** δ 9.80 (*s*, 1H, C(=O)**H**), 8.77 (*s*, 1H, H-6), 8.04 (*s*, 1H, N**H**), 7.67

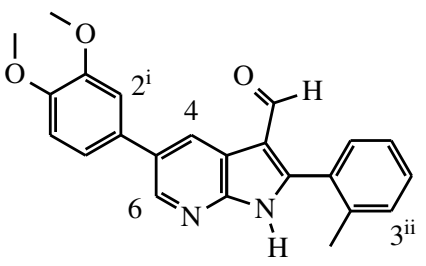
(*dd*, J = 11.1 Hz, 8.0 Hz, 1H, H-6^i), 7.54 (*dd*, J = 13.6 Hz, 6.4 Hz, 1H, H-4^i), 7.51 - 7.40 (*m*, 2H, H-4 & H-5^i), 7.38 (*t*, J = 7.4 Hz, 1H, H-3^i), 2.54 (*s*, 3H, C**H**$_3$), 2.40 (*s*, 3H, C**H**$_3$) **^{13}C NMR (126 MHz, CDCl$_3$):** δ 186.35 (**C**=O), 150.97, 137.53, 132.17, 131.94, 131.42, 131.22, 130.93, 128.56, 127.92, 126.71, 126.63, 126.22, 113.84, 20.41 (**C**H$_3$), 18.57 (**C**H$_3$) **HRMS:** [M+H]$^+$ Calculated: 251.1179 Found: 251.1148

5-Chloro-2-(2-methylphenyl)-1*H*-pyrrolo[2,3-*b*]pyridine-3-carbaldehyde (113)



CAS: Novel **Yield:** 35% **MP:** 144-146 °C **IR (cm^{-1}):** $\bar{\nu}$ 2756 (*s, br*), 1649 (*l*), 1579 (*m*), 1458 (*l*), 1276 (*l*), 1097 (*l*), 891 (*m*), 696 (*l*) **^{1}H NMR (500 MHz, CDCl$_3$):** δ 11.96 (*s*, 1H, N**H**), 9.77 (*s*, 1H, C(=O)**H**), 8.68 (*d*, J = 2.4 Hz, 1H, H-6), 7.96 (*d*, J = 2.4 Hz, 1H, H-4), 7.54 (*dd*, J = 7.6 Hz, 1.4 Hz, 1H, H-5^i), 7.48 (*td*, J = 15.2 Hz, 7.6 Hz, 2H, H-6^i & H-3^i), 7.41 (*t*, J = 7.4 Hz, 1H, H-4^i), 2.39 (*s*, 3H, C**H**$_3$) **^{13}C NMR (126 MHz, CDCl$_3$):** δ 186.18 (**C**=O), 150.66, 146.48, 142.52, 137.29, 131.16, 131.15, 130.80, 130.61, 128.59, 127.09, 126.26, 119.56, 113.71, 20.30 (**C**H$_3$) **HRMS:** [M+H]$^+$ Calculated: 271.0633 Found: 271.0634

5 - (3,4-Dimethoxyphenyl) -2- (2-methylphenyl) -1*H*- pyrrolo [2,3-*b*] pyridine -3- carbaldehyde (142)

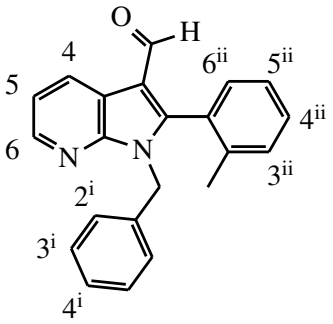


CAS: Novel **Yield:** 26% **MP:** 201-205 °C **IR (cm^{-1}):** $\bar{\nu}$ 3010 (*s, br*), 2850 (*s, br*), 1776 (*s, br*), 1654 (*m*), 1465 (*m*), 1249 (*l*), 1026 (*l*), 694 (*l*) **^{1}H NMR (400 MHz, CDCl$_3$):** δ 11.20 (*s*, 1H, N**H**), 9.82 (*s*, 1H, C(=O)**H**), 8.85 (*d*, J = 2.2 Hz, 1H, H-6), 8.41 (*d*, J = 2.2 Hz, 1H, H-4), 7.52 (*dd*, J = 8.1 Hz, 6.8 Hz, 1H), 7.40 (*m*, 3H), 7.20 (*dd*, J = 8.3 Hz, 2.1 Hz, 1H, H-6^i), 7.14 (*d*, J = 2.1 Hz, 1H, H-2^i), 7.01 (*d*, J = 8.3 Hz, 1H, H-5^i), 4.00 (*s*, 3H, C**H**$_3$), 3.96 (*s*, 3H, C**H**$_3$), 2.42 (*s*, 3H, C**H**$_3$) **^{13}C NMR (101 MHz, CDCl$_3$):** 186.54, 150.01, 149.50, 148.98, 147.58, 143.42, 137.52, 131.56, 131.36, 131.05, 130.49, 128.87, 128.56, 126.15, 119.88, 116.99, 114.45, 111.79, 110.71, 56.13, 56.11, 20.41 **HRMS:** [M+H]$^+$ Calculated: 373.1547 Found: 373.1547

4.2.14 A typical formylation procedure with $POCl_3$

$POCl_3$ was added to a cooled solution of dried DMF and the reaction mixture left to stir at room temperature for 30 min. To the solution the respective 1-H benzyl protected 7-azaindole was added and stirred for a further 2 hrs. The mixture was then cooled and a 1M aqueous NaOH solution added drop wise with cooling. After the addition of 20 ml the resulting mixture was then heated under reflux for 1 hr after which the reaction mixture was poured into water and was then extracted with several portions of diethyl ether (40 ml). The organic layer was then dried with anhydrous Na_2SO_4 and evaporated under vacuum. The resulting crude product was then purified using silica chromatography with a hexane:EtOAc solvent system of 10:1 to yield **72**.

1-Benzyl-2-(2-methylphenyl)-1*H*-pyrrolo[2,3-*b*]pyridine-3-carbaldehyde (72)



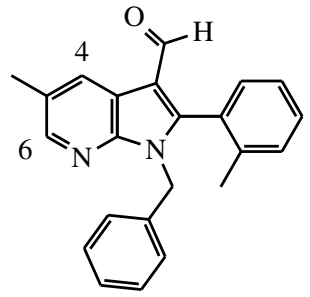
CAS: Novel **Yield:** 45% **IR (cm^{-1}):** $\bar{\nu}$ 3018 (*s*), 2956 (*s*), 2744 (*s*), 1772 (*s*), 1658 (*l*), 1423 (*l*), 1137 (*m*), 1035 (*m*), 742 (*l*), 698 (*l*) **^{1}H NMR (300 MHz, $CDCl_3$):** δ 9.56 (*s*, 1H, C(=O)**H**), 8.65 (*dd*, J = 1.5 Hz, 7.8 Hz, 1H, H-6), 8.48 (*dd*, J = 1.5 Hz, 4.8 Hz, 1H, H-4), 7.43 (*t*, J = 7.8 Hz, 1H, H-5), 7.34 - 7.26 (*m*, 3H, H-4^i & H-2^i), 7.20 - 7.12 (*m*, 4H, H-3^i & H-4^{ii} & H-5^{ii}), 6.87 - 6.84 (*m*, 2H, H-6^{ii} & H-3^{ii}), 5.33 (*d*, J = 3.0 Hz, 2H, C**H**$_2$), 1.88 (*s*, 3H, C**H**$_3$) **^{13}C NMR (75 MHz, $CDCl_3$):** δ 186.0 (**C**=O), 150.9, 148.5, 145.0, 130.9, 130.5, 130.4, 128.4, 127.7, 127.7, 125.8, 119.3, 117.7, 114.4, 46.0 (**C**H$_2$), 19.7 (**C**H$_3$) **HRMS:** $[M+H]^+$ Calculated: 327.1492 Found: 327.1491

4.2.15 A typical benzylation procedure

The formylated 7-azaindole **114**, **113**, **142** or **115** (3.04 mmol) was dissolved in NMP (10 ml) and solid freshly ground KOH (1.7 g, 30.4 mmol) was added and the mixture stirred for 30 min. Benzyl bromide (571 mg, 3.34 mmol) was then added and the mixture stirred for 2 hrs after which water was added and the extracted with several portions of diethyl ether and dried over anhydrous Na_2SO_4 after which the solvent evaporated

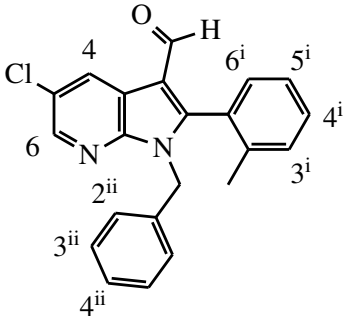
under vacuum. The crude product was then purified using silica chromatography with a hexane:EtOAc solvent system of 10:1 to yield **72**, **118**, **119** or **143**.

1-Benzyl-5-methyl-2-(2-methylphenyl)-pyrrolo[2,3-*b*]pyridine-3-carbaldehyde (118)



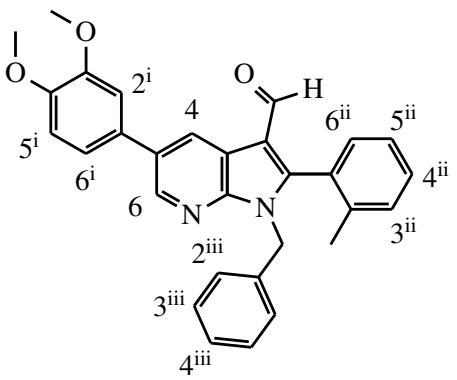
CAS: Novel **Yield:** (Calculated with next step) **MP:** Liquid **IR (cm^{-1}):** $\bar{\nu}$ 3008 (*s*), 2790 (*s*), 2366 (*s*), 1768 (*m*), 1660 (*l*), 1421 (*m*), 1375 (*m*), 1245 (*m*), 759 (*m*), 704 (*m*) **^{1}H NMR (500 MHz, CDCl$_3$):** δ 9.53 (*s*, 1H, C(=O)**H**),8.47 (*d*, J = 2.2 Hz, 1H, H-6), 8.31 (*d*, J = 2.2 Hz, 1H, H-4),7.44 (*dt*, J = 7.6 Hz, 1.5 Hz, 1H),7.29 (*m*, 2H),7.15 (*m*, 4H),6.85 (*m*, 2H),5.30 (*q*, J = 15.1 Hz, 2H, (*s*, 2H, C**H**$_2$)),2.51 (*s*, 3H, C**H**$_3$),1.88 (*s*, 3H, C**H**$_3$) **^{13}C NMR (126 MHz, CDCl$_3$):** δ 186.10, 151.01, 147.10, 145.76, 138.36, 136.57, 130.84, 130.41, 130.33, 130.30, 128.79, 128.36, 128.01, 127.66, 127.62, 125.78, 117.51, 114.00, 45.97, 19.68, 18.57 **HRMS:** [M+H]$^+$ Calculated: 341.1648 Found: 341.1649

1-Benzyl-5-chloro-2-(2-methylphenyl)-pyrrolo[2,3-*b*]pyridine-3-carbaldehyde (119)



CAS: Novel **Yield:** 61% **MP:** 151-153 °C **IR (cm^{-1}):** $\bar{\nu}$ 3095 (*s*), 2798 (*s*), 1612 (*l*), 1446 (*l*), 1406 (*l*), 1367 (*l*), 1282 (*l*), 1228 (*l*), 1172 (*l*), 906 (*l*), 858 (*l*), 729 (*l*) **^{1}H NMR (500 MHz, CDCl$_3$):** δ 9.76 (*s*, 1H, C(=O)**H**), 8.81 (*d*, J = 1.8 Hz, 1H, H-6), 7.80 (*d*, J = 1.9 Hz, 1H, H-4), 7.49 - 7.39 (*m*, 3H), 7.36 - 7.33 (*m*, 5H), 7.29 (*dt*, J = 7.1 Hz, 2.0 Hz, 1H), 5.89 (*s*, 2H, C**H**$_2$), 2.41 (*s*, 3H, C**H**$_3$) **^{13}C NMR (126 MHz, CDCl$_3$):** δ 186.30 (**C**=O), 169.70, 149.74, 137.33, 134.29, 133.86, 133.10, 131.29, 130.75, 129.24, 129.08, 128.95, 128.84, 128.69, 125.42, 121.30, 115.58, 56.31 (**C**H$_2$), 20.53 (**C**H$_3$) **HRMS:** [M+H]$^+$ Calculated: 361.1102 Found: 361.1103

1-Benzyl-5- (3,4-dimethoxyphenyl) -2- (2-methylphenyl) -pyrrolo [2,3-*b*] pyridine -3- carbaldehyde (143)

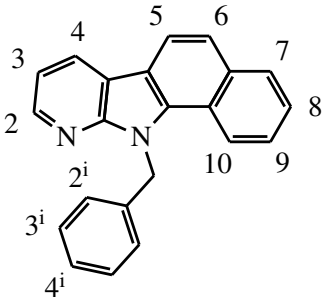


CAS: Novel **Yield:** 58% **MP:** 95-97 °C **IR (cm^{-1}):** $\bar{\nu}$ 3005 (*s, br*), 2848 (*s, br*), 1772 (*s*), 1658 (*m*), 1606 (*m*), 1521 (*m*), 1425 (*l*), 1245 (*l*), 1028 (*l*), 761 (*l*), 700 (*l*) **^{1}H NMR (300 MHz, CDCl$_3$):** δ 9.78 (*s*, 1H, C(=O)**H**), 9.04 (*d*, J = 1.5 Hz, 1H, H-6), 8.02 (*d*, J = 1.5 Hz, 1H, H-4), 7.50 - 7.48 (*m*, 3H), 7.37 - 7.08 (*m*, 6H), 7.11 - 7.10 (*m*, 2H), 7.96 (*d*, J = 9 Hz, H-6^i), 6.01 (*s*, 2H, C**H**$_2$), 3.95 (*s*, 3H, OC**H**$_3$), 3.92 (*s*, 3H, OC**H**$_3$), 2.42 (*s*, 3H, C**H**$_3$) **^{13}C NMR (75 MHz, CDCl$_3$):** δ 186.3 (**C**=O), 175.0, 169.1, 150.2, 149.6, 149.4, 137.4, 134.9, 134.8, 132.1, 131.3, 130.7, 129.7, 129.2, 129.1, 129.0, 128.8, 128.7, 128.6, 125.3, 119.8, 116.0, 111.9, 110.8, 56.3 (O**C**H$_3$), 56.1 (O**C**H$_3$), 49.4 (**C**H$_2$), 20.6 (**C**H$_3$) **HRMS:** [M+H]$^+$ Calculated: 463.2016 Found: 463.2018

4.2.16 A typical light mediated ring closure procedure

The aldehyde **72**, **118**, **119** or **143** (2.74 mmol) was dissolved in dried DMF (20 ml) and degassed. To this solution *t*-BuOK (1.34 g, 10.99 mmol) was added and the reaction mixture heated to 70° and irradiated with a high pressure vapour mercury lamp. After ten minutes the reaction mixture was poured into water and stirred for 30 min after which the solid was filtered and washed with *i*-PrOH. If no precipitate formed the reaction mixture was extracted with EtOAc and dried over anhydrous Na_2SO_4 and the solvent removed under vacuum. α-Carbolines **71**, **121**, **120**, **144** and **145** were isolated.

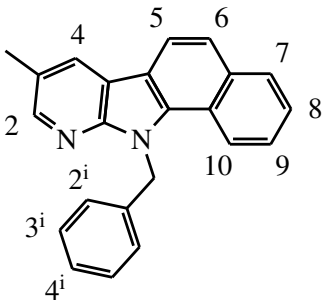
11-Benzyl-11*H*-benzo[*g*]pyrido[2,3-*b*]indole (71)



CAS: Novel **Yield:** 82% **MP:** 137-139 °C **IR (cm^{-1}):** $\bar{\nu}$ 2997 (*s*), 1770 (*l*), 1384 (*m*), 1247 (*l*), 1062 (*m*) **^{1}H NMR (300 MHz, CDCl$_3$):** δ 8.55 (*dd*, J = 4.8 Hz, 1.7 Hz, 1H, H-2), 8.44 (*dd*, J = 7.7 Hz, 1.6 Hz, 1H, H-4), 8.33 (*dd*, J = 8.4 Hz, 0.6 Hz,

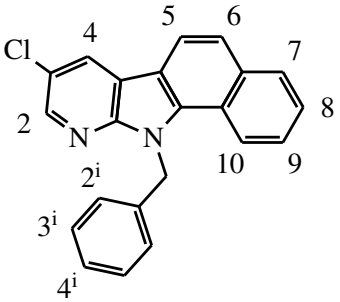
1H, H-10), 8.17 (*d*, J = 8.5 Hz, 1H, H-5), 7.99 (*dd*, J = 8.0 Hz, 1.4 Hz, 1H, H-7), 7.72 (*d*, J = 8.5 Hz, , H-6), 7.47 (*ddd*, J = 8.1 Hz, 7.0 Hz, 1.3 Hz, 1H, H-8), 7.40 (*ddd*, J = 8.3 Hz, 6.9 Hz, 1.5 Hz, 1H, H-9), 7.29 (*dd*, J = 7.7 Hz, 4.8 Hz, 1H, H-3), 7.26 - 7.19 (*m*, 3H), 7.16 (*dd*, J = 4.4 Hz, 3.7 Hz, 2H, H-2^i), 6.29 (*s*, 2H, C$\underline{\mathbf{H}}_2$) **^{13}C NMR (75 MHz, CDCl$_3$):** δ 151.4, 145.6, 137.8, 134.7, 133.8, 129.3, 128.9, 127.6, 127.2, 125.9, 125.7, 125.2, 122.7, 122.1, 121.6, 119.1, 116.8, 116.2, 115.9, 47.4 ($\underline{\mathbf{C}}$H$_2$) **HRMS:** [M+H]$^+$ Calculated: 309.1386 Found: 309.1378

11-Benzyl-8-methyl-11*H*-benzo[*g*]pyrido[2,3-*b*]indole (121)



CAS: Novel **Yield:** 37% (over two steps) **MP:** 170-172 °C **IR (cm^{-1}):** $\bar{\nu}$ 3018 (*s*), 2927 (*s*), 1772 (*m*), 1377 (*l*), 1249 (*l*), 804 (*l*), 732 (*l*), 609 (*l*) **^{1}H NMR (500 MHz, CDCl$_3$):** δ 8.39 (*d*, J = 1.9 Hz, 1H, H-2), 8.33 (*d*, J = 8.6 Hz, 1H), 8.27 (*dd*, J = 2.0 Hz, 0.9 Hz, 1H, H-4), 8.16 (*s*, 1H, H-6), 7.98 (*d*, J = 8.0 Hz, 1H, H-7), 7.70 (*d*, J = 8.4 Hz, 1H, H-10), 7.46 (*ddd*, J = 8.1 Hz, 6.8 Hz, 1.1 Hz, 1H, H-8), 7.39 (*ddd*, J = 8.4 Hz, 6.8 Hz, 1.4 Hz, 1H, H-9), 7.24 (*s*, 1H, H-5), 7.21 (*d*, J = 7.4 Hz, 1H, H-6), 7.16 (*d*, J = 7.2 Hz, 2H), 6.27 (*s*, 2H, C$\underline{\mathbf{H}}_2$), 2.57 (*s*, 3H, C$\underline{\mathbf{H}}_3$) **^{13}C NMR (126 MHz, CDCl$_3$):** δ 146.36, 139.01, 137.95, 133.74, 129.27, 128.87, 127.83, 127.15, 125.93, 125.60, 125.10, 122.63, 121.29, 119.14, 115.58, 47.44, 18.63 **HRMS:** [M+H]$^+$ Calculated: 323.1543 Found: 323.1540

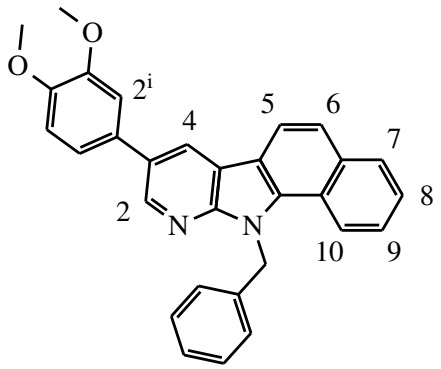
11-Benzyl-8-chloro-11*H*-benzo[*g*]pyrido[2,3-*b*]indole (120)



CAS: Novel **Yield:** 4% (low pressure mercury lamp) **MP:** 185-190 °C **IR (cm^{-1}):** $\bar{\nu}$ 3057 (*s*), 3030 (*s*), 2945 (*s*), 1656 (*m*), 1450 (*m*), 1419 (*m*), 1377 (*m*), 1271 (*m*), 1190 (*m*), 1087 (*m*), 1029 (*m*), 933 (*m*), 854 (*m*), 808 (*m*), 748 (*l*), 732 (*l*), 694 (*l*) **^{1}H NMR (300 MHz, DMSO):** δ 8.45 (*d*, J = 2.3 Hz, 1H, H-2), 8.33 (*d*, J = 2.3 Hz, 1H, H-4), 8.27 (*d*, J = 8.4 Hz, 1H, H-10), 8.04 (*d*, J = 8.5 Hz, 1H, H-3), 7.96 (*d*, J = 7.8 Hz, 1H, H-7), 7.68 (*d*, J

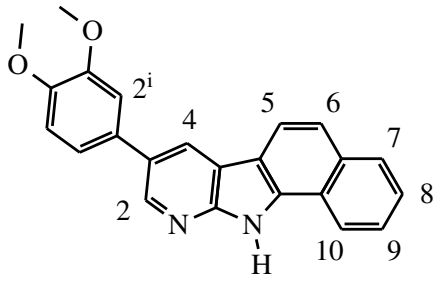
= 8.5 Hz, 1H, H-4), 7.47 (*dt*, J = 11.0 Hz, 4.9 Hz, 1H, H-8), 7.39 (*ddd*, J = 8.3 Hz, 6.9 Hz, 1.3 Hz, 1H, H-9), 7.27 - 7.22 (*m*, 3H), 7.19 (*t*, J = 7.2 Hz, 1H, H-4^i), 7.11 (*d*, J = 7.2 Hz, 2H, H-2^i), 6.17 (*s*, 2H, C$\underline{\mathbf{H}}_2$) **^{13}C NMR (75 MHz, CDCl$_3$):** δ 171.1, 149.4, 144.0, 137.4, 135.5, 134.0, 129.3, 128.9, 127.3, 126.9, 125.9, 125.8, 125.6, 124.0, 122.6, 122.0, 121.9, 118.9, 116.4, 115.8, 47.5 ($\underline{\mathbf{C}}$H$_2$) **HRMS:** [M+H]$^+$ Calculated: 343.0997 Found: 343.0996

11-Benzyl-8-(3,4-dimethoxyphenyl)-11*H*-benzo[*g*]pyrido[2,3-*b*]indole (144)



CAS: Novel **Yield:** 15% (low pressure mercury lamp) **MP:** 186-189 °C **IR (cm^{-1}):** $\bar{\nu}$ 3080 (*s, br*), 2970 (*s, br*), 2866 (*s*), 1593 (*s*), 1523 (*m*), 1467 (*m*), 1247 (*l*), 1028 (*m*), 808 (*l*), 742 (*l*) **^{1}H NMR (500 MHz, CDCl$_3$):** δ 8.76 (*d*, J = 2.2 Hz, 1H, H-2), 8.58 (*d*, J = 2.1 Hz, 1H, H-3), 8.36 (*d*, J = 8.5 Hz, 1H, H-7), 8.24 (*d*, J = 8.5 Hz, 1H, H-6), 8.01 (*dd*, J = 8.1 Hz, 1.3 Hz, 1H, H-10), 7.75 (*d*, J = 8.4 Hz, 1H, H-5), 7.49 (*ddd*, J = 80 Hz, 6.8 Hz, 1.1 Hz, 1H, H-8), 7.43 (*ddd*, J = 8.3 Hz, 6.9 Hz, 1.4 Hz, 1H, H-9), 7.27 (*m*, 7H), 7.04 (*d*, J = Hz, 1H, H-2^i), 6.34 (*s*, 2H, C$\underline{\mathbf{H}}_2$), 4.01 (*s*, 3H, C$\underline{\mathbf{H}}_3$), 3.97 (*s*, 3H, C$\underline{\mathbf{H}}_3$)**^{13}C NMR (126 MHz, CDCl$_3$):** δ 150.68, 149.45, 148.64, 144.70, 137.76, 135.26, 132.42, 130.09, 129.35, 128.94, 127.26, 125.94, 125.80, 125.32, 122.63, 122.12, 121.68, 119.77, 119.16, 116.84, 111.83, 110.90, 56.08, 47.58, 30.92 **HRMS:** [M+H]$^+$ Calculated: 445.1911 Found: 445.1903

8-(3,4-Dimethoxyphenyl)-11*H*-benzo[*g*]pyrido[2,3-*b*]indole (145)



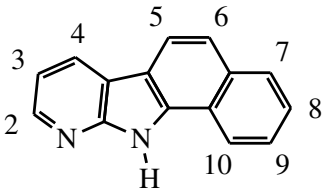
CAS: Novel **Yield: 10% MP:** 229-231 °C **IR (cm^{-1}):** $\bar{\nu}$ 2927 (), 2837 (*s*), 1589 (*m*), 1523 (*m*), 1442 (*m*), 1375 (*m*), 1251 (*m*), 1151 (*m*), 1028 (*m*), 839 (*m*), 810 (*l*), 734 (*m*), 682 (*m*) **^{1}H NMR (500 MHz, DMSO):** δ 12.81 (*s*, 1H, N$\underline{\mathbf{H}}$), 8.86 (*d*, J = 2.2 Hz, 1H, H-2), 8.79 (*d*, J = 2.2 Hz, 1H, H-4), 8.62 (*dd*, J = 8.4 Hz, 1.1 Hz, 1H,

H-7), 8.32 (*d*, J = 8.6 Hz, 1H, H-6), 8.07 (*d*, J = 8.3 Hz, 1H, H-10), 7.73 (*d*, J = 8.6 Hz, 1H, H-5), 7.66 (*ddd*, J = 8.2 Hz, 6.8 Hz, 1.3 Hz, 1H, H-8), 7.60 (*ddd*, J = 8.2 Hz, 6.9 Hz, 1.3 Hz, 1H, H-9), 7.41 (*d*, J = 2.2 Hz, 1H, H-2^i), 7.36 (*dd*, J = 8.3 Hz, 2.2 Hz, 1H, H-6^i), 7.11 (*d*, J = 8.3 Hz, 1H, H-5^i), 3.92 ($\underline{\mathbf{C}}H_3$), 3.83 ($\underline{\mathbf{C}}H_3$) **^{13}C NMR (126 MHz, DMSO):** δ 150.86, 149.74, 148.74, 144.43, 135.78, 132.78, 131.95, 129.09, 128.80, 126.29, 126.24, 126.22, 122.77, 121.69, 120.47, 120.43, 119.48, 116.42, 115.93, 112.92, 111.29, 79.71, 79.44, 79.18, 56.16, 56.13 **HRMS:** $[M+H]^+$ Calculated: 355.1441 Found: 355.1449

4.2.17 A typical oxidative debenzylation procedure

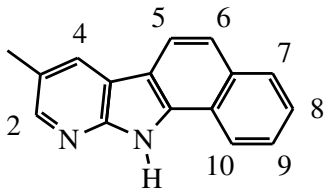
The α-carboline **71**, **121** or **120** (1.0 mmol) in THF (20 ml) and DMSO (788 mg, 10.0 mmol). *t*-BuOK (784 mg, 7.0 mmol) was added and O_2 bubbled through the reaction mixture with continuous stirring for 20 min. After this the resulting mixture was poured into water (200 ml) and stirred for 20 min and filtered. The filtrate was then washed with several portions of *i*-PrOH and dried under vacuum to yield the unprotected α-carboline **70**, **133** or **132**.

11*H*-Benzo[*g*]pyrido[2,3-*b*]indole (70)



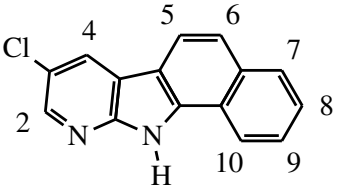
CAS: 78750-85-3[214] **Yield:** 24% **MP:** Decomposed at 250 °C **IR (cm^{-1}):** $\bar{\nu}$ **^{1}H NMR (500 MHz, DMSO):** δ 12.78 (*s*, 1H, N$\underline{\mathbf{H}}$), 8.63 (*dd*, J = 8.0 Hz, 1.0 Hz, 1H, H-2), 8.58 (*dd*, J = 7.5 Hz, 1.5 Hz, 1H, H-4), 8.25 (*d*, J = 9.0 Hz, 1H, H-5), 8.06 (*dd*, J = 8.5 Hz, 8.0 Hz, 1H, H-8), 7.72 (*d*, J = 8.5 Hz, 1H, H-6), 6.65 (*t*, J = 7.5 Hz, 1H, H-9), 7.61 (*dd*, J = 7.0 Hz, 1.5 Hz, 1H, H-10), 7.59 (*dd*, J = 7.0 Hz, 1.5 Hz, 1H, H-7), 7.30 (*dd*, J = 7.5 Hz, 8.0 Hz, 1H, H-3) **^{13}C NMR (126 MHz, DMSO:** δ 151.6, 145.7, 135.1, 132.7, 129.1, 128.5, 126.2, 122.8, 121.6, 120.5, 120.2, 116.3, 116.1, 115.7 **HRMS:** $[M+H]^+$ Calculated: 219.0917 Found: 219.0917

8-Methyl-11*H*-benzo[*g*]pyrido[2,3-*b*]indole (133)



Reaxys: 12969446[118] **Yield:** 18% **MP:** Decomposition after 240 °C **IR (cm^{-1}):** $\bar{\nu}$ 3149 (*s*), 3057 (*s*), 1591 (*s*), 1531 (*s*), 1382 (*m*), 1267 (*m*), 810 (*m*), 788 (*l*), 736 (*l*), 678 (*l*) **^{1}H NMR (300 MHz, DMSO):** δ 12.64 (*s*, 1H, N**H**), 8.60 (*d*, J = 8.2 Hz, 1H, H-2), 8.39 (*d*, J = 1.3 Hz, 1H, H-10), 8.33 (*d*, J = 1.3 Hz, 1H, H-7), 8.20 (*d*, J = 2.0 Hz, 1H, H-6), 8.05 (*d*, J = 8.0 Hz, 1H, H-4), 7.68 (*d*, J = 8.5 Hz, 1H, H-5), 7.65 (*ddd*, J = 8.2 Hz, 6.9 Hz, 1.2 Hz, 1H, H-8), 7.58 (*ddd*, J = 8.1 Hz, 6.9 Hz, 1.2 Hz, 1H, H-9), 3.34 (*s*, 3H, C**H**$_3$) **^{13}C NMR (125 MHz, DMSO):** δ 149.2, 141.9, 138.9, 136.3, 132.6, 131.1, 129.5, 128.5, 128.2, 126.1, 121.8, 115.8, 100.4, 21.2 (**C**H$_3$) **HRMS:** [M+H]$^+$ Calculated: 233.1073 Found: 233.1224

8-Chloro-11*H*-benzo[*g*]pyrido[2,3-*b*]indole (132)



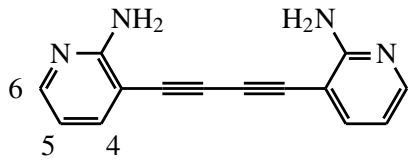
CAS: 140138-72-3[215] **Yield:** 25% **MP:** decomposed 240 °C **^{1}H NMR (500 MHz, DMSO):** δ 12.97 (*s*, 1H, N**H**), 8.77 (*d*, J = 2.4 Hz, 1H, H-2), 8.62 (*d*, J = 8.2 Hz, 1H, H-10), 8.48 (*d*, J = 2.4 Hz, 1H, H-4), 8.26 (*d*, J = 8.6 Hz, 1H, H-6), 8.07 (*d*, J = 7.9 Hz, 1H, H-7), 7.68 (*ddd*, J = 7.9 Hz, 7.0 Hz, 1.1 Hz, 1H, H-8), 7.63 (*ddd*, J = 8.1 Hz, 7.0 Hz, 1.2 Hz, 1H, H-9) **^{13}C NMR (75 MHz, CDCl$_3$):** δ 149.8, 143.7, 136.4, 133.0, 129.1, 128.0, 126.8, 126.5, 122.9, 121.6, 121.0, 120.4, 117.5, 115.1 **HRMS:** [M+H]$^+$ Calculated: 253.0527 Found: 253.0540

4.2.18 A typical copper catalyzed alkyne dimerisation procedure

The coupling of alkynes follows a modified procedure designed by Balaraman and Kesavan[139]. The respective alkyne **76** or **87**) (8.48 mmol) was added to an acetonitrile (50 ml) and copper acetate solution (169 mg, 0.847 mmol). To this solution piperidine (970 μl, 8.48 mmol) was added and the mixture allowed to stir for 3 hrs. In the case of a precipitate the solution was filtered, washed with acetonitrile (50 ml) and dried. However, when the alkyne dimer was still in solution a diethyl ether extraction (50 ml x 2) together with the addition of water (20 ml) was used. The diethyl ether layer was then washed with an aqueous saturated ammonium chloride solution (10 ml, 0.2 g NaOH)

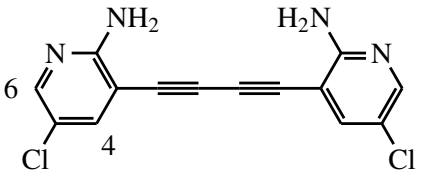
followed by brine (10 ml). The diethyl ether solution was then dried with anhydrous Na_2SO_4 and filtered.

[4-(2-Amino-3-yl)buta-1,3-diyn-1-yl]-2-amine (93)



Yield: Quantitative **MP:** decomposed at 200 °C **IR (cm^{-1}):** $\bar{\nu}$ 3467 (*s*), 3296 (*s*), 3129 (*s, br*), 2134 (*s*), 1631 (*l*), 1561 (*l*), 1466 (*l*), 1440 (*l*), 1250 (*l*), 1191 (*l*), 789 (*l*), 760 (*l*), 555 (*l*) **^{1}H NMR (500 MHz, AcetoneD$_6$):** δ 8.04 (*dd*, J = 2.7 Hz, 0.6 Hz, 1H, H-6), 7.63 (*dd*, J = 4.5 Hz, 1.2 Hz, 1H, H-4), 6.62 (*dd*, J = 4.5 Hz, 3.0 Hz, 1H, H-5), 5.96 (*s*, 2H, N$\underline{\mathbf{H}}_2$) **^{13}C NMR (125 MHz, AcetoneD$_6$):** δ 160.9, 149.4, 140.8, 112.6, 100.0, 79.0 ($\underline{\mathbf{C}}$≡C), 78.8 ($\underline{\mathbf{C}}$≡C) **HRMS:** [M+H]$^+$ Calculated: 235.0978 Found: 235.0979

[4-(2-Amino-5-chloropyridin-3-yl)buta-1,3-diyn-1-yl]-5-chloropyridin-2-amine (92)



CAS: Novel **Yield:** 96% **IR (cm^{-1}):** $\bar{\nu}$ 3393 (*s, br*), 3315 (*s, br*), 3170 (*s, br*), 1657 (*s*), 1601 (*m*), 1546 (*m*), 1446 (*m*), 1397 (*m*), 1233 (*m*), 912 (*m*), 891 (*m*), 760 (*m*), 564 (*l*) **^{1}H NMR (300 MHz, DMSO):** δ^* 8.02 (*d*, J = 2.7 Hz, 2H, H-6^i), 7.96 (*d*, J = 2.1 Hz, 1H, H-6^{ii}), 7.75 (*d*, J = 2.4 Hz, 2H, H-4^i), 7.63 (*d*, J = 2.4 Hz, 2H, H-4^{ii}), 6.73 (*s*, 4H, N$\underline{\mathbf{H}}_2$), 6.39 (*s*, 2H, N$\underline{\mathbf{H}}_2$) **^{13}C NMR (75 MHz, DMSO):** δ 159.4, 158.7, 147.7, 146.5, 139.6, 139.1, 117.0, 116.9, 101.8, 100.3, 87.5 ($\underline{\mathbf{C}}$≡C), 78.0 ($\underline{\mathbf{C}}$≡C), 78.4 ($\underline{\mathbf{C}}$≡C) **HRMS:** [M+H]$^+$ Calculated: 302.0199 Found: 302.0199

*Note that even though symmetry is seen in the molecule there is limited rotation and so similar protons are in different environments arising to the increased integration values

References

[1] *Cambridge Crystallographic Database User Manual*; Crystallographic Data Centre, 1978.

[2] Christensen, B.; Kockrow, E. *Foundations and Adult Health Nursing*; Mosby, 2005.

[3] Purich, D. *Contemporary Enzyme Kinetics and Mechanism*; Selected methods in enzymology; Academic Press, 1996.

[4] Aller, S. G.; Yu, J.; Ward, A.; Weng, Y.; Chittaboina, S.; Zhuo, R.; Harrell, P. M.; Trinh, Y. T.; Zhang, Q.; Urbatsch, I. L.; Chang, G. *Science* **2009**, *323*, 1718–1722.

[5] Piafsky, K. M.; Borga, O. *Clinical Pharmacology & Therapeutics* **1977**, *22*, 545–549.

[6] Fiala, R.; Sulová, Z.; El-Saggan, A.; Uhrák, B.; Liptaj, T.; Dovinová, I.; Hanušovská, E.; Drobná, Z.; Barančik, M.; Breier, A. *Biochimica et Biophysica Acta (BBA) - Molecular Basis of Disease* **2003**, *1639*, 213–224.

[7] Thor, H.; Smith, M. T.; Hartzell, P.; Bellomo, G.; Jewell, S. A.; Orrenius, S. *Journal of Biological Chemistry* **1982**, *257*, 12419–12425.

[8] Wardman, P. *Current Medicinal Chemistry* **2001**, *8*, 739–761.

[9] Grove, J.; Marsh, M. *The Journal of Cell Biology* **2011**, *195*, 1071–1082.

[10] Boulant, S.; Stanifer, M.; Lozach, P.-Y. *Viruses* **2015**, *7*, 2794–2815.

[11] Gallagher, J.; MacDougall, C. *Antibiotics Simplified*; Jones & Bartlett Learning, 2011.

[12] Dougherty, T.; Pucci, M. *Antibiotic Discovery and Development*; SpringerLink : Bücher; Springer US, 2011.

[13] Kubinyi, H. *Die Pharmazie* **1995**, *50*, 647—662.

[14] Patel, D. V. In *Annual Reports in Combinatorial Chemistry and Molecular Diversity*; Moos, W. H., Pavia, M. R., Kay, B. K., Ellington, A. D., Eds.; Springer Netherlands: Dordrecht, 1997; pp 78–89.

[15] Martin, Y. C.; Kofron, J. L.; Traphagen, L. M. *Journal of Medicinal Chemistry* **2002**, *45*, 4350–4358.

[16] Berg, J.; Tymoczko, J.; Stryer, L. *Biochemistry, Fifth Edition*; W.H. Freeman, 2002.

[17] González-Bello, C. *ChemMedChem* **2016**, *11*, 22–30.

[18] Rink, S. M.; Hopkins, P. B. *Biochemistry* **1995**, *34*, 1439–1445.

[19] Barceló, F.; Capó, D.; Portugal, J. *Nucleic Acids Research* **2002**, *30*, 4567–4573.

[20] Patel, M. N.; Chhasatia, M. R.; Patel, S. H.; Bariya, H. S.; Thakkar, V. R. *Journal of Enzyme Inhibition and Medicinal Chemistry* **2009**, *24*, 715–721.

[21] Wang, J. Y. *Current Opinion in Cell Biology* **1998**, *10*, 240–247.

[22] Norbury, C. J.; Zhivotovsky, B. *Oncogene* **2004**, *23*, 2797–2808.

[23] Fenech, M.; Crott, J.; Turner, J.; Brown, S. *Mutagenesis* **1999**, *14*, 605–612.

[24] Pradeep, P. The Suzuki-Miyaura Cross Coupling Reaction as a key Step for the Synthesis of Oxygen and Nitrogen Containing Hetero-aromatic compounds. Ph.D. thesis, University of the Witwatersrand, 2015.

[25] Patel, D. J.; Canuel, L. L. *European Journal of Biochemistry* **1978**, *90*, 247–254.

[26] Rasko, I.; Downes, C. *Genes in Medicine: Molecular biology and human genetic disorders*; Springer Netherlands, 1994.

[27] Hardie, D. *Biochemical Messengers: Hormones, Neurotransmitters and Growth Factors*; Springer, 1991.

[28] Anand, P.; Kunnumakara, A.; Sundaram, C.; Harikumar, K.; Tharakan, S.; Lai, O.; Sung, B.; Aggarwal, B. *Pharmaceutical Research* **2008**, *25*, 2097–2116.

[29] Klug, W.; Cummings, M. *Concepts of Genetics*; Macmillan, 1994.

[30] Fulda, S.; Debatin, K.-M. *When Cells Die II*; John Wiley & Sons, Inc., 2005; pp 461–481.

[31] Gavande, N. S.; VanderVere-Carozza, P. S.; Hinshaw, H. D.; Jalal, S. I.; Sears, C. R.; Pawelczak, K. S.; Turchi, J. J. *Pharmacology & Therapeutics* **2016**, *160*, 65–83.

[32] Shay, J.; Bacchetti, S. *European Journal of Cancer* **1997**, *33*, 787–791, Special Issue: Telomeres and Telomerase in Cancer.

[33] Peyrone, M. *Justus Liebigs Annalen der Chemie* **1844**, *51*, 1–29.

[34] Rosenberg, B.; Van Camp, L.; Krigas, T. *Nature* **1965**, *205*, 698–699.

[35] Rosenberg, B.; Vancamp, L.; Trosko, J. E.; Mansour, V. H. *Nature* **1969**, *222*, 385–386.

[36] Carpenter, D. *Reputation and Power: Organizational Image and Pharmaceutical Regulation at the FDA*; Princeton University Press, 2010.

[37] Florea, A.-M.; Basselberg, D. *Cancers* **2011**, *3*, 1351–1371.

[38] Minotti, G.; Menna, P.; Salvatorelli, E.; Cairo, G.; Gianni, L. *Pharmacological Reviews* **2004**, *56*, 185–229.

[39] Ames, M. *Cancer Treatment Reviews* **1991**, *18*, 3–14.

[40] Alcamo, I.; Warner, J. *Schaum's Outline of Microbiology*, second edition ed.; Schaum's Outline Series; McGraw-Hill Education, 2009.

[41] Vaughan, A. M.; Aly, A. S.; Kappe, S. H. *Cell Host & Microbe 4*, 209–218.

[42] Hide, G.; Tait, A.; Maudlin, I.; Welburn, S. *Parasitology Today* **1996**, *12*, 50–55.

[43] Brun, R.; Hecker, H.; Lun, Z.-R. *Veterinary Parasitology* **1998**, *79*, 95–107.

[44] Caraballo, H.; King, K. *Emergency medicine practice* **2014**, *16*, 1.

[45] Carter, R.; Mendis, K. N. *Clinical Microbiology Reviews* **2002**, *15*, 564–594.

[46] Butler, N.; Schmidt, N.; Vaughan, A.; Aly, A.; Kappe, S.; Harty, J. *Cell Host & Microbe* **2011**, *9*, 451–462.

[47] Cowman, A. F.; Berry, D.; Baum, J. *The Journal of Cell Biology* **2012**, *198*, 961–971.

[48] Talisuna, A. O.; Okello, P. E.; Erhart, A.; Coosemans, M.; D'Alessandro, U. *The American Journal of Tropical Medicine and Hygiene* **2007**, *77*, 170–180.

[49] Medicine, I.; Health, B.; Drugs, C.; Gelband, H.; Panosian, C.; Arrow, K. *Saving Lives, Buying Time: Economics of Malaria Drugs in an Age of Resistance*; National Academies Press, 2004.

[50] Woodward, R. B.; Doering, W. E. *Journal of the American Chemical Society* **1944**, *66*, 849–849.

[51] Plowe, C. V. In *Malaria: Drugs, Disease and Post-genomic Biology*; Compans, R. W., Cooper, M. D., Honjo, T., Koprowski, H., Melchers, F., Oldstone, M. B. A., Olsnes, S., Potter, M., Vogt, P. K., Wagner, H., Sullivan, D. J., Krishna, S., Eds.; Springer Berlin Heidelberg: Berlin, Heidelberg, 2005; pp 55–79.

[52] Chen, P. M.; Gombart, Z. J.; Chen, J. W. *Cell & Bioscience* **2011**, *1*, 10.

[53] Kim, E. L.; Wüstenberg, R.; Rübsam, A.; Schmitz-Salue, C.; Warnecke, G.; Bücker, E.-M.; Pettkus, N.; Speidel, D.; Rohde, V.; Schulz-Schaeffer, W.; Deppert, W.; Giese, A. *Neuro-Oncology* **2010**, *12*, 389–400.

[54] Schlagenhauf, P.; Adamcova, M.; Regep, L.; Schaerer, M. T.; Rhein, H.-G. *Malaria Journal* **2010**, *9*, 357.

[55] Liao, F. *Molecules* **2009**, *14*, 5362–5366.

[56] White, N. J. *Antimicrobial Agents and Chemotherapy* **1997**, *41*, 1413–22.

[57] Lundkvist, G. B.; Kristensson, K.; Bentivoglio, M. *Physiology* **2004**, *19*, 198–206.

[58] Brun, R.; Blum, J.; Chappuis, F.; Burri, C. *The Lancet* **2010**, *375*, 148–159.

[59] Koff, A. B.; Rosen, T. *Journal of the American Academy of Dermatology* **1994**, *31*, 693 – 708.

[60] Sands, M.; Kron, M. A.; Brown, R. B. *Review of Infectious Diseases* **1985**, *7*, 625–6344.

[61] Bray, P. G.; Barrett, M. P.; Ward, S. A.; de Koning, H. P. *Trends in Parasitology* **2003**, *19*, 232 – 239.

[62] Fairlamb, A.; Bowman, I. *Molecular and Biochemical Parasitology* **1980**, *1*, 315 – 333.

[63] Docampo, R.; Moreno, S. N. *Parasitology Research* **2003**, *90*, S10–S13.

[64] Burri, C.; Brun, R. *Parasitology Research* **2003**, *90*, S49–S52.

[65] Hall, B. S.; Bot, C.; Wilkinson, S. R. *Journal of Biological Chemistry* **2011**, *286*, 13088–13095.

[66] Burri, C.; Nkunku, S.; Merolle, A.; Smith, T.; Blum, J.; Brun, R. *The Lancet* **2000**, *355*, 1419 – 1425.

[67] Van Order, R. B.; Lindwall, H. G. *Chemical Reviews* **1942**, *30*, 69–96.

[68] Rodriguez, A. L.; Koradin, C.; Dohle, W.; Knochel, P. *Angewandte Chemie International Edition* **2000**, *39*, 2488–2490.

[69] Yue, D.; Yao, T.; Larock, R. C. *The Journal of Organic Chemistry* **2006**, *71*, 62–69.

[70] Chen, Y.; Xie, X.; Ma, D. *The Journal of Organic Chemistry* **2007**, *72*, 9329–9334.

[71] Kumar, M. P.; Liu, R.-S. *The Journal of Organic Chemistry* **2006**, *71*, 4951–4955.

[72] Wei, Y.; Deb, I.; Yoshikai, N. *Journal of the American Chemical Society* **2012**, *134*, 9098–9101.

[73] Ali, M.; Punniyamurthy, T. *Synlett* **2011**, *2011*, 623–626.

[74] Kraus, G. A.; Guo, H. *Organic Letters* **2008**, *10*, 3061–3063.

[75] Lu, B. Z.; Zhao, W.; Wei, H.-X.; Dufour, M.; Farina, V.; ; Senanayake, C. H. *Organic Letters* **2006**, *8*, 3271–3274.

[76] Hannon, J.; Hoyer, D. *Behavioural Brain Research* **2008**, *195*, 198–213, Serotonin and cognition: mechanisms and applications.

[77] Jimenez, P. C.; Wilke, D. V.; Takeara, R.; Lotufo, T. M.; Pessoa, C.; de Moraes, M. O.; Lopes, N. P.; Costa-Lotufo, L. V. *Comparative Biochemistry and Physiology Part A: Molecular & Integrative Physiology* **2008**, *151*, 391–398.

[78] Gul, W.; Hamann, M. T. *Life Sciences* **2005**, *78*, 442–453.

[79] Bobzin, S. C.; Faulkner, D. J. *The Journal of Organic Chemistry* **1991**, *56*, 4403–4407.

[80] Shinonaga, H.; Shigemori, H.; Kobayashi, J. *Journal of Natural Products* **1994**, *57*, 1603–1605.

[81] Nibbs, A. Indoles in Organic Synthesis: Something Old, Something New, Something Heterocyclic, Something Blue. 2008.

[82] Taber, D. F.; Tirunahari, P. K. Indole synthesis: A review and proposed classification. 2011.

[83] Bischler, A. *Berichte der deutschen chemischen Gesellschaft* **1892**, *25*, 2860–2879.

[84] Sridharan, V.; Perumal, S.; Avendao, C.; Menandez, J. C. *Synlett* **2006**, 0091–0095.

[85] Jia, Y.; Zhu, J. *The Journal of Organic Chemistry* **2006**, *71*, 7826–7834.

[86] Kudzma, L. *Synthesis* **2003**, *2003*, 1661–1666.

[87] Bauer, I.; Knölker, H.-J. In *Alkaloid Synthesis*; Knölker, H.-J., Ed.; Topics in Current Chemistry 309; Springer Berlin Heidelberg, 2012; pp 203–253.

[88] de Koning, C. B.; Michael, J. P.; Rousseau, A. L. *Tetrahedron Letters* **1998**, *39*, 8725–8728.

[89] de Koning, C. B.; Michael, J. P.; Rousseau, A. L. *Journal of the Chemical Society, Perkin Transactions 1* **2000**, 1705–1713.

[90] Pagano, N.; Wong, E. Y.; Breiding, T.; Liu, H.; Wilbuer, A.; Bregman, H.; Shen, Q.; Diamond, S. L.; Meggers, E. *The Journal of Organic Chemistry* **2009**, *74*, 8997–9009.

[91] Pathak, R.; Nhlapo, J. M.; Govender, S.; Michael, J. P.; van Otterlo, W. A.; de Koning, C. B. *Tetrahedron* **2006**, *62*, 2820–2830.

[92] Pelly, S. C.; Parkinson, C. J.; van Otterlo, W. A. L.; de Koning, C. B. *The Journal of Organic Chemistry* **2005**, *70*, 10474–10481.

[93] Ackermann, L.; Althammer, A.; Mayer, P. *Synthesis* **2009**, *2009*, 3493–3503.

[94] Deane, F. M.; O'Sullivan, E. C.; Maguire, A. R.; Gilbert, J.; Sakoff, J. A.; McCluskey, A.; McCarthy, F. O. *Organic & Biomolecular Chemistry* **2013**, *11*, 1334–1344.

[95] Forke, R.; Jager, A.; Knölker, H.-J. *Organic & Biomolecular Chemistry* **2008**, *6*, 2481–2483.

[96] Hughes, I.; Nolan, W. P.; Raphael, R. A. *Journal of the Chemical Society , Perkin Transactions 1* **1990**, 2475–2480.

[97] Bhattacharyya, P.; Chowdhury, B. K. *Journal of Natural Products* **1985**, *48*, 465–466.

[98] Meragelman, K. M.; McKee, T. C.; ; Boyd, M. R. *Journal of Natural Products* **2000**, *63*, 427–428.

[99] Knölker, H.-J. *Chemistry Letters* **2009**, *38*, 8–13.

[100] Knölker, H.-J., H.-J. In *Natural Products Synthesis II*; Mulzer, J., Ed.; Topics in Current Chemistry; Springer Berlin Heidelberg, 2005; Vol. 244; pp 115–148.

[101] Knölker, H.-J.; ; Reddy, K. R. *Chemical Reviews* **2002**, *102*, 4303–4428.

[102] Nozaki, K.; Takahashi, K.; Nakano, K.; Hiyama, T.; Tang, H.-Z.; Fujiki, M.; Yamaguchi, S.; Tamao, K. *Angewandte Chemie International Edition* **2003**, *42*, 2051–2053.

[103] Campeau, L.-C.; Parisien, M.; Jean, A.; ; Fagnou, K. *Journal of the American Chemical Society* **2006**, *128*, 581–590.

[104] Walker, S. R.; Carter, E. J.; Huff, B. C.; Morris, J. C. *Chemical Reviews* **2009**, *109*, 3080–3098.

[105] Echalier, A.; Bettayeb, K.; Ferandin, Y.; Lozach, O.; Clément, M.; Valette, A.; Liger, F.; Marquet, B.; Morris, J. C.; Endicott, J. A.; Joseph, B.; Meijer, L. *Journal of Medicinal Chemistry* **2008**, *51*, 737–751.

[106] Van Baelen, G. *et al. Bioorganic & Medicinal Chemistry* **2009**, *17*, 7209–7217.

[107] Sun, X.; Wang, C.; Li, Z.; Zhang, S.; Xi, Z. *Journal of the American Chemical Society* **2004**, *126*, 7172–7173.

[108] Alajaran, M.; Molina, P.; Vidal, A. *Journal of Natural Products* **1997**, *60*, 747–748.

[109] Song, J. J.; Reeves, J. T.; Gallou, F.; Tan, Z.; Yee, N. K.; Senanayake, C. H. *Chemical Society Reviews* **2007**, *36*, 1120–1132.

[110] Dixit, B.; Balog, J.; Riedl, Z.; Drahos, L.; Hajas, G. *Tetrahedron* **2012**, *68*, 3560–3565.

[111] Leboho, T. C. Novel Syntheses of 5- and 7-Azaindole Derivatives. Ph.D. thesis, University of the Witwatersrand, 2013.

[112] Davis, M. L.; Wakefield, B. J.; Wardell, J. A. *Tetrahedron* **1992**, *48*, 939–952.

[113] Robinson, M. M.; Robison, B. L. *Journal of the American Chemical Society* **1955**, *77*, 457–460.

[114] Wang, L.; Switalska, M.; Mei, Z.-W.; Lu, W.-J.; Takahara, Y.; Feng, X.-W.; El-Sayed, I. E.-T.; Wietrzyk, J.; Inokuchi, T. *Bioorganic & Medicinal Chemistry* **2012**, *20*, 4820–4829.

[115] Luniewski, W.; Wietrzyk, J.; Godlewska, J.; Switalska, M.; Piskozub, M.; Peczynska-Czoch, W.; Kaczmarek, L. *Bioorganic & Medicinal Chemistry Letters* **2012**, *22*, 6103–6107.

[116] Hostyn, S.; Tehrani, K. A.; Lemiare, F.; Smout, V.; Maes, B. U. *Tetrahedron* **2011**, *67*, 655–659.

[117] Phani Babu Tiruveedhula, V. V. N.; Methuku, K. R.; Deschamps, J. R.; Cook, J. M. *Organic and Biomolecular Chemistry* **2015**, *13*, 10705–10715.

[118] Mineno, M.; Sera, M.; Ueda, T.; Mizuno, M.; Yamano, M.; Mizufune, H.; Zanka, A. *Tetrahedron* **2014**, *70*, 5550–5557.

[119] Bracca, A. B. J.; Heredia, D. A.; Larghi, E. L.; Kaufman, T. S. *European Journal of Organic Chemistry* **2014**, *2014*, 7979–8003.

[120] Aukasz Kaczmarek, R. B. *Archiv der Pharmazie* **2006**, *321*, 463 – 467.

[121] Jonckers, T. H. M. *et al. Journal of Medicinal Chemistry* **2002**, *45*, 3497–3508.

[122] Frolov, A. N.; Baklanov, M. V. *Mendeleev Communications* **1992**, *2*, 22–23.

[123] Leboho, T. C.; van Vuuren, S. F.; Michael, J. P.; de Koning, C. B. *Organic and Biomolecular Chemistry* **2014**, *12*, 307–315.

[124] Meunier, B. *Accounts of Chemical Research* **2008**, *41*, 69–77.

[125] Arnaud, C. H. *Chemical & Engineering News* **2007**, *85*, 46–48.

[126] Graham, L. A.; Suryadi, J.; West, T. K.; Kucera, G. L.; Bierbach, U. *J Med Chem* **2012**, *55*, 7817–7827.

[127] Saadeh, H. A.; Mosleh, I. M.; Mubarak, M. S. *Molecules* **2009**, *14*, 1483–1494.

[128] Dos Santos, J. L.; Lanaro, C.; Chelucci, R. C.; Gambero, S.; Bosquesi, P. L.; Reis, J. S.; Lima, L. M.; Cerecetto, H.; Gonzalez, M.; Costa, F. F.; Chung, M. C. *J Med Chem* **2012**, *55*, 7583–7592.

[129] Gagnon, V.; St-Germain, M. E.; Descoteaux, C.; Provencher-Mandeville, J.; Parent, S.; Mandal, S. K.; Asselin, E.; Berube, G. *Bioorg Med Chem Lett* **2004**, *14*, 5919–5924.

[130] Zhao, P.; Huang, J.-W.; Ji, L.-N. *Journal of Coordination Chemistry* **2011**, *64*, 1977–1990.

[131] Colacot, T., Ed. *New Trends in Cross-Coupling*; RSC Catalysis Series; The Royal Society of Chemistry, 2015; pp P001–864.

[132] Chinchilla, R.; Najera, C. *Chemical Society Reviews* **2011**, *40*, 5084–5121.

[133] Sonogashira, K. *Journal of Organometallic Chemistry* **2002**, *653*, 46–49.

[134] Sonogashira, K.; Tohda, Y.; Hagihara, N. *Tetrahedron Letters* **1975**, *16*, 4467–4470.

[135] Dieck, H.; Heck, F. *Journal of Organometallic Chemistry* **1975**, *93*, 259–263.

[136] Dasaradhan, C.; Kumar, Y. S.; Prabakaran, K.; Khan, F.-R. N.; Jeong, E. D.; Chung, E. H. *Tetrahedron Letters* **2015**, *56*, 784–788.

[137] de Koning, C. B.; Michael, J. P.; Rousseau, A. L. *Tetrahedron Letters* **1997**, *38*, 893–896.

[138] Rozen, S.; Zamir, D.; Menachem, Y.; Brand, M. *The Journal of Organic Chemistry* **1988**, *53*, 1123–1123.

[139] Balaraman, K.; Kesavan, V. *Synthesis* **2010**, *2010*, 3461–3466.

[140] Fomina, L.; Vazquez, B.; Tkatchouk, E.; Fomine, S. *Tetrahedron* **2002**, *58*, 6741–6747.

[141] Stefani, H. A.; Guarezemini, A. S.; Cella, R. *Tetrahedron* **2010**, *66*, 7871–7918.

[142] Gelman, D.; Buchwald, S. L. *Angewandte Chemie International Edition* **2003**, *42*, 5993–5996.

[143] Fourie, E.; van Rensburg, J. M. J.; Swarts, J. C. *Journal of Organometallic Chemistry* **2014**, *754*, 80–87.

[144] Nataro, C.; Fosbenner, S. M. *Journal of Chemical Education* **2009**, *86*, 1412.

[145] Stepnicka, P. *Ferrocenes: Ligands, Materials and Biomolecules*; Wiley, 2008.

[146] Ullmann, F. *Justus Liebigs Annalen der Chemie* **1904**, *332*, 38–81.

[147] Ohsawa, K.; Yoshida, M.; Doi, T. *The Journal of Organic Chemistry* **2013**, *78*, 3438–3444.

[148] Chen, Y.-y.; Zhang, N.-n.; Ye, L.-m.; Chen, J.-h.; Sun, X.; Zhang, X.-j.; Yan, M. *RSC Adv.* **2015**, *5*, 48046–48049.

[149] Crowell, E. P. **1962**,

[150] Fleming, I. *Molecular Orbitals and Organic Chemical Reactions*; John Wiley & Sons, Ltd, 2009; pp 299–325.

[151] Porco, J.; Schreiber, S. L. *Comprehensive Organic Synthesis* **1992**, *2*, 151–192.

[152] Vogt, F.; Jádicke, K.; Schröder, J.; Bach, T. *Synthesis* **2009**, *2009*, 4268–4273–.

[153] Haddach, A. A.; Kelleman, A.; Deaton-Rewolinski, M. V. *Tetrahedron Letters* **2002**, *43*, 399–402.

[154] Martinez-Montero, L.; Diaz-Rodriguez, A.; Gotor, V.; Gotor-Fernandez, V.; Lavandera, I. *Green Chemistry* **2015**, *17*, 2794–2798.

[155] Baltzly, R.; Russell, P. B. *Journal of the American Chemical Society* **1953**, *75*, 5598–5602.

[156] Jarowicki, K.; Kocienski, P. *Journal of the Chemical Society , Perkin Transactions 1* **1998**, 4005–4037.

[157] Zhang, Y.; Li, C.-J. *Journal of the American Chemical Society* **2006**, *128*, 4242–4243.

[158] Pradeep, P.; Ngwira, K. J.; Reynolds, C.; Rousseau, A. L.; Lemmerer, A.; Fernandes, M. A.; Johnson, M. M.; de Koning, C. B. *Tetrahedron* **2016**, *72*, 8417–8427.

[159] Leboho, T. C.; Giri, S.; Popova, I.; Cock, I.; Michael, J. P.; de Koning, C. B. *Bioorganic & Medicinal Chemistry* **2015**, *23*, 4943–4951.

[160] Hecht, S. M. *Journal of Natural Products* **2000**, *63*, 158–168.

[161] Cafeo, G.; Carbotti, G.; Cuzzola, A.; Fabbi, M.; Ferrini, S.; Kohnke, F. H.; Papanikolaou, G.; Plutino, M. R.; Rosano, C.; White, A. J. P. *Journal of the American Chemical Society* **2013**, *135*, 2544–2551.

[162] Dam, J.; Ismail, Z.; Kurebwa, T.; Gangat, N.; Harmse, L.; Marques, H. M.; Lemmerer, A.; Bode, M. L.; de Koning, C. B. *European Journal of Medicinal Chemistry* **2017**, *126*, 353–368.

[163] Fabre, S.; Prudhomme, M.; Rapp, M. *Bioorganic & Medicinal Chemistry* **1993**, *1*, 193–196.

[164] Ragg, U. T.; Gillian, B. *Trends in Pharmacological Sciences* **1989**, *10*, 218–220.

[165] Caravatti, G.; Meyer, T.; Fredenhagen, A.; Trinks, U.; Mett, H.; Fabbro, D. *Bioorganic & Medicinal Chemistry Letters* **1994**, *4*, 399–404.

[166] Stepczynska, A.; Lauber, K.; Engels, I. H.; Janssen, O.; Kabelitz, D.; Wesselborg, S.; Schulze-Osthoff, K. *Oncogene* **2001**, *20*, 1193–1202.

[167] Zhang, X. D.; Gillespie, S. K.; Hersey, P. *Molecular Cancer Therapeutics* **2004**, *3*, 187–197.

[168] Deshmukh, M.; Johnson, E. *Cell Death & Differentiation* **2000**, *7*.

[169] Karaman, M. W. *et al. Nat Biotech* **2008**, *26*, 127–132.

[170] Omura, S.; Iwai, Y.; Hirano, A.; Nakagawa, A.; Awaya, J.; Tsuchiya, H.; Takahashi, Y.; Asuma, R. *The Journal of Antibiotics* **1977**, *30*, 275–282.

[171] Funato, N.; Takayanagi, H.; Konda, Y.; Toda, Y.; Harigaya, Y.; Iwai, Y.; Yamura, S. *Tetrahedron Letters* **1994**, *35*, 1251–1254.

[172] Link, J. T.; Raghavan, S.; Danishefsky, S. J. *Journal of the American Chemical Society* **1995**, *117*, 552–553.

[173] Fischer, T. *et al. Journal of Clinical Oncology* **2010**, *28*, 4339–4345.

[174] Faul, M. M.; Winneroski, L. L.; Krumrich, C. A. *The Journal of Organic Chemistry* **1999**, *64*, 2465–2470.

[175] Wang, J.; Rosingana, M.; Watson, D. J.; Dowdy, E. D.; Discordia, R. P.; Soundarajan, N.; Li, W.-S. *Tetrahedron Letters* **2001**, *42*, 8935–8937.

[176] Messaoudi, S.; Anizon, F.; Peixoto, P.; David-Cordonnier, M.-H.; Golsteyn, R. M.; Léonce, S.; Pfeiffer, B.; Prudhomme, M. *Bioorganic & Medicinal Chemistry* **2006**, *14*, 7551 – 7562.

[177] Steglich, W.; Steffan, B.; Kopanski, L.; Eckhardt, G. *Angewandte Chemie International Edition in English* **1980**, *19*, 459–460.

[178] Gaudáncio, S. P.; Santos, M. M.; Lobo, A. M.; Prabhakar, S. *Tetrahedron Letters* **2003**, *44*, 2577–2578.

[179] Wada, Y.; Nagasaki, H.; Tokuda, M.; Orito, K. *The Journal of Organic Chemistry* **2007**, *72*, 2008–2014.

[180] Raju, P.; Gobi Rajeshwaran, G.; Mohanakrishnan, A. K. *European Journal of Organic Chemistry* **2015**, *2015*, 7131–7145.

[181] Beccalli, E. M.; Gelmi, M. L.; Marchesini, A. *Tetrahedron* **1998**, *54*, 6909–6918.

[182] Fox, J. C.; Gilligan, R. E.; Pitts, A. K.; Bennett, H. R.; Gaunt, M. J. *Chemical Science* **2016**, *7*, 2706–2710.

[183] Kastl, A.; Wilbuer, A.; Merkel, A. L.; Feng, L.; Fazio, P. D.; Ocker, M.; Meggers, E. *Chemical Communications* **2012**, *48*, 1863–1865.

[184] Pelly, S. C.; Parkinson, C. J.; van Otterlo, W. A. L.; de Koning, C. B. *The Journal of Organic Chemistry* **2005**, *70*, 10474–10481.

[185] Brown, R. J. C.; Brown, R. F. C. *Journal of Chemical Education* **2000**, *77*, 724.

[186] Pinal, R. *Organic and Biomolecular Chemistry* **2004**, *2*, 2692–2699.

[187] Nazaré, M.; Schneider, C.; Lindenschmidt, A.; Will, D. W. *Angewandte Chemie International Edition* **2004**, *43*, 4526–4528.

[188] Liu, S.-F.; Wu, Q.; Schmider, H. L.; Aziz, H.; Hu, N.-X.; Popovi, Z.; Wang, S. *Journal of the American Chemical Society* **2000**, *122*, 3671–3678.

[189] Dam, J. Synthetic, Mechanistic and Biological Studies of Novel Metal-Imidazo[1,2-a]pyridines and Xanthones. Ph.D. thesis, University of the Witwatersrand, 2016.

[190] Bruker, SAINT+. Version 6.02 (includes XPREP and SADABS). Bruker AXS Inc.: Madison, Wisconsin, USA, 1999.

[191] Sheldrick, G. M. SADABS. University of Gottingen: Germany, 1996.

[192] Bruker, SHELXTL. Version 5.1 (includes XS, XL, XP, XSHELL). Bruker AXS Inc.: Madison, Winsconsin, USA.

[193] Spek, A. L. *Acta Crystallographica Section D Biological Crystallography* **2009**, *65*, 148–155.

[194] Farrugia, L. J. *Journal of Applied Crystallography* **1997**, *30*, 565–565.

[195] Brignell, P. J.; Jones, P. E.; Katritzky, A. R. *Journal of the Chemical Society B* **1970**, 117–121.

[196] Xu, T.; Zhou, W.; Wang, J.; Li, X.; Guo, J.-W.; Wang, B. *Tetrahedron Letters* **2014**, *55*, 5058–5061.

[197] Zanatta, N.; Faoro, D.; Silva, S. C.; Bonacorso, H. G.; Martins, M. A. *Tetrahedron Letters* **2004**, *45*, 5689–5691.

[198] Al-Awadi, N. A.; Al-Bashir, R. F.; ElDusouqui, O. M. *Tetrahedron* **1990**, *46*, 2903–2910.

[199] Pauli, L.; Tannert, R.; Scheil, R.; Pfaltz, A. *Chemistry A European Journal* **2015**, *21*, 1482–1487.

[200] Rossy, C.; Fouquet, E.; Felpin, F.-X. *Beilstein Journal of Organic Chemistry* **2013**, *9*, 1426–1431.

[201] National institute of advanced industrial science and technology (Japan), *AIST: Integrated spectral database system of organic compounds*; CAS (SciFinder), 2013.

[202] Niu, L.; Zhang, H.; Yang, H.; Fu, H. *Synlett* **2014**, *25*, 995–1000.

[203] Xu, C.; Du, W.; Zeng, Y.; Dai, B.; Guo, H. *Organic Letters* **2014**, *16*, 948–951.

[204] de Mattos, M. C.; Alatorre-Santamaría, S.; Gotor-Fernández, V.; Gotor, V. *Synthesis* **2007**, *2007*, 2149–2152.

[205] Palmisano, G.; Penoni, A.; Sisti, M.; Tibiletti, F.; Tollari, S.; M Nicholas, K. *Current Organic Chemistry* **2010**, *14*, 2409–2441.

[206] Kim, J.; Kim, H.; Chang, S. *Organic Letters* **2012**, *14*, 3924–3927.

[207] Fiandanese, V.; Bottalico, D.; Marchese, G.; Punzi, A. *Tetrahedron* **2008**, *64*, 53–60.

[208] Chappie, T.; Verhoest, P.; Patel, N.; Hayward, M. Azabenzimidazole compounds. 2015; `https://www.google.com/patents/US9120788`, US Patent 9,120,788.

[209] Carpita, A.; Ribecai, A.; Stabile, P. *Tetrahedron* **2010**, *66*, 7169–7178.

[210] Sakai, N.; Tamura, K.; Shimamura, K.; Ikeda, R.; Konakahara, T. *Organic Letters* **2012**, *14*, 836–839.

[211] Bellenie, B. R.; Bloomfield, G. C.; Bruce, I.; Culshaw, A. J.; Hall, E. C.; Hollingworth, G. J.; Neef, J.; Spendiff, M.; Watson, S. J. Amino pyridine derivatives as phosphatidylinositol 3-kinase inhibitors. 2017; `https://www.google.com/patents/US20170037032`.

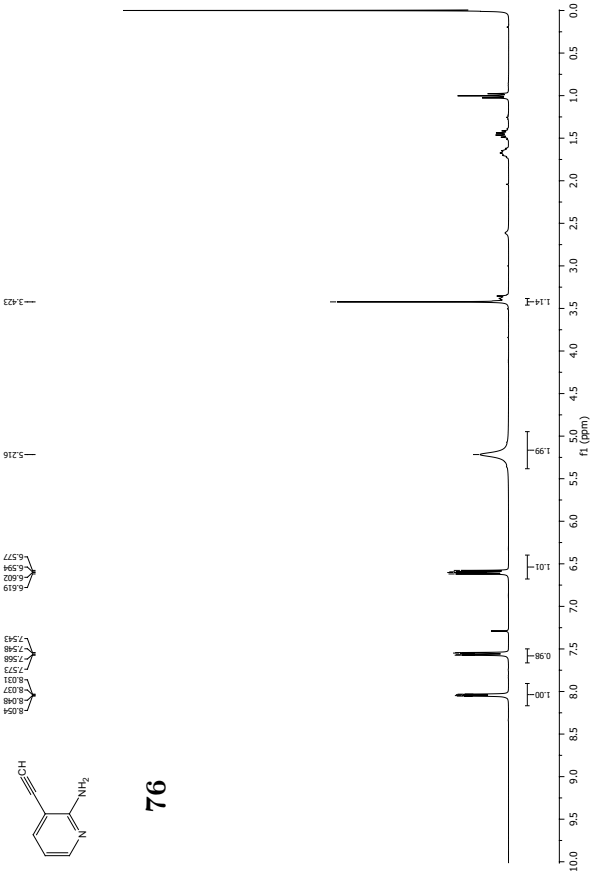
[212] Bhunia, S.; Ghorpade, S.; Huple, D. B.; Liu, R.-S. *Angewandte Chemie International Edition* **2012**, *51*, 2939–2942.

[213] Sharma, H. A.; Todd Hovey, M.; Scheidt, K. A. *Chemical Communications* **2016**, *52*, 9283–9286.

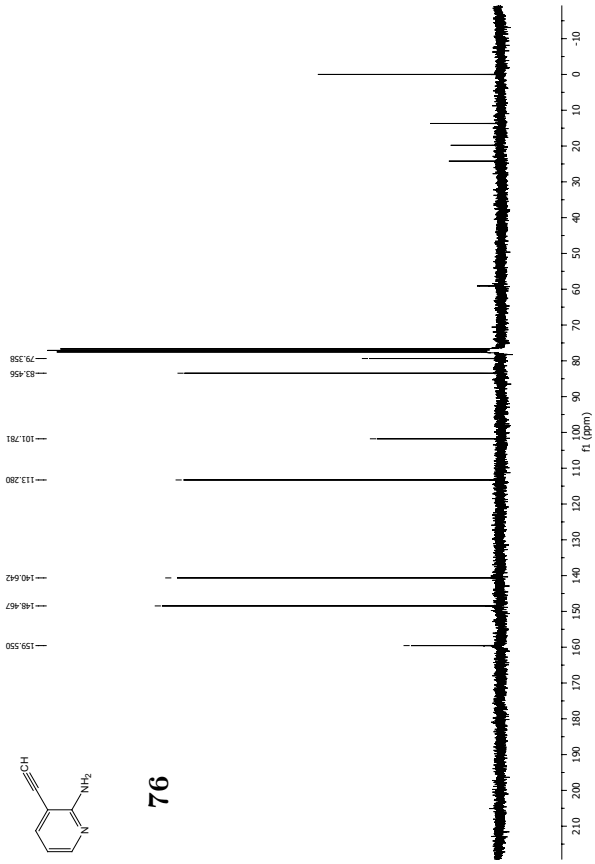
[214] Kaczmarek, L.; Balicki, R.; Nantka-Namirski, P.; Peczyńska-Czoch, W.; Mordarski, M. *Archiv der Pharmazie* **1988**, *321*, 463–467.

[215] Frolov, A. N.; Baklanov, M. V. *Journal of organic chemistry of the USSR* **1991**, *27*, 2153–2157.

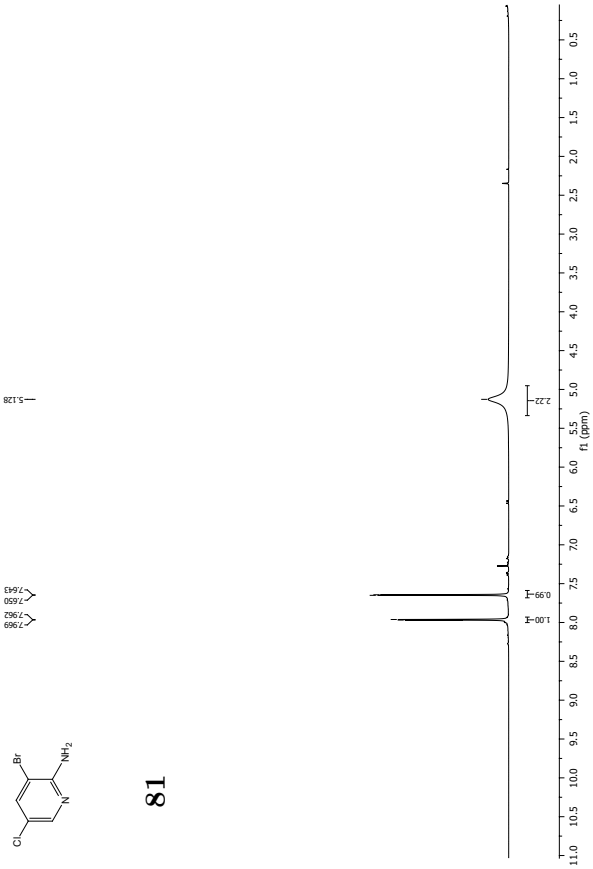
Appendix: NMR spectra


8.054
8.048
8.037
8.031
7.573
7.568
7.548
7.543
6.619
6.602
6.594
6.577
5.216
3.423
1.00
0.98
1.01
1.99
1.14
f1 (ppm)

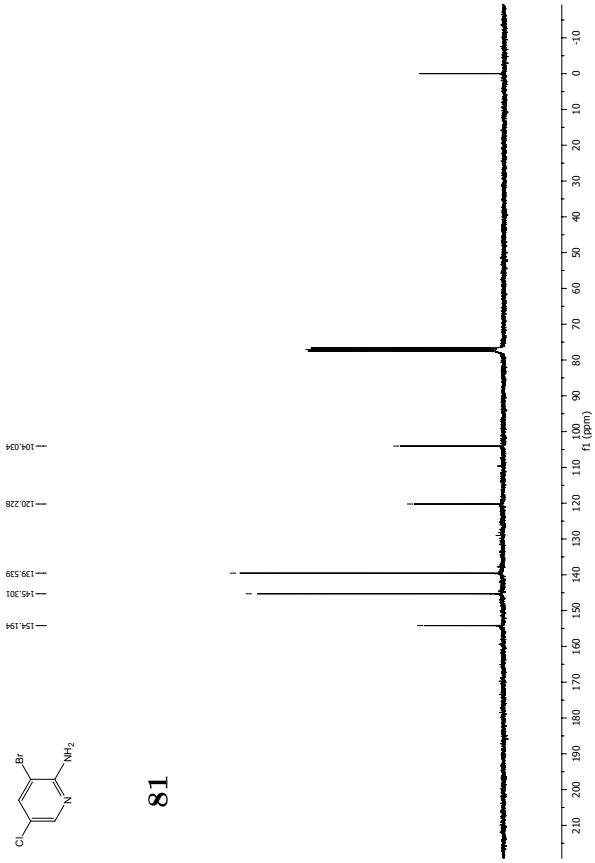
76


159.550
148.967
140.642
113.280
101.781
83.456
79.358
f1 (ppm)

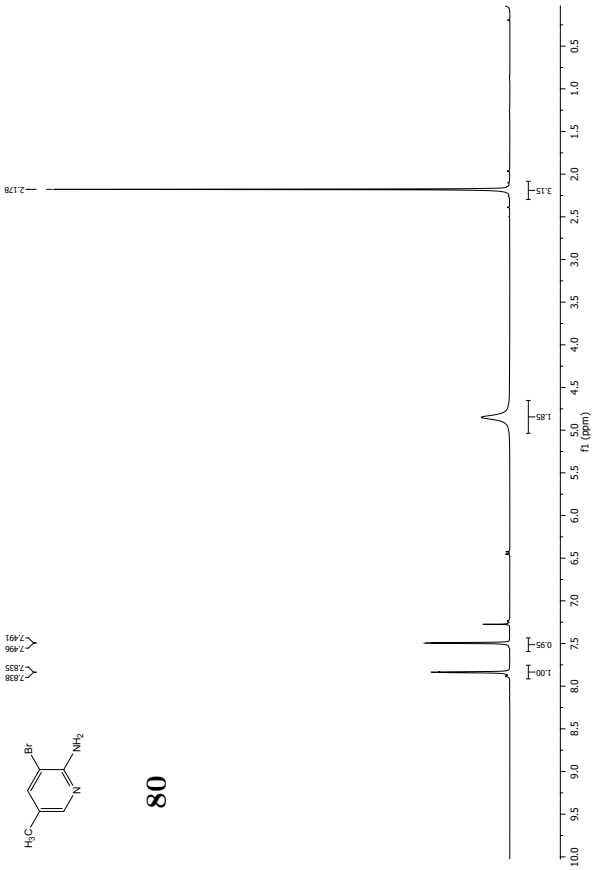
76

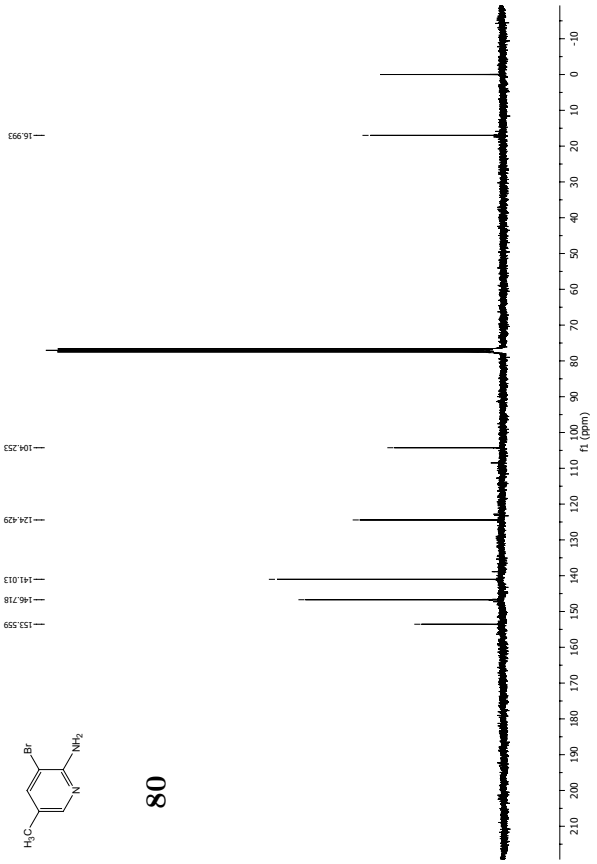

7969
7962
7650
7643
5.128
1.00
0.99
2.22
f1 (ppm)

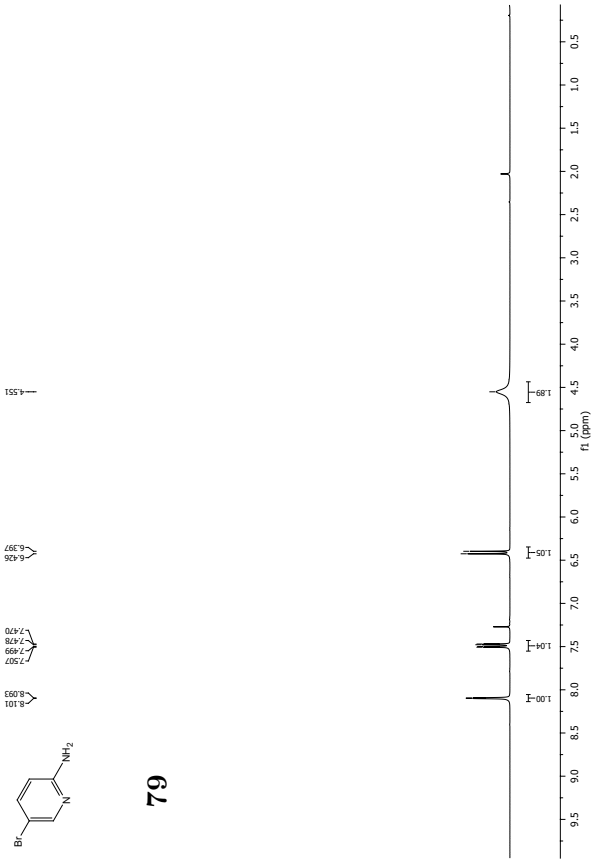
81

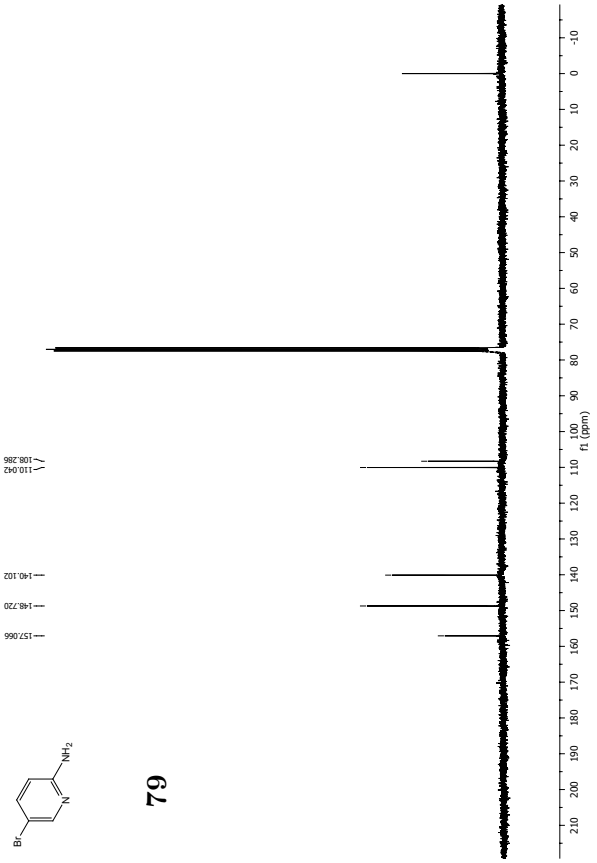

154.194
145.301
139.539
120.228
104.034
f1 (ppm)

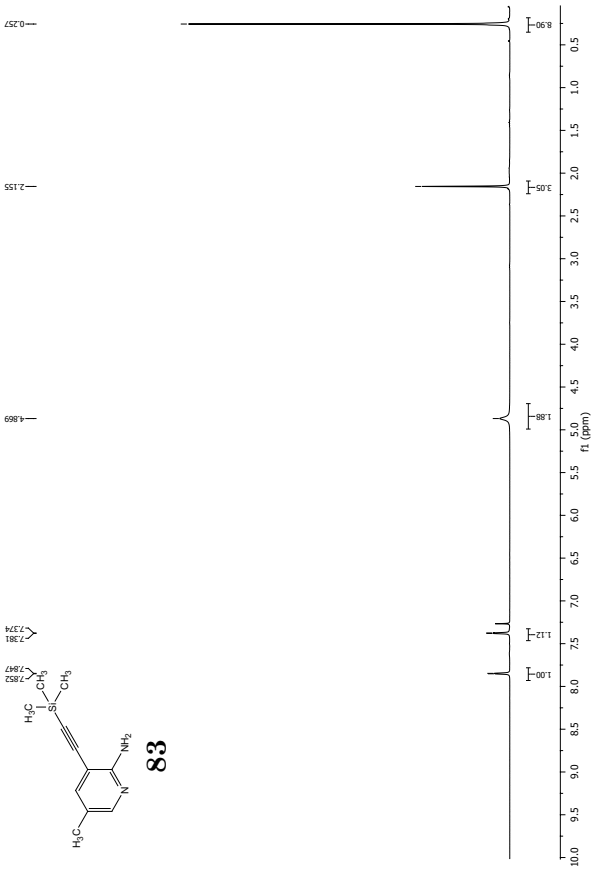
81

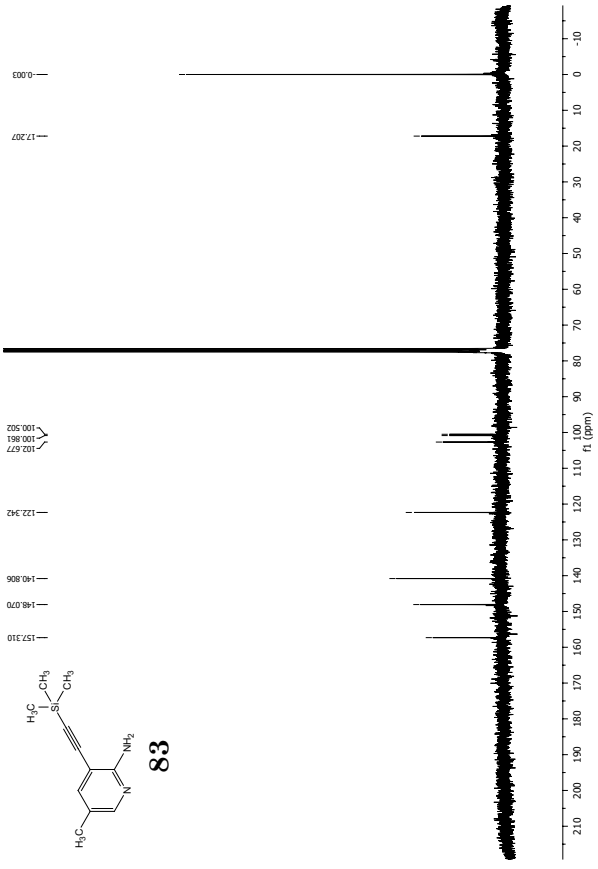

2.178
7.838
7.835
7.496
7.491
3.15
1.85
0.95
1.00
f1 (ppm)
80

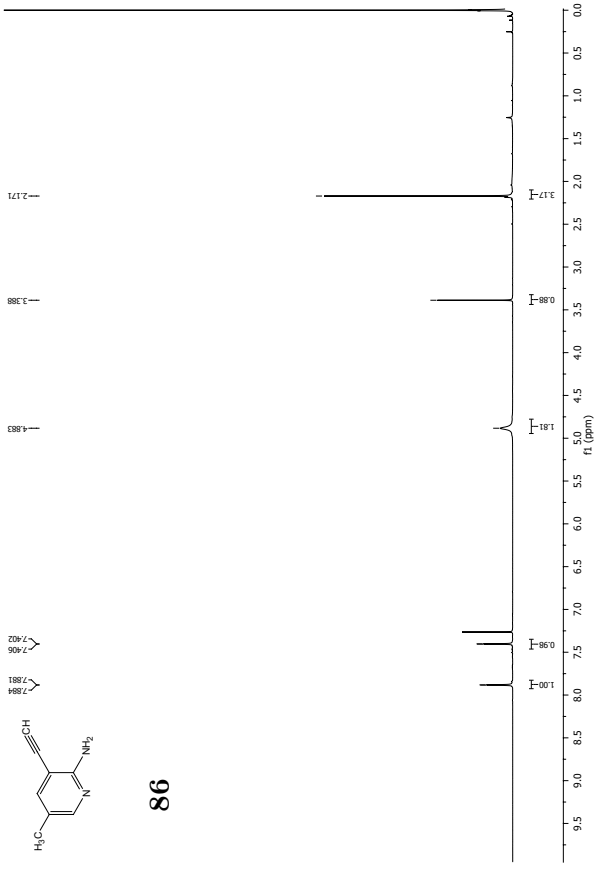

16.993
104.253
124.429
141.013
146.718
153.559
f1 (ppm)
80

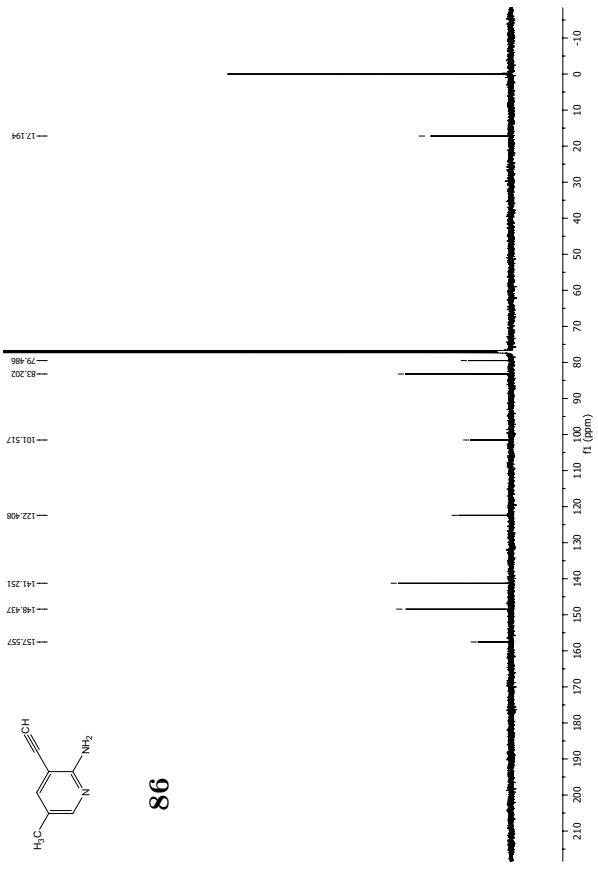

4.551
8.101
8.093
7.507
7.499
7.428
7.420
6.426
6.397
1.89
1.05
1.04
1.00
f1 (ppm)
67

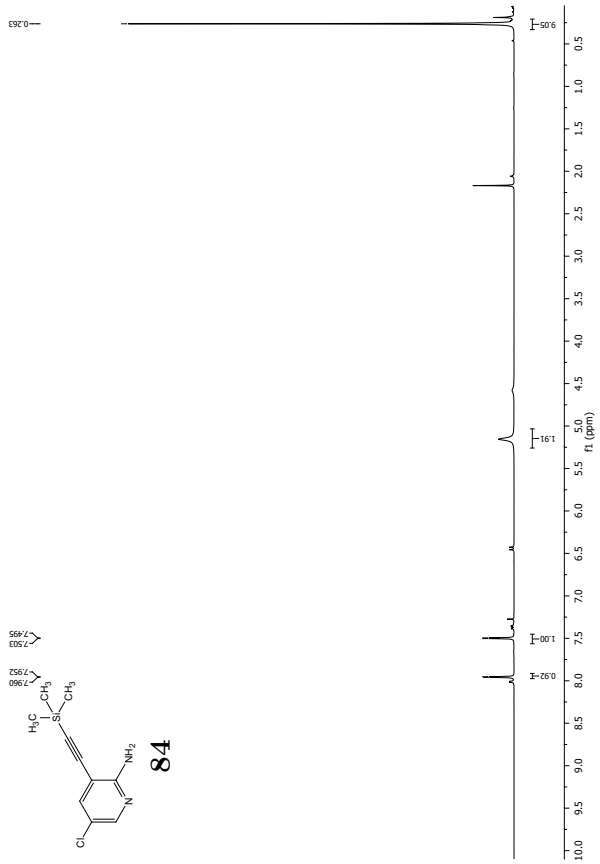

110.042
108.286
140.102
148.720
157.066
f1 (ppm)
67

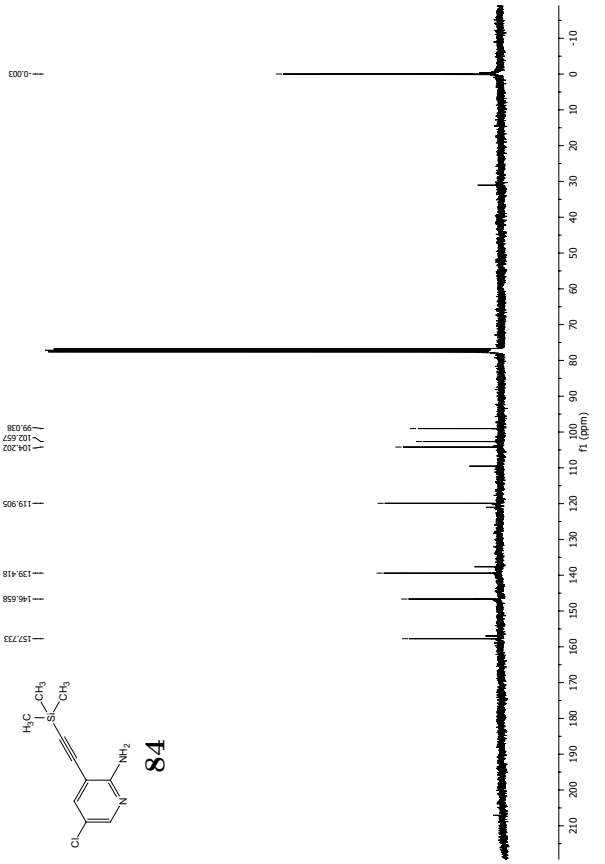

0.257
2.155
4.869
7.381
7.324
7.852
7.847
8.90
3.05
1.88
1.12
1.00
f1 (ppm)
83

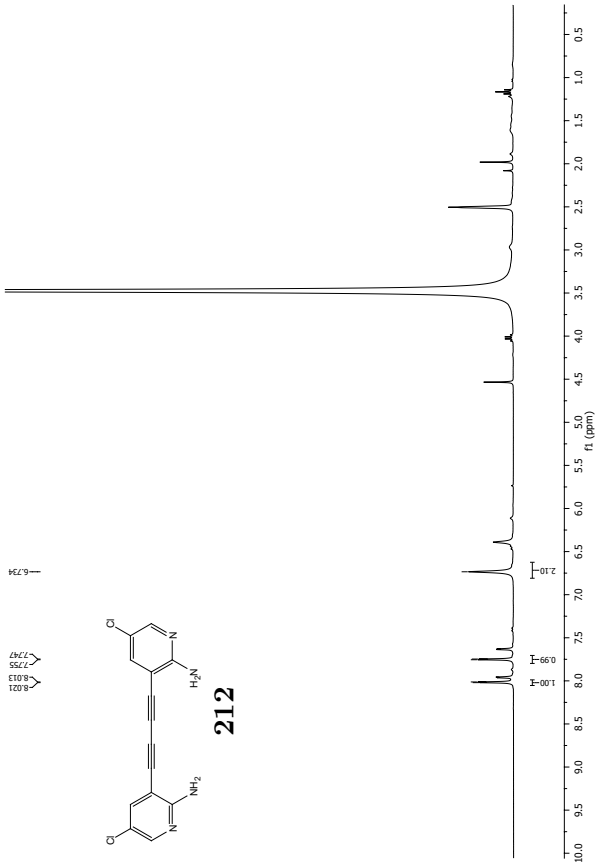

0.003
17.207
102.677
100.861
100.502
122.342
140.806
148.070
157.310
f1 (ppm)
83

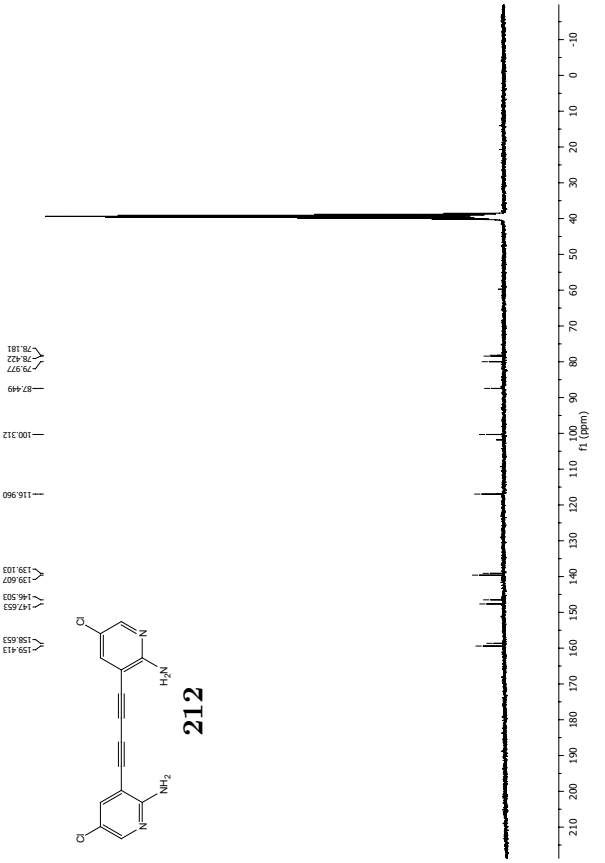

2.171
3.388
4.883
7.884
7.881
7.406
7.402
3.17
0.88
1.81
0.98
1.00
f1 (ppm)
86

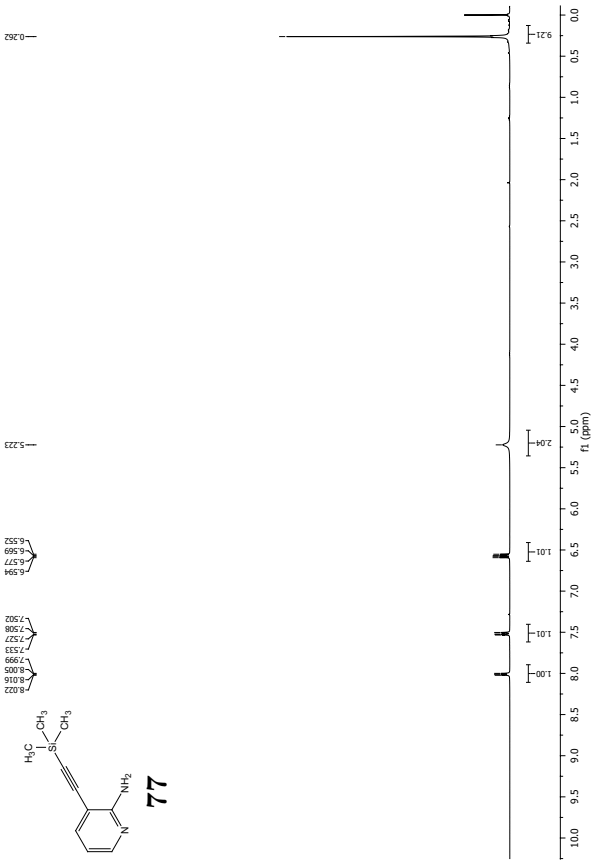

17.194
79.486
83.202
101.517
122.408
141.251
148.437
157.557
f1 (ppm)
86

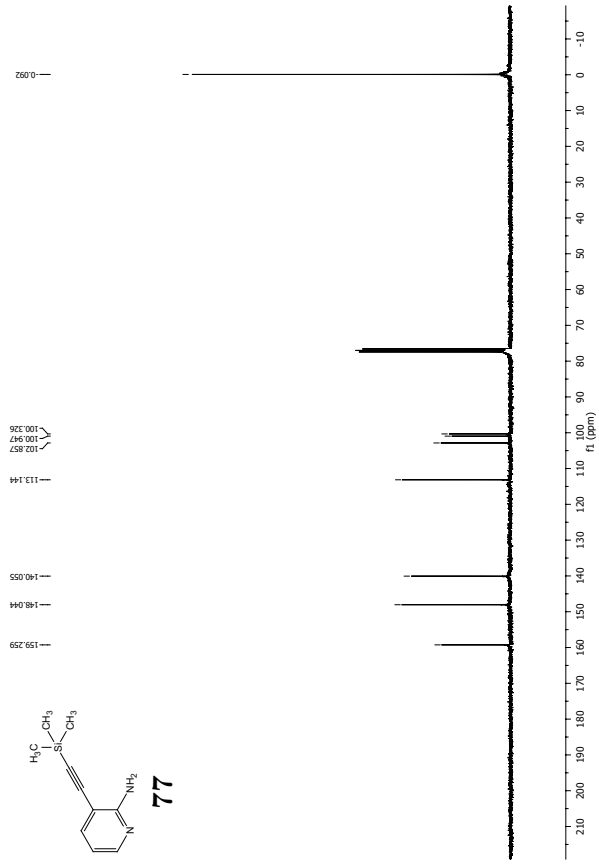

0.263
7.503
7.495
7.960
7.952
9.05
1.91
1.00
0.92
84

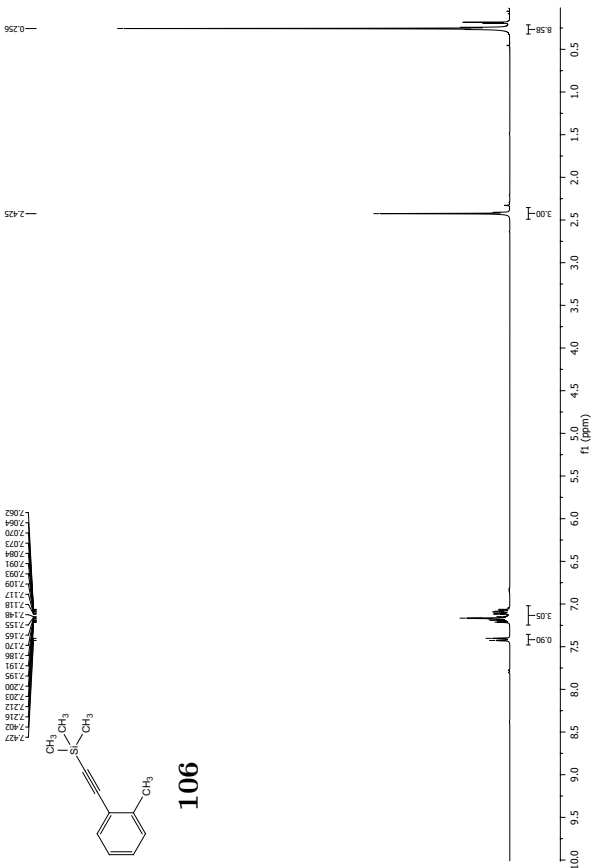

0.003
157.733
146.658
139.418
119.905
104.202
102.657
99.038
84

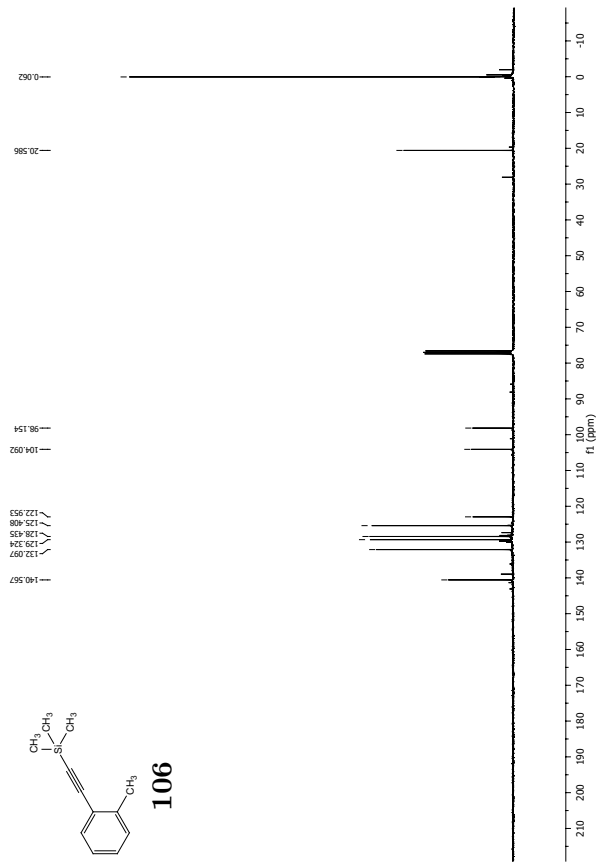

6.734
8.021
8.013
7.755
7.747
2.10
1.00
0.99
212

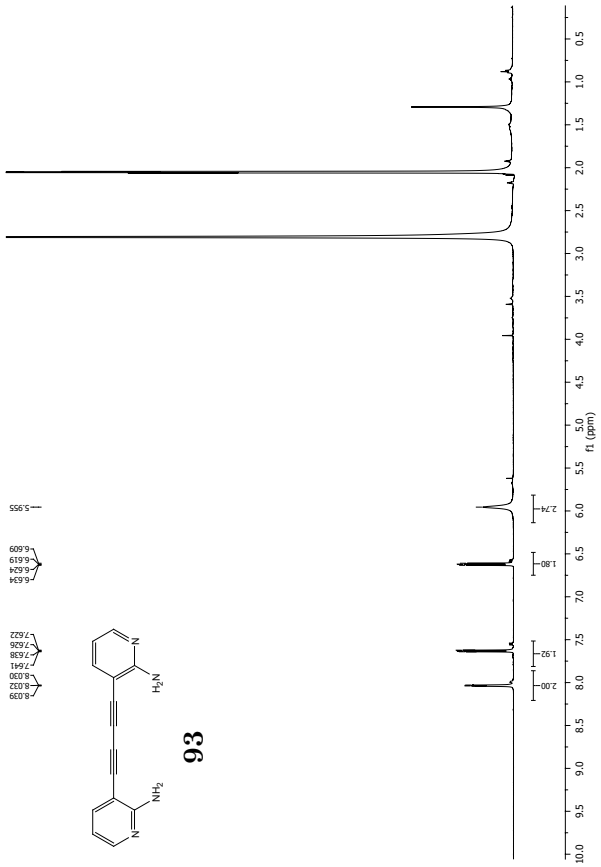

159.413
158.653
147.653
146.503
139.607
139.103
116.960
100.312
87.449
79.577
78.422
78.181
212

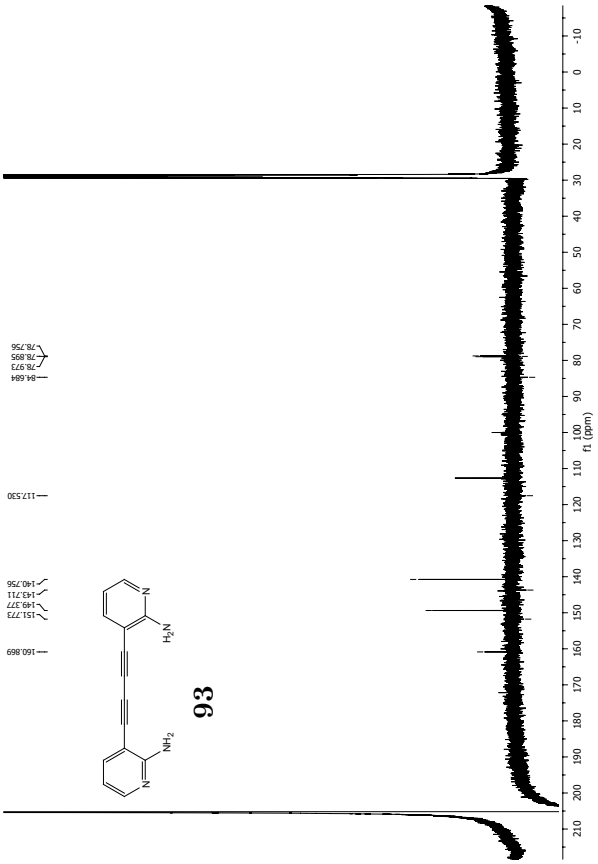

0.262
9.21
5.223
2.04
1.01
1.01
1.00
6.594
6.577
6.569
6.552
8.022
8.016
8.005
7.999
7.533
7.527
7.508
7.502
77
f1 (ppm)

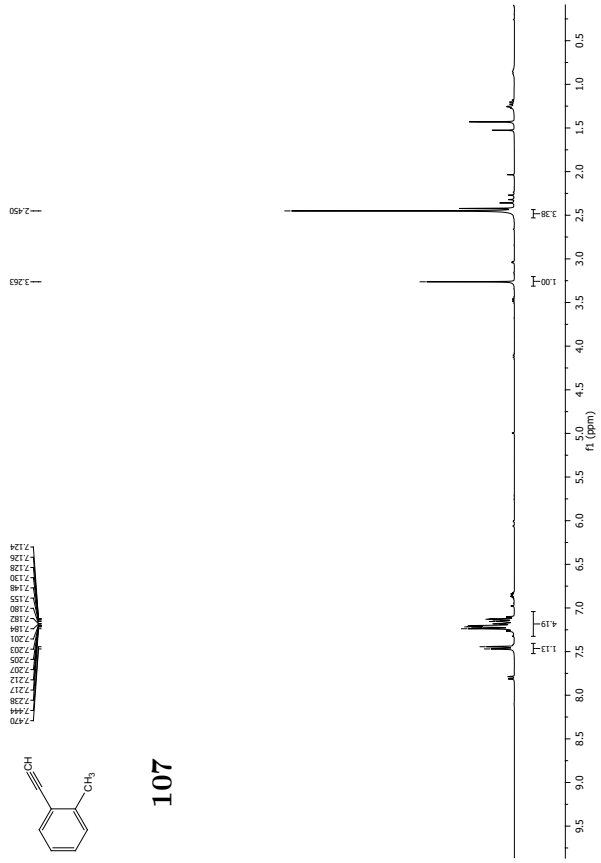

0.092
159.259
148.044
140.055
113.144
102.857
100.947
100.326
77
f1 (ppm)

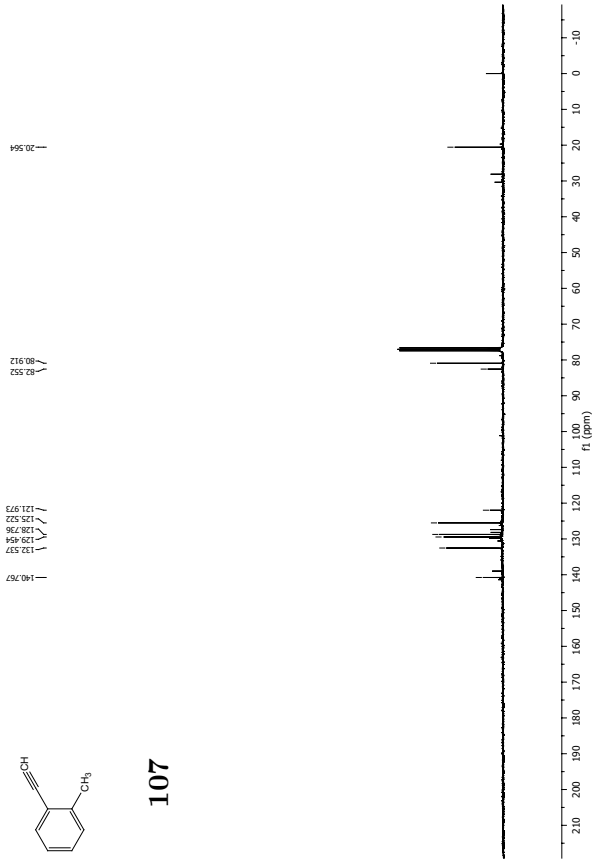

0.256
8.58
2.425
3.00
3.05
0.90
7.427
7.402
7.216
7.212
7.203
7.200
7.191
7.195
7.186
7.170
7.165
7.155
7.148
7.118
7.117
7.109
7.093
7.091
7.084
7.073
7.070
7.064
7.062
106
f1 (ppm)

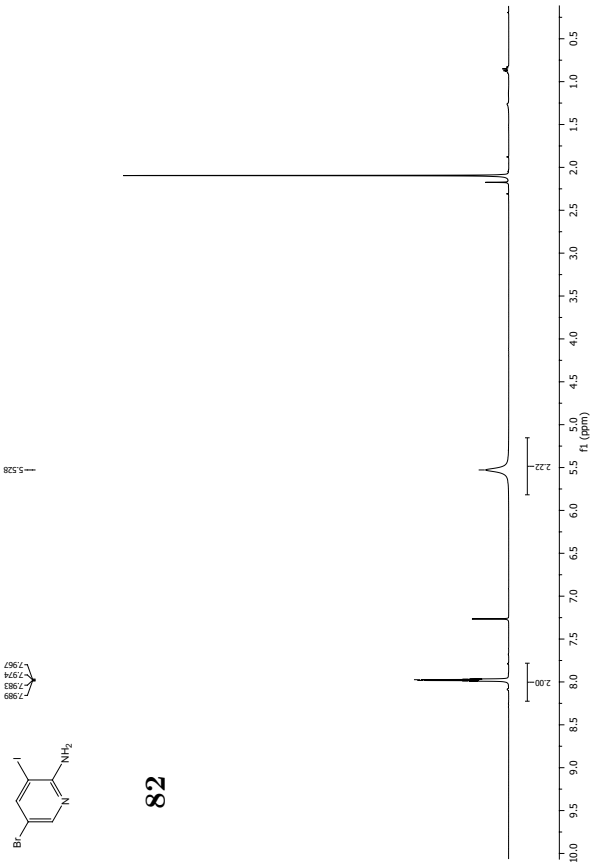

0.062
20.586
140.567
132.097
128.435
125.408
122.953
104.092
98.154
106
f1 (ppm)


8.039
8.030
8.024
7.644
7.638
7.626
7.622
6.634
6.624
6.619
6.609
5.955
2.74
1.80
1.92
2.00
f1 (ppm)
93

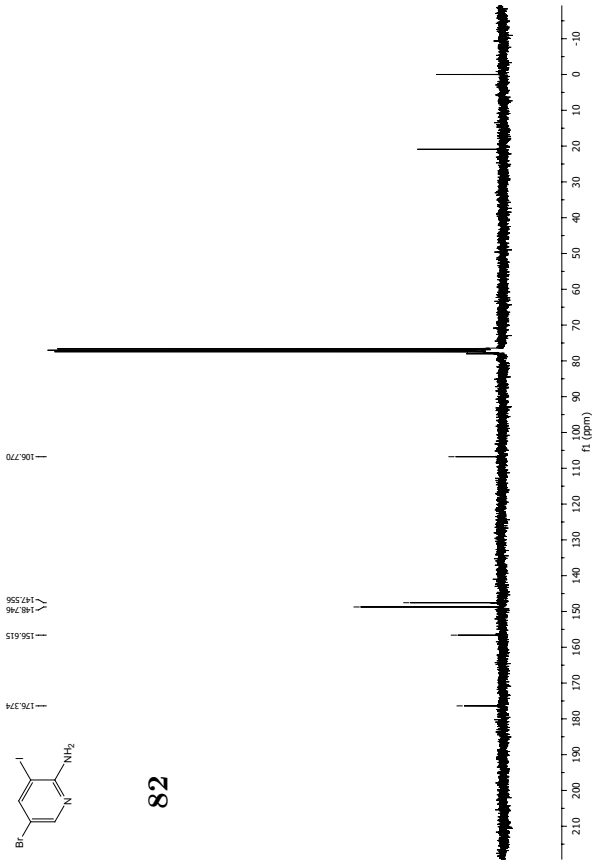

160.869
151.773
149.377
143.711
140.756
117.530
84.684
78.973
78.895
78.756
f1 (ppm)
93


7.470
7.444
7.238
7.217
7.212
7.207
7.205
7.203
7.201
7.194
7.182
7.155
7.148
7.130
7.128
7.126
7.124
3.363
2.450
4.19
1.13
1.38
1.00
f1 (ppm)
107

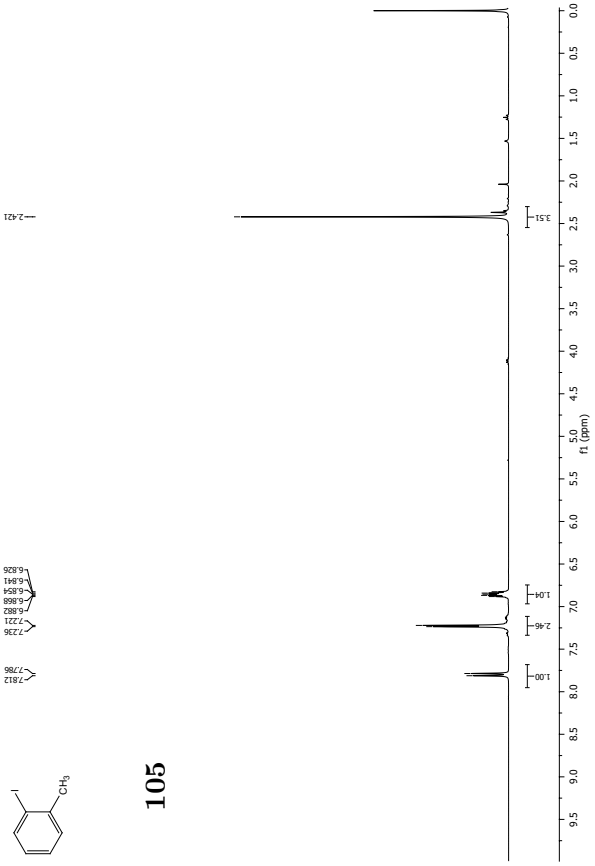

140.767
132.537
129.454
128.736
125.522
121.973
82.552
80.912
20.564
f1 (ppm)
107


5.528
7.989
7.983
7.974
7.967
2.22
2.00
f1 (ppm)

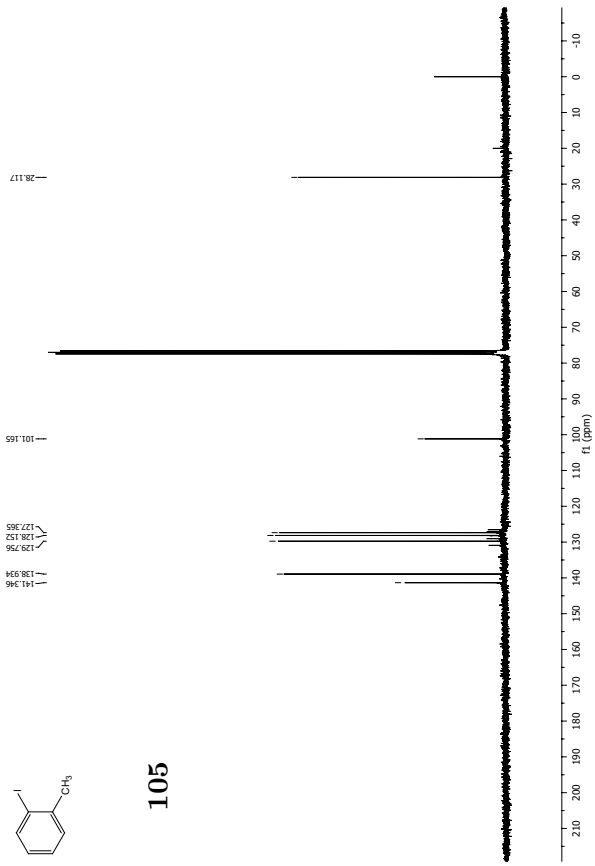
82


106.770
148.746
147.556
156.615
176.374
f1 (ppm)

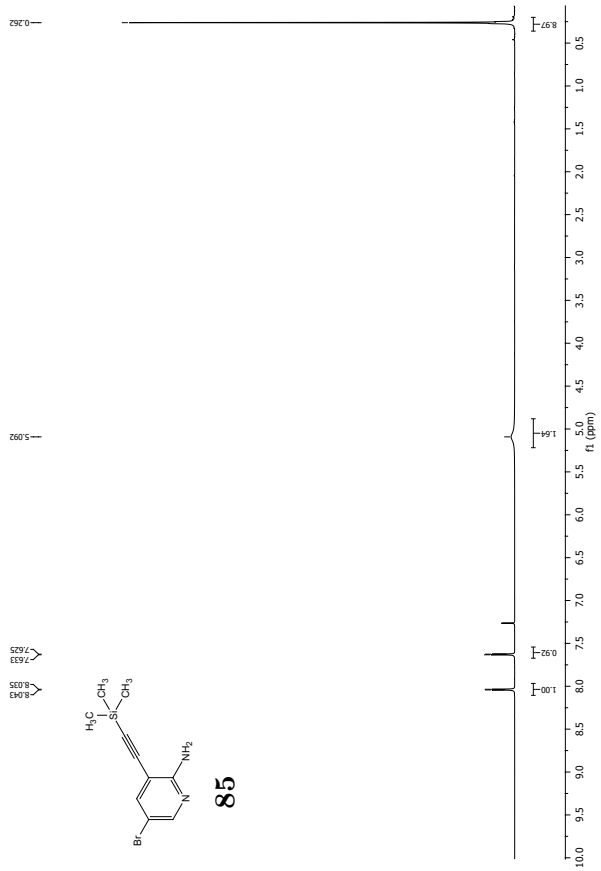
82

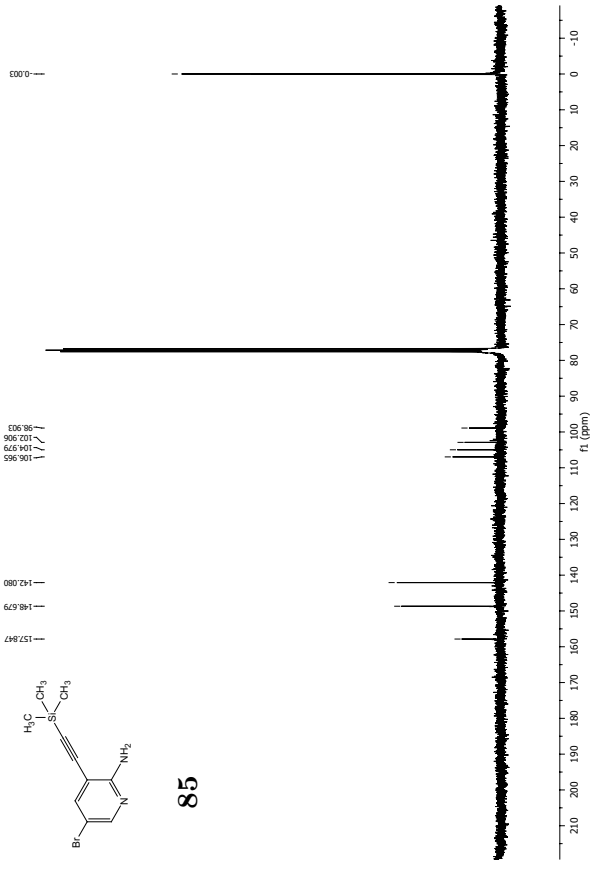

2.421
7.812
7.786
7.236
7.221
6.882
6.868
6.854
6.841
6.826
3.51
2.46
1.04
1.00
f1 (ppm)

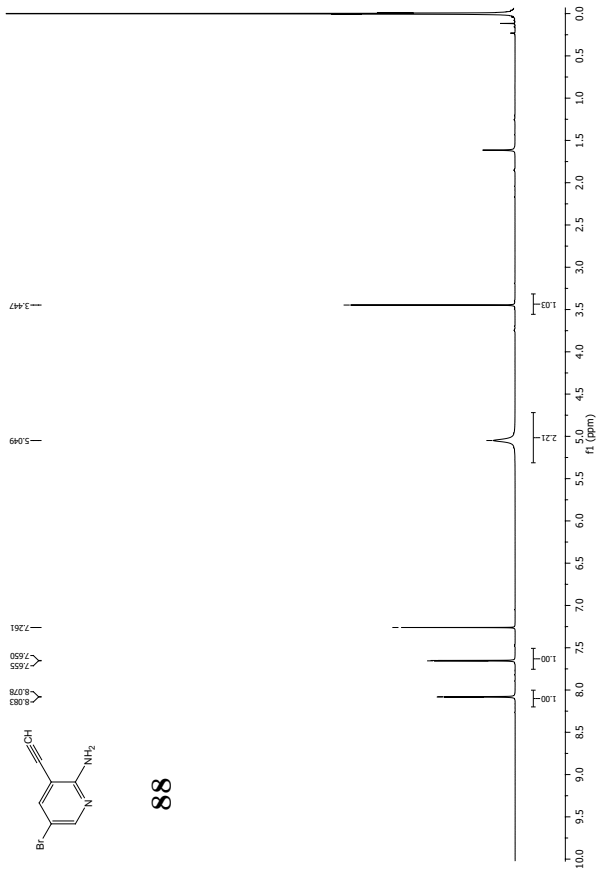
105

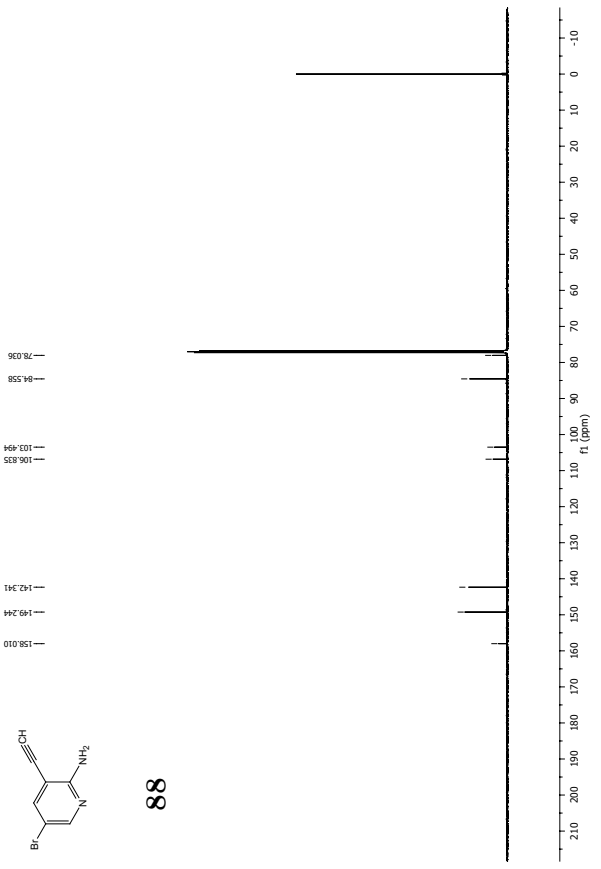

28.117
101.165
141.346
138.934
129.756
128.152
127.365
f1 (ppm)

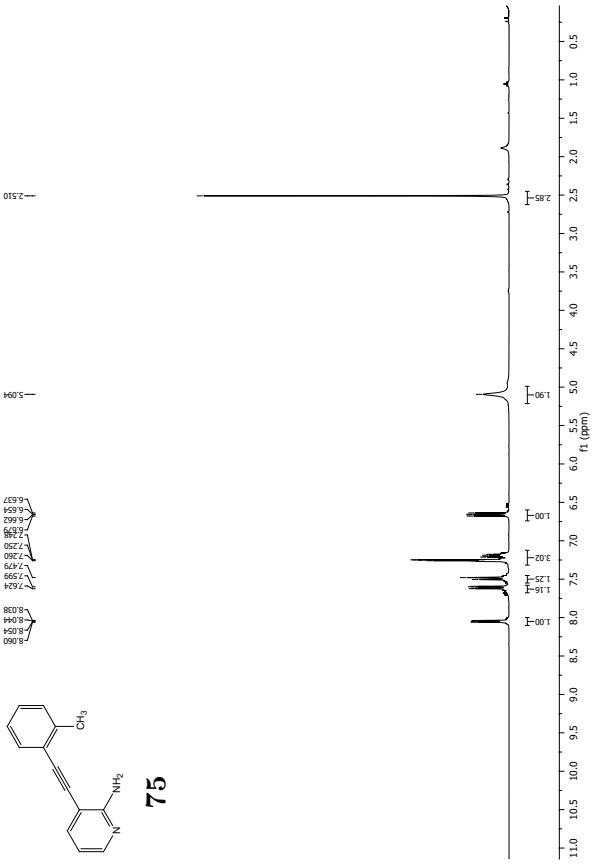
105


0.262
8.97
5.092
1.64
7.633
7.625
8.043
8.035
0.92
1.00
f1 (ppm)
85

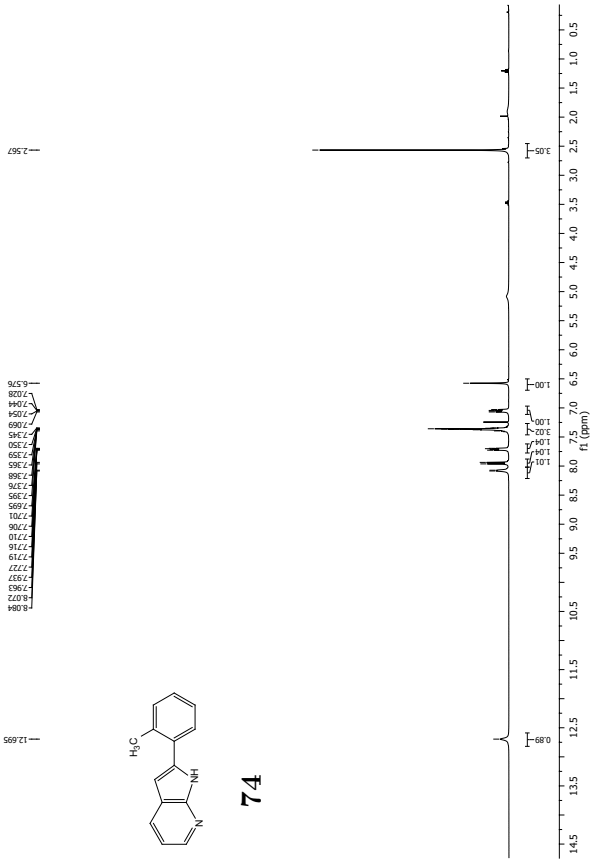

0.003
106.965
104.979
102.906
98.903
142.080
148.679
157.847
f1 (ppm)
85


3.447
5.049
7.261
7.655
7.650
8.083
8.078
1.03
2.21
1.00
1.00
f1 (ppm)
88

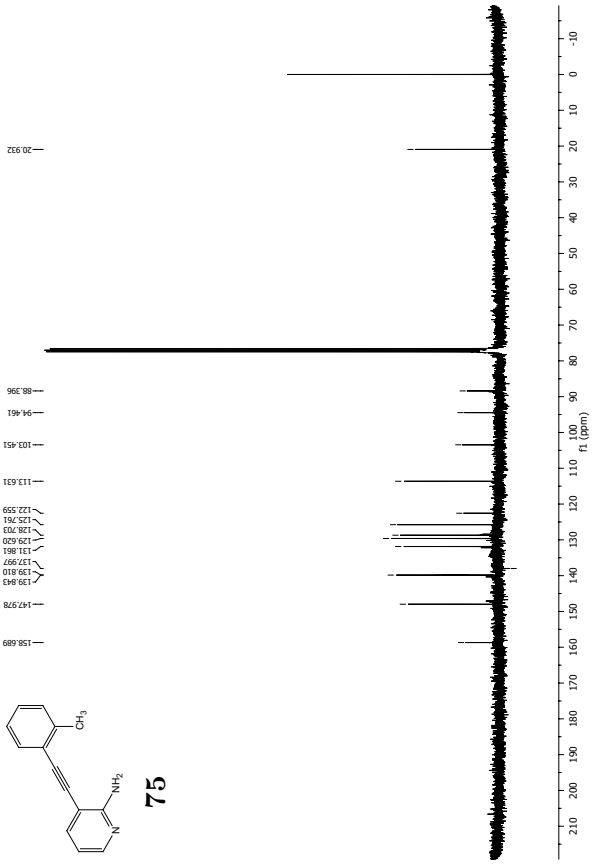

78.036
84.558
106.835
103.494
142.341
149.244
158.010
f1 (ppm)
88


8.060
8.054
8.044
8.038
7.624
7.599
7.479
7.260
7.250
7.248
6.662
6.654
6.637
5.094
2.510
1.00
1.16
1.25
3.02
1.00
1.90
2.85
f1 (ppm)
CH3
NH2
N

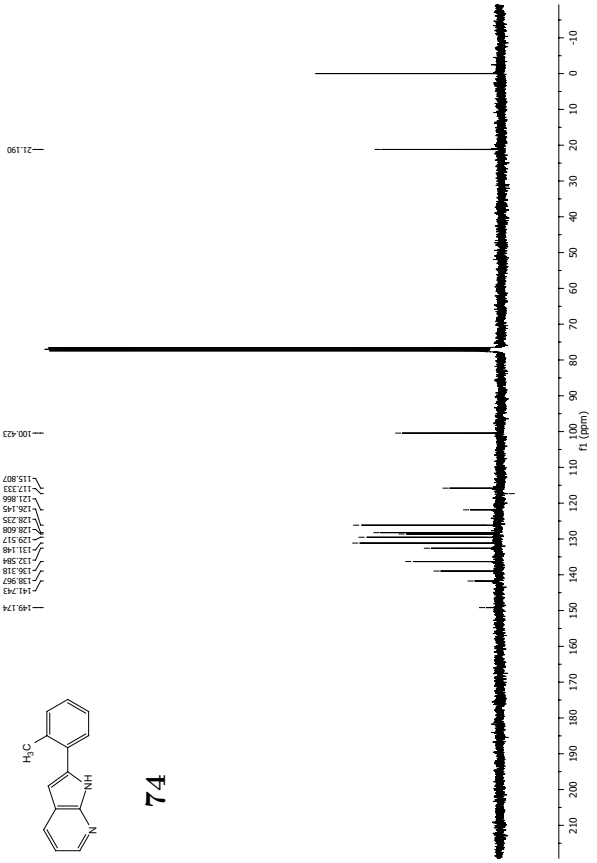
75


8.084
8.072
7.963
7.937
7.727
7.719
7.710
7.706
7.695
7.691
7.395
7.376
7.368
7.365
7.359
7.350
7.345
7.069
7.054
7.044
7.028
6.576
12.695
0.89
1.00
1.04
1.04
1.01
1.00
3.02
1.00
3.05
2.567
f1 (ppm)
H3C
NH
N

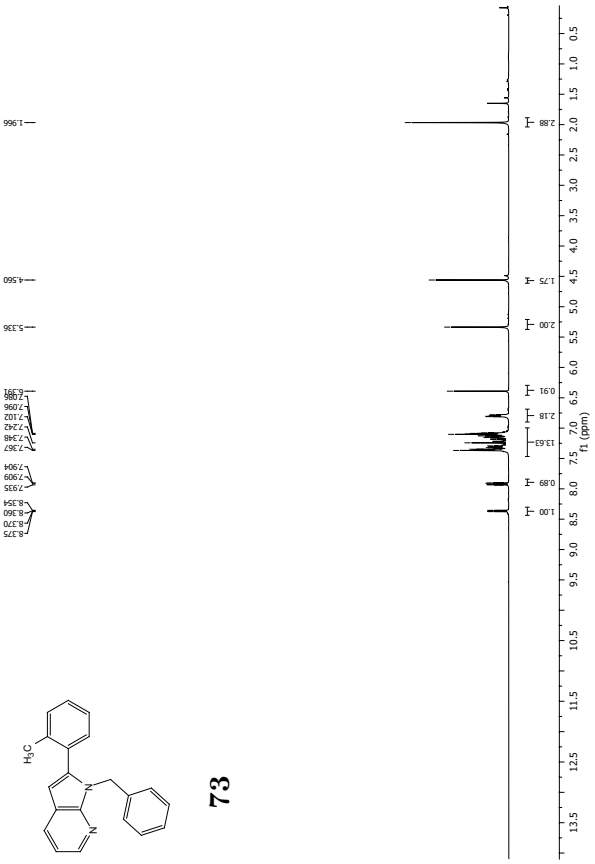
74


158.689
147.978
139.843
139.810
137.997
131.861
129.620
128.703
125.761
122.559
113.631
103.451
94.461
88.396
20.932
f1 (ppm)
CH3
NH2
N

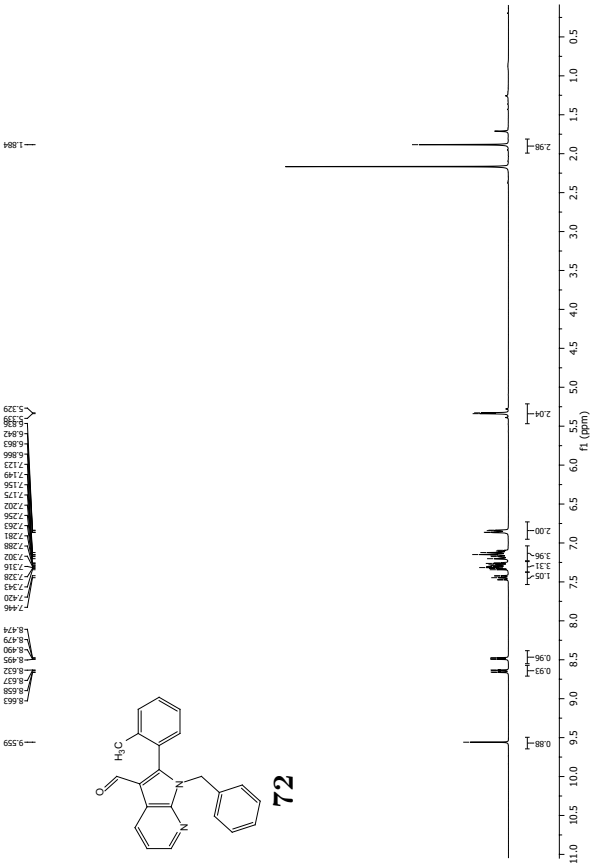
75


149.174
141.743
138.967
136.318
132.584
131.148
129.517
128.808
128.235
126.145
121.865
117.333
115.807
100.423
21.190
f1 (ppm)
H3C
NH
N

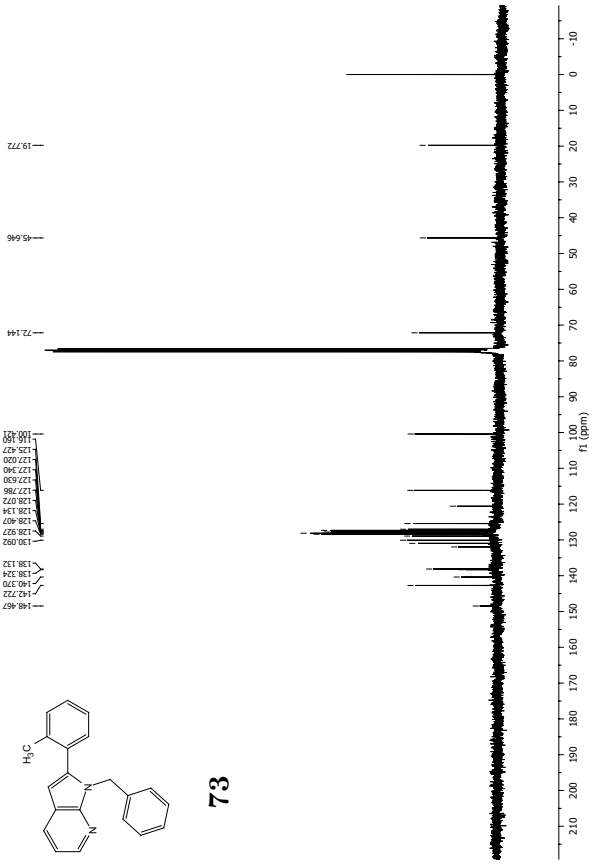
74


1.966
4.560
5.336
7.291
7.298
7.309
7.342
7.367
7.504
7.909
7.935
8.354
8.360
8.375
2.88
1.75
2.00
0.91
2.18
13.63
0.89
1.00
f1 (ppm)
H3C
N
N

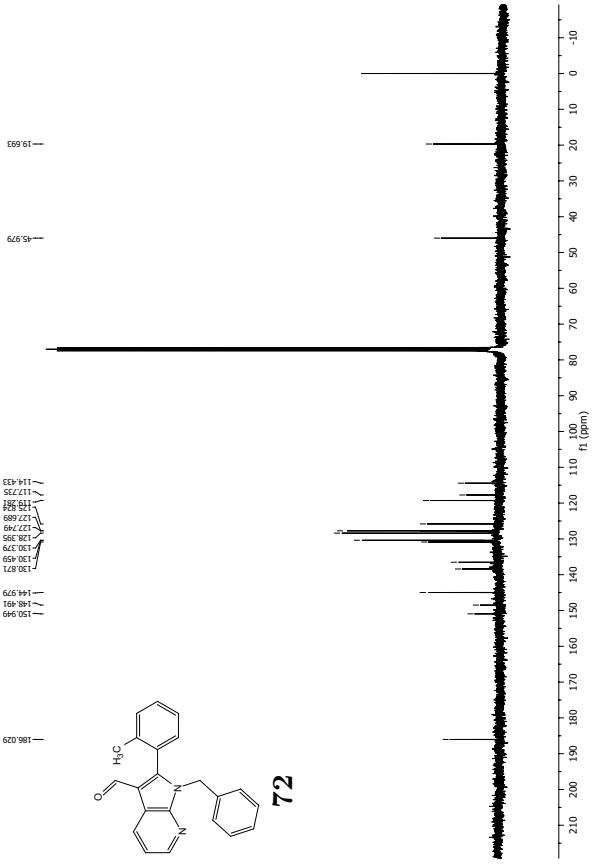
73


1.884
5.329
6.836
6.842
6.863
6.866
7.123
7.149
7.156
7.175
7.202
7.236
7.263
7.281
7.288
7.302
7.316
7.328
7.343
7.420
7.446
8.474
8.479
8.490
8.495
8.532
8.537
8.558
8.663
9.559
2.98
2.04
2.00
1.05
3.31
3.96
0.93
0.96
0.88
f1 (ppm)
H3C
O
N
N

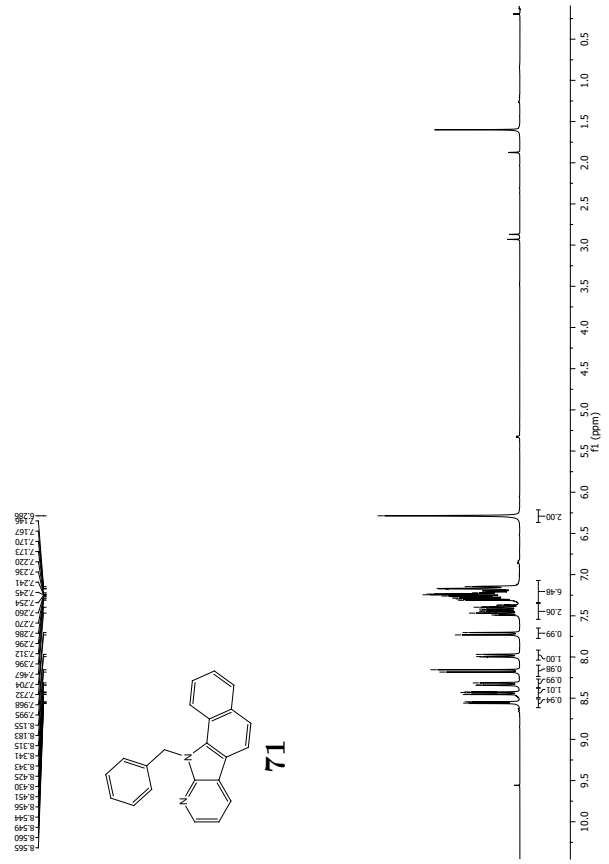
72

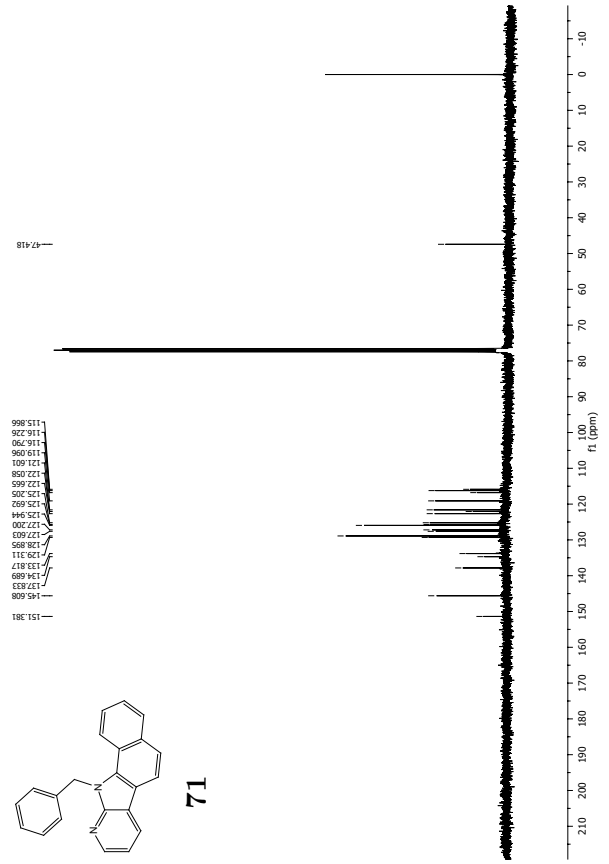

19.772
45.646
72.144
100.421
116.160
125.427
127.020
127.240
127.630
127.786
128.072
128.134
128.407
129.927
130.092
138.132
138.324
140.370
142.722
148.467
f1 (ppm)
H3C
N
N

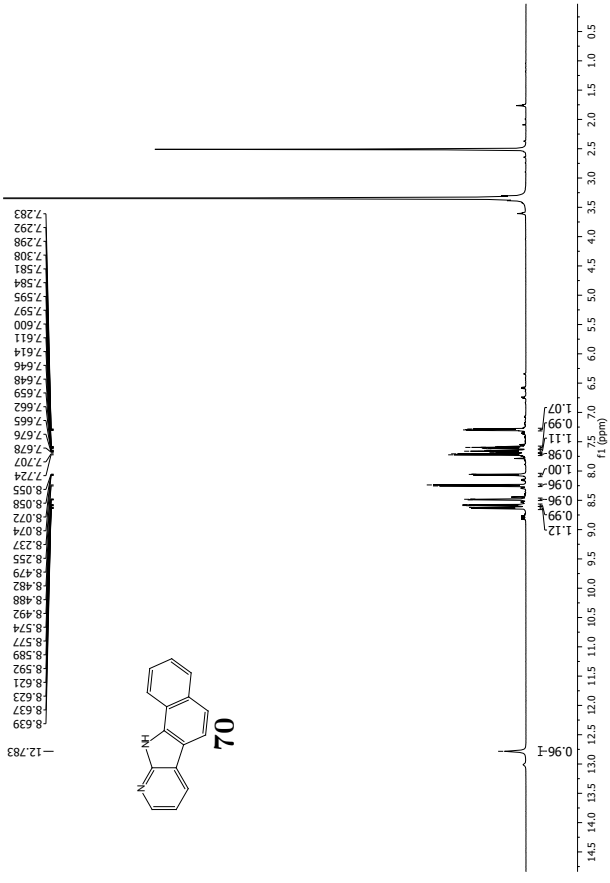
73

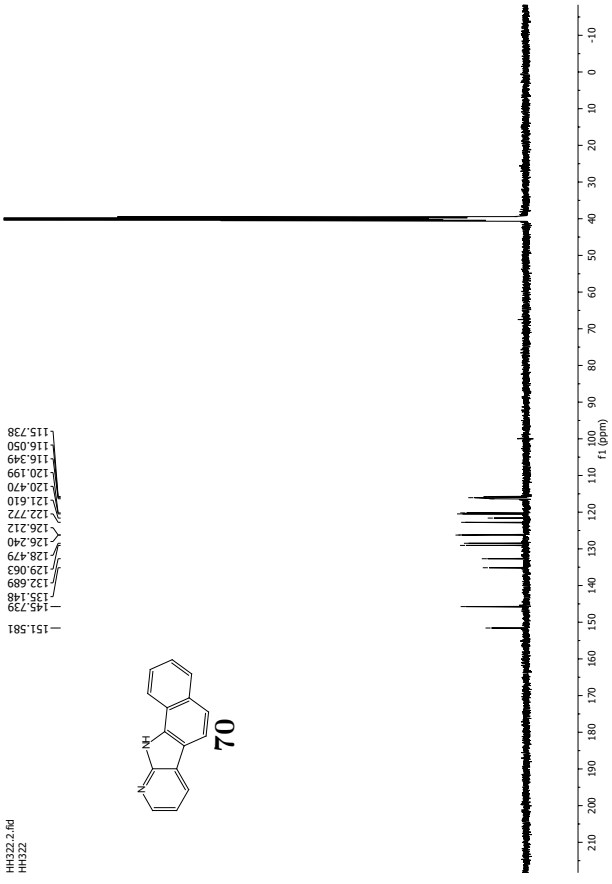

19.693
45.979
114.433
117.735
123.384
123.581
127.689
127.749
128.395
130.379
130.459
130.871
144.979
148.491
150.949
186.029
f1 (ppm)
H3C
O
N
N

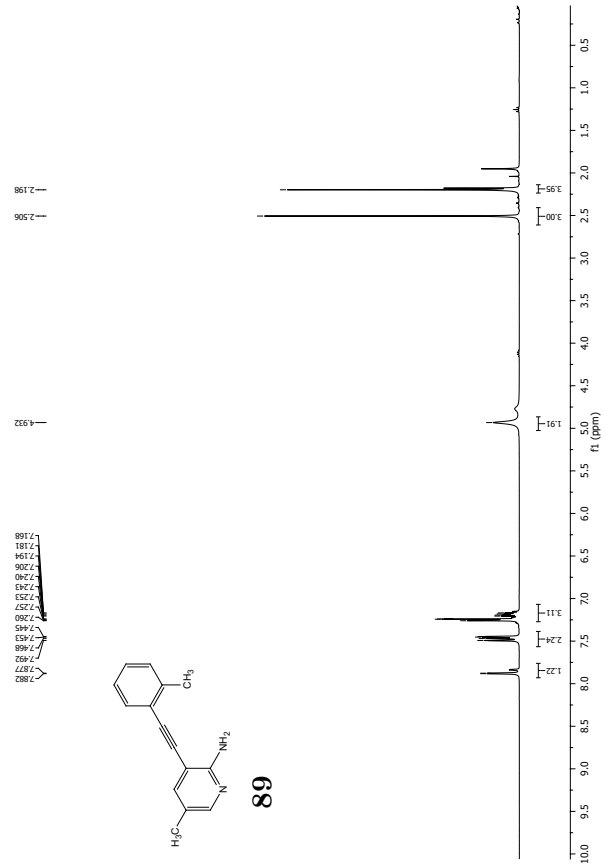
72

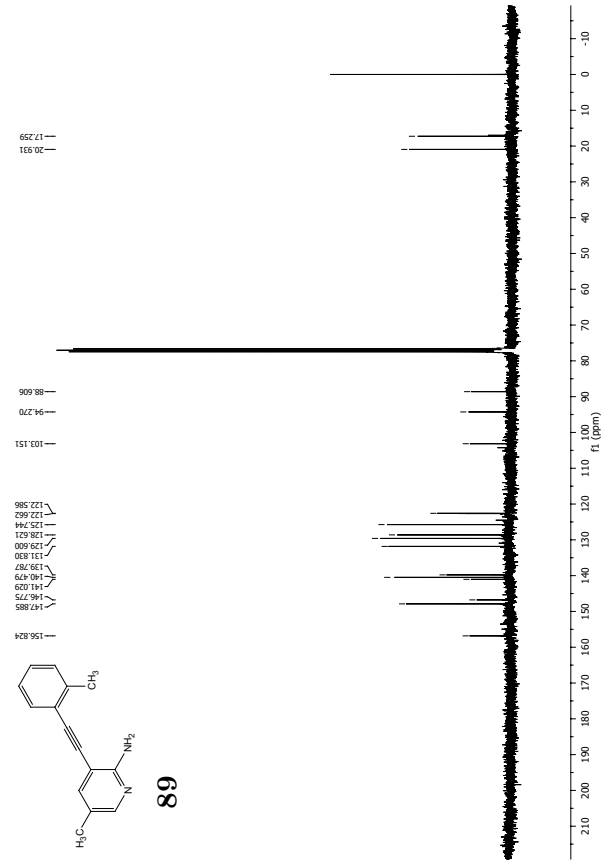

71
f1 (ppm)

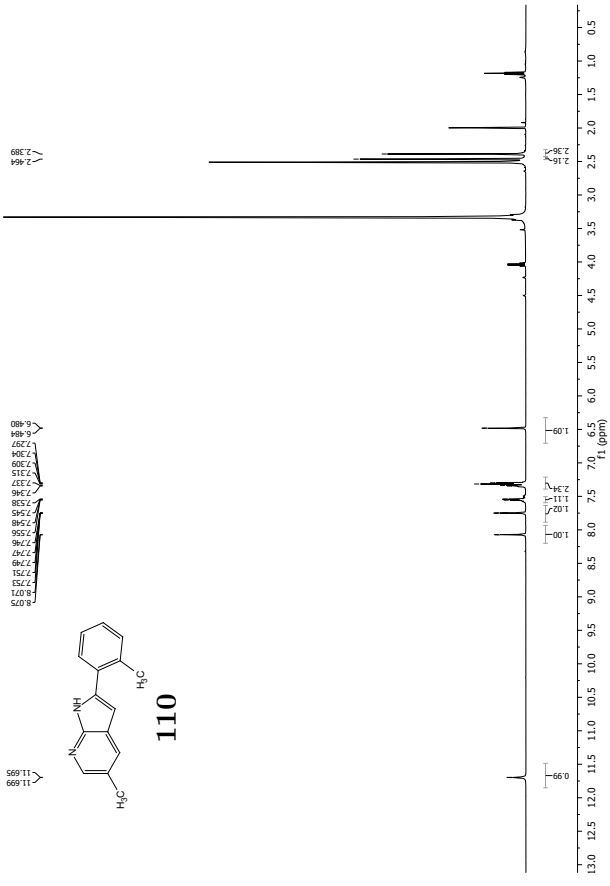

71
f1 (ppm)

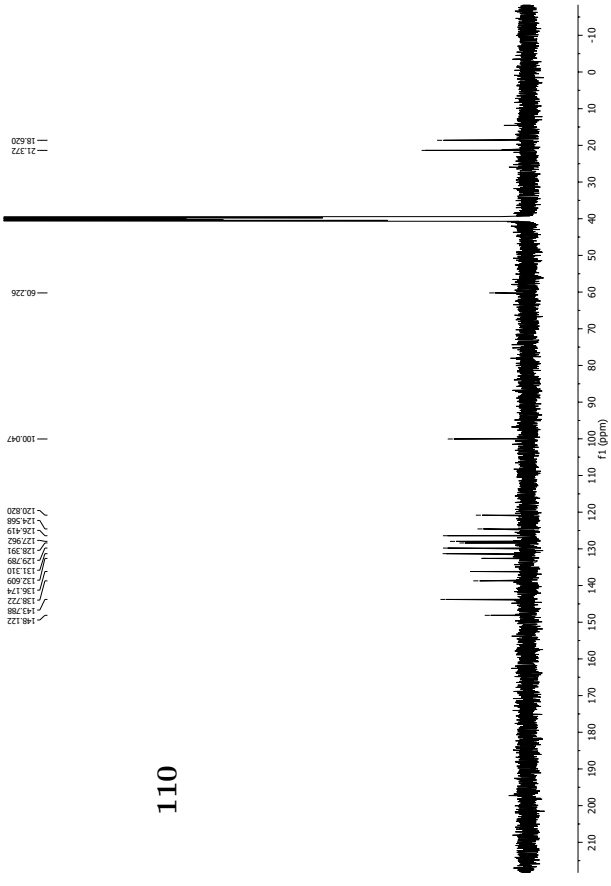

70
f1 (ppm)

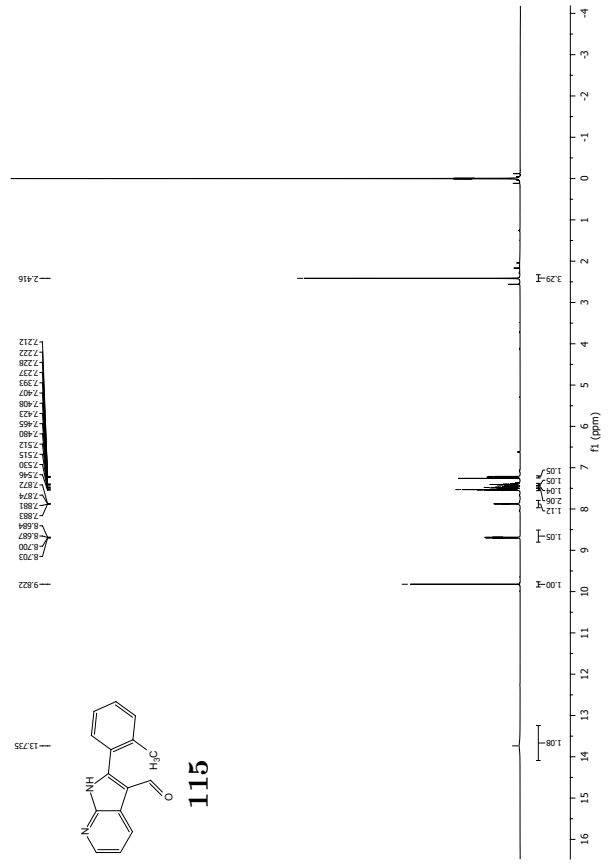

70
f1 (ppm)

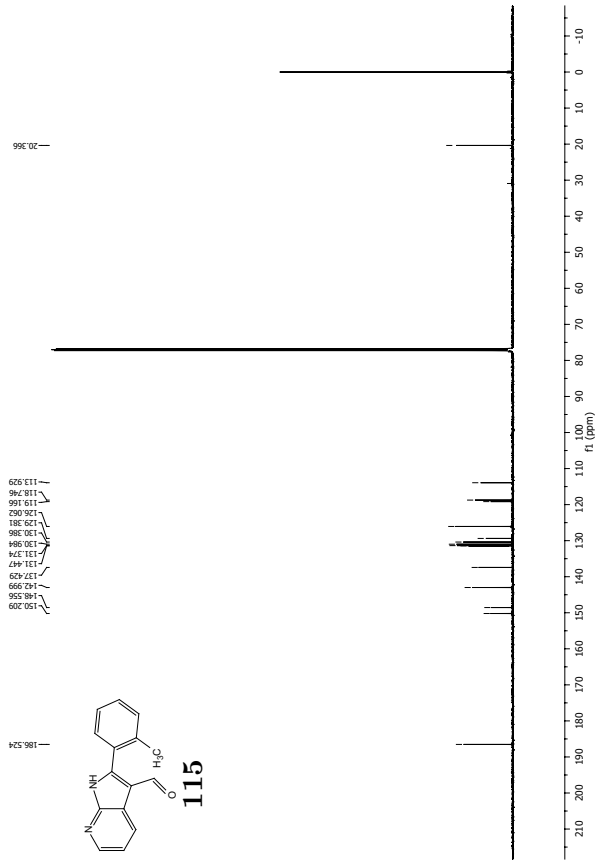

89
f1 (ppm)

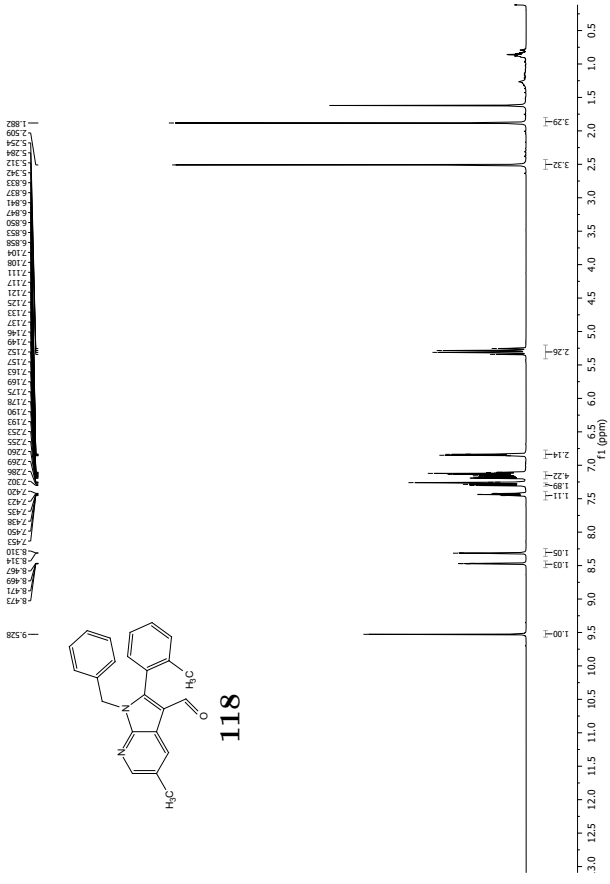

89
f1 (ppm)

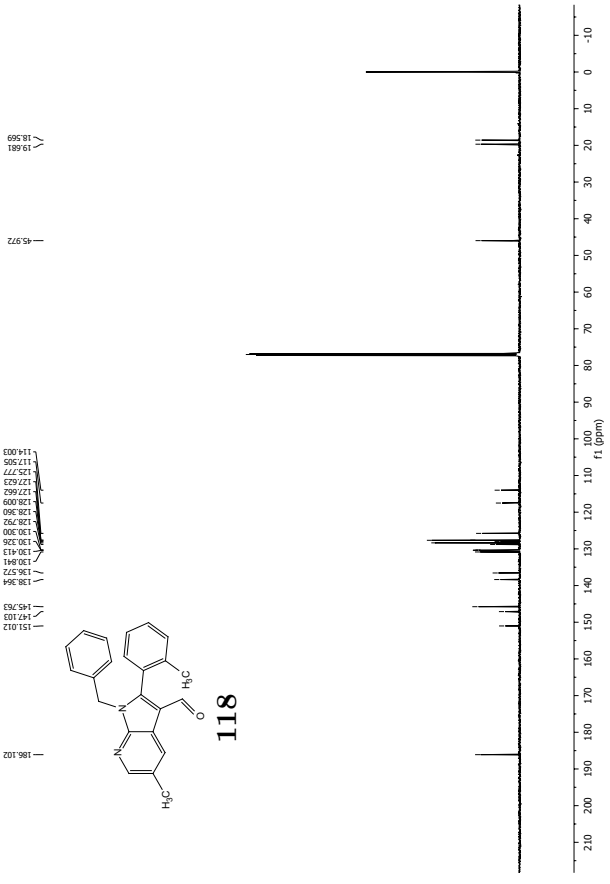

110
f1 (ppm)

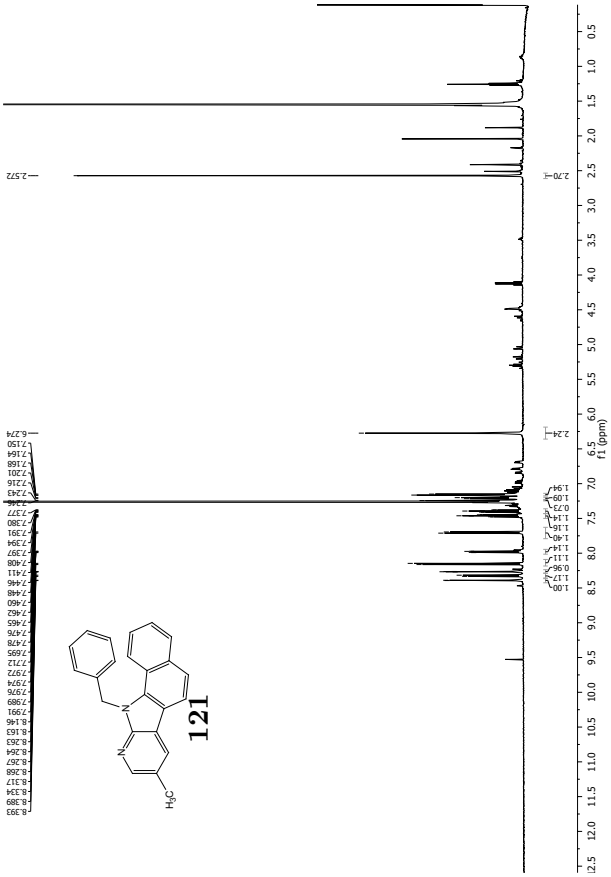

110
f1 (ppm)

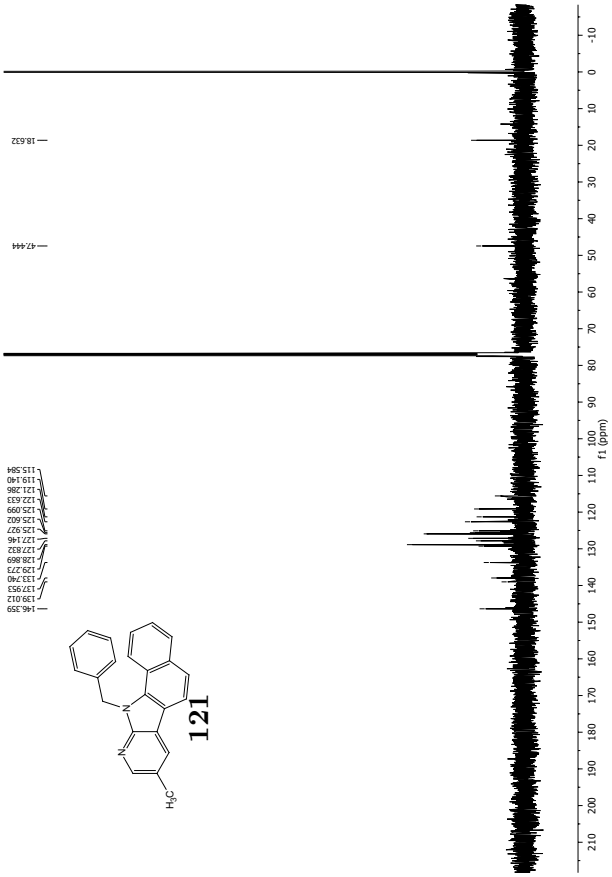

115
f1 (ppm)

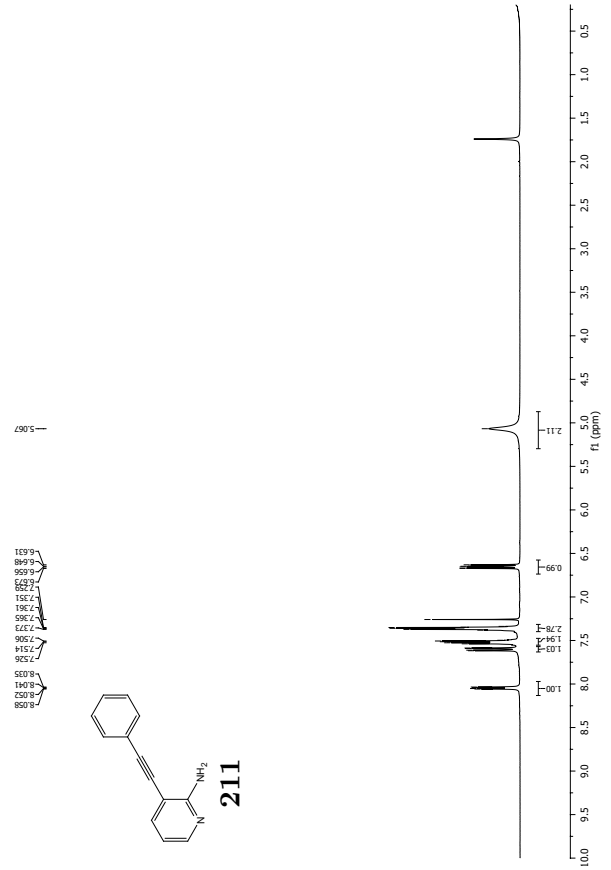

115
f1 (ppm)

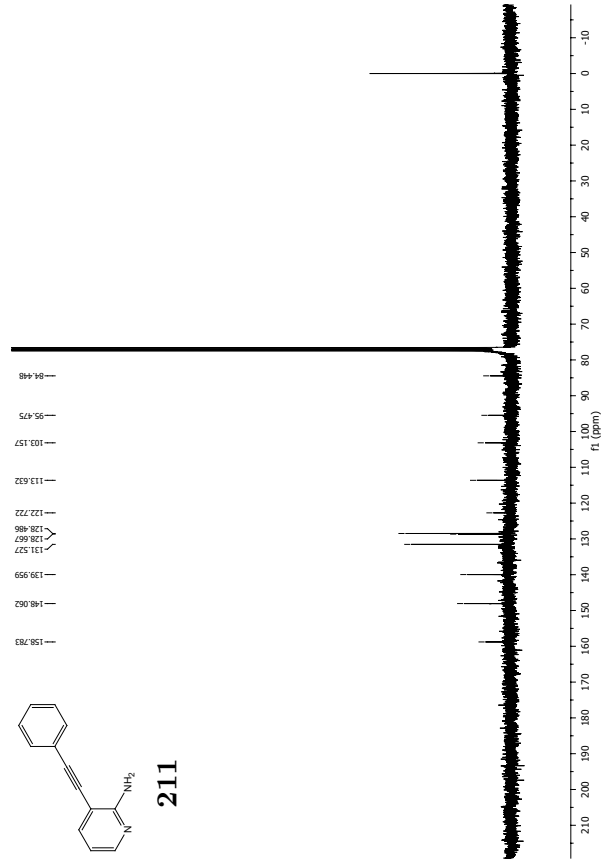

118
f1 (ppm)

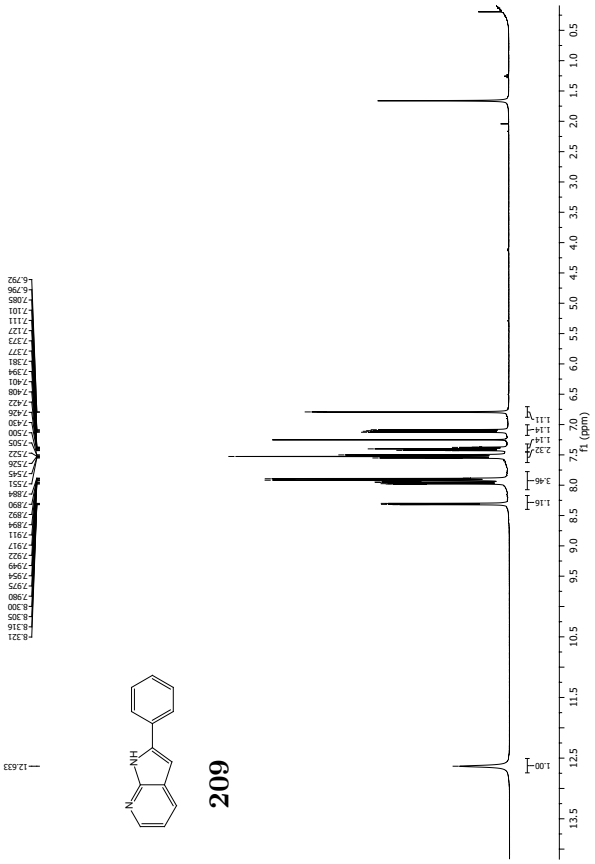

118
f1 (ppm)


121
f1 (ppm)

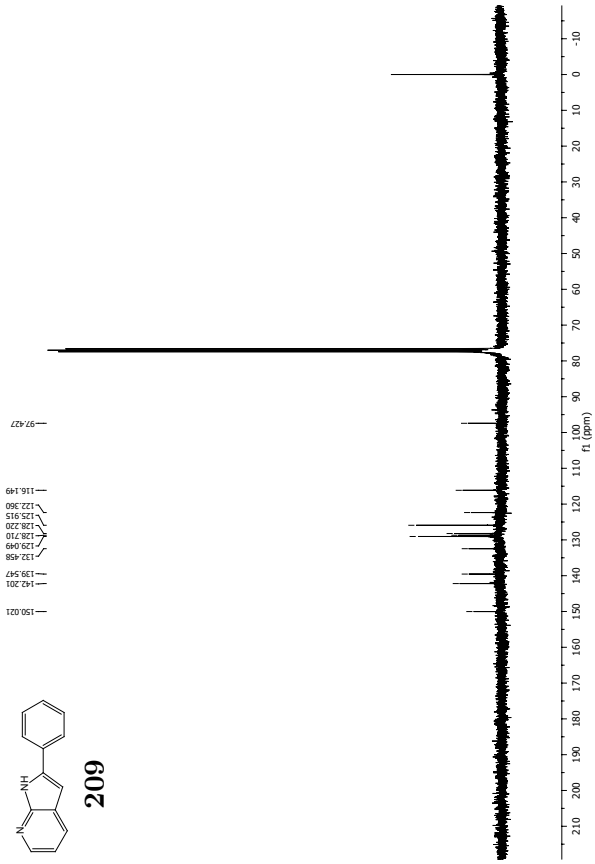

121
f1 (ppm)


211
f1 (ppm)

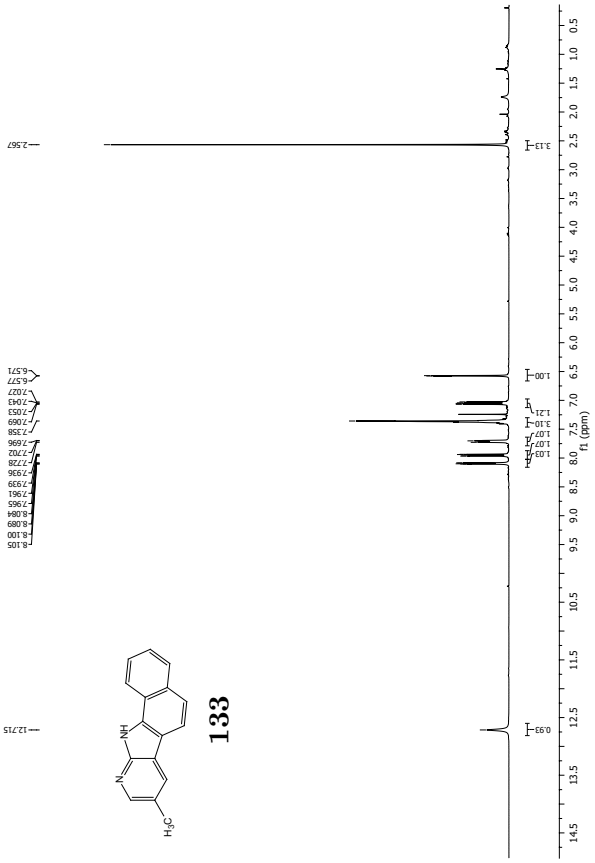

211
f1 (ppm)



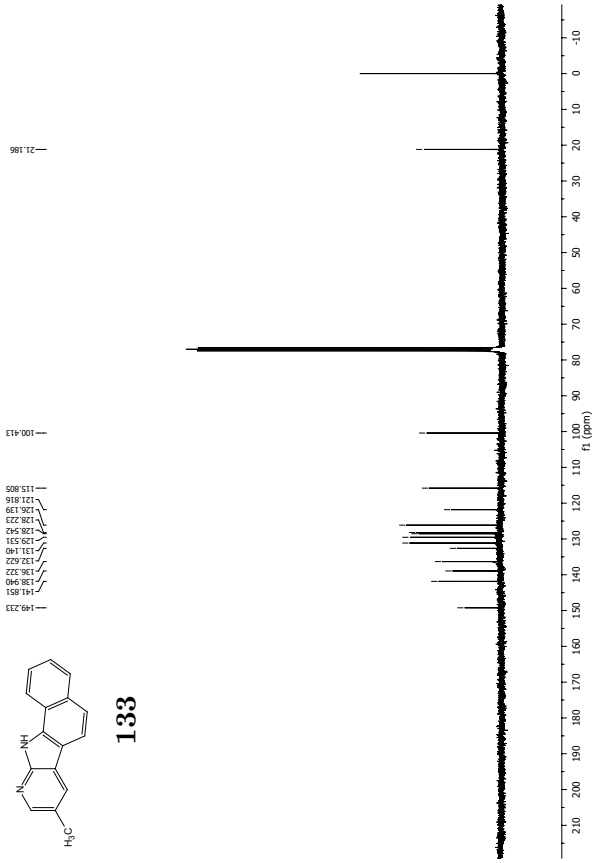
209



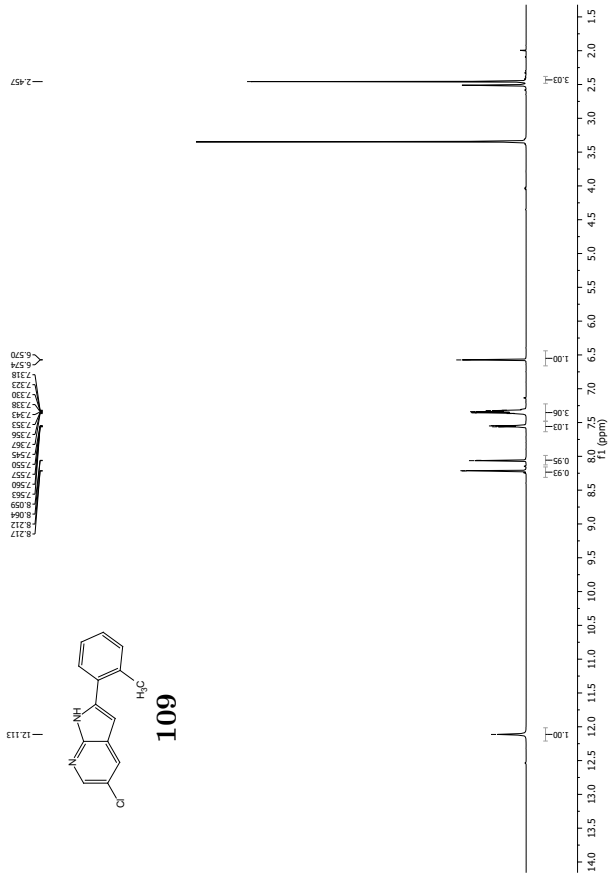
209

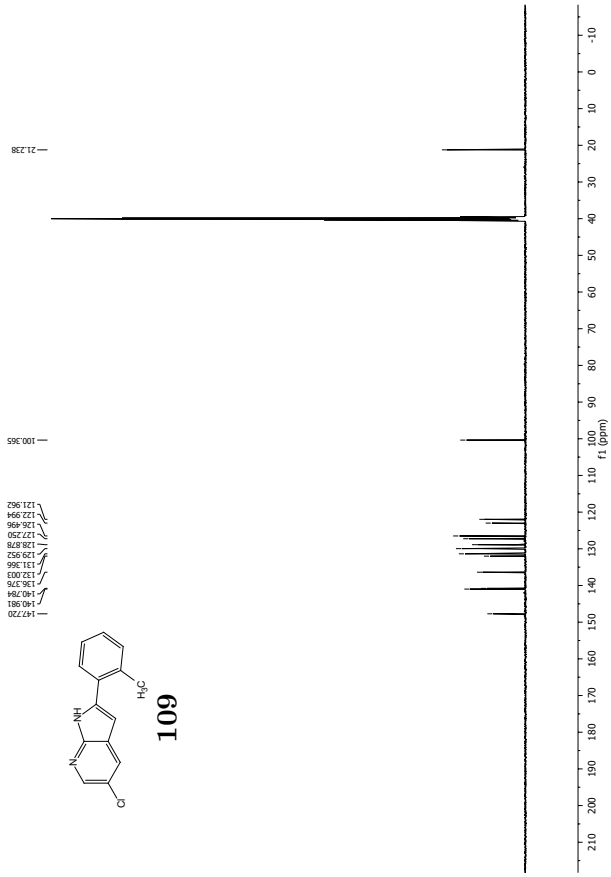


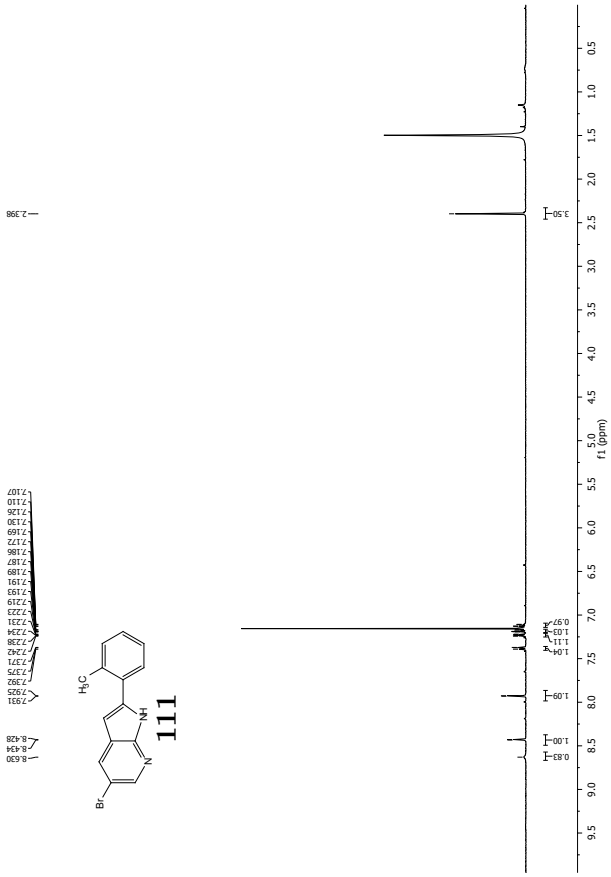
133

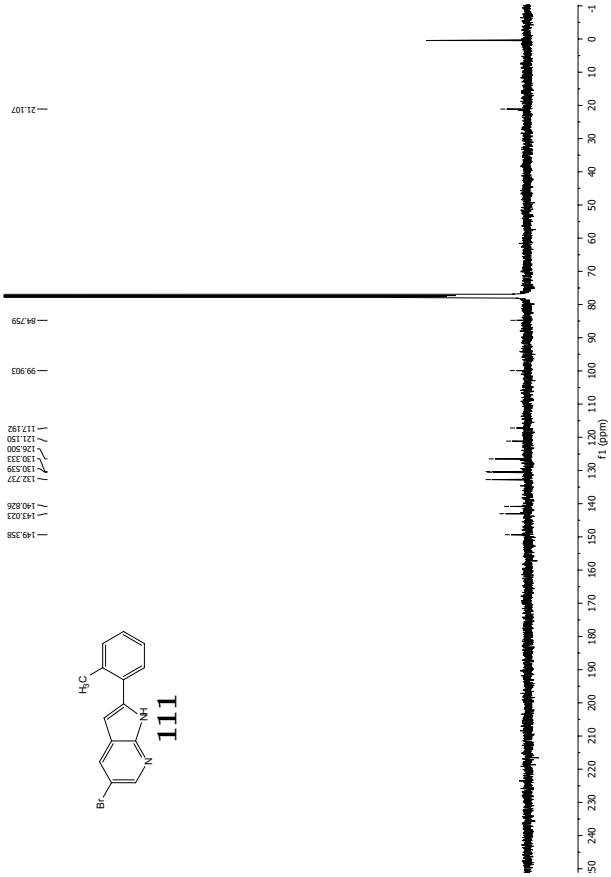


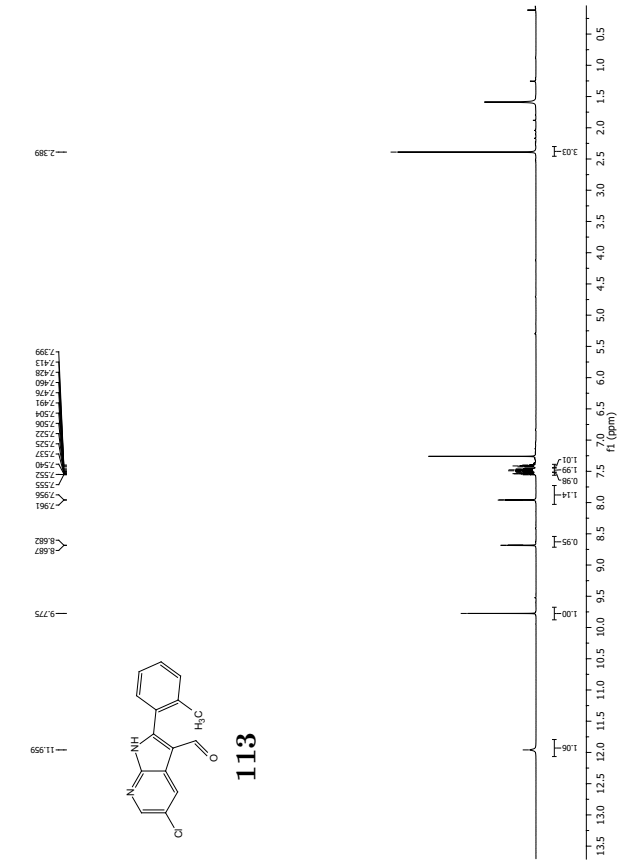
133

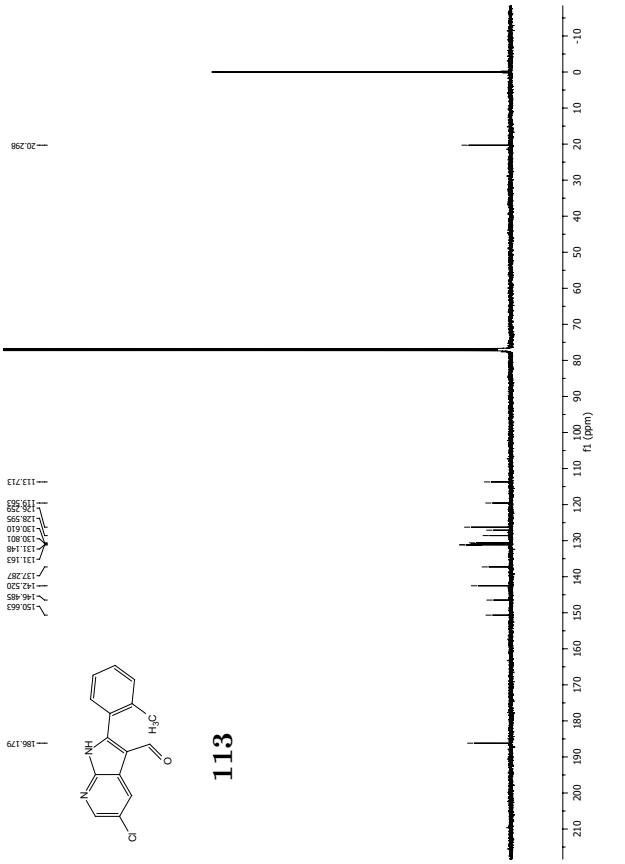

109
f1 (ppm)

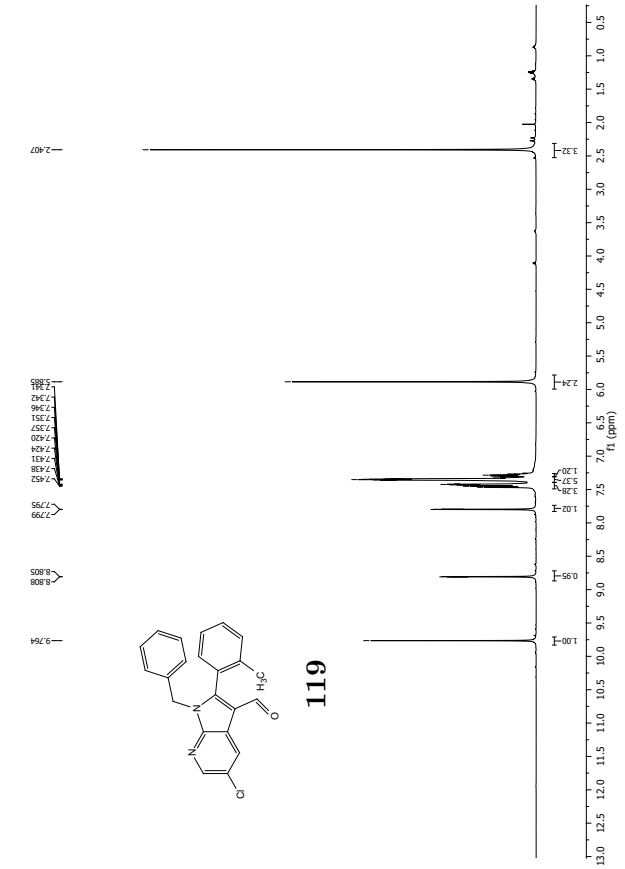

109
f1 (ppm)

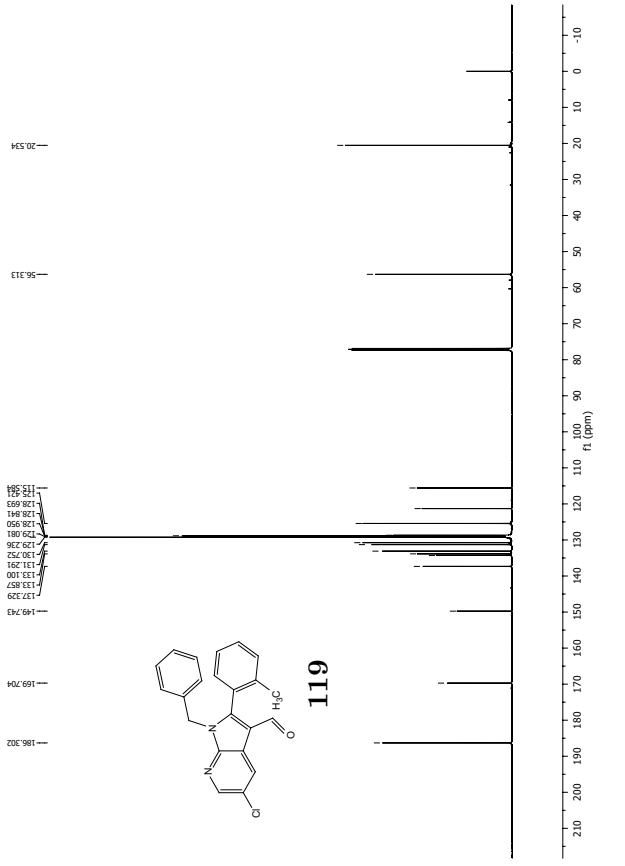

111
f1 (ppm)

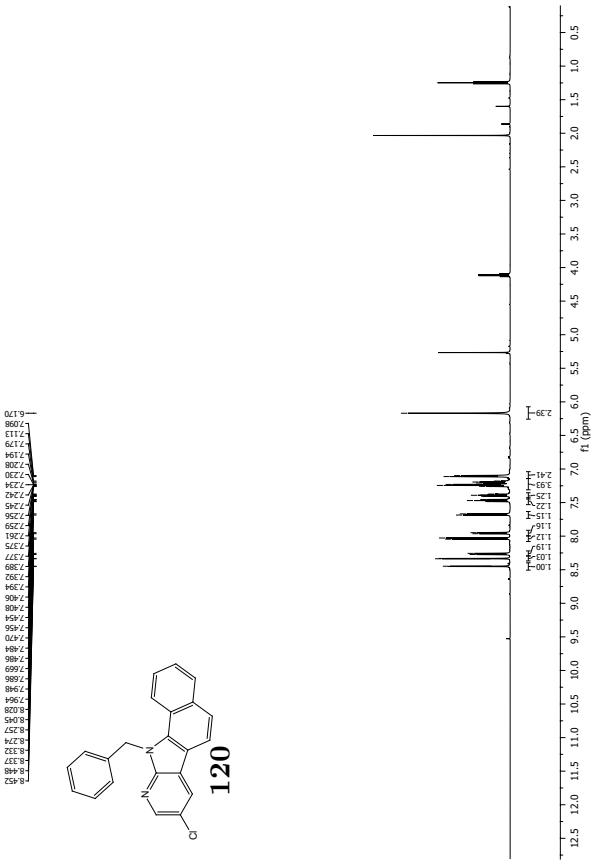

111
f1 (ppm)

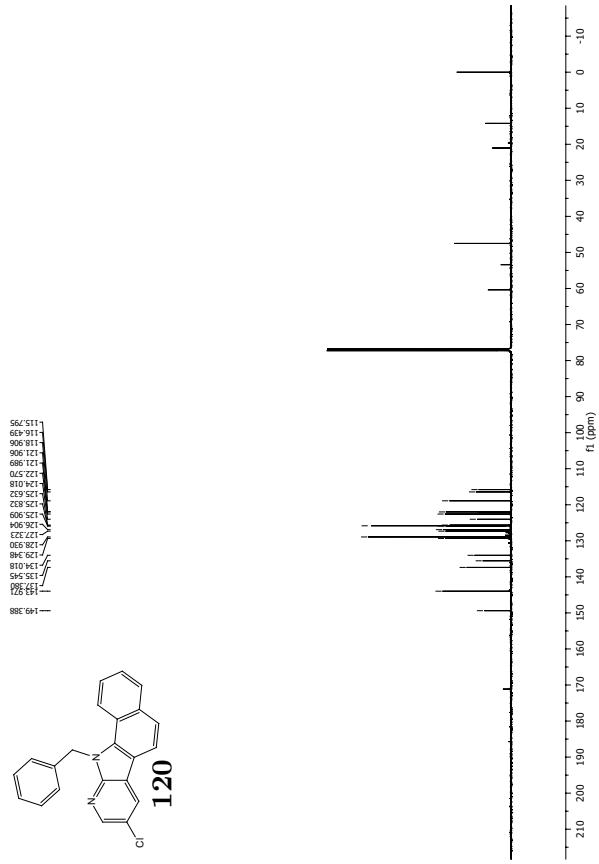

113
f1 (ppm)

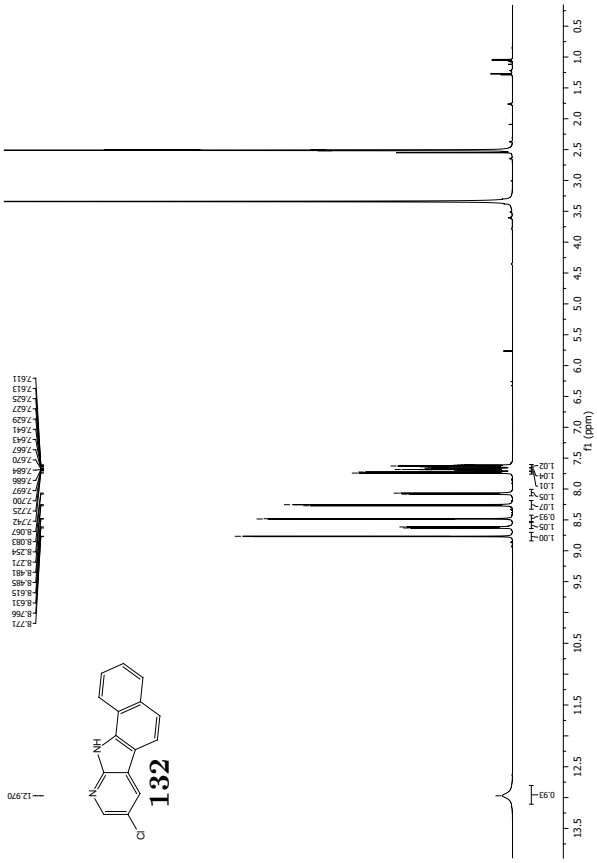

113
f1 (ppm)

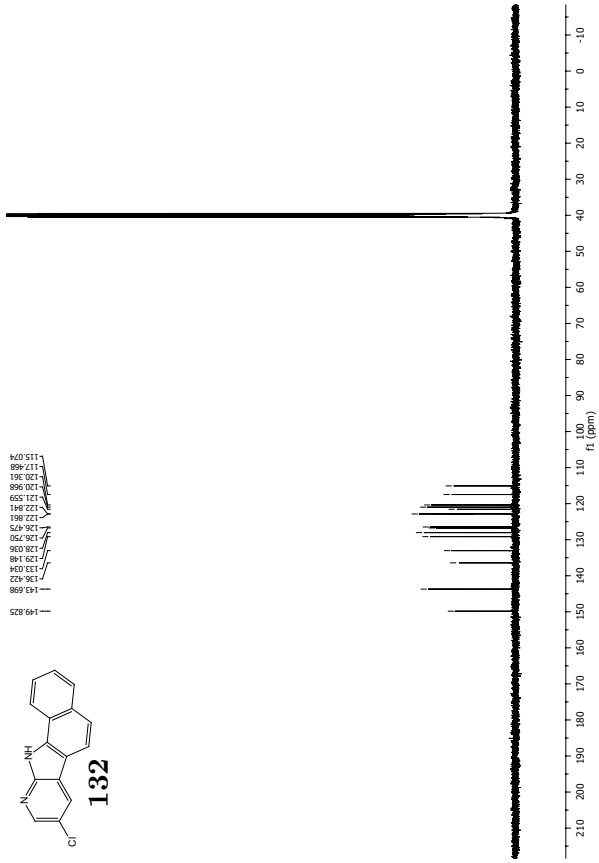

119
f1 (ppm)

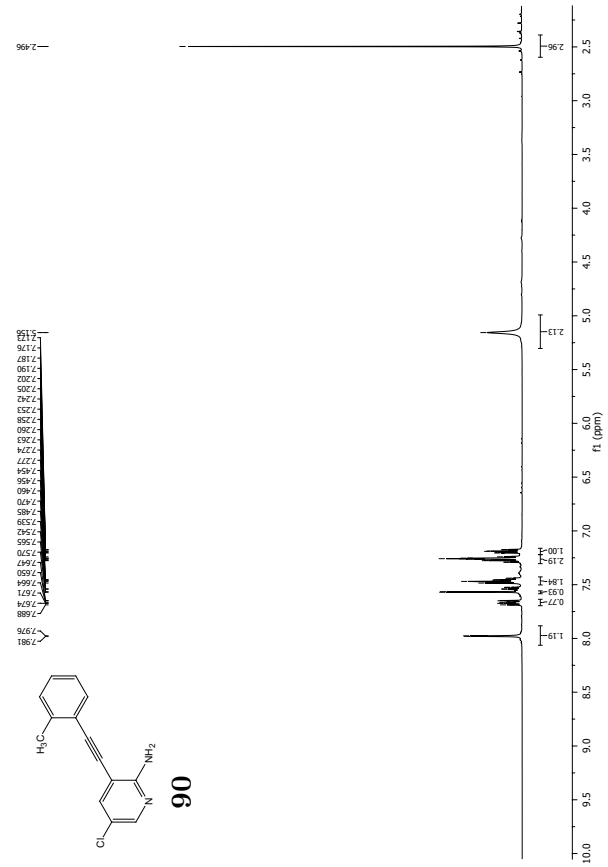

119
f1 (ppm)

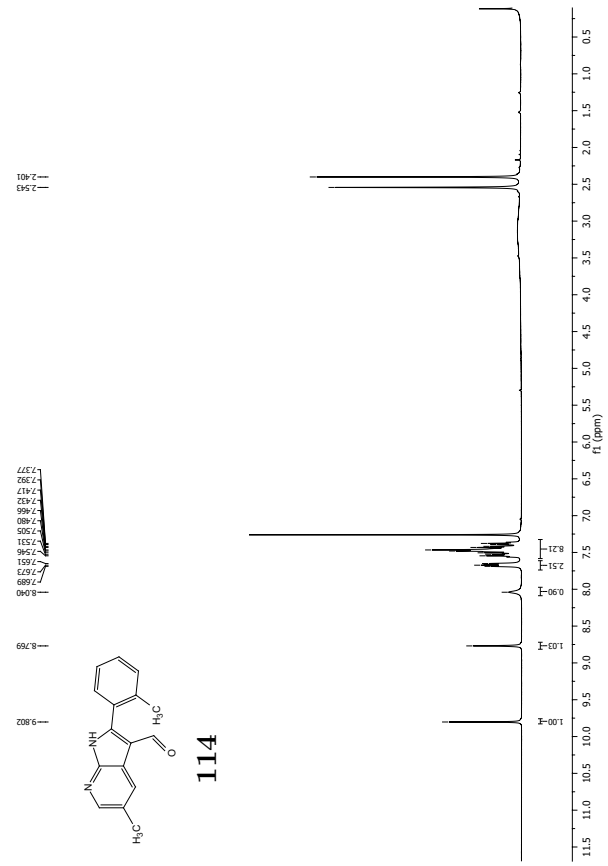

120
f1 (ppm)

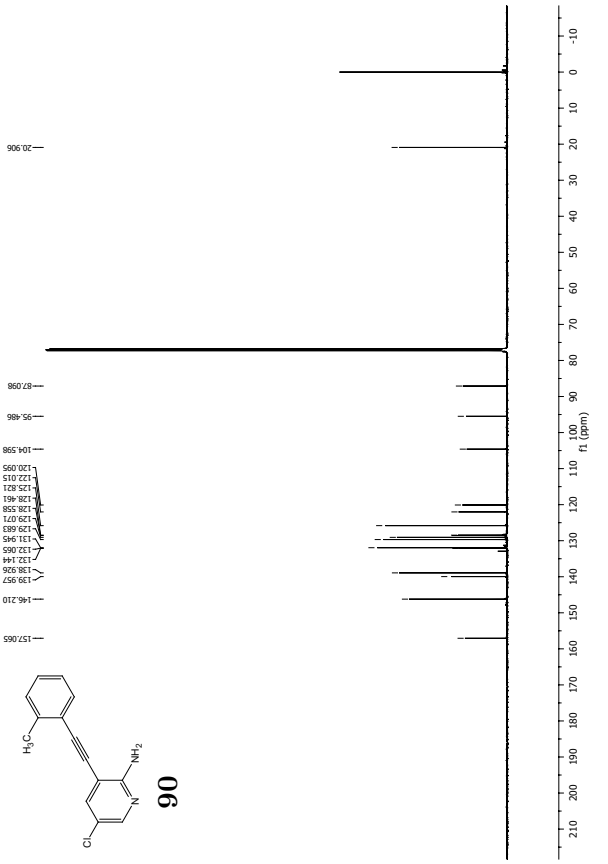

120
f1 (ppm)

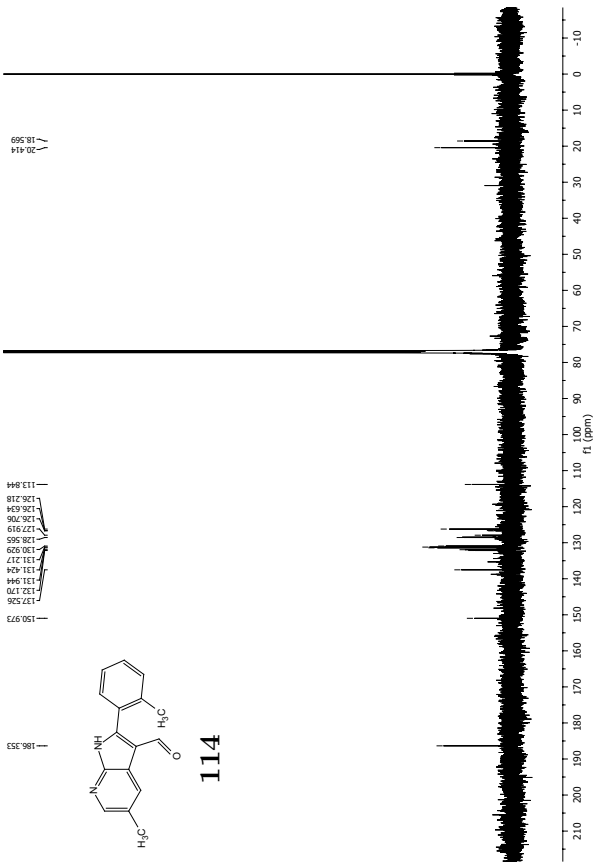

132
f1 (ppm)

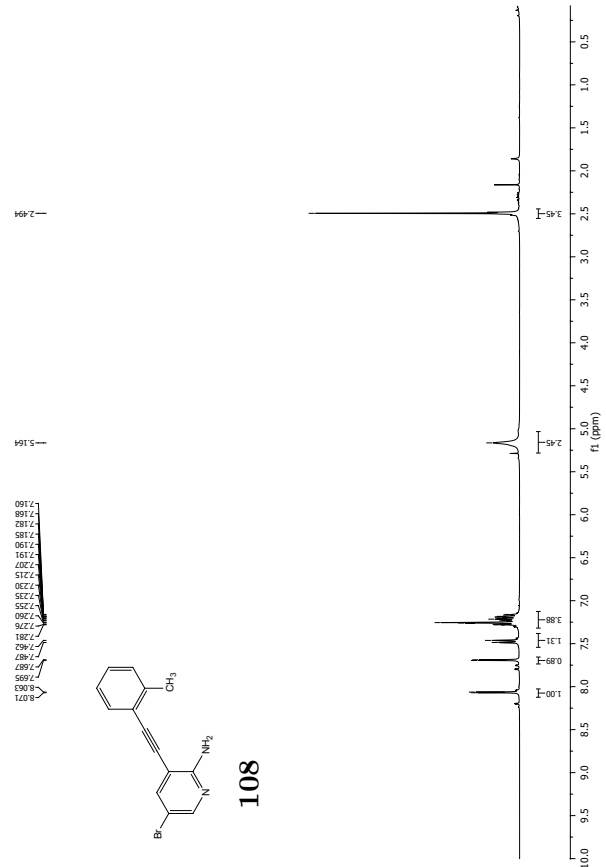

132
f1 (ppm)

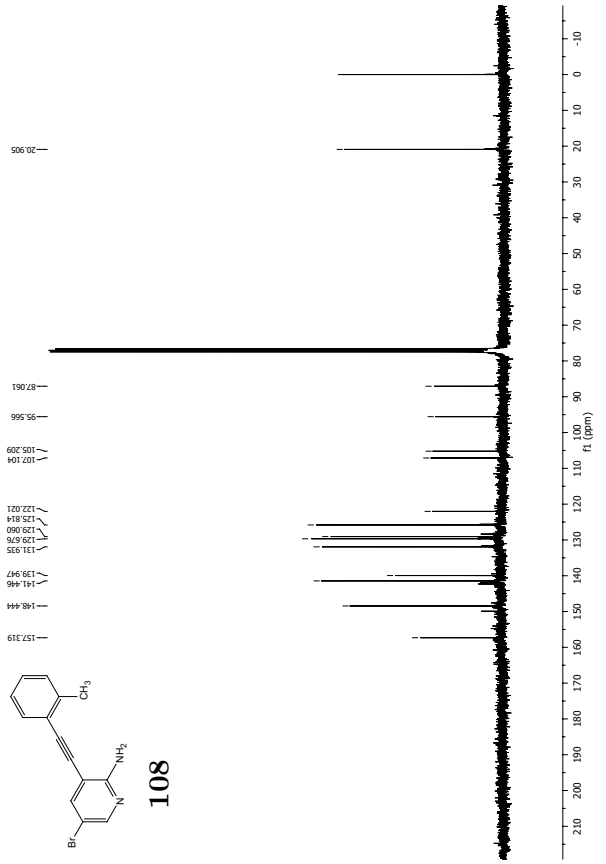

2.496
7.981
7.976
7.688
7.624
7.571
7.564
7.547
7.520
7.650
7.647
7.565
7.542
7.539
7.485
7.470
7.460
7.456
7.454
7.277
7.263
7.260
7.258
7.242
7.205
7.202
7.190
7.187
7.176
7.173
5.158
2.96
2.13
2.19
1.00
1.84
0.93
0.77
1.19
f1 (ppm)
90

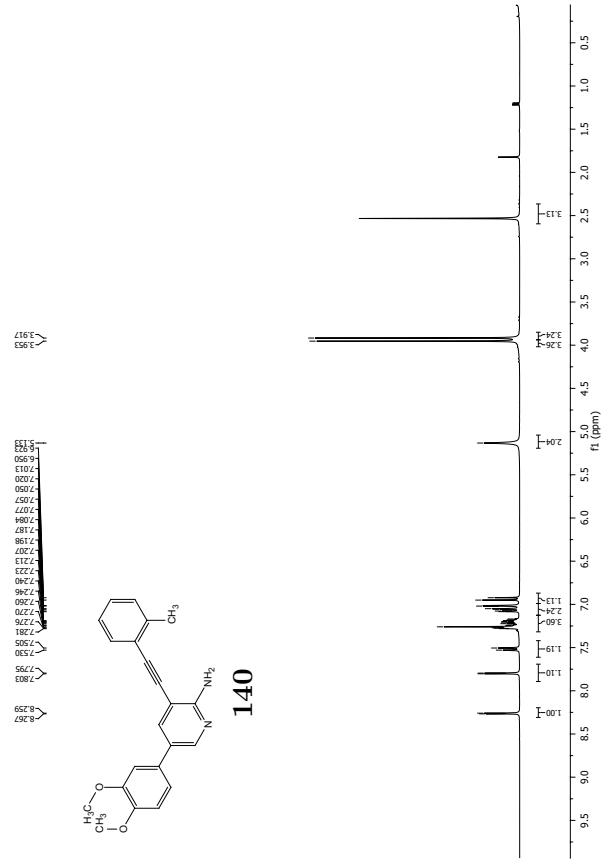

9.802
8.769
8.040
7.689
7.673
7.651
7.596
7.531
7.505
7.480
7.466
7.422
7.417
7.392
7.377
2.543
2.401
1.00
1.03
0.90
2.51
8.21
f1 (ppm)
114

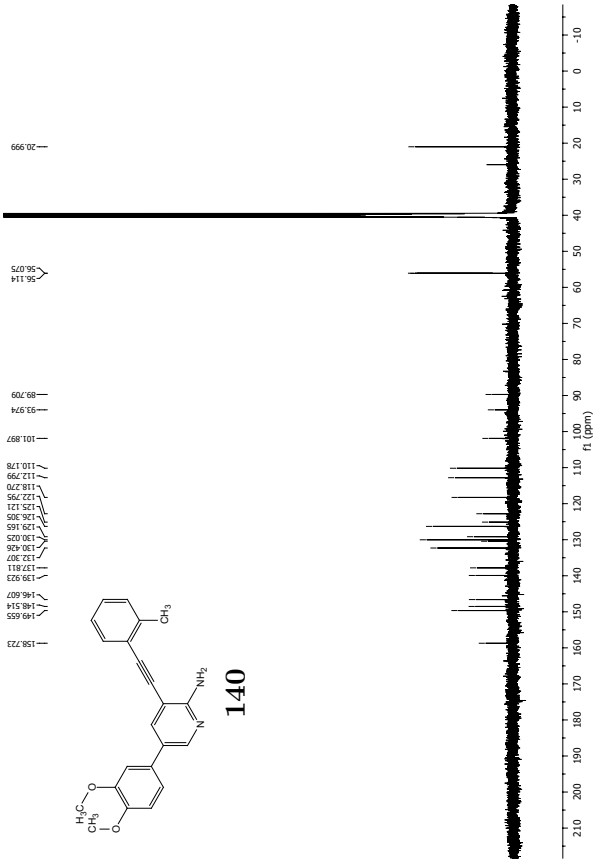

157.065
146.210
139.957
138.926
132.144
132.065
131.945
129.683
129.071
128.558
128.461
125.821
123.015
120.095
104.598
95.486
87.098
20.906
f1 (ppm)
90

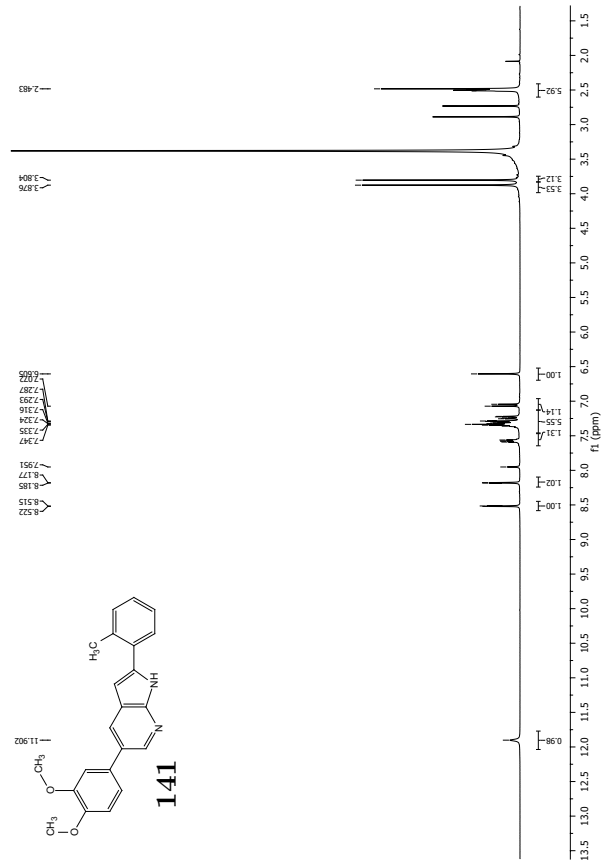

186.353
150.973
137.526
132.170
131.944
131.424
130.929
128.565
127.919
126.786
126.634
126.218
113.844
20.414
18.569
f1 (ppm)
114

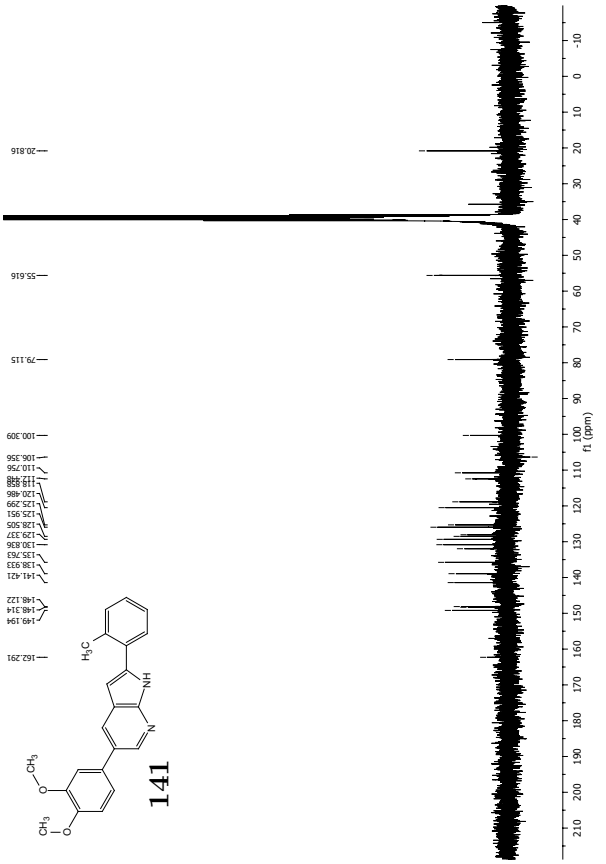

108
f1 (ppm)

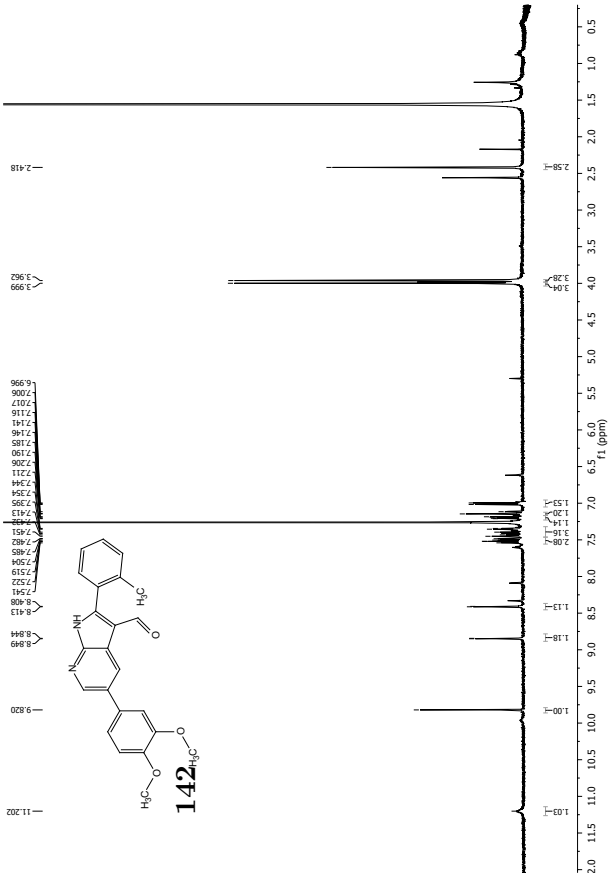

108
f1 (ppm)

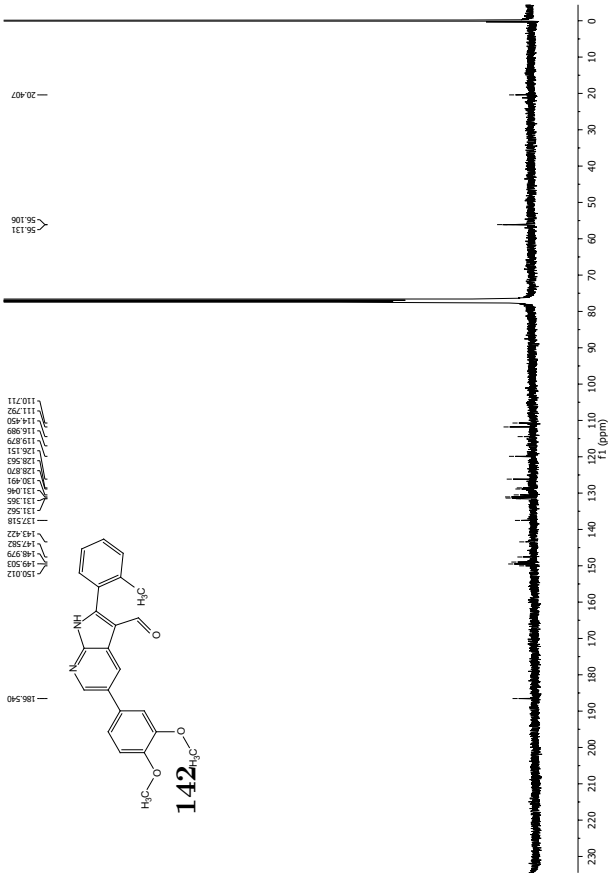

140
f1 (ppm)

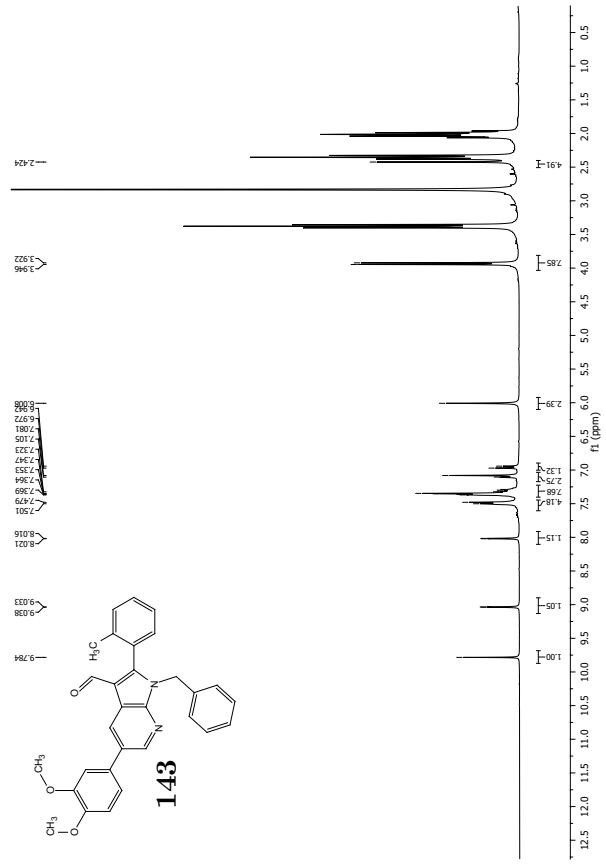

140
f1 (ppm)

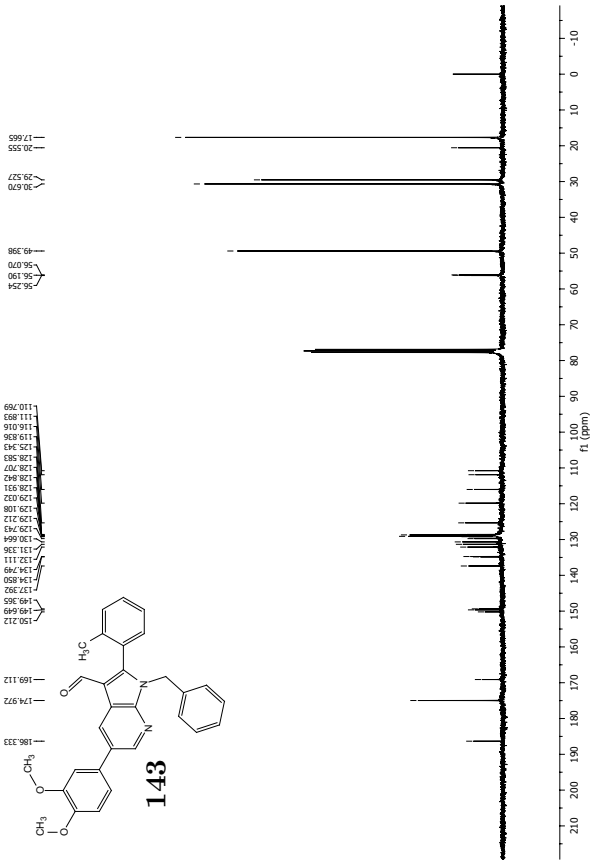

141
f1 (ppm)

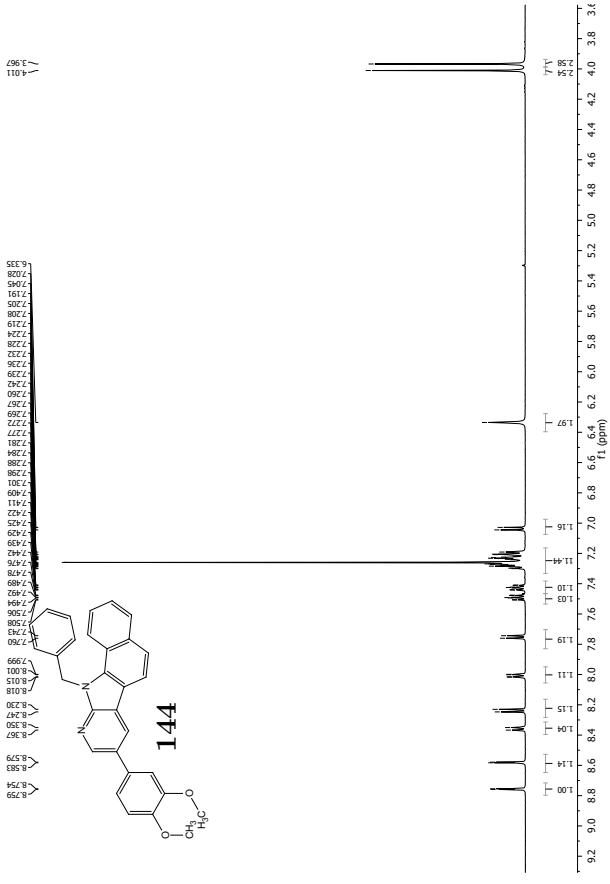

141
f1 (ppm)

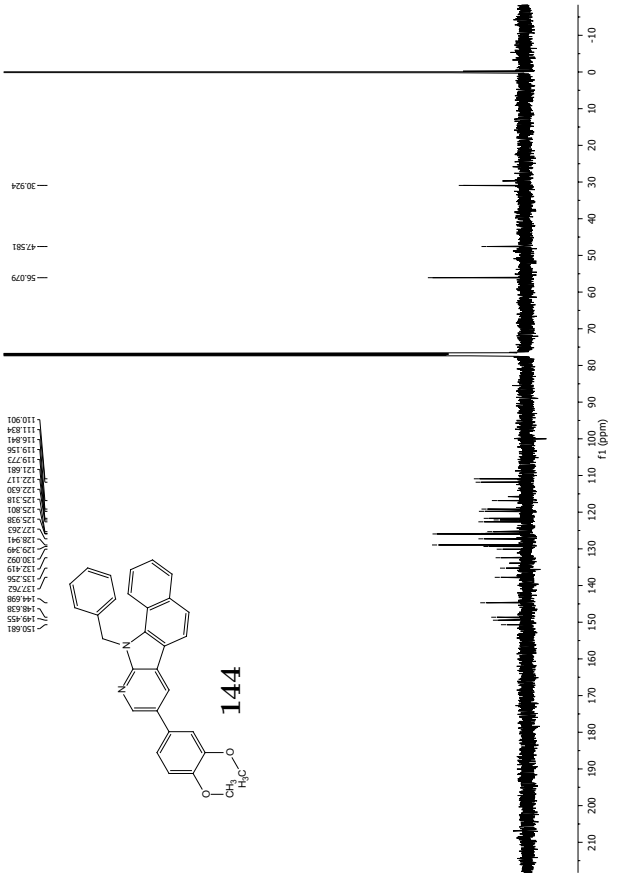

142
f1 (ppm)

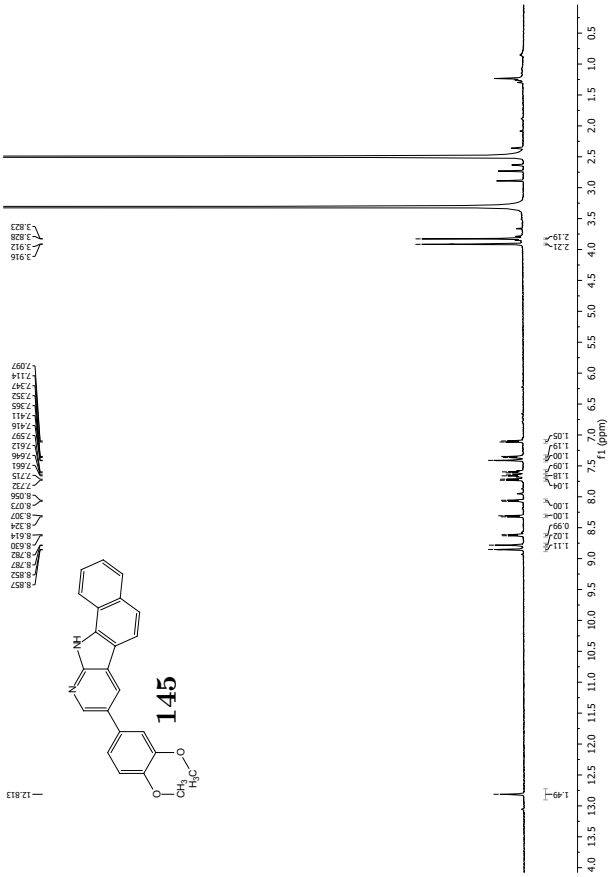

142
f1 (ppm)

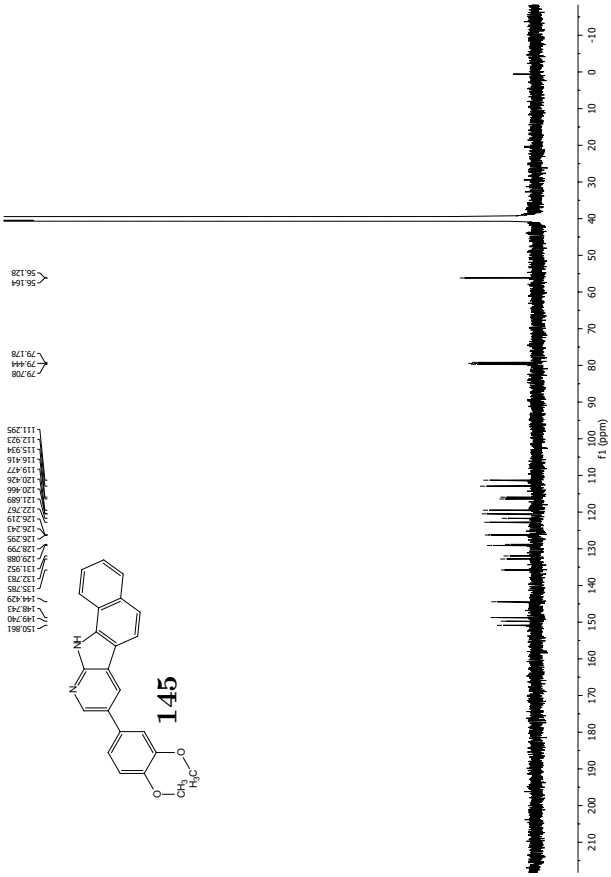

143
f1 (ppm)

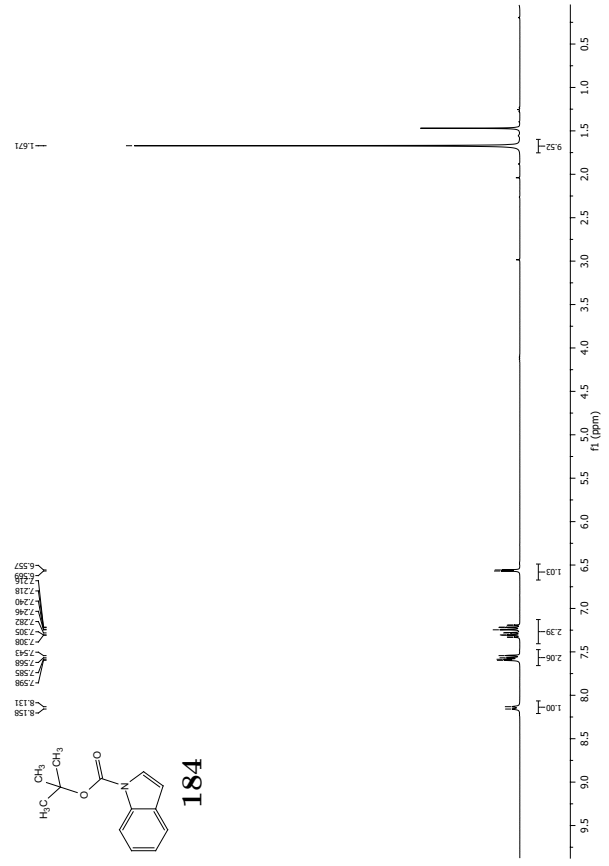

143
f1 (ppm)

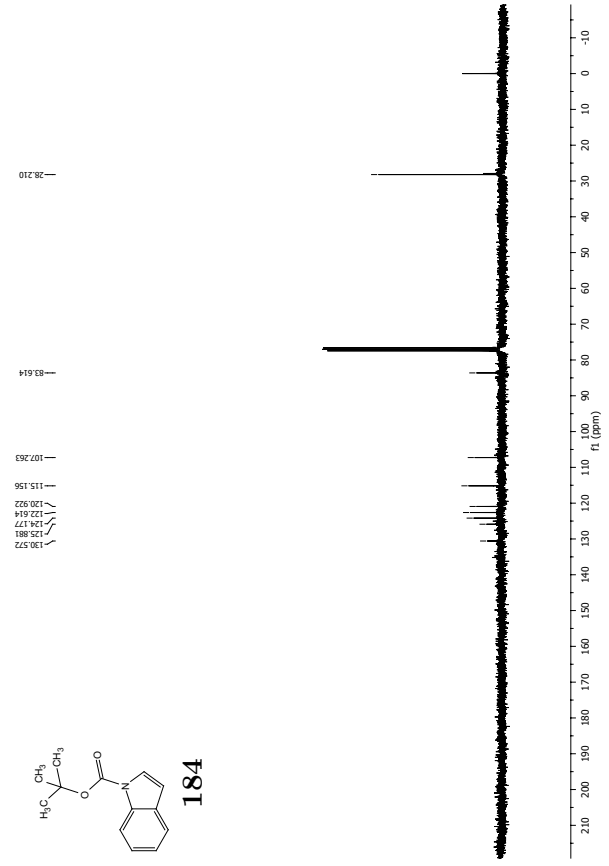

144
f1 (ppm)

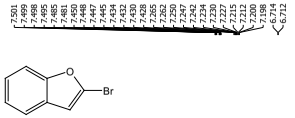

144
f1 (ppm)


145
f1 (ppm)

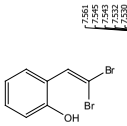

145
f1 (ppm)


184
f1 (ppm)

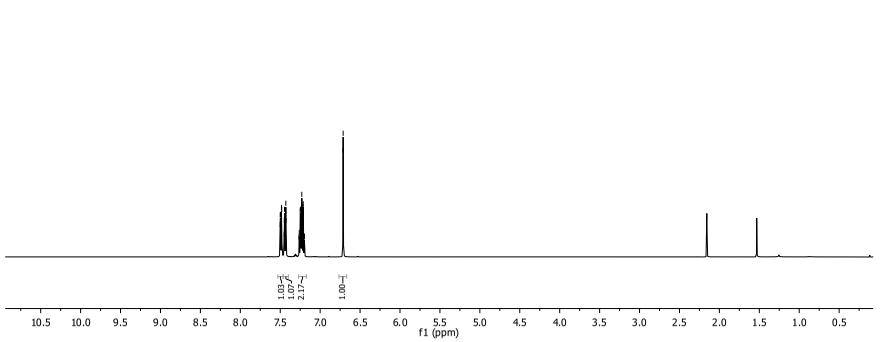

184
f1 (ppm)

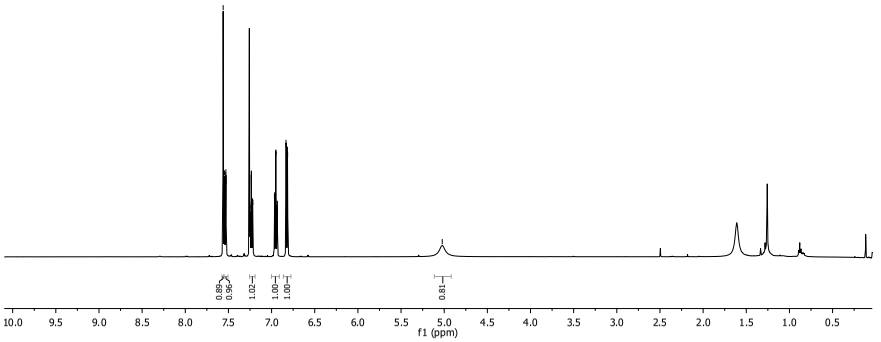


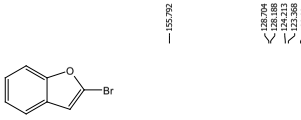
186



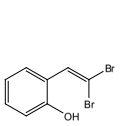
210



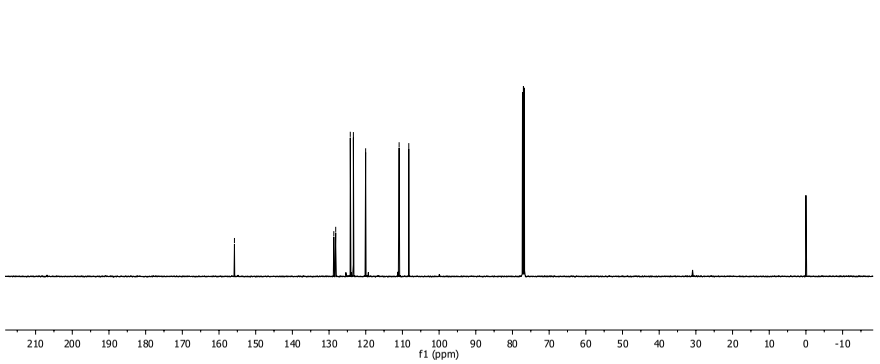


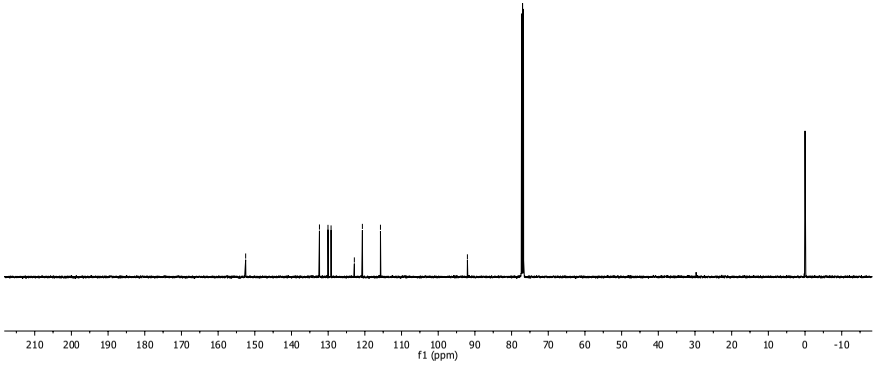


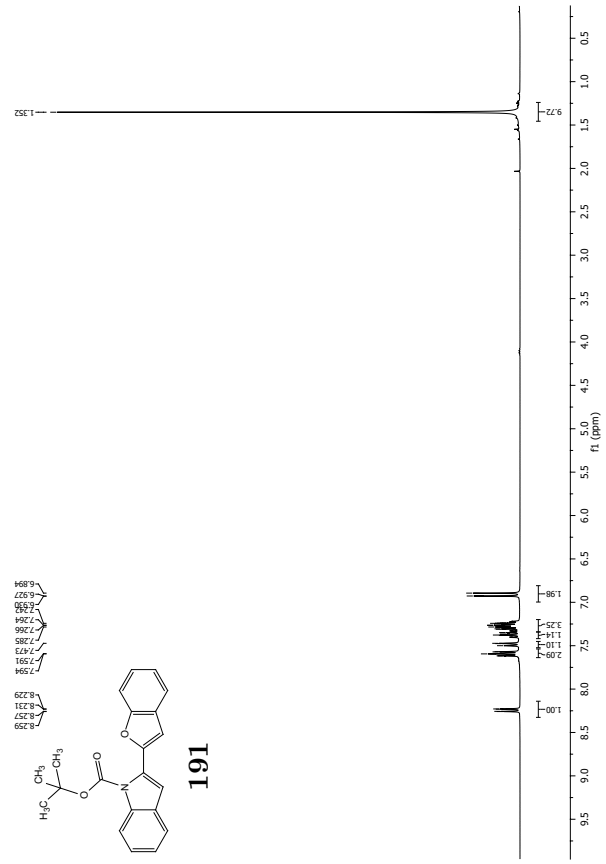
186

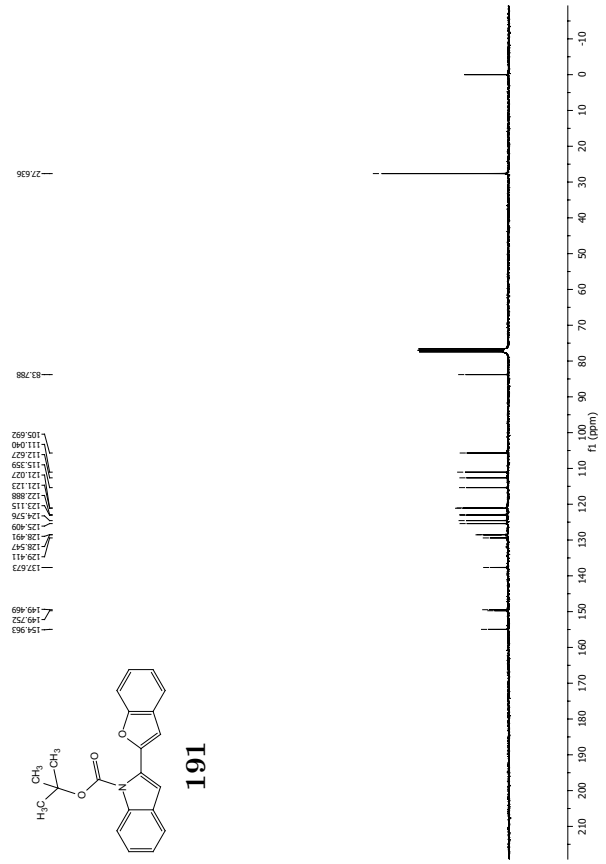


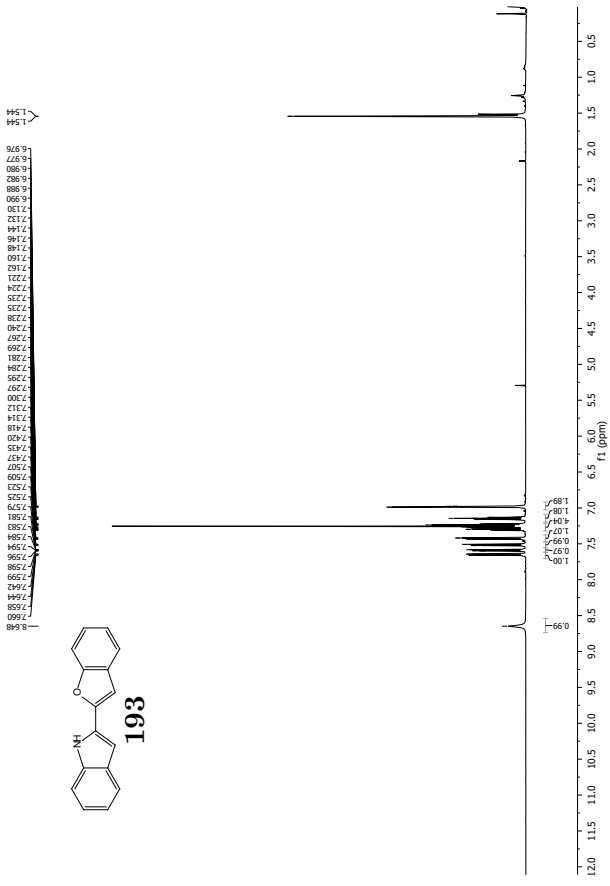
210

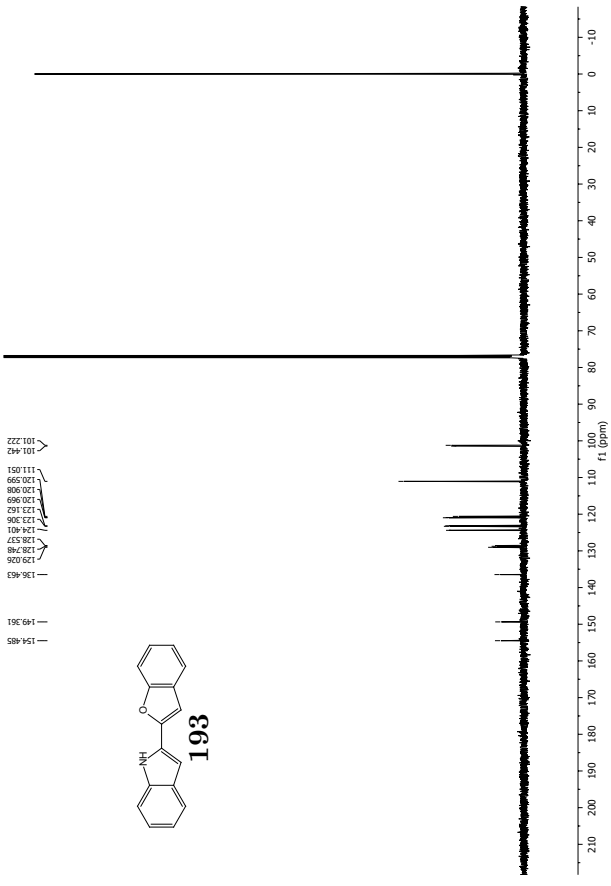


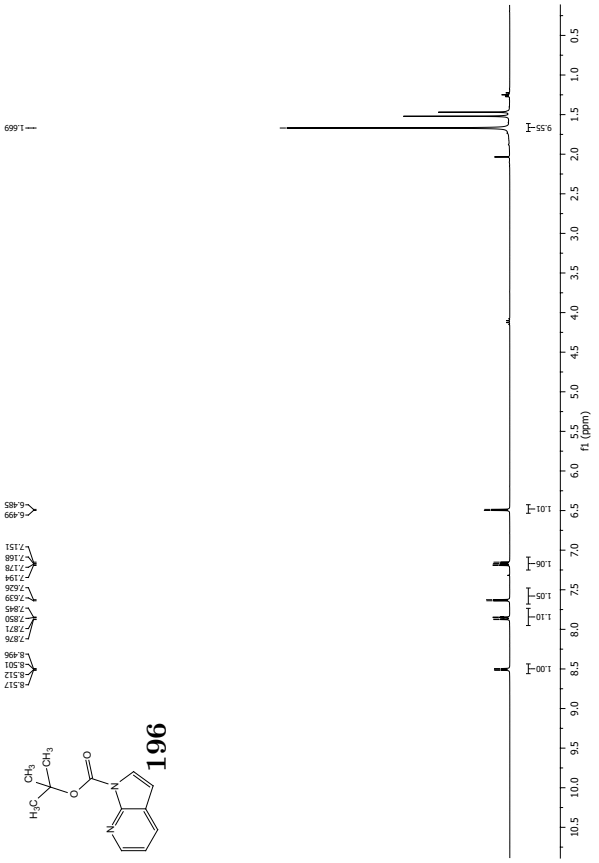



191

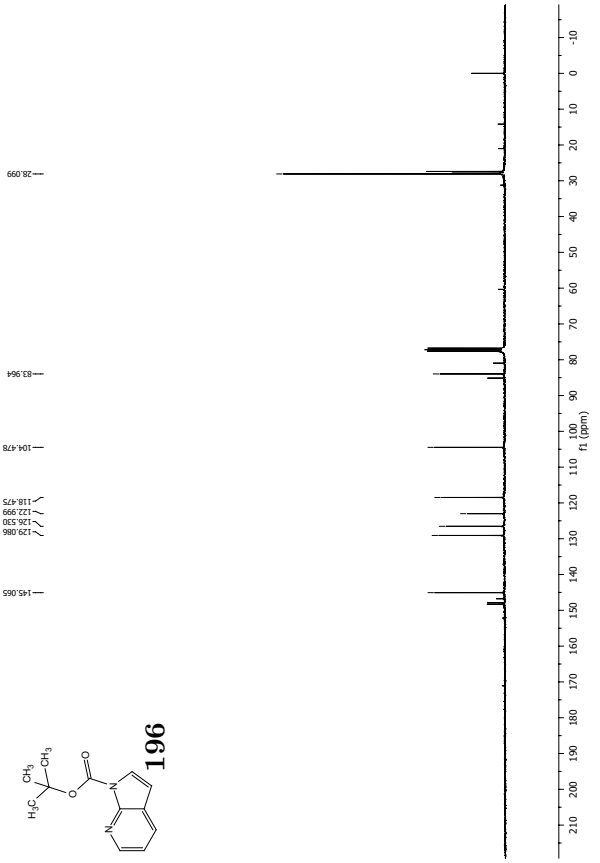

191


193

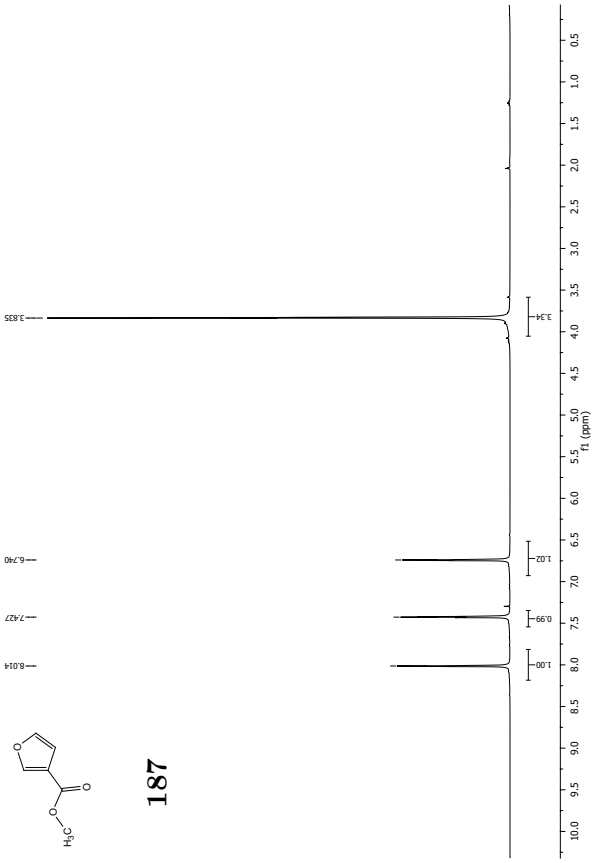

193



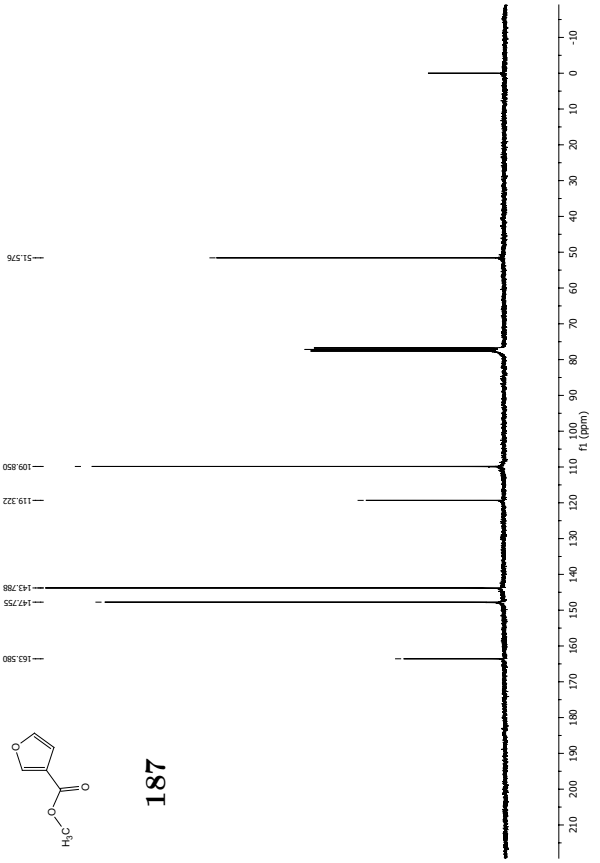
196



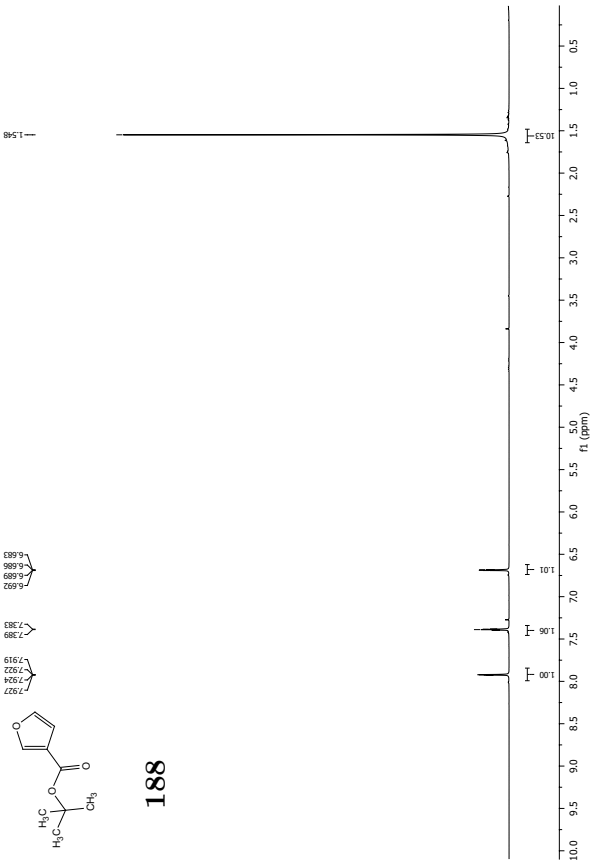
196

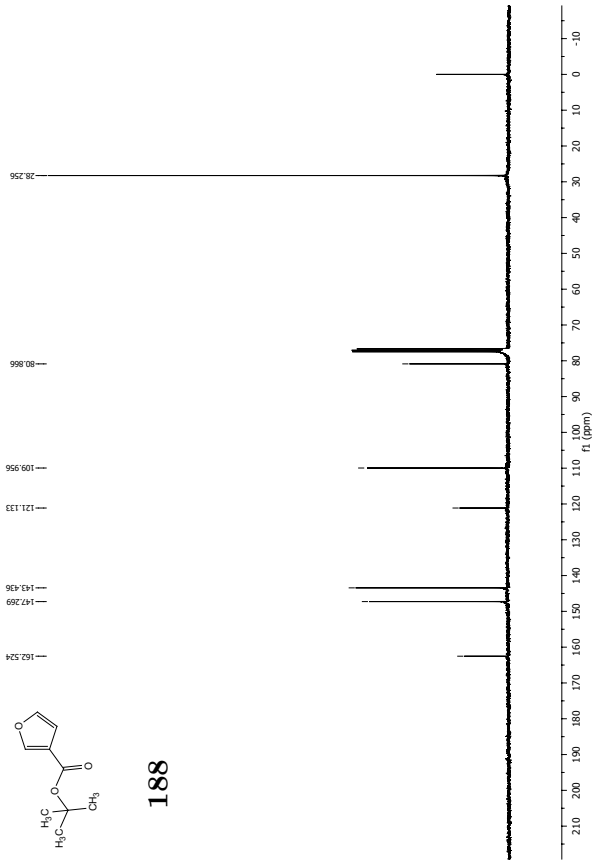


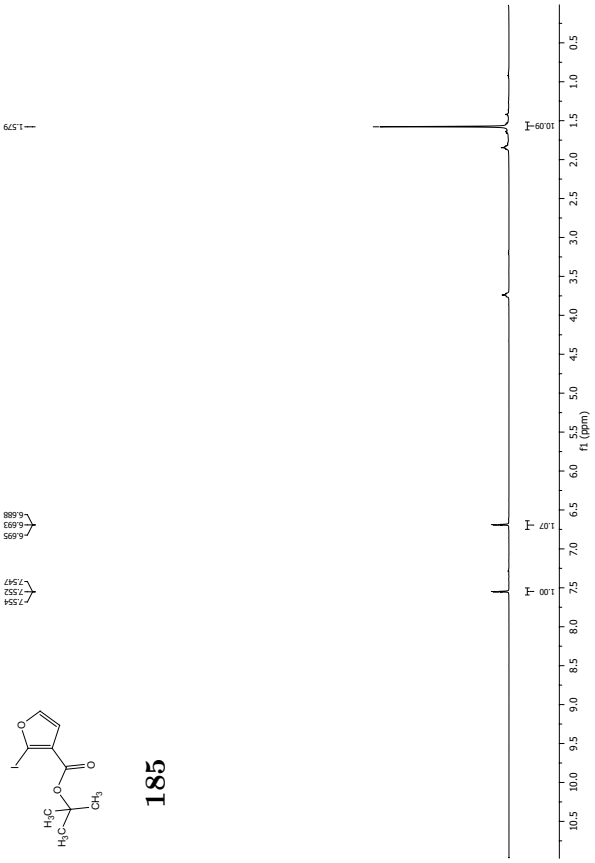
187

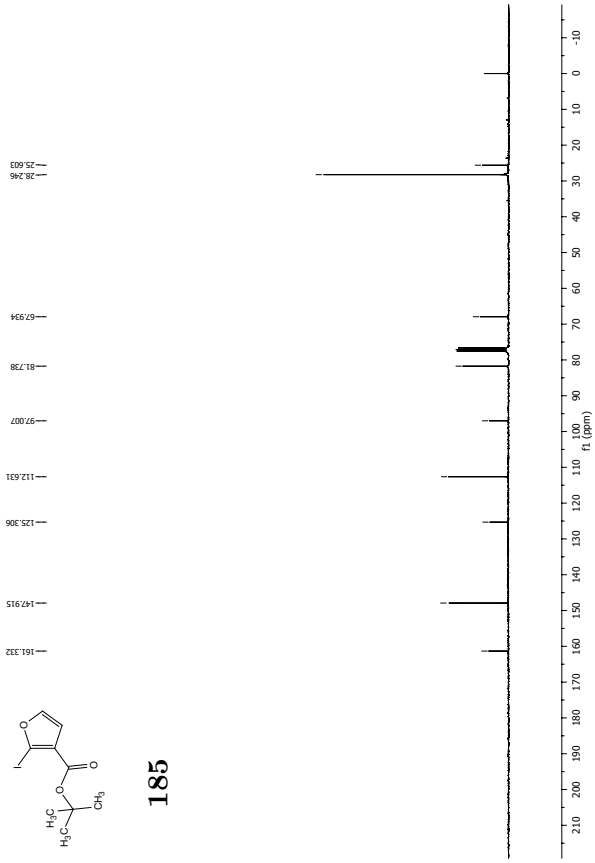


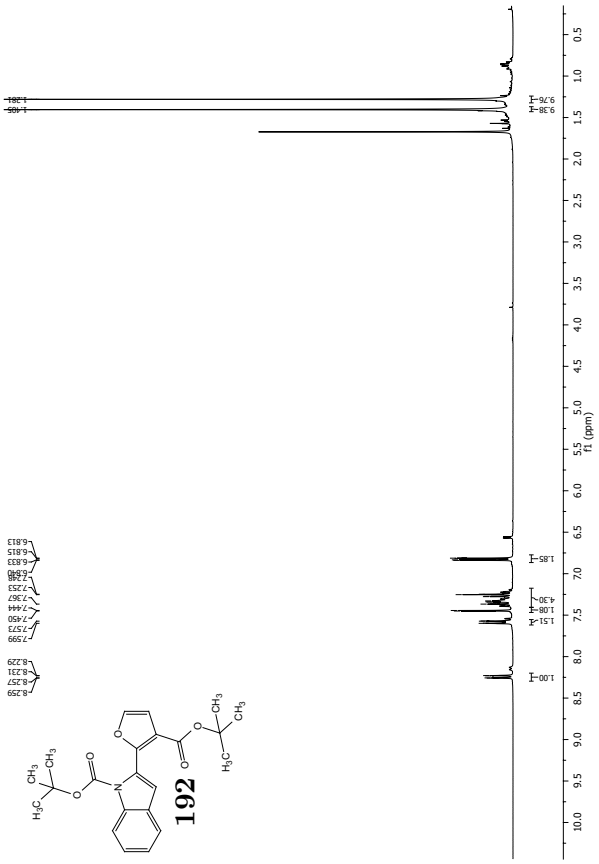
187

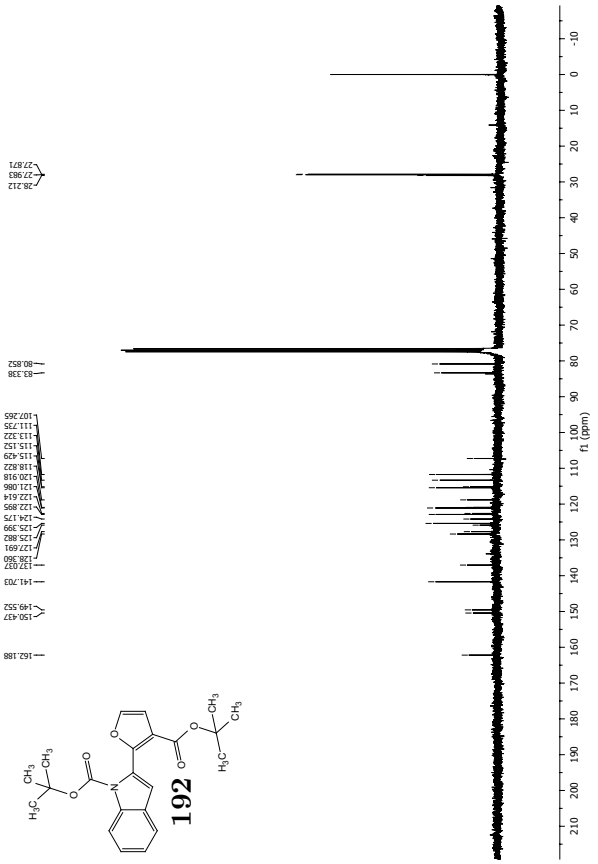

1.548
7.383
7.389
6.683
6.686
6.689
6.692
7.907
7.919
7.922
7.924
10.53
1.01
1.06
1.00
f1 (ppm)
188

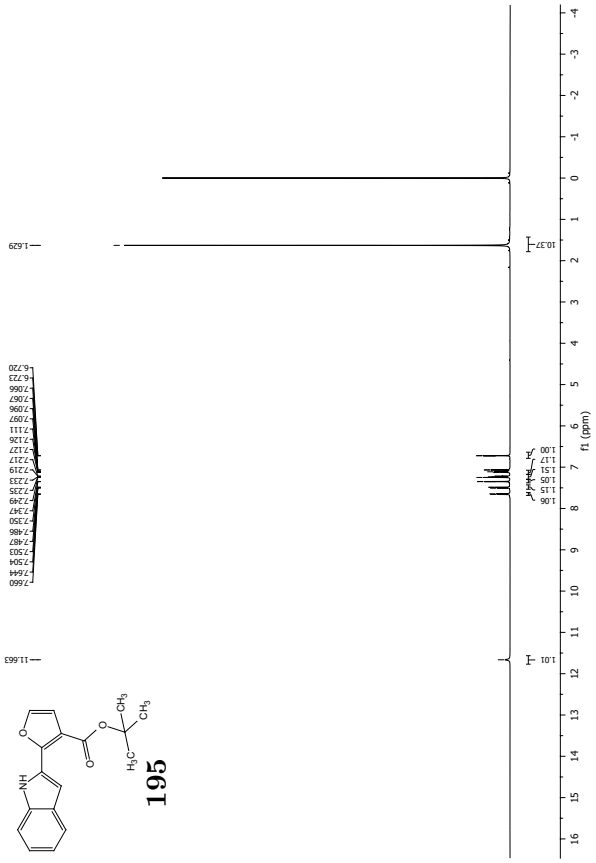

28.256
80.866
109.956
121.133
143.436
147.269
162.524
f1 (ppm)
188

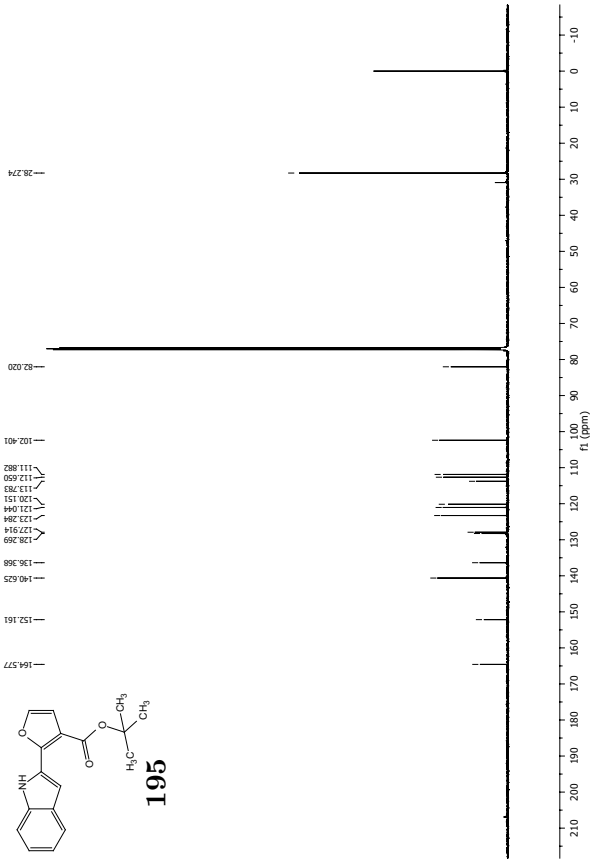

1.579
6.688
6.693
6.695
7.547
7.552
7.554
10.09
1.07
1.00
f1 (ppm)
185

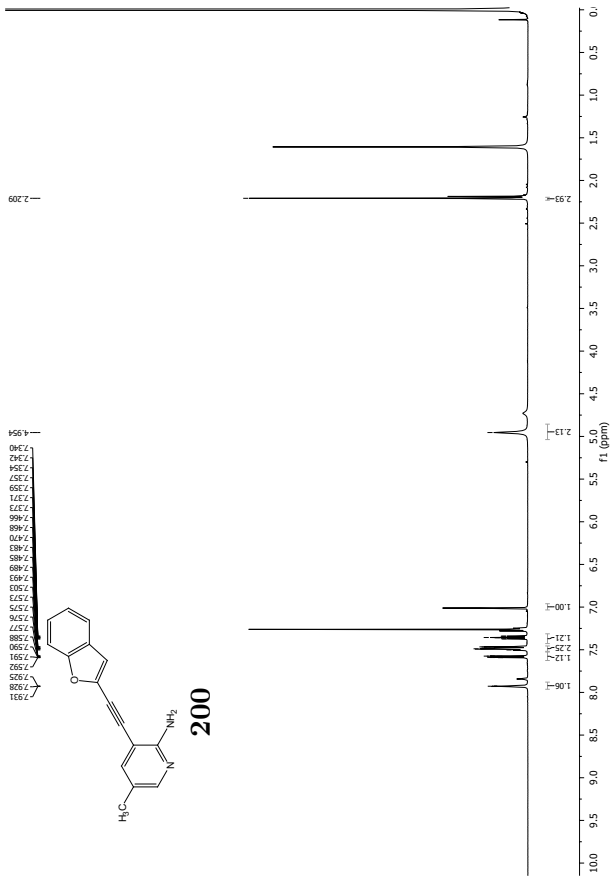

25.603
28.246
67.934
81.738
97.007
112.631
125.306
142.915
161.332
f1 (ppm)
185

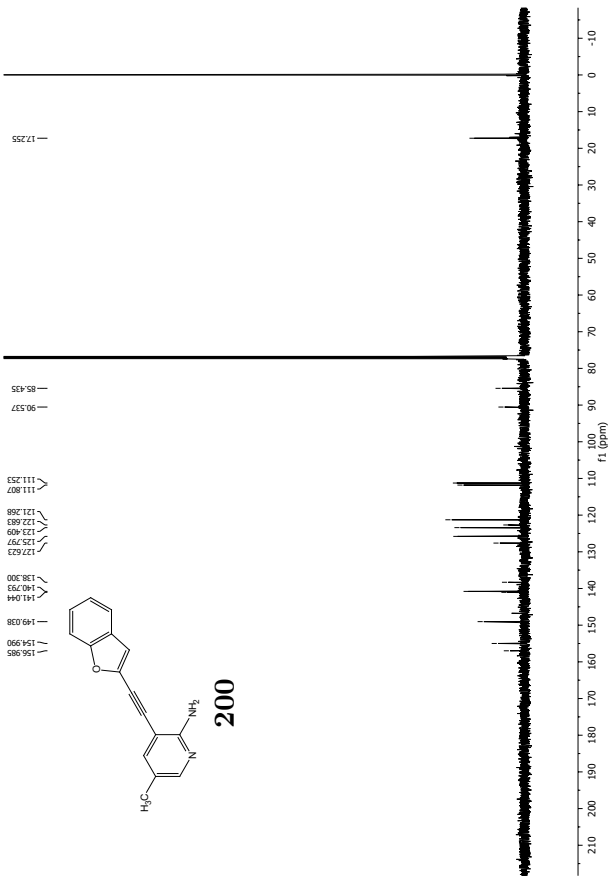

192

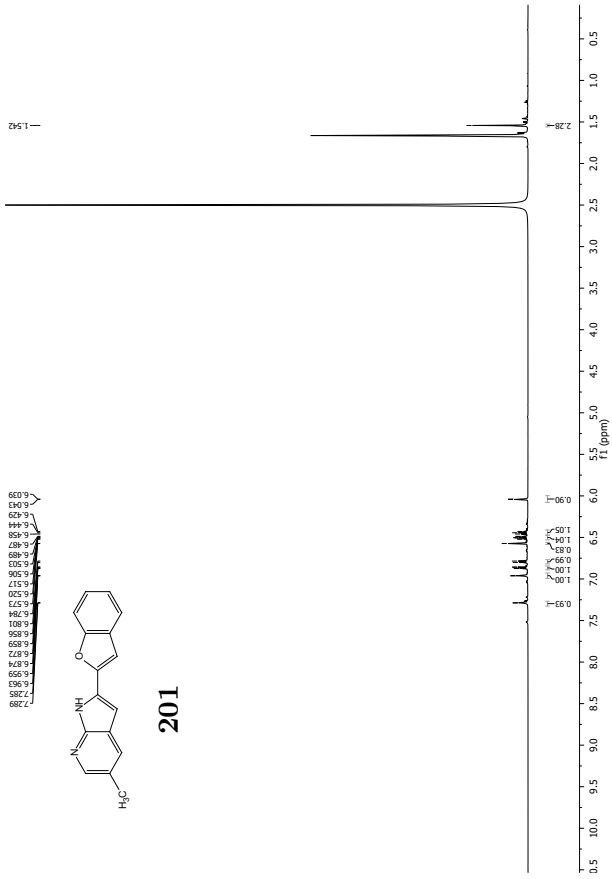

192

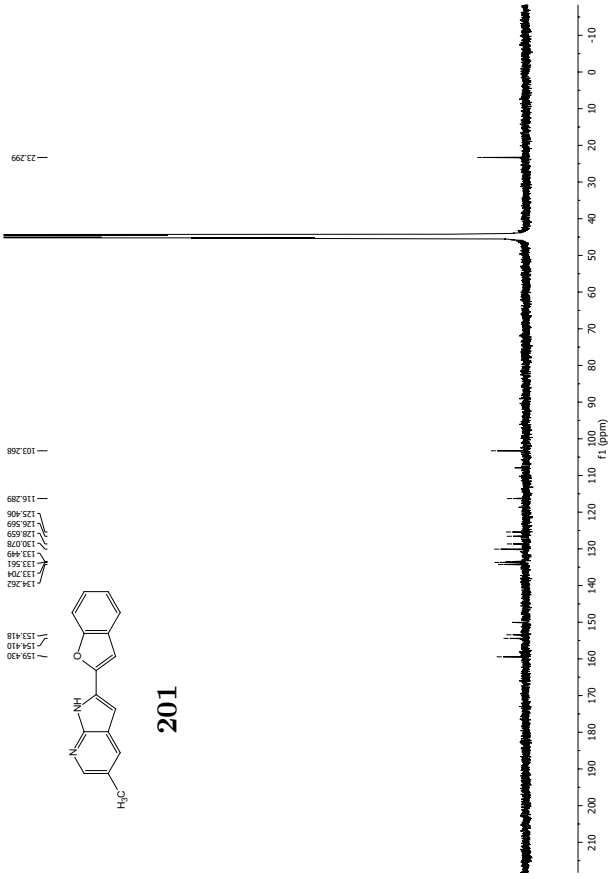

195

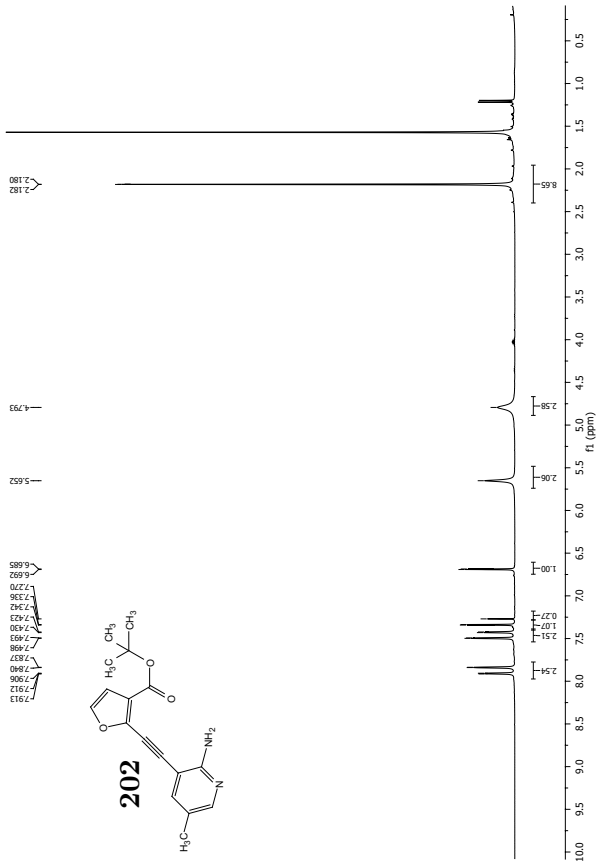

195

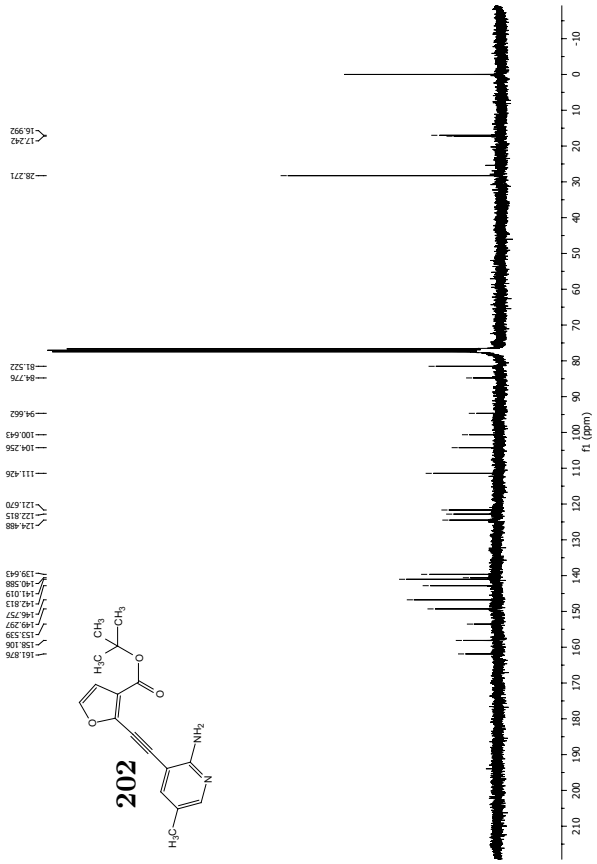

200
f1 (ppm)


200
f1 (ppm)


201
f1 (ppm)

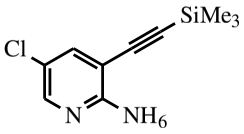
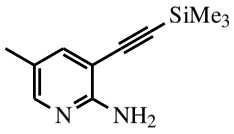
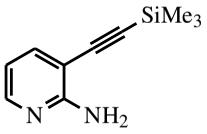
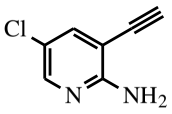
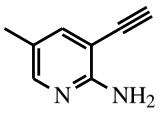
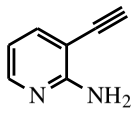

201
f1 (ppm)


2.182
4.793
5.652
6.685
6.682
7.270
7.336
7.342
7.423
7.430
7.493
7.498
7.837
7.840
7.906
7.912
7.913
8.65
2.58
2.06
1.00
1.07
0.27
2.51
2.54
f1 (ppm)
202


16.992
17.242
28.271
81.522
84.776
94.662
100.643
104.256
111.426
121.670
122.815
124.488
139.643
140.588
141.019
142.813
146.757
149.297
153.539
158.106
161.876
f1 (ppm)
202

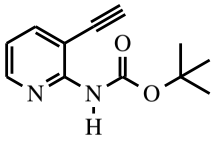
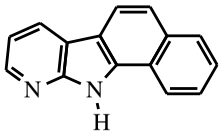
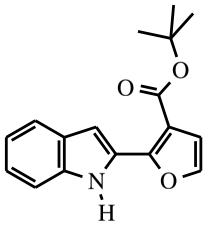
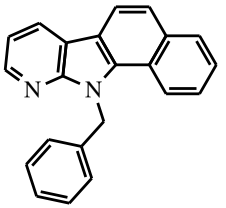
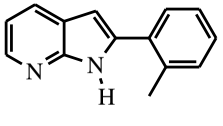
Appendix: Crystallography data

TABLE 1: Collection data of elucidated structures

Compound	 **84**	 **83**	 **77**	 **87**	 **86**	 **76**
Empirical formula	$C_{10}H_{13}Cl_1N_2Si_1$	$C_{11}H_{16}N_2Si_1$	$C_{10}H_{14}N_2Si_1$	$C_7H_6N_2$	$C_8H_8N_2$	$C_7H_6N_2$
Formula weight	224.76	204.35	190.32	118.14	132.16	118.14
Temperature	173.0(2) K	173.0(10) K	173.0(2) K	173.0(2) K	173.0(2) K	173.0(2) K
Wavelength	0.71073 Å	0.71073 Å	0.71073 Å	0.71073 Å	0.71073	0.71073 Å
Crystal system	Monoclinic	Monoclinic	Monoclinic	Monoclinic	Monoclinic	Monoclinic
Space group	P 21/n	P 21/n	C 2/c	P 21/n	P 21/c	P 21/n
Unit cell dimensions						
a	6.1555(2) Å	5.7804(2) Å		8.1199(2) Å	15.4791(4) Å	8.1199(2) Å
b	20.9072(6) Å	19.1377(6) Å	7.8254(2) Å	6.3376(2) Å	8.8958(2) Å	6.3376(2) Å
c	9.4985(3) Å	10.7436(3) Å	14.5560(4) Å	12.4126(3) Å	11.1615(3) Å	12.4126(3) Å
α	90°	90°	90°	90°	90°	90°
β	95.4480(10)°	92.805(2)°	108.7830(10)°	102.9350(10)°	111.007(2)°	102.9350(10)°
γ	90°	90°	90°	90°	90°	90°
Volume	1216.88(7) $Å^3$	1187.07(6) $Å^3$	2241.08(10) $Å^3$	622.55(3) $Å^3$	1434.78(7) $Å^3$	622.55(3) $Å^3$
Z	4	4	8	4	8	4
Density (calculated)	1.227 Mg/m^3	1.143 Mg/m^3		1.260 Mg/m^3		
Absorption coefficient	0.378 mm^{-1}	0.164 mm^{-1}		0.079 mm^{-1}		
F(000)	472	440	816	248	560	248

Crystal size (mm^3)	0.557 x 0.341	0.433 x 0.213	0.637 x 0.369	0.28 x 0.246	0.308 x 0.229	0.28 x 0.246
	x 0.196	x 0.164	x 0.326	0.16 mm^3	x 0.209	x 0.16
	$1.95°to28.29°$	$2.13°to28°$	$2.07°to28.27°$	$2.742°to27.997°$	$1.41°to28°$	$2.74°to28.00°$
Index ranges						
	$-8 \preceq h \preceq 8$	$-7 \preceq h \preceq 7$	$-26 \preceq h \preceq 27$		$-20 \preceq h \preceq 20$	$-10 \preceq h \preceq 9$
	$-27 \preceq k \preceq 27$	$-24 \preceq k \preceq 25$	$-10 \preceq k \preceq 10$		$-11 \preceq k \preceq 11$	$-7 \preceq k \preceq 8$
	$-11 \preceq l \preceq 12$	$-14 \preceq l \preceq 11$	$-16 \preceq l \preceq 19$		$-14 \preceq l \preceq 13$	$-16 \preceq l \preceq 15$
Reflections collected	29454	11039	10023	11264	17343	11264
Independent reflections	3014	2859	2783	1507	3476	1507
R(int)	0.0442	0.0371	0.0306	0.0348	0.0254	0.0348
Completeness	99.70%	99.40%	99.90%	100.00%	100.00%	100.00%
Refinement method	Full-matrix least-squares on F^2					
Data / restraints / parameters	3014 / 0 / 138	2859 / 0 / 139	2783 / 0 / 129	1507 / 0 / 90	3476 / 0 / 199	1507 / 0 / 90
Goodness-of-fit on F^2	1.064	1	1.038	1.038	1.058	1.05
	$R1 = 0.0299$	$R1 = 0.0381$	$R1 = 0.0463$	$R1 = 0.0400$	$R1 = 0.0412$	$R1 = 0.0402$
	$wR2 = 0.0814$	$wR2 = 0.0859$	$wR2 = 0.1256$	$wR2 = 0.1010$	$wR2 = 0.0989$	$wR2 = 0.1022$
R indices (all data)	$R1 = 0.0339$	$R1 = 0.0536$	$R1 = 0.0524$	$R1 = 0.0493$	$R1 = 0.0642$	$R1 = 0.0496$
	$wR2 = 0.0841$	$wR2 = 0.0939$	$wR2 = 0.1303$	$wR2 = 0.1086$	$wR2 = 0.1132$	$wR2 = 0.1098$
Largest diff. peak and hole($e.Å^{-3}$)	0.316 / -0.334	0.313 / -0.251	0.688 / -0.229	0.274 / -0.226	0.247 / -0.217	0.275 / -0.225

Table 2: Collection data of elucidated structures 2

Compound					
	213	**70**	**195**	**71**	**74**
Empirical formula	$C_{12}H_{14}N_2O_2$	$C_{15}H_{10}N_2$	$C_{17}H_{17}NO_3$	$C_{22}H_{17}N_2$	$C_{14}H_{12}N_2$
Formula weight	218.25	218.32	283.32	309.38	208.26
Temperature	173.0(2) K	173.0(2) K	173.0(2) K	173.0(2) K	173.0(2) K
Wavelength	0.71073 Å	0.71073 Å	0.71073 Å	0.71073 Å	0.71073 Å
Crystal system	Orthorhombic	Monoclinic	Monoclinic	Monoclinic	Monoclinic
Space group	P b c a	P2(1)/c	P2(1)/n	P2(1)/c	P2(1)/c
Unit cell dimensions					
a	9.2470(3) Å	11.477(6) Å	10.4765(4) Å	5.5833(2) Å	3.8759(2) Å
b	14.5102(4) Å	4.886(3) Å	7.7837(3) Å	18.2498(6) Å	23.5592(8) Å
c	17.4380(6) Å	19.046(11) Å	18.1482(7) Å	15.3217(5) Å	11.4047(5) Å
α	90°	90°	90°	90°	90°
β	90°	96.09(2)°	101.666(2)°	93.940(2)°	91.651(2)°
γ	90°	90°	90°	90°	90°
Volume	2339.76(13) $Å^3$	1061.9(11) $Å^3$	1449.34(10) $Å^3$		

Z	8	4	4	4	4
Density (calculated)		1.365 Mg/m^3	1.298 Mg/m^3	1.319 Mg/m^3	1.329 Mg/m^3
Absorption coefficient		0.082 mm^{-1}	0.089 mm^{-1}	0.078 mm^{-1}	0.080 mm^{-1}
F(000)	928	456	600	652	440
Crystal size (mm^3)	0.355 x 0.165	0.24 x 0.11	0.46 x 0.28	0.374 x 0.263	
	x 0.09	x 0.02	x 0.11	x 0.116	
	$2.86°to27.99°$	1.78ĉirc to 26.00ĉirc	$2.08°to28.00°$	$1.74°to28.35°$	$1.73°to28.00°$
Index ranges					
	-12⪯h⪯11	-13⪯h⪯14	-13⪯h⪯13	-7⪯h⪯7	-5⪯h⪯4
	-19⪯k⪯19	-6⪯k⪯6	-10⪯k⪯10	-21⪯k⪯24	-31⪯k⪯31
	-23⪯l⪯22	-23 ⪯l⪯23	-23⪯l⪯23	-20⪯l⪯20	-14⪯l⪯50
Reflections collected	19630	8638	12764	23975	10479
Independent reflections	2811	2065	3501	3902	2495
R(int)	0.0325	0.0988	0.0412	0.0408	0.0586
Completeness	99.70%	99.50%	100.00%	99.90%	99.90%
Refinement method			Full-matrix least-squares on F^2		
Data / restraints / parameters	2811 / 0 / 152	2065 / 0 / 154	3501 / 0 / 193	3902 / 0 / 217	2495 / 0 / 150
Goodness-of-fit on F^2	1.26	0.99	0.578	1.003	1.037
	R1 = 0.0428	R1 = 0.0676	R1 = 0.0392	R1 = 0.0403	R1 = 0.0533
	wR2 = 0.1089	wR2 = 0.1723	wR2 = 0.1200	wR2 = 0.0922	wR2 = 0.1144
R indices (all data)	R1 = 0.0697	R1 = 0.1576	R1 = 0.0558	R1 = 0.0530	R1 = 0.0916
	wR2 = 0.1469	wR2 = 0.2259	wR2 = 0.1454	wR2 = 0.1008	wR2 = 0.1285
Largest diff. peak and hole($e.Å^{-3}$)	0.590 / -0.881	0.335 / -0.292	0.272 / -0.261	0.319 / -0.193	0.473 / -0.206